Novel Fast Techniques for Online Voltage and T/D Power Exchange Control in Smart Distribution Grids Considering Voltage Stability Issues

by

Khaled ALZAAREER

MANUSCRIPT-BASED THESIS PRESENTED TO ÉCOLE DE TECHNOLOGIE SUPÉRIEURE IN PARTIAL FULFILLMENT FOR THE DEGREE OF DOCTOR OF PHILOSOPHY
Ph.D.

MONTREAL, DECEMBER 17,2020

ÉCOLE DE TECHNOLOGIE SUPÉRIEURE
UNIVERSITÉ DU QUÉBEC

BOARD OF EXAMINERS

THIS THESIS HAS BEEN EVALUATED

BY THE FOLLOWING BOARD OF EXAMINERS

Mr. Maarouf Saad, Thesis Supervisor
Department of Electrical Engineering, École de technologie supérieure

Mr. Hasan Mehrjerdi, Thesis Co-supervisor
Department of Electrical Engineering, Qatar University

Mr. Jean-Pierre Kenné, President of the Board of Examiners
Department of Mechanical Engineering, École de technologie supérieure

Mr. Ambrish Chandra, Member of the jury
Department of Electrical Engineering, École de technologie supérieure

Mrs. Dalal Asber, External Evaluator
Research Institute of Hydro-Quebec

Mr. Innocent Kamwa, Independent External Evaluator
Research Institute of Hydro-Quebec

THIS THESIS WAS PRENSENTED AND DEFENDED

IN THE PRESENCE OF A BOARD OF EXAMINERS AND PUBLIC

ON DECEMBER 14 2020

AT ÉCOLE DE TECHNOLOGIE SUPÉRIEURE

ACKNOWLEDGMENT

I would like to express my gratitude to my supervisor, Professor. Maarouf Saad, for his generosity, enthusiasm and help throughout this project. I am grateful not only for his role in achieving this work, but also for his invaluable guidance, patience, and his enormous qualities as a mentor and as a person. Without his support, the achievement of the present work would have not been possible.

Great thanks to my co-supervisor, Professor. Hasan Mehrjerdi, for his availability, support, suggestions and his valuable advice. Without his support, the achievement of the present work would have not also been possible. I thank him very much.

I wish to express my gratitude to the committee members who agreed to review and evaluate this research.

Finally, I would like to express my thanks to my mother, my brothers, and my sister who encourage me and make me feel loved and accompanied wherever I go.

Nouvelles techniques rapides pour le contrôle de la tension et de la puissance en temps réel sur le réseau de distribution intelligent en tenant compte des problèmes de stabilité de la tension

Khaled ALZAAREER

RÉSUMÉ

L'intégration des unités de production distribuées (PD) dans les réseaux de distribution (RD) a augmenté ces dernières années. L'augmentation d'intégration de l`unités PD peut ajouter de nouveaux défis au fonctionnement, à la stabilité et au contrôle du système d'alimentation. Ces défis sont a) les problèmes de surtension / sous-tension causés par la génération intermittente de PD, b) les conflits opérationnels entre les unités PD et les dispositifs conventionnels de contrôle de tension, c) le problème de stabilité de tension dû à l'augmentation des distances électriques entre les nœuds du générateur et les nœuds de charge, et d) un problème de commande de puissance active et réactive à l'interface de transport / distribution (T/D) pour répondre aux exigences émises par les règlements de connexion à la demande internationaux à ce point. Bien que de nombreux efforts de recherche se soient concentrés sur l'utilisation des unités de production distribuées pour résoudre les deux premiers problèmes grâce au contrôle de tension coordonné (CTC), les deux derniers problèmes n'ont pas encore été complètement étudiés. En outre, le temps de calcul nécessaire pour obtenir le contrôle global via CTC peut ne pas répondre aux exigences du réseau intelligent.

Cette thèse vise à développer de nouvelles techniques en temps réel pour le contrôle CTC et d'échange de puissance à l'interface T/D pour les DN intelligents tout en tenant compte des problèmes de stabilité de la tension et du support côté haute tension (HT). La vitesse de calcul rapide associée à ces techniques les rend uniques. L'inclusion du coût dans l'analyse ajoute également une caractéristique importante aux techniques.

La CTC est la commande d'échange de puissance de T/D est principalement basée sur la relation entre les tensions du réseau et les variables de commande. Ainsi, une méthode d'analyse rapide de sensibilité en tension (modèle ABCD) est proposée via la dérivée directe des grandeurs nodales (puissance, courant et tension) par rapport aux injections de puissance. De plus, une nouvelle technique CTC en temps réel pour choisir un groupe global des variables de contrôle les plus efficaces compte tenu de celles à faible coût est proposée. Cette technique est basée sur le concept des distances électriques pour définir l'efficacité des variables de contrôle, et sur la méthode descendante/ascendante pour la sélection des contrôles. En outre, une nouvelle technique de contrôle de stabilité de tension statique en temps réel pour les RD intelligents est développée en utilisant la sensibilité de la charge et les impédances équivalentes pour contrôler les variables. Les sensibilités d'impédance peuvent être utilisées pour évaluer la marge d'impédance de charge de Thevenin. Enfin, un contrôle d'échange de puissance T/D multimodes en temps réel est développé en formulant le problème en tant que problème d'optimisation quadratique à entiers mixtes. La coordination entre différents types de ressources de contrôle, y

compris les appareils appartenant au client et les appareils appartenant aux services publics est réalisée à cet effet.

Mots-clés: Réseaux de distribution intelligents, Génération distribuée, contrôle de tension, stabilité de tension, analyse de sensibilité.

Novel Fast Techniques for Online Voltage and T/D Power Exchange Control in Smart Distribution Grids Considering Voltage Stability Issues

Khaled ALZAAREER

ABSTRACT

The integration of Distributed Generation (DG) units into Distribution Networks (DNs) has been raised in the recent years. Hosting high penetration levels of DG units can add new challenges to power system operation, stability, and control. Such challenges are a) over/under voltage problems caused by the intermittent generation of DGs, b) operational conflicts between DG units and convention voltage control devices, c) voltage stability problem due to increase the electrical distances between the generator nodes and load nodes, and d) active and reactive power control problem at Transmission/Distribution (T/D) interface to meet the requirements issued by international Demand Connection Codes (DCC) at this point. Although numerous research efforts have focused to utilize DG units to solve the first two problems through Coordinated Voltage Control (CVC), the last two problems have not yet been fully studied. Besides, the calculation time needed to obtain the global control through CVC may not meet smart grid requirements.

This thesis aims to develop novel online techniques for CVC and power exchange control at T/D interface for smart DNs while considering the voltage stability issues and high-voltage (HV) side support. The fast-computational speed associated with these techniques makes them unique. Including the cost in the analysis also adds an important feature to the techniques.

The CVC and T/D power exchange control are mainly based on the relation between network voltages and control variables. Thus, a fast voltage sensitivity analysis method (ABCD model) is proposed via the direct derivative of system nodal quantities (power, current and voltage) with respect to power injections. Moreover, a new online CVC technique for choosing a global group of the most effective control variables considering the ones with low cost is proposed. This technique is based on the concept of electrical distances to define the effectiveness of control variables, and on top-down/bottom-up method for control selection. Besides, a new technique for online static voltage stability control for smart DNs is developed by using the sensitivity of the load and the equivalent impedances to control variables. The impedance sensitivities can be used to evaluate the Thevenin Load Impedance Margin (TLIM). Finally, an online multi-modes T/D power exchange control is developed by formulating the problem as Mixed-integer Quadratically Constrained Optimization Problem (MIQCP). Coordination among different types of control resources, including the customer-owned devices and utility-owned devices is achieved for this purpose.

Keywords: Smart distribution networks, Distributed Generation, voltage control, voltage stability, sensitivity analysis.

TABLE OF CONTENTS

Page

LIST OF TABLES

Page

LIST OF FIGURES

LIST OF ABREVIATIONS

T/D	Transmission/ Distribution
HV	High-Voltage
DG	Distributed Generation
DNs	Distribution Networks
DCC	Demand Connection Codes
CVC	Coordinated Voltage Control
TLIM	Thevenin Load Impedance Margin
MIQCP	Mixed-integer Quadratically Constrained Optimization Problem
TN	Transmission Network
OLTC	On Load Tap Changer
CBs	Shunt Capacitors
VRs	Voltage Regulators
R/X	Resistance/Reactance ratio
ENTSO-E	European Network of Transmission System Operators for Electricity
P & O	Perturb and Observe
MPC	Model Predictive Control
CPF	Continuation Power Flow
PMU	Phasor Measurement Units
MINLP	Mixed-integer Nonlinear Optimization Problem
CI	Correction Index
DR	Demand Response

LPF	Linear Power Flow
DMS	Distribution Management System
SCADA	Supervisory Control and Data Acquisition

LIST OF SYMBOLS AND UNIT OF MEASUREMENT

$ABCD$	Submatrices A, B, C and D
J	Jacobian matrix
Z	System impedance matrix
Q_{ex}	Reactive power exchange
V_T	Transmission network voltage
Y	System admittance matrix
N	Number of system nodes
G, L, T	Generator, Load, and Tie buses
Z_L , Z_{eq}	Load and equivalent impedances
E_{th} or V_{eq}	Thevenins' equivelent voltage
V_L , I_L	Load voltage and current phasors
u	Set of control variables
u_x	Control variable 'x'
k	Time instant
ΔE	The change in the target objective function
t	Time
s or sec	Second
h	Set of system quantities
G_{ij} , B_{ij}	The ijth line conductance and susceptance
$V_{j,r} , V_{j,im}$	The real and the imaginary parts of the voltage at bus i
$I_{i,r} , I_{i,im}$	The real and the imaginary parts of the load current of bus i

S_i	The complex power of bus i
$P_\mathrm{i}\ and\ Q_\mathrm{i}$	The real and reactive power of bus i
M	Number of PQ buses
$a_{ij}, b_{ij}, c_{ij}, d_{ij}$	The ijth element of the submatrices A, B, C, and D
I_p , I_q	Vectors of the real and the imaginary parts of load currents
V_{re}, V_{im} or V^{re}, V^{im}	Vectors of the real and the imaginary parts of the node voltages
V_g	The voltage at PV buses
Q_g	Reactive power injection by PV buses
N_g	Number of PV buses
$\|V\|$	Vector of node voltage magnitudes
J^{-1}	Inverse of J
"T"	Array transposition
ε	Vector of slack variables
θ	Vector of voltage angles
H	Set of equations for reactive power injection of all PQ buses
H_V , H_u	Partial derivatives of the injected reactive power with respect to the voltages and control variables
α_{ij}	The attenuation between the two nodes i and j
D_{ix}	Electrical distance between the two buses 'x' and 'i'.
d_{ix}	Normalized electrical distance between the two buses 'x' and 'i'.
d_x	Vector of normalized electrical distances between network nodes and the control variable u_x

dx'	Vector of normalized electrical distances including the cost
C_x	Unit cost for the control variable u_x
Γ	Vector of all violated voltages
φ	Set of the most effective control variables
$£$	Vector of the voltages obtained by top-down method
φ'	Result set by top-down method
φ''	The final result set of the most effective controls with low cost.
ΔVCD_i	The change in the ith voltage control device.
pf_{lim}	Power factor limit
P_{ex}	Active power exchange at T/D interface
Q_{lim}^{pf}	Limits of the reactive power exchange at T/D interface
Q_{lim}	Limits of reactive power exchange
V_T^S	Setpoint voltage at HV side
ΔV_T^S	Voltage deviation at HV side
Q_O, P_O, V_O	Nominal values of load power and voltage
G_L , B_L	The equivalent conductance and susceptance for each load
$I_{L,p}$, $I_{L,q}$	The real and imaginary parts of equivalent current source for each load
I_p^L , I_q^L	Vectors of the real and imaginary parts of the load currents
I_p^{DG} , I_q^{DG}	The real and imaginary parts of the current injection by DG unit
$I_{p,i}$, $I_{q,i}$	The real and imaginary parts of the net current at bus i
S_{sub} , V_{sub}	The power and the voltage at T/D interface
I_{sub}	The current drawn from the substation

$I_{p,sub}$, $I_{q,sub}$	The real and the imaginary parts of the current drawn from the substation
PF	Power factor at T/D interface
$C^{ca}, C^{DG},$ C^{cl} C^{ε}	Change cost of the capacitors, output power of DGs, the controllable loads, and using the slack variable
N_{ca}, N_{DG}, N_{cl}	Number of the capacitors, DGs, and the controllable loads used for the control
$e(i)$	Status of "on" or "off" of the capacitor at bus i
N_{ex}	Number of the controlled quantities at T/D interface.
C_i, P_i^{DG}, Q_i^{DG}, P_i^{cl}	Status of the capacitor i, active and reactive power injected by the DG i, and demand of the controllable load i, respectively.
λ	Demand curtailment contract or percentage of curtailed demand
I_{ij}	Magnitude of the current flowing through ijth branch
DR_P, DR_Q	Active and reactive power requested by TN

CHAPTER 1

INTRODUCTION

1.1 Background

Power distribution network is a major part of the electric grid which connects the Transmission Network (TN) and the consumers. The environmental issues, demand increase, and the dependence on traditional power plants are concerning problems today. To meet such problems, renewable energy resources have been used as DG units into DNs (Gama et al., 2009). The size and power generation of these DG units are very small compared to our traditional power generation resources (Short, 2014). The renewable energy-based DGs can reduce the dependence on conventional generation units (Wang & Lan, 2011). However, integration of DGs with DNs will consequently changes some characteristics of existing distribution grids (i.e. transforms the DNs from passive to active ones due to their properties).

1.1.1 Voltage control in distribution networks

Voltage regulation is one of the operational challenges in DNs. Voltage regulation aims to maintain the node voltages inside acceptable limits. This can be achieved by either directly controlling the node voltages or by controlling the reactive power flow which in turn can affect the voltage drop. On Load Tap Changer (OLTC) transformers, Capacitor Banks (CBs) and Voltage Regulators (VRs) are conventional voltage controls that are normally used for this purpose (Short, 2014), (Gönen, 1986). However, such controls are designed for passive DNs where the power flow is unidirectional (i.e. the power flows from the substation to the loads).

The connection of DGs with DNs may cause bidirectional power flow (Viawan, 2008). This will create new challenges in voltage control, especially in case of high penetration levels of DG units (Atwa et al., 2010). If DGs are operated at leading power factor mode, the node voltages can be increased by injecting reactive power to the system. The direction and magnitude of the power might change according to DG location and size (Shivarudraswamy

& Gaonkar, 2012) (Lopes et al., 2007). Thus, some considerations have to be taken into account to avoid the negative impacts of DG integration into the network like voltage rise. To avoid such problem, one may try to limit the amount of the power injected by DG units and install them near the load centers. However, this reduces the benefits that DG units could provide to the system. The intermittent nature of renewable energy resources can also add additional challenges on system control, stability and operation.

The integration of multiple DG units into DNs can cause over/under voltage problems as well as operational conflicts with other conventional voltage control devices (Ranamuka et al., 2016). These problems can grow as DNs meet structural changes (Ranamuka et al., 2015). Thus, it is required to operationally update the voltage control devices in active DNs. One of the favorable ways of reducing the adverse impacts of the operational conflicts among voltage control devices is control coordination. Control coordination aims to restrict the voltages within the normal range under different operating conditions such as the load variation and random output. Generally speaking, CVC techniques can update the control actions based on control rules or optimization techniques.

DG units can be actively involved in power systems for voltage regulation (Ranamuka et al., 2015). Voltage control techniques are mainly based on the relation between the network voltages and control variables (i.e. power injections). The sensitivity analysis is usually used to find the voltage sensitivity coefficients with respect to nodal reactive and real power injections. These sensitivities can be used to evaluate the node voltages due to performing control actions for CVC.

IEEE Standard 1547 (Photovoltaics et al., 2009) states a requirement regarding how much voltage violation is allowed with or without the presence of DG units. Voltage variations must remain within acceptable limits.

1.1.2 Power exchange control at T/D interface and HV side support

The adoption of renewable energy-based DG units has been raised in the recent years. This will reduce the dependence on the conventional generating units or transmission lines. The IEEE Std 1547.4 (Photovoltaics et al., 2009) considers utilization of DG units to provide the power to distribution grids and expand their capabilities for the overall TN support. In other words, DNs are requested to provide ancillary services by exporting reactive power to the TN, especially during its unexpected system failures. However, injecting power into TN may add new challenges to TN operator in the regard of voltage control (Lin et al., 2016). Indeed, high production from DG units of DNs and during light loading can increase the connection point voltage. Currently, DN operators are not responsible for power exchange control at T/D interface. TN operator is normally responsible for managing this problem. As a result, control of power exchange between transmission and distribution systems is one of the new requirements for modern power networks.

1.1.3 Voltage stability in distribution networks

Voltage stability is defined as the ability of a power system to maintain acceptable voltages at all nodes in the network under normal condition and after being subjected to a disturbance (kundur et al., 2004). Voltage stability analysis can be classified into transient and steady-state analysis. However, in this thesis, only the static models are applied for analysis to obtain voltage stability margin. Voltage stability margin is defined as the minimum distance between the current operating point and the maximum loadability point (Bahmanyar & Karami et al., 2014).

Voltage stability is usually studied for transmission networks. With the rapid increase in hosting large penetration levels of DG units, voltage stability problem has raised a main concern for DNs (Bolognani & Zampieri, 2015), (Wang et al., 2016), (Aolaritei et al 2018). Integration high penetration levels of DG units will pose more challenges in voltage stability assessment due to its intermittent nature and displacement of a significant portion of the synchronous generation. Moreover, as DNs continue in hosting DG units, the electrical

distances between generator nodes and load nodes become larger, which can cause major changes in the stability of DNs (Nazari & Ilic, 2014). In addition, some types of DG units, especially fixed speed wind turbines, always consume reactive power, which may cause long-term voltage stability in DNs (Liu & Chu, 2014). It is also known that DNs continuously witness fast load increase with a slow expansion in its grid, which can also affect the voltage stability. Another essential issue is that when TN meet accidents, the voltage stability in DNs can significantly be affected during post disturbances periods (Aristidou et al., 2017). For all these reasons, it is expected that future DNs will face several challenges in system operation and stability.

The methods of voltage stability analysis that have been developed are mainly oriented to HV networks. Voltage stability of DNs had a less attention by researches. Most of researchers focused on improving voltage profiles for DNs. However, a good voltage profile cannot guarantee that the network is stable since voltage magnitude is not a good indicator of voltage stability (Lof et al., 1992).

1.2 Problem statement

As mentioned in previous sections, integration of large scale of renewable DG units into DNs adds new challenges on system operation and control. The existing solutions are not enough to meet these challenges, especially in the context of online applications. The motivation behind of this thesis research is to a) find solutions for the new challenges associated with active DNs and b) enhance the computational speed and convergence. This motivation can be explained into four main points as follows:

a. Sensitivity Analysis plays a significant role in voltage prediction and control of power networks. The inverse of the Jacobian J (Borghetti et al., 2010), (Zhou et al., 2007) is a well-known approach that depends on solving a Newton Raphson power flow. However, the sensitivity coefficients have to be updated with any change in the system operating condition. This requires performing new Newton Raphson-based power flow calculations

(Peschon et al., 1968), and therefore more computation time is required. Besides, the convergence may not be obtained by this method. Such methods developed for transmission load flow studies are not suitable for distribution systems due to the poor convergence (Kersting, 2012). Such problems (convergence problems and the remarkable calculation time) add new challenges for online applications, especially in the context of optimization problems and practical systems.

b. The integration of DG units into DN voltage control may create operational interactions with other conventional voltage control devices. The structural changes can also increase the possibility to create control conflicts. Control rules-based voltage control methods are not suitable for large scale networks where large number of control choices are available or when many various objectives are included in the control. Similarly, optimization-based voltage control methods are impractical to implement since many control variables have to be used to obtain the optimal solution. Another issue is that the wide distribution of control variables and the possibility of occurring many voltage violations among the network makes it is hard to provide coordination of the controls while activating only the required number of controls. Besides, it is not easy to rank the most effective control variables during multi violated voltages while considering a set of aspects as cost. Thus, it is necessary to obtain the cheapest and the most effective controls for global voltage control in DNs.

c. The incorporation of high penetration levels of DG units in DNs could impose a new challenge on network stability. This is due to displacement of a significant portion of the synchronous generation and increase the electrical distances between nodes (Nazari et al., 2014). Moreover, DG unavailability (or outage) and the continuously fast load increase can also significantly affect the voltage stability in DNs. Besides, some types of DG units (i.e. fixed speed wind turbines) always consume reactive power, which may cause voltage instability in DNs (Liu et al., 2014). Another essential issue is that when TN is subjected to disturbances, the voltage stability in DNs may be affected during post disturbance periods. For all these reasons, it is necessary to design voltage control considering voltage

stability issues in future DNs. Besides, there is a need for guiding information regarding the decisions of control measures for voltage stability prediction and control. The information of how each control variable contributes in voltage stability control is an important issue for network operators.

d. The high production from DG units of DNs and during light loading can increase the voltage at T/D connection point and, in turn, cause problems for TN. In contrast, active DNs are strongly requested to support TN (i.e. providing ancillary services) during its unexpected system failures. Thus, future requirements will be posed for DN operators to manage the power exchange. One of these requirements is issued by the 'Network Code on Demand Connection' of the European Network of Transmission System Operators for Electricity (ENTSO-E) (European Commission, 2016). According to this code, the reactive power transfer should be inside a range depending on the import or export capability. Such a code is beneficial for both networks to keep the system secure and reliable. However, there are open questions about how to steer the power exchange at T/D interface from DN side. It is requested that DNs have the ability to maintain their own voltages while managing the power exchange at T/D interface.

1.3 Literature review

1.3.1 Voltage sensitivity analysis

Many approaches have been developed in the literature for voltage sensitivity analysis. One of the well-known approaches is based on the matrix J (Borghetti et al., 2010), (Zhou et al., 2007). This approach is a classical method and depends on the solving a Newton Raphson power flow which requires iterative process (Peschon et al., 1968). The voltage sensitivities are found by taking the inverse of J at one operating condition. One of the disadvantages of iterative methods is that the convergence may not be obtained. Although this kind of sensitivity analysis appears in recent studies for real-time applications such as voltage control (Alzaareer et al., 2020) and

voltage stability issues (Kamel et al., 2017), the analysis is done offline and only at normal operating conditions.

Many other sensitivity methods have been discussed in the literature. An approach based on the Gauss-Seidel method of load flow is developed (Zhou et al., 2008). The approach depends on the impedance matrix of the network and uses iteration process with a fixed number of iterations. Therefore, the accuracy of this method is low. An approach in which the network impedance matrix was used with the constant-current model of loads to develop a sensitivity approach (Conti et al., 2010). However, this approach depends on the approximated representation of the network lines. A direct voltage sensitivity analysis method is developed which is based on the topological structure of the network and independent of the network operating points (Zad et al., 2015). An approach starting from branch currents is used for sensitivity analysis (Khatod et al., 2006). However, this method requires a base load flow solution. Other methods based on the use of the so-called adjoint network are also proposed (Gurram et al., 1999), (Ferreira et al., 1990), (Bandler et al., 1980), (Bandler et al., 1982). Another approach based on the Perturb-And-Observe (P &O) Power Flow is proposed (Sansawatt et al., 2012). It considers the current state of the network and two power flows with a small change in the active (or reactive) power at the interested bus. An approach based on historical data is also presented (Weckx et al., 2014). However, these works suffer from inaccuracy and/or low-speed calculations.

1.3.2 Coordinated voltage control

Numerous research efforts have focused to utilize DG units in voltage control in distribution networks. A CVC for active DNs is proposed (Richardot et al., 2006) to show the ability of DG units to regulate the system voltage. Generally speaking, CVC techniques can update the control actions based on control rules or optimization techniques.

A novel CVC method is based on installing remote terminal units at DG units is developed (Elkhatib et al., 2011). A CVC method based on control rules algorithm is proposed (Kulmala

et al., 2014). A dynamic master/slave CVC method is presented (Moursi et al., 2014). A method based on power flow sensitivity factor for output control of multiple DG units is presented (Jupe et al., 2010). An online combined local and remote voltage control in the presence of induction machine-based DG unit is presented (Viawan et al., 2007). A CVC method for coordination of OLTC, VR, and DG unit is presented (Muttaqi et al., 2015). The method is based on the concept of control zone, line drop compensation, as well as the controllers' parameters. A real-time CVC employing plug-in electric vehicles, DG, and OLTC is proposed (Azzouz et al., 2015). However, all the above-mentioned studies do not consider the coordination process in case of multiple conventional voltage control devices and multiple DG units. An online CVC method to operationally avoid the impact of simultaneous responses of multiple voltage control devices and DG units is developed (Ranamuka et al., 2013). However, it does not consider the impacts of non-simultaneous operations of DG units and the conventional devices. To minimize the impact of non-simultaneous operations, an online CVC by allowing voltage control devices to operate in accordance with a priority scheme is proposed (Ranamuka et al., 2015). However, defining of control rules in large scale power system is a complex task.

In the literature, many optimization-based CVC methods are proposed for active DNs. A CVC for DNs is presented to maintain voltages at their set-point value (Biserica et al., 2011). A CVC model based on sensitivity analysis is proposed (Zhou et al., 2007) to minimize the curtailment in active power production of DG units. A short-term scheduling of a DN is presented (Borghetti et al., 2010) to minimize the variation in the output of DG units and node voltages. An CVC method is developed (Oshiro et al., 2011) to reduce the voltage deviation in DNs using DG units. An optimal voltage control to minimize the deviation in the voltage at pilot bus and the power production by DG units is proposed (Castro et al., 2016). A CVC method is proposed by formulating a large-scale optimization problem and solving it using a genetic algorithm-based solver (Senjyu et al., 2008). A CVC method based on dynamic programming method is proposed (Kim et al., 2012). A new mutation fuzzy adaptive particle swarm optimization algorithm is presented to mitigate the overvoltage and minimize total loss in active DNs (Yang et al., 2015). A CVC of tap changers and DG units is presented to maximize

daily DG production and minimize the daily losses (Jakus et al., 2015). A voltage control framework for day-ahead operation is presented with the objective to minimize the power losses and voltage violations in active DNs (Degefa et al., 2015). A nonintrusive control strategy using voltage and reactive power for DNs based on PV and the nine-zone diagram is presented (Dou et al., 2019). A multiagent-based dispatching scheme for DG units for voltage support on distribution feeders is proposed (Baran et al., 2007). A CVC method aims to enable high solar penetrations in DNs while minimizing the voltage deviations and tap operations is proposed (Li et al., 2018). Advanced CVC scheme is proposed for smart microgrids to maximize power generated by DG units (Olival et al., 2017). A CVC approach exploits the reactive power capability of DG units to minimize the power losses and mitigating overvoltages is developed (Kryonidis et al., 2019). A comprehensive decentralized Volt/VAr control strategy is proposed for coordination of conventional control devices and synchronous machine-based DG units (Viawan et al., 2008). A multiple line drop compensation voltage control technique for under-load tap changer transformers is proposed (Choi et al., 2001), where the desired tap positions are obtained by solving an integer optimization problem. A Trust Region Sequential Quadratic Programming technique for CVC in active DNs is presented (Sheng et al., 2015). Optimal power flow is used for voltage control in medium voltage networks with the objective to minimize the curtailment of DG units and reduce the shedding of controllable loads (Meirinhos et al., 2017). The aforementioned methods formulate the problem as a single step optimization. To compensate the modeling inaccuracies, the MPC method to correct the voltages in active DNs is proposed (Valverde et al., 2013). Multi-step optimization is used in the literature to speed-up the computation and to avoid numerical problems (Alamo et al., 2015), (Guo et al., 2017). However, by using optimization-based methods, large number of control variables have to be activated to obtain the best solution, which is not suitable for practical systems. Moreover, those works do not fully consider the impacts of structural changes in voltage control.

1.3.3 Voltage stability assessment

For static voltage stability analysis, the critical condition of power systems can be determined based on the singularity point of power flow Jacobian. The Newton-Raphson method may fail to converge, which adds a challenge for singularity point calculation. To address this problem, Iwamoto's approach (Iwamoto & Tamura, 1981), Continuation Power Flow (CPF) (Ajjarapu, & Christy, 1992), (Sheng & Chiang, 2013) and holomorphic embedding approach (Trias, 2012), have been used. Some stability indicators are also developed based on eigen-decomposition of the power flow Jacobian at the singularity point (Gao et al., 1992), (Lof et al., 1993). Another method is characterized by the eigenvector with respect to the zero eigenvalue of power flow Jacobian (Dobson et al., 1992). Other methods are based on Thevenin equivalent to reduce the system into two-bus network (Vu, 1999), (Milosevic & Begovic¸2003), (Smon et al., 2006), (Corsi & Taranto, 2008), (Wang et al., 2011). Branch equivalents are also adopted in the literature for network reduction (Jasmon et al., 1991), (Chakravorty & Das, 2001), (Yu et al., 2014).

For voltage stability analysis in DNs, several techniques have been proposed: CPF (Dou et al., 2017), probabilistic evaluation (Liu et al., 2015) and modal analysis technique (Chou et al., 2014)). However, all these approaches require extensive calculations that are not suitable for real-time applications. Several voltage stability indicators have been presented by reducing the DN into two-bus system (Gubina et al., 1997), (Jasmon et al., 1991), (Hamada et al., 2010). However, those indicators are derived only at one operating point and none of them can involve the dynamic nonlinear behavior of loads. The equivalent nodal analysis (Wang et al., 2011) was extended to be used in DNs (Alzaareer & Saad, 2018) for voltage stability assessment. The same concept was also used (Liu et al., 2014) to detect the voltage instability of fixed-speed induction generator in DNs. The equivalent nodal analysis is simple such that Thevenin circuit seen by a load bus can be easily obtained and, then, incorporated into voltage stability assessment.

1.3.4 Power exchange control and HV side support

Although some works deal with the role of DNs in TN support, employing DNs for online power exchange control and considering practical issues has not yet been fully studied. However in the literature, a coordinative sub-transmission voltage control for reactive power management between TN and DNs is proposed (Ke et al., 2018). In this method, all the decisions are done by HV side. The enhanced utilization of voltage control variables by maximizing the DG reactive power output is proposed (Keane et al., 2010). A method for minimizing the reactive power transfer by the TN to the DNs is presented (Ochoa et al., 2011). Reactive power management at T/D interconnection is proposed (Ali et al., 2015). An optimal reactive power control for transmission connected distribution network with wind farms is proposed (Stock et al., 2016). A MPC for reactive power control in transmission connected DNs is proposed (Stock et al., 2016). These works present passive control methods and do not aim to solve the problem online. Moreover, most of them depend on non-linear power flow equations to perform optimal power flow technique for problem solving. Other methods based on real-time measurements are used for TN support (Valverde et al., 2013), (Morin et al., 2016). However, the high required number of monitoring devices is one of the main challenges in these methods.

1.4 Research objectives

This thesis aims to develop novel fast methods for online CVC in smart DNs. The developed methods also provide solutions for other important problems in DNs as well as TN. Voltage stability issues, power exchange control at T/D interface and HV side support are such problems that are considered in this thesis. To solve the problems mentioned in section 1.2, this thesis presents four main objectives as follows:

- Since CVC and power exchange control mainly depend on voltage sensitivity analysis, it is necessary to speed-up voltage sensitivity analysis for online application purposes. Therefore, the first objective of this thesis is to develop fast voltage sensitivity analysis

method using analytical derivation for smart DNs. The method does not require iterative process to update the sensitivity coefficients and therefore it can be implemented for online applications in smart distribution networks. The method represents an analytical development for sensitivity analysis, such that it is not limited to a particular type of network or governed by a particular power flow method. The method can also be considered as an alternative technique for the classical ones but with an extra advantage of fast computations.

- To provide a feasible solution for practical implementation for online CVC in active DNs, the second objective is to develop a new identification method for global group of controls. The proposed method takes into consideration five aspects: the effectiveness, availability, and cost of the control variables as well as the structural changes of networks and the coordination between control variables to simultaneously eliminate the violation in the voltages. By this method, the cheapest and the most effective control variables can be selected as a global control set. This means that only the minimum required number of control variables can be used for voltage control. Besides, the proposed method is capable of ranking the control variables to multi violated voltages (not only one violated voltage) and simultaneously (with no time delay) eliminating all the multi violations with only the most effective controls, low computational efforts and high speed. It is worth noting that the proposed method does not aim to find the optimal voltage control, which requires operation of most, if not all, the control variables, but provides a group of the most effective control variables.

- To consider the static voltage stability issues while performing CVC in DNs, the third objective is to develop an online centralized CVC method aiming to maximize the voltage stability margin in the network. The objective can be achieved by optimally dispatch the outputs of DG units without needing for a detailed system model and complex calculation to find the critical point. This feature makes the proposed method suitable for real-time voltage control in DNs. The method also aims to evaluate the sensitivity of the load and the equivalent impedances of load buses to control variables to obtain the contribution of

each DG unit in change the impedances and, hence, in the voltage stability margin. The impedance sensitivity provides an analysis of not only how other buses affect the impedances of a specific load bus but also how the specific bus can affect the impedances of other load buses.

- To consider HV side support while performimg CVC in DNs, the fourth objective is to develop a MIQCP-based multi mode online power exchange control at T/D interface while keeping DN voltages within acceptable limits. The control method is centralized and can meet the requirements issued by international DCC at T/D interface or fulfill the Demand Response (DR) requirements from TN as well as DN voltages. The proposed control method provides the option for DNs to operate in different modes: isolated mode, passive mode, active mode, and DR mode. Both active and reactive power exchanges are considered for the control. The control can be implemented at the distribution side, without needing for any interactive mechanism (or data exchange) between TN and DNs or any extra monitoring devices for DNs. The method also aims to formulate the problem as MIQCP problem, which can be efficiently solved for its global optimum solution. To increase the responsibility degree of DNs for problem control, the method involves controllable loads, along with DGs and CBs, in the control.

  The relation between the aformentioned four objectives in order to investigate the global objective can be understood in Figure 1.1. It can be seen that the first objective is used to mainly evaluate the changes in the voltages and impedances in the other three objectives. The othre three objectives are generally developed for CVC. The third objective can also maximize the system voltage stability margin while the forth objective consider HV side support.

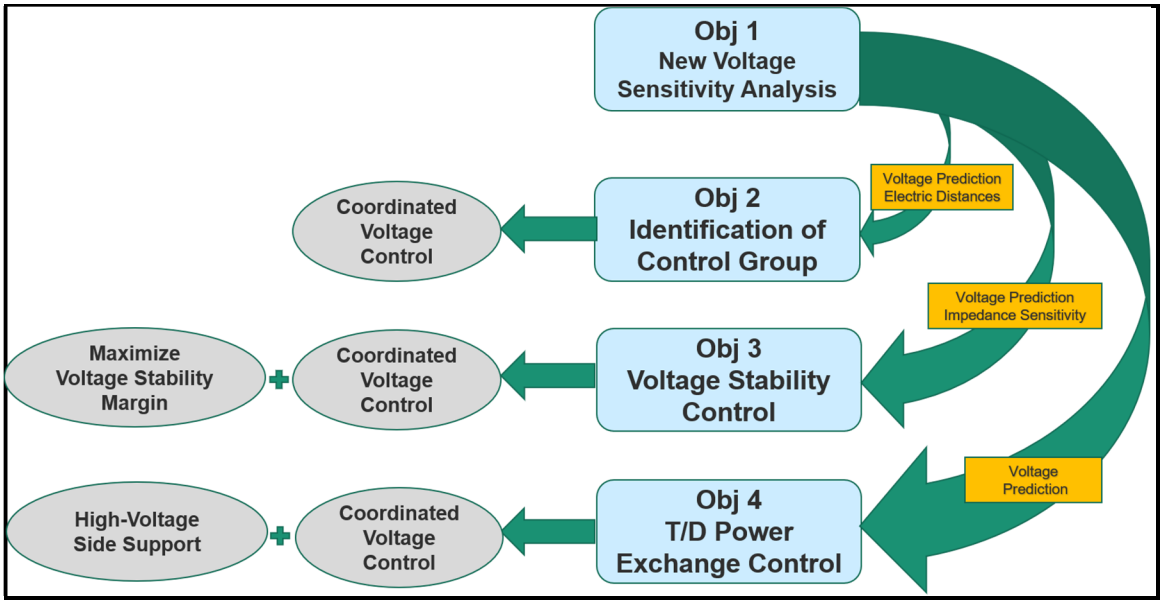

Figure 1.1 The relation between the work objectives

1.5 Methodology overview

To achieve the four objectives presented in the previous section, the following methodology were applied:

a. The fast voltage sensitivity analysis is developed by taking the direct derivatives of nodal power equations with respect to power injections, and then constructing the ABCD matrix (refer to equation (3.25)). The nodal quantities (power, current and voltage) are expressed in Cartesian coordinates to make a complete separation between the sensitivities to active and the sensitivities to reactive power injections. ABCD elements represent coefficients for the partial derivatives of node voltages (in Cartesian form) and their values remain constant regardless of the bus on which the power is injected.

b. The proposed identification method for global control group is developed based on the concept of electrical distances between the voltage control devices and network nodes. An index, namely Correction Index (CI), is derived based on the electrical distances and the

control cost to represent the level of effectiveness of each control variable with respect to all violated voltages. This means that the CI can be used for control ranking. The index is then implemented in two phase algorithms (top–down and bottom- up) to identify the global group of controls (the cheapest and the most efficient ones) to simultaneously eliminate the violation in voltages.

c. For voltage stability control in distribution networks, a Thevenin-based Load Impedance Margin (TLIM) derived from the nodal measurements is used. This margin takes into the consideration the changes in the system operation, especially those caused by the rapid-response devices of DG units. Sensitivity analysis is then performed on the load and the equivalent impedances (terms of TLIM) to obtain the contribution of each control variable in the change of TLIM. The sensitivity analysis is investigated via the derivation of nodal voltage and current with respect to control variables. The changes of the impedances of pilot bus, which has the smallest value among all the TLIMs, are formulated in a multi-step optimization problem in terms of impedance sensitivities for the optimal dispatch of controls.

d. Power exchange control at T/D interface is achieved by performing the problem as a MIQCP. To do that, a Linear Power Flow (LPF) taking into account the voltage dependence of loads is used for the analysis. The analysis is done at the distribution level without any interaction with TN. A mathematical relation for power drawn by the substation is determined using LPF, and thus there is no need for interactive mechanism with TN or any extra monitoring devices. To increase the responsibility degree of DNs in fulfilling DCC or DR requirements, controllable loads are involved in the control strategy.

1.6 Thesis contribution

This thesis research focuses on finding solutions for voltage and T/D power exchange control in active DNs while taking into account the voltage stability issues as well as HV side support. The thesis solutions are fast enough, such that it has a high potential to be implemented in

online applications for large-scale DNs. Following the literature review, although numerous researches deal with some voltage control problem, few of them are concerned with voltage stability and T/D power exchange control in DNs. Besides, their solutions are still not fast enough to meet the challenges associated with renewable DG integration and/or practical power systems.

The key contributions of this thesis can be summarized as follows:

1. A new analytical and fast approach for voltage sensitivity analysis of power systems is proposed via the derivative of the real and imaginary parts of the nodal quantities with respect to power injections. It can be extended to compute the sensitivities with respect to different types of control variables. It is also suitable for any network (TN or DN, radial or meshed networks). The proposed method mainly depends on the construction of ABCD matrix to derive one general mathematical expression for sensitivity analysis. Indeed, it does not require to update ABCD matrix with changing the bus on which the power is injected. One important feature for ABCD model that it was able to completely separate between the sensitivities to active and the sensitivities to reactive power injections. This can be achieved by expressing the nodal quantities (power, voltage, and current) and network admittances in Cartesian coordinates and making an assumption that the real or reactive power injections at a particular bus is independent of any other power injections in the system.

2. A novel identification method is proposed, to our best knowledge for the first time, to select a global set of the most effective control variables for voltage control in DNs. The method is feasible for practical implementation. Compared to optimization-based voltage control techniques, only the required number of controls are selected for control. Compared with control rules-based CVC methods, the proposed method is suitable for large networks where a large number of control choices exist or when many various objectives are included in the control. Indeed, most of the rules-based methods are not capable to simultaneously eliminate the violations due to the time delay associated with conventional controls. Besides, the proposed identification control method shows a high level of

flexibility such that it can take into consideration the five aspects to eliminate the violation in the voltages: the effectiveness, availability, and the cost of each control action as well as the structural changes of distribution network and the coordination among control actions.

3. Using the common optimization methods for voltage control in DNs, the normal operating limits of voltage follow an economical purpose (i.e. the objective function is to minimize the cost, loss,…etc.). In contrast, this thesis formulates the problem to maximizes the voltage stability margin in smart DNs. Besides, the impedance sensitivity analysis is presented for the first time in order to evaluate the changes in the load and the equivalent impedances of any load bus (i.e. terms of voltage stability margin) to control variables. The proposed sensitivities provide an analysis of not only how other buses affect the impedances of a specific load bus, but also how the specific bus can affect the impedances of other load buses.

4. The thesis provides a flexible online control framework for DN to steer the power exchange at T/D interface without needing interactive mechanism (or data exchange) between TN and DNs or any extra monitoring devices for DNs. The framework can work under different modes: isolated mode, passive mode, active mode and DR mode. Although some works deal with the role of DNs in TN support, employing DNs for online power exchange control and considering practical issues has not yet been fully studied. Besides, T/D power control considers not only the reactive power but also the active power exchange. Furthermore, formulating the problem as MIQCP problem instead of MINLP problem makes the proposed method more applicable for smart grid. Such a programming problem can be efficiently solved to its optimal or sub-optimal solution while reducing the high-computational burdens, compered to MINLP problems.

1.7 Thesis outline

The organization of this thesis is given as follows:

The first chapter provides an introduction to this thesis. It presents a general background on DNs. It also states the motivation, literature survey, research objectives and the contributions of this thesis.

The second chapter describes some of the fundamental concepts that are used to achieve this thesis. Such concepts are required for online voltage and power exchange control in smart DNs.

The third chapter presents a fast method, namely ABCD model, for voltage sensitivity analysis in smart grids. This chapter represents one of the thesis articles and it was submitted for publication in International Journal of Electrical Power & Energy Systems.

The fourth chapter presents a new identification method for global control group for online CVC in smart DNs. This chapter represents one of the thesis articles and it was published in IEEE Transactions on smart grid (Alzaareer et al., 2020b).

The fifth chapter presents an impedance sensitivity-based method for online voltage control in smart DNs. This chapter represents one of the thesis articles and it was published in Electric Power System Research Journal (Alzaareer et al., 2020a).

The sixth chapter presents a MIQCP-Based Multi-Modes Online Power Exchange Control at T/D Interface. This chapter represents one of the thesis articles and it was submitted for publication in IEEE Transactions on smart grid.

The conclusion and recommendation of the thesis are stated at the end of this thesis.

CHAPTER 2

FUNDAMENTAL CONCEPTS

2.1 Introduction

As mentioned in chapter 1, this thesis aims to investigate four objectives. This chapter provides some fundamental concepts used to achieve the four objectives. The link among the next chapters and the coherency between them are also explained.

2.2 Nodal current equation

Nodal power equation is widely used for power system issues. This equation relates the node voltages V with the node currents I by using the system admittance matrix Y as follows:

$$[I] = [Y][V] \tag{2.1}$$

In general, the system buses can be divided into generator buses G, load buses L and tie buses T. Accordingly, the nodal current equation can be expressed as:

$$\begin{bmatrix} I_G \\ -I_L \\ 0 \end{bmatrix} = \begin{bmatrix} Y_{GG} & Y_{GL} & Y_{GT} \\ Y_{LG} & Y_{LL} & Y_{LT} \\ Y_{TG} & Y_{TL} & Y_{TT} \end{bmatrix} \begin{bmatrix} V_G \\ V_L \\ V_T \end{bmatrix} \tag{2.2}$$

For any load bus i, the current injection can be written in terms of the system admittances and node voltages as:

$$I_i = \sum_{j=0}^{N} Y_{ij} V_j \tag{2.3}$$

Where N is the number of system buses. Y_{ij} is the admittance between the nodes i and j. I_i is the current injection at bus "i" while V_j is the voltage of bus "j". The expression represented in (2.3) can be written in polar and rectangular terms as:

$$I_i = |I_i|\angle\alpha_i = I_{i,r} + jI_{i,im} \tag{2.4}$$

To explain nodal current equation, let us consider the simple distribution network shown in Figure 2.1. The load power at each node and the power produced by DG unit are represented by current injections (refer to Figure 2.1 (a)). The system admittances are constants in normal cases. If the admittance values and the load currents are available, the network voltages can be obtained according to (2.2). If the structure or the topology of the network is changed, the corresponding admittances should be changed by ΔY. Similarly, if the load power consumption or the power output by DG at any node is changed, the current injection of that node will be changed by ΔI. By performing (2.2) again, we can find that the network voltages will be changed by ΔV. Not only the voltage of one node will be changed, but also all the node voltages having sensitivity to that particular change (i.e. topology or power change). As a result, the network voltages are governed by nodal current equation.

According to nodal current equation, the nodal power of any node can be presented as:

$$S_i = V_i I_i^* = V_i \left(\sum_{j=0}^{N} Y_{ij} V_j \right)^* = P_i + jQ_i \tag{2.5}$$

Where S_i, P_i, Q_i are the complex, real and reactive power of bus i, respectively. The symbol "*" denotes the conjugate.

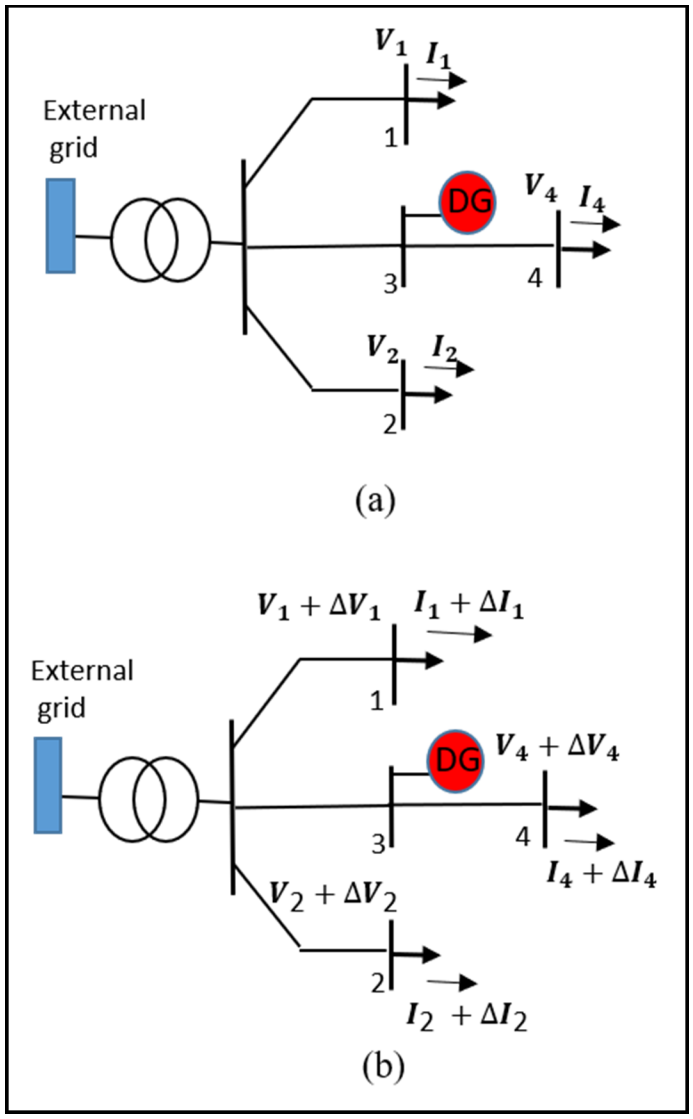

Figure 2.1 The concept of nodal current equation (a) before and (b) after the control

This thesis mainly depends on nodal current equations to derive the expressions and develop the proposed control methods for smart DNs. This equation is simple, easy to handle, and can accurately represents the network model.

2.3 Voltage sensitivity Analysis

The voltage sensitivity analysis is mainly used to find the dependence between the node voltages and power injections. Voltage sensitivity analysis is very necessary to evaluate the

network voltages for solving many problems. In this thesis, voltage sensitivity is used to evaluate the network voltages for voltage control problem and assess the system voltage stability margin for voltage stability analysis.

One of the well-known methods for voltage sensitivity analysis is the Jacobian-based method (Alzaareer et al., 2020c). Jacobina matrix (J) usually links the nodal power mismatch with nodal voltage changes as:

$$\begin{pmatrix} \Delta P_2 \\ \vdots \\ \Delta P_N \\ \hline \Delta Q_2 \\ \vdots \\ \Delta Q_N \end{pmatrix} = \begin{pmatrix} \frac{\partial P_2}{\partial \theta_2} & \cdots & \frac{\partial P_2}{\partial \theta_N} & \frac{\partial P_2}{\partial |V_2|} & \cdots & \frac{\partial P_2}{\partial |V_N|} \\ \vdots & \ddots & \vdots & \vdots & \ddots & \vdots \\ \frac{\partial P_N}{\partial \theta_2} & \cdots & \frac{\partial P_N}{\partial \theta_N} & \frac{\partial P_N}{\partial |V_2|} & \cdots & \frac{\partial P_N}{\partial |V_N|} \\ \frac{\partial Q_2}{\partial \theta_2} & \cdots & \frac{\partial Q_2}{\partial \theta_N} & \frac{\partial Q_2}{\partial |V_2|} & \cdots & \frac{\partial Q_2}{\partial |V_N|} \\ \vdots & \ddots & \vdots & \vdots & \ddots & \vdots \\ \frac{\partial Q_N}{\partial \theta_2} & \cdots & \frac{\partial Q_N}{\partial \theta_N} & \frac{\partial Q_N}{\partial |V_2|} & \cdots & \frac{\partial Q_N}{\partial |V_N|} \end{pmatrix} \begin{pmatrix} \Delta \theta_2 \\ \vdots \\ \Delta \theta_N \\ \hline \Delta |V_2| \\ \vdots \\ \Delta |V_N| \end{pmatrix} \quad (2.6)$$

Where ΔP and ΔQ denote the real and reactive power mismatch, respectively. $\Delta\theta$ and $\Delta|V|$ denote the change in the voltage phase and magnitude, respectively. $\partial P/\partial|V|$ and $\partial Q/\partial|V|$ denote the partial derivatives of the real and reactive power injection to voltage magnitude, respectively. $\partial P/\partial\theta \ and \ \partial Q/\partial\theta$ denote the partial derivatives of the real and reactive power injection to voltage angle, respectively.

It is worth mentioning that the relation illustrated in (2.6) can be modified according to the number of PQ and PV buses in the network. Bus 1 is assumed to be slack bus and therefore it is omitted from (2.6). The relation in (2.6) can be written as:

$$\begin{aligned} \begin{pmatrix} \Delta P \\ \Delta Q \end{pmatrix} &= \begin{pmatrix} J_1 & J_2 \\ J_3 & J_4 \end{pmatrix} \begin{pmatrix} \Delta \theta \\ \Delta |V| \end{pmatrix} \\ &= (J) \begin{pmatrix} \Delta \theta \\ \Delta |V| \end{pmatrix} \end{aligned} \quad (2.7)$$

Where, J_1, J_2, J_3, J_4 are the Jacobian matrix elements. Assuming that the control variables are only nodal power injection, the sensitivity of voltage magnitudes and angles to power injections can be obtained from the inverse of J as:

$$\begin{bmatrix} \Delta|V| \\ \Delta\theta \end{bmatrix} = [J]^{-1} \begin{bmatrix} \Delta P \\ \Delta Q \end{bmatrix} = \begin{bmatrix} \frac{\partial|V|}{\partial P} & \frac{\partial|V|}{\partial Q} \\ \frac{\partial\theta}{\partial P} & \frac{\partial\theta}{\partial Q} \end{bmatrix} \begin{bmatrix} \Delta P \\ \Delta Q \end{bmatrix} \quad (2.8)$$

Where $\partial|V|/\partial P \; and \; \partial|V|/\partial Q$ are the sensitivity vectors of nodal voltage magnitudes to real and reactive power injection, respectively. $\partial\theta/\partial P \; and \; \partial\theta/\partial Q$ are the sensitivity vectors of nodal voltage angles to real and reactive power injection, respectively.

The voltage sensitivity of any load bus to any power injection (i.e. dV_i/dP_x and dV_i/dQ_x) can then be calculated as:

$$\frac{dV_i}{dP_x} = e^{j\theta_i}\left(\frac{d|V_i|}{dP_x} + j|V_i|\frac{d\theta_i}{dP_x}\right) \quad (2.9)$$

$$\frac{dV_i}{dQ_x} = e^{j\theta_i}\left(\frac{d|V_i|}{dQ_x} + j|V_i|\frac{d\theta_i}{dQ_x}\right) \quad (2.10)$$

To speed up the calculation time of voltage sensitivity analysis, ABCD model is proposed in chapter 3. The steps for developing ABCD method can be described as follows:

- For each load bus, the real or reactive powers at 1st instant is expressed in terms of real and imaginary parts of the network voltages and currents as:

$$P_1 = f(V_r, V_{im}, I_r, I_{im})$$
$$Q_1 = g(V_r, V_{im}, I_r, I_{im}) \quad (2.11)$$

Where V_r and V_{im} are the real and the imaginary parts of the node voltage.

- For each load bus, the real or reactive powers at 2nd instant is also expressed in terms of real and imaginary parts of the network voltages and currents as:

$$P_2 = f(V_r + \Delta V_r,\ V_{im} + \Delta V_{im},\ I_r + \Delta I_{re},\ I_{im} + \Delta I_{im})$$
$$Q_2 = g(V_r + \Delta V_r,\ V_{im} + \Delta V_{im},\ I_r + \Delta I_{re},\ I_{im} + \Delta I_{im}) \quad (2.12)$$

- For each load bus, the change in active or reactive power injection can be obtained as:

$$\Delta P = P_2 - P_1 = f'(V_r, V_{im}, I_r, I_{im})$$
$$\Delta Q = Q_2 - Q_1 = g'(V_r, V_{im}, I_r, I_{im}) \quad (2.13)$$

- Ignore the very small values of the terms implied in (2.11), divide (2.11) by amount of real or reactive power injection at bus "x" (ΔP_x or ΔQ_x), and then take the limit of the expressions in (2.11) as $\Delta P_x \rightarrow 0$ or $\Delta Q_x \rightarrow 0$.
- By organizing the obtained equations, we get:

$$[A \quad \mathrm{B}]\begin{bmatrix}\frac{\partial V_r}{\partial P_x}\\ \frac{\partial V_{im}}{\partial P_x}\end{bmatrix} = \left[\frac{\partial P}{\partial P_x}\right] \quad (2.14)$$

$$[\mathrm{C} \quad \mathrm{D}]\begin{bmatrix}\frac{\partial V_r}{\partial Q_x}\\ \frac{\partial V_{im}}{\partial Q_x}\end{bmatrix} = \left[\frac{\partial Q}{\partial Q_x}\right] \quad (2.15)$$

Where $\frac{\partial P}{\partial P_x}$ and $\frac{\partial Q}{\partial Q_x}$ are sensitivity vectors of the active and reactive power of PQ nodes with respect to active and reactive power injection at node "x", respectively. $\frac{\partial V_r}{\partial P_x}$, $\frac{\partial V_{im}}{\partial P_x}$, $\frac{\partial V_r}{\partial Q_x}$ and $\frac{\partial V_{im}}{\partial Q_x}$ are sensitivity vectors of real and imaginary parts of PQ voltages with respect to active

and reactive power injection at node "x", respectively. A, B, C, and D are submatrices with constant values.

The sensitivity analysis can also be used to find the voltage sensitivity to any control variable u_x (i.e. OLTC, VR, CB, DG) as:

$$\frac{dV}{du_x} = -\left[\frac{dV}{dP}\right]\left[\frac{dP}{du_x}\right] \tag{2.16}$$

Or

$$\frac{dV}{du_x} = -\left[\frac{dV}{dQ}\right]\left[\frac{dQ}{du_x}\right] \tag{2.17}$$

Where $\frac{dV}{du_x}$ is a vector of the partial derivatives of network voltages with respect to the control variable u_x. $\frac{dV}{dP}$ and $\frac{dV}{dQ}$ are matrices of the partial derivatives of network voltages with respect to real and reactive power injection, respectively. $\frac{dP}{du_x}$ and $\frac{dQ}{du_x}$ are vectors of the partial derivatives of real and reactive power injection with respect to the control variable u_x, respectively. Elements of $\frac{dV}{dP}$ and $\frac{dV}{dQ}$ can be found as mentioned early (i.e. the inverse of J or using ABCD method). Elements of $\frac{dP}{du_x}$ and $\frac{dQ}{du_x}$ are known vectors and represent how the real and reactive power injection change with varying the control variable u_x. Based on the type of the control variable, (2.16) or (2.17) is used.

2.4 Electrical distances

The electrical distance is a concept used to obtain the coupling degrees among different nodes. In this thesis, the electrical distances are determined based on the effect of control variables. The electrical distance between any two nodes D_{ij} can be obtained by:

$$D_{ij} = -Log\left(\alpha_{ij}.\alpha_{ji}\right) \tag{2.18}$$

Where $\alpha_{ij} = \alpha_{ji}$ represents the attenuation between the two nodes i and j. It normally depends on the relative variation in the voltage between any two buses due to the change in the control variable located at one of the buses, and can be calculated as (Ranamuka et al., 2015):

$$\alpha_{ij} = \frac{\partial V_i}{\partial u_j} / \frac{\partial V_j}{\partial u_j} \tag{2.19}$$

The electrical distance concept is used in chapter 4 to sort the promising control variables for the violated voltages.

2.5 Thevenin-Based Load Impedance Margin (TLIM)

The TLIM is an index developed in chapter 5 for voltage stability analysis in distribution networks. It is used to find the distance to voltage collapse or instability in the network. By this method, the DN seen by a load bus can be simplified to Thevenin equivalent circuit as shown in Figure 2.2. Where Z_L and Z_{eq} are the load and the equivalent impedances referred to the load bus. E_{th} is the Thevenins equivelent voltage. $V_L$and I_L are the voltage and the current of the load bus.

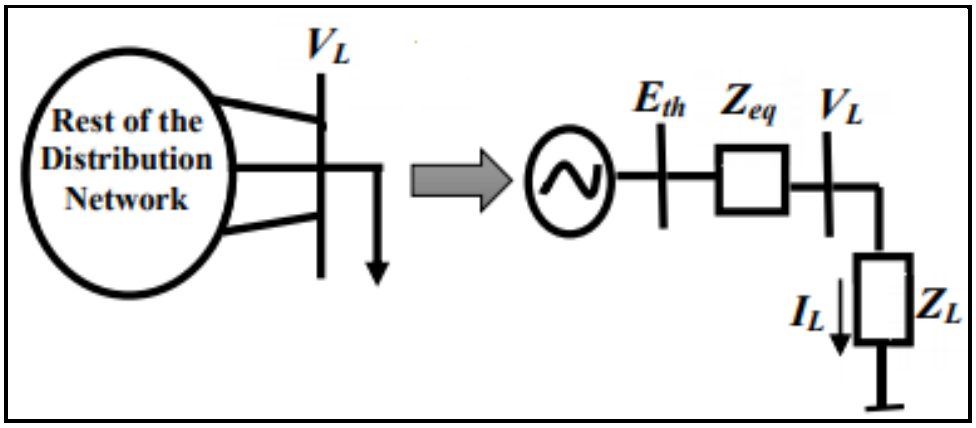

Figure 2.2 Simplified DN using Thevenin theorem
Taken from Alzaareer & Saad (2018)

The equivalent impedance Z_{eq} can be calculated using different techniques. However, this work uses the equivalent nodal model to capture the dynamic nonlinear changes of loads. The equivalent nodal model used the nodal current equation presented in (2.2) to obtain the load voltages. By reorganizing (2.2), we obtain that the voltage of load bus i is:

$$V_i = \sum_{j \in G} Z_{ij} I_j - \left(Z_{ii} + \sum_{\substack{j \in L \\ i \neq j}} Z_{ij} \frac{I_j}{I_i} \right) I_i = E_{eq,i} - Z_{eq,i} I_i \tag{2.20}$$

Where Z_{ii} and Z_{ij} are elements of the submatrix Z_{LL} which is obtained from (2.2) as:

$$Z_{LL} = \left(Y_{LL} - Y_{LT} {Y_{TT}}^{-1} Y_{TL} \right)^{-1} \tag{2.21}$$

Based on the Thevenin impedance theory, the maximum power transfer to a load bus is obtained when the load impedance equals the equivalent impedance of the rest of the network. (i.e. $|Z_{eq}| = |Z_L|$). Thus, a load impedance margin (i.e. voltage stability index) can be formulated as:

$$TLIM = \frac{|Z_L| - |Z_{eq}|}{|Z_L|} \tag{2.22}$$

Where TLIM denotes Thevenin-based Load Impedance Margin. The value of the TLIM ranges from 0 to 1, and TLIM $= 0$ represents the instability point where $|Z_{eq}|$=$|Z_L|$. The impedance $|Z_L|$ can be obtained by taking the ratio between the voltage and current phasors of the network bus.

The concept of TLIM can be understood using the r-x plane presented in Figure 2.3. As the load varies, the load impedance Z_L changes in the plane. When Z_L crosses the Thevenin circle

(with radius $|Z_{eq}|$), the voltage instability occurs. On the other side, the system equivalent impedance Z_{eq} also varies due to the changes in the system operating condition. This means that $|Z_{eq}|$ can be increased or decreased, resulting in changing the voltage stability margin.

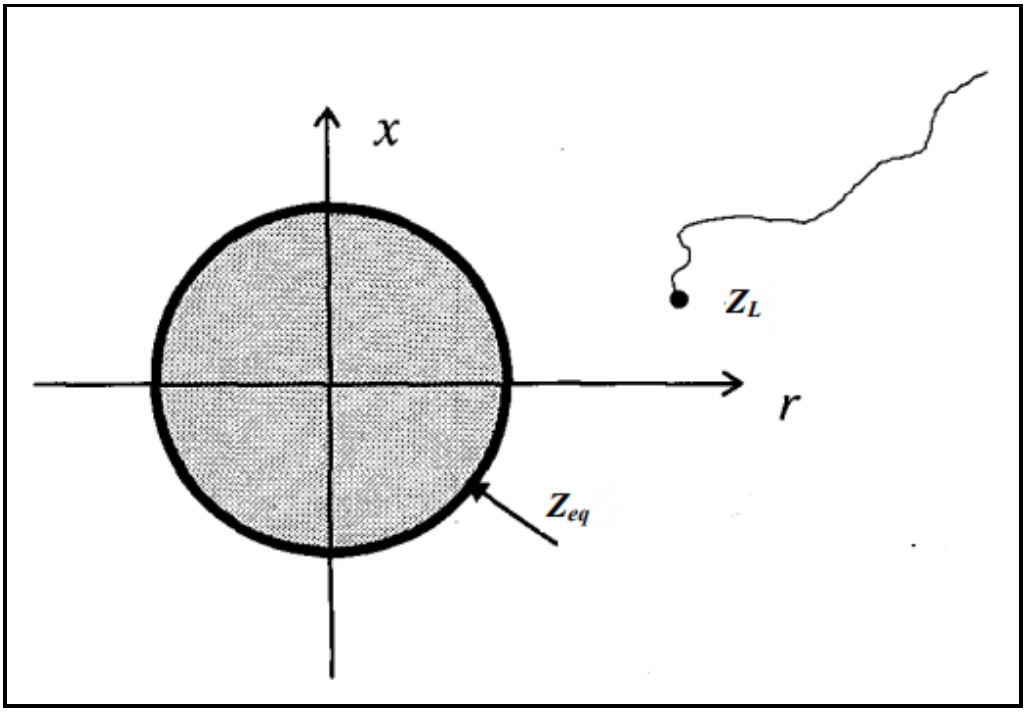

Figure 2.3 r-x Plane for static sensitivity analysis
Taken from Vu et al. (1999)

2.6 Impedance sensitivity analysis

It is concluded from Figure 2.1 that any change in load power consumption will change the load current and voltage. This will result in an increase or decrease in the load impedance (i.e. ΔZ_L). Similarly, any change in the current or voltage of other load buses will result in an increment or decrement in the equivalent impedance (i.e. ΔZ_{eq}) seen by that load bus. This can definitely change the TLIM of the system. To assess the impedance changes, an impedance sensitivity analysis is proposed in chapter 5 for voltage stability control in distribution networks.

Since the impedances $Z_L$and Z_{eq} referred to any load bus i can be written as:

$$Z_{L,i} = f(V_i, I_i) \tag{2.23a}$$

$$Z_{eq} = g(I_i, I_j, Z_{ij}) \tag{2.23b}$$

The impedance sensitivities with respect to control variable u_x can be expressed as:

$$\frac{dZ_{L,i}}{du_x} = f'\left(V_i, I_i, \frac{dV_i}{du_x}\right) \tag{2.24a}$$

$$\frac{dZ_{eq,i}}{du_x} = g'\left(V_i, I_i, V_j, I_j, Z_{ij}, \frac{dV_i}{du_x}, \frac{dV_j}{du_x}\right) \tag{2.24b}$$

It is worth noting that the impedance sensitivities depend on the voltage sensitivity analysis (i.e. $\frac{dV_i}{du_x}$). The voltage sensitivity is already mentioned in section 2.3. By obtaining the sensitivities $dZ_{L,i}/du_x$ and $dZ_{eq,i}/du_x$, we can evaluate the change in the impedances referred to bus i due to control variable u_x as:

$$\Delta Z_{L,i} = \frac{dZ_{L,i}}{du_x}\,\Delta u_x \tag{2.25a}$$

$$\Delta Z_{eq,i} = \frac{dZ_{eq,i}}{du_x}\,\Delta u_x \tag{2.25b}$$

Whrere Δu_x represents the change in the control variable u_x. The change in $TLIM$ can also be evaluated as*:*

$$\begin{aligned} \Delta TLIM_i &= \frac{\left|\Delta Z_{L,i}\right| - \left|\Delta Z_{eq,i}\right|}{\left|\Delta Z_{L,i}\right|} \\ &= \frac{\left|\frac{dZ_{L,i}}{du_x}\,\Delta u_x\right| - \left|\frac{dZ_{eq,i}}{du_x}\,\Delta u_x\right|}{\left|\frac{dZ_{L,i}}{du_x}\,\Delta u_x\right|} \end{aligned} \tag{2.26}$$

2.7 Multi-step optimization problem

As mentioned in chapter 1, most of the optimization-based methods for voltage and T/D power exchange control have been formulated as single-step optimization problems. Such formulations normally depend on sensitivity analysis. However, the sensitivity analysis cannot reflect the exact behavior of the system. The sensitivity coefficients suffer from the inaccuracy due to the assumptions associated with load modeling. Indeed, the response of network loads to voltage is still not well-known. Moreover, single-step optimization problems cannot show a smooth response to reach the target point. Besides, the measurement noises can also affect the control (Valverde & Cutsem, 2013).

To avoid the aforementioned problems, the optimization-based control methods presented in this thesis are formulated as multi-step optimization problems. They are based on MPC to optimally dispatch the control variables while satisfying the security constraints. The MPC-based multi-step optimization problem finds a sequence of control actions in Nc steps and predicts the response of these actions in Np steps (Zhang et al., 2018), (Glavic et al. 2011). Sensitivity analysis is used through the multi-step optimization problems to assess the performance of the system over a future interval of N_P.

At discrete time, the controller determines the optimal changes of the control variables u ,at instants k, $k+1$,…, $+N_C-1$ with the objective of progressively bringing the calculated or monitored voltages inside the desired interval (Valverde & Cutsem, 2013). According to the principle of MPC, only the first control action Δu_k of the sequence is applied at time k. where Δu_k is a set of the control variables. At the next time step, the whole control sequence is recomputed and again only the first step is applied (Maciejowski, 2002). This receding-horizon scheme allows compensating for model inaccuracies and measurement noise (Valverde & Cutsem, 2013).

At time k, a standard Quadratic Programming problem can be formulated as:

$$\sum_{k=0}^{N_c-1} \| \Delta E(t+k) \|_G^2 \tag{2.27}$$

s.t

$$V^{min} \leq V(t+k) \leq V^{max}$$

$$V(t+k) = V(t+k-1) + \frac{\partial |V|}{\partial u} \Delta u(t+k)$$

$$h^{min} \leq h(t+k) \leq h^{max}$$

Where ΔE is the change in the target objective function (i.e. cost, voltage stability margin,…etc.). G is a diagonal weighting matrix to distinguish between the control variables. $V(t+k)$ is the predicted voltage magnitudes of network buses given the measurements (or calculation) at time instant t. $V(t+k-1)$ is the measured (or calculated) voltage magnitudes of network buses at time instant t and it was evaluated using voltage sensitivity analysis mentioned in section 2.2. $\frac{\partial |V|}{\partial u}$ is the sensitivity matrix of bus voltage magnitudes with respect to the control variables. V^{min} and V^{max} are the minimum and the maximum limits of network voltages. h is a set of the other system quantities. h^{min} and h^{max} are the minimum and the maximum limits of the other network quantities.

The MPC-based multi-step optimization method aims at progressively bringing DN voltages in a pre-specified range of values. This can be explained in Figure 2.4. At time k, the method uses an internal model to predict the performance of the system over a future prediction interval with Np discrete steps, and computes an optimal sequence of Nc control actions, where Nc ≤ Np (Maciejowski, 2002). The solid lines in Figure 2.4 show the constraints imposed on voltage to restore the voltage to acceptable value at the end of the prediction interval (Valverde et al., 2013).

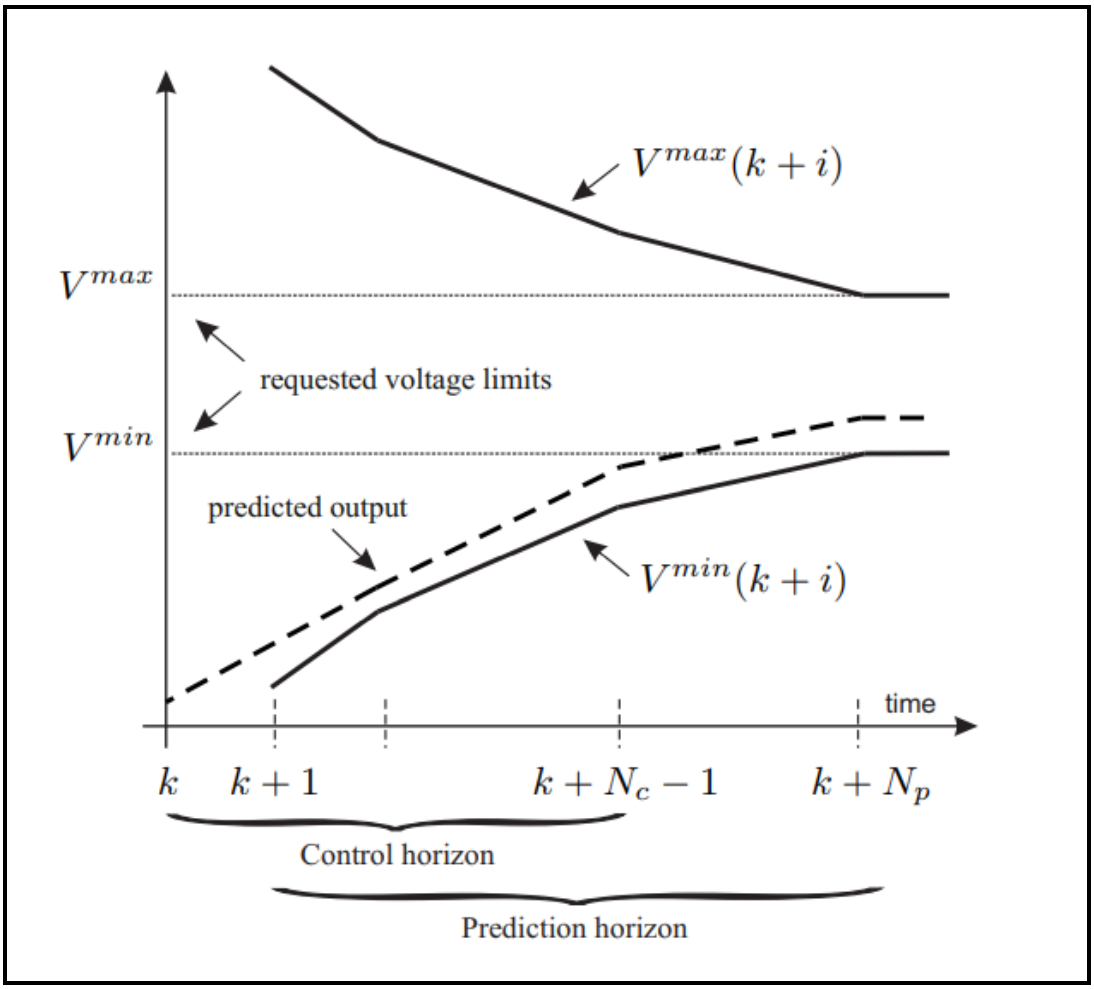

Figure 2.4 Concept of the MPC-based multi-optimizationproblem appliedfor CVC
Taken from Valverde & Cutsem (2013b)

In this thesis, multi-step optimization problem is used in chapter 5 for voltage stability control in distribution networks and in chapter 6 for power exchange control at T/D interface. For voltage stability control, the problem is formulated with an objective function mainly to maximize TLIM of pilot bus as:

$$min \sum_{k=0}^{N_C-1} \left\| \frac{|Z_{eq} + \Delta Z_{eq}(t+k)|}{|Z_L + \Delta Z_L(t+k)|} \right\|^2 \quad (2.28)$$

The load and the equivalent impedances are evaluated inside the optimization problem using the impedance sensitivity analysis mentioned in section 2.6.

For T/D power exchange, the problem is formulated with an objective function mainly to minimize the cost.

2.8 Linear power flow (LPF)

Nonlinear power flow can be replaced by LPF for fast solutions of different problems in smart grids, especially in the context of optimization problems. According to (marti et al., 2013), the power flow equations can be described as:

$$\begin{bmatrix} G & -B \\ B & G \end{bmatrix} \begin{bmatrix} V^{re} \\ V^{im} \end{bmatrix} = \begin{bmatrix} I_p^L \\ I_q^L \end{bmatrix} \tag{2.29}$$

For N number of network buses, *G* and *B* are submatrices (each of N×N dimension) of the real and the imaginary parts of the new admittance matrix, respectively. V^{re} and V^{im} are vectors (each of N×1 dimension) of the real and the imaginary parts of the node voltages, respectively. I_p^L and I_q^L are vectors (each of N×1 dimension) of the parts of the load currents.

The LPF is used in chapter 6 to formulate the T/D power exchange control problem as MIQCP, which can be solved efficiently to its global optimum solution. To achieve that, the active and reactive power drawn from the substation (i.e. $P_{ex}\ and\ Q_{ex}$) is formulated based on LPF as:

$$P_{ex} = V_{sub} \sum_{j=1}^{N} \left(G_{sub,j} V_j^{re} - B_{sub,j} V_j^{im} \right) \tag{2.30}$$

$$Q_{ex} = -V_{sub} \sum_{j=1}^{N} \left(G_{sub,j} V_j^{im} + B_{sub,j} V_j^{re} \right) \tag{2.31}$$

Where *sub* denotes substation. The expressions illustrated in (2.30) and (2.31) can be used as constraints for the optimization problem of T/D power exchange.

2.9 Top-down approach and Bottom-up approach

Top-down and bottom-up are both strategies of data treatment and knowledge organizing used in chapter 4 to identify a group of control variables to simultaneously correct the voltages in active distribution networks. According to Top-down approach, the main problem is divided into many smaller subproblems to easily understand it. Each subproblem is separately analyzed to solve the global problem. In contrast, the bottom-up method works in an inverse manner for top-down method. The bottom-up method defines a set of rules for the individual performances and the interactions and then are combined into the entire problem. Figure 2.5 represents the concept of the two approaches. Since the bottom-up approach implemented on the basis of the concept of the information hiding, it can omit the redundancies in the results obtained via Top-down method. A comparison between Top-down approach and Bottom-up approach is described in Table 2.1.

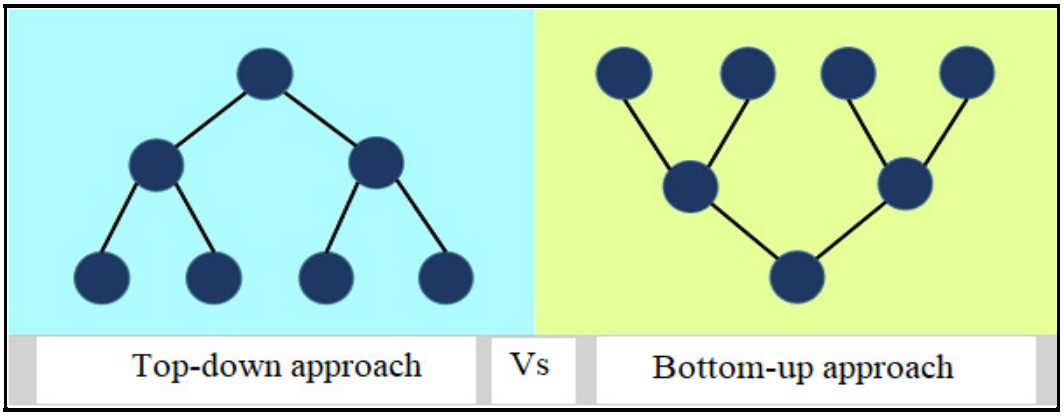

Figure 2.5 Top-down approach Vs Bottom-up approach

Table 2.1 A comparison between Top-down approach and Bottom-up approach

Issue	Top-down	Bottom-up
Basic	Breaks the massive problem into smaller subproblems.	Solves the fundamental low-level problem and integrates them into a larger one.
Process	Submodules are solitarily analyzed.	Examine what data is to be encapsulated, and implies the concept of information hiding.
Communication	Not required in the top-down approach.	May need some communication
Redundancy	Contain redundant information.	Redundancy can be eliminated.
Application	Documentation	Testing

In this thesis, the two approaches have been used for identifying the global group of controls for voltage control in active DNs. The top-down approach uses aggregate control to obtain the global group, which is then allocated to individual control variables on the basis of their ranking in correction index (CI) index. The bottom-up approach employs individual control variables to test the voltage estimation process.

2.10 Distribution management system

Distribution Management System (DMS) is a group of applications (or devices) designed to help the control room and network operators with the monitoring and control DNs. This could increase the system reliability, especially in terms of eliminating outages and maintaining acceptable frequency and voltages. DMS can support various functions for DNs. In the context of this work, DMS can easily identify the network or components. In other word, it can capture the system operating state and structure (i.e. radial or meshed mode). Besides, it can perform load flow analysis and Volt-VAR control of the network.

The work in this thesis depends on the feature of the use of DMS for online voltage and T/D power exchange control. The DMS is assumed to be a substation centered system. The softwares of control methods can be implemented with the aid of the advanced DMS for online voltage control (NR Electric Corporation, 2012), (Uluski,2011), (ABB Pvt, 2012). The hardware modules for other functions can be also embedded in the DMS. The control methods normally use pseudo measurements of loads and DG power generations, and the updated topology data of the system as inputs. A general overview of the DMS used for this work can be understood in Figure 2.6.

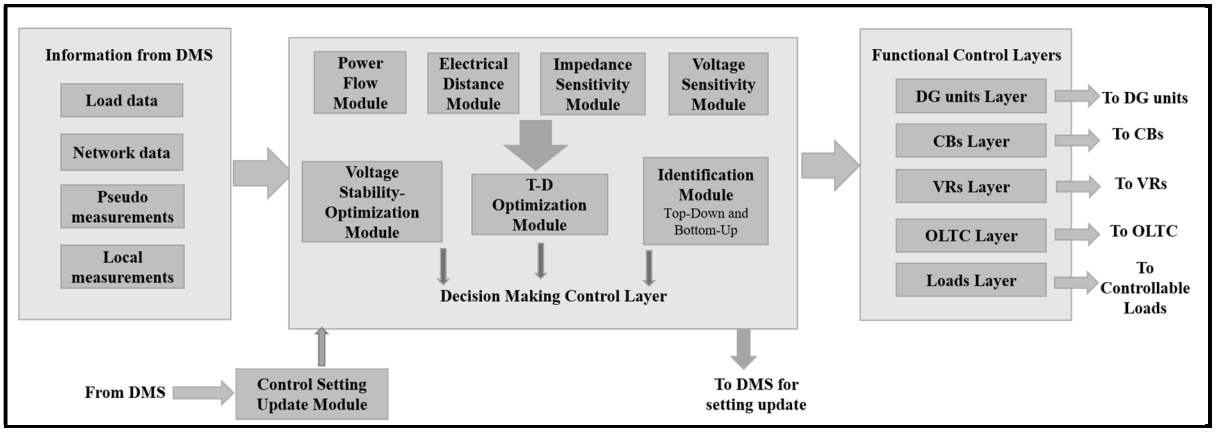

Figure 2.6 General overview of DMS used in this work

The figure shows the DMS contains power flow module, electric distance module, impedance sensitivity module, voltage sensitivity module, voltage stability-based optimization module, T/D optimization module, identification control module and control setting update module. Each module is used for a specific function. The power flow module is for obtaining the network voltages. The electric distance module is for obtaining the electrical distances between DG units and network nodes. The impedance sensitivity module and voltage sensitivity module are for obtaining the impedance and voltage sensitivities, respectively. The voltage stability-based optimization module is for maximizing the voltage stability margin in DNs while fulfilling a set of system constraints. T/D optimization module is for power exchange control at T/D interface. The identification control module is for selecting a global group of controls for CVR in DNs. The control setting update module is for updating the control parameters. A decision making control layer with separate functional control layers for DG units, CBs, VRs,

OLTC, and controllable loads can also be included for enacting the control devices according to the information provided by the decision making control layer. Operation of DNs by involving reactive power capabilities of DG units is explained in (Zou et al., 2011). To transmit the real-time information about the status of control variables to DMS modules, the control panels of the control variables are proposed to be equipped with Supervisory Control and Data Acquisition (SCADA) facilities (Ranamuka et al., 2016).

CHAPTER 3

NEW VOLTAGE SENSITIVITY ANALYSIS FOR SMART DISTRIBUTION GRIDS USING ANALYTICAL DERIVATION: ABCD MODEL

Khaled Alzaareer[1], Maarouf Saad[1], Hasan Mehrjerdi[2], Dalal Asber[3] and Serge Lefebvre[3]

[1] Département of Electrical Engineering, École de Technologie Supérieure, 1100 Notre-Dame Ouest, Montréal, Québec, Canada H3C 1K3
[2] Department of Electrical Engineering, Qatar University, University Street, Doha, Qatar 2713
[3] Power Systems and Mathematics, Research Institute of Hydro-Quebec 1740 Boul Lionel-Boulet, Varennes, Québec, Canada J3X 1S1

Paper submitted to *International Journal of Electrical Power & Energy Systems*, September 2020

Abstract

Sensitivity Analysis plays a significant role in voltage prediction and control of power networks. However, the classical sensitivity methods require significant computation time. As active distribution networks require real-time implementation for voltage control, reducing the computation time becomes a necessary task for network operators, especially in the context of optimization techniques. In this work, a new and fast voltage sensitivity analysis method is developed via the derivative of the nodal quantities (power, current and voltage) with respect to power injections. The proposed method mainly depends on the construction of ABCD matrix. The values of the matrix elements remain the same regardless of the bus on which the power is injected. Thus, it has a high potential to be implemented in online applications. To make a complete separation between the sensitivities to active and the sensitivities to reactive power injections, the analytical formulations are expressed in Cartesian coordinates. A radial distribution network including several DG units are used to verify and assess the proposed sensitivity method under different scenarios.

Keywords: Sensitivity Analysis; Voltage Control; Smart Power Networks; Distributed Generation, Jacobian Matrix; Cartesian Coordinates.

3.1 Introduction

Future Power networks will meet new challenges in voltage control due to the high penetration levels of Distributed Generation (DG) units (Walling et al., 2008). DG units can be actively involved in power systems for voltage regulation (Ochoa et al., 2009). Voltage control techniques are mainly based on the relation between the network voltages and control variables (i.e. power injections). The sensitivity analysis is usually used to find the voltage sensitivity coefficients with respect to nodal reactive and real power injections. These sensitivities can be actively used to manage control variables to solve voltage problems in an accurate way. Many approaches have been proposed in the literature to compute these sensitivities.

One of the well-known approaches is based on the Jacobian matrix (Borghetti et al., 2010), (Zhou et al., 2007). This approach is a classical method and depends on the solving a Newton Raphson power flow (Peschon et al., 1968). The voltage sensitivities are found by taking the inverse of J at one operating condition. However, the sensitivity coefficients have to be updated with any change in system state (e.g. changes of demand, generation, topology, and/or network parameters). This requires performing new Newton Raphson-based power flow calculations and, therefore, more computation time is required. Besides, the convergence may not be obtained by this method. Such methods developed for transmission load flow studies are not suitable for distribution networks due to poor convergence (Kersting, 2012). This is due to the radial structure and the high R/X ratio of distribution networks. Thus, these issues may add a new challenge for real-time voltage control. Although this kind of sensitivity analysis appears in recent studies for real-time applications such as voltage control (Alzaareer et al., 2020) and voltage stability issues (Kamel et al., 2017), the analysis is done offline and only at normal operating conditions.

Many other sensitivity methods have been discussed in the literature. An approach based on the Gauss-Seidel method of load flow is developed (Zhou et al., 2008). The approach depends

on the impedance matrix of the network and uses iteration process with a fixed number of iterations. Therefore, the accuracy of this method is low. An approach in which the network impedance matrix was used with the constant-current model of loads to develop a sensitivity approach (Khatod et al., 2006). However, this approach depends on the approximated representation of the network lines. An approach starting from branch currents is used for sensitivity analysis (Conti et al., 2010). This method requires a base load flow solution. Other methods based on the use of the so-called adjoint network are also proposed (Gurram et al., 1999), (Ferreira et al., 1990), (Bandler et al., 1980), (Bandler et al., 1982). Another approach based on the Perturb-And-Observe (P &O) Power Flow is proposed (Sansawatt et al., 2012). It considers the current state of the network and two power flows with a small change in the active (or reactive) power at the interested bus. An approach based on historical data is also presented (Weckx et al., 2014). A direct voltage sensitivity analysis method is developed which is based on the topological structure of the network and independent of the network operating points (Zad et al., 2015). However, these works suffer from inaccuracy and/or low-speed calculations.

As power systems continue in hosting large penetration levels of DG units, the need for online voltage control approaches is advanced. Sensitivity analysis represents the main role in voltage prediction and control. However, most of the common sensitivity techniques may not meet the requirements of future distribution networks to continuously update the sensitivities. The convergence problems and the remarkable calculation time associated with the common sensitivity analysis methods add new challenges for online applications, especially in the context of optimization problems and practical systems. In this regard, this work aims to develop a new and fast approach for voltage sensitivity analysis in power systems. The sensitivities are obtained via the direct derivative of nodal quantities (power, voltages, and currents) with respect to active and reactive power injections. The proposed method, namely ABCD model, mainly depends on the construction of ABCD matrix (refer to equation (3.25)). ABCD elements represent coefficients for the partial derivatives of node voltages (in Cartesian form). Their values remain constant regardless of the bus on which the power is injected.

The method developed in this work is oriented for online applications in smart grids. The problem is formulated such that the sensitivities can be directly obtained using the final expression (refer to equation (3.24)). The final expression illustrated in (3.24) can be considered to be a general formula for sensitivity analysis in distribution networks. The method is also flexible, such that it is not limited to a particular type of network or governed by a particular power flow method. The method can also be extended to include PV buses effect and different types of control variables (i.e. load tap changers). The ABCD model can be used as an alternative technique for the classical ones but with an extra advantage of fast computations.

The characteristics associated with ABCD method make the proposed method unique. These significant characteristics are: a) ABCD matrix is constant regardless of the node on which the power is injected, b) the expressions are in Cartesian coordinates for fast calculations and c) the complete separation between the sensitivities to active and the sensitivities to reactive power injections.

The features of the ABCD method can be summarized as:

- It depends on sparse submatrices, which can also speed up the computation.
- It is an accurate method such that the errors in the sensitivities or in the predicted voltages are very small.
- It does not require to update ABCD matrix with changing the bus on which the power is injected. This will also reduce the computation time.
- It can account for any change in the demand, generation, or network parameters.
- It is strongly related to the parts of system admittance bus. Thus, it can take into accounts the structural changes in the networks.
- It completely separates between the sensitivities to active and the sensitivities to reactive power injections.
- It can be extended to compute the sensitivities with respect to different types of control variables.
- It is suitable for any network (transmission or distribution, radial or meshed networks).

The key contributions of this work are:

5. Development of a new and fast approach for voltage sensitivity analysis of power systems via the direct derivative of the real and imaginary parts of the nodal quantities with respect to power injections, which to the best to our knowledge, is not done in literature.
6. Construction of ABCD matrix, which the proposed method depends on, and derivation of one mathematical expression to find the sensitivities with respect to any power injection. The value of ABCD matrix elements of a particular system remains the same regardless of the bus on which the power is injected.
7. The complete separation between the sensitivities to active and the sensitivities to reactive power injections.
8. Validation of the fast computation of the proposed method and its applicability in online voltage control.

The remainder of this work is organized as follows. Section II derives the mathematical development for nodal power injections in Cartesian coordinates. Section III presents the proposed sensitivity analysis method. Simulation results are presented in section IV. Section V provides the conclusions.

3.2 Mathematical model in Cartesian coordinates formula for nodal power injections

This section aims to find the mathematical relation for the network states and parameters in Cartesian coordinates.

3.2.1 Nodal current injection in Cartesian coordinates

The nodal bus currents I can be written in terms of nodal voltages V and system admittance Y as:

$$\begin{bmatrix} I_1 \\ \vdots \\ I_i \\ \vdots \\ I_N \end{bmatrix} = \begin{bmatrix} Y_{11} \dots Y_{1i} \dots Y_{1N} \\ \vdots \quad \vdots \quad \vdots \\ Y_{i1} \dots Y_{ii} \dots Y_{iN} \\ \vdots \quad \vdots \quad \vdots \\ Y_{N1} \dots Y_{Ni} \dots Y_{NN} \end{bmatrix} \begin{bmatrix} V_1 \\ \vdots \\ V_i \\ \vdots \\ V_N \end{bmatrix} \tag{3.1}$$

Where N denotes the number of system nodes. The element Y_{ij} can be written as $G_{ij} + jB_{ij}$, where G and B denote the conductance and susceptance, respectively. Similarly, the voltage V_j can be written as $V_{j,r} + j\, V_{j,im}$, where $V_{j,r}\ and\ V_{j,im}$ are the real and the imaginary parts, respectively. Accordingly, the current I_i can be expressed as:

$$I_i = \sum_{j\,\epsilon\,N} Y_{ij} V_j$$

$$= \sum_{j\,\epsilon\,N} \left(\left(G_{ij} V_{j,r} - B_{ij}\, V_{j,im} \right) + j \left(G_{ij}\, V_{j,im} + B_{ij} V_{j,r} \right) \right) \tag{3.2}$$

Thus, the real and the imaginary parts of the current I_i (i.e. $I_{i,r}\ and\ I_{i,im}$, respectively) can be obtained as:

$$I_{i,r} = \sum_{j\,\epsilon\,N} \left(G_{ij} V_{j,r} - B_{ij}\, V_{j,im} \right) \tag{3.3}$$

$$I_{i,im} = \sum_{j\,\epsilon\,N} \left(G_{ij}\, V_{j,im} + B_{ij} V_{j,r} \right) \tag{3.4}$$

3.2.2 Nodal power injection in Cartesian coordinates

The complex power at node i (S_i) can be written in terms of real and reactive power (i.e. $P_{\mathrm{i}}\ and\ Q_{\mathrm{i}}$, respectively) as:

$$\begin{aligned} S_i &= V_i\, I_i^* \\ &= (V_{i,r} + j\, V_{i,im})(I_{i,r} - j\, I_{i,im}) \\ &= (V_{i,r}I_{i,r} + V_{i,im}I_{i,im}) + j(V_{i,im}I_{i,r} - V_{i,r}\, I_{i,im}) \end{aligned} \tag{3.5}$$

Thus, we obtain:

$$P_i = (V_{i,r}I_{i,r} + V_{i,im}I_{i,im}) \tag{3.6}$$

$$Q_i = \left(V_{i,im}I_{i,r} - V_{i,r}\, I_{i,im}\right) \tag{3.7}$$

By substituting (3.3) and (3.4) into (3.6) and (3.7), we obtain:

$$P_i = V_{i,r} \sum_{j\,\epsilon\,N} \left(G_{ij}V_{j,r} - B_{ij}\, V_{j,im}\right) + V_{i,im} \sum_{j\,\epsilon\,N} \left(G_{ij}\, V_{j,im} + B_{ij}V_{j,r}\right) \tag{3.8}$$

$$Q_i = V_{i,im} \sum_{\mathrm{j}\,\epsilon\,N} \left(G_{ij}V_{j,r} - B_{ij}\, V_{j,im}\right) - V_{i,r} \sum_{\mathrm{j}\,\epsilon\,N} \left(G_{ij}\, V_{j,im} + B_{ij}V_{j,r}\right) \tag{3.9}$$

It is clear from (3.8) and (3.9) that the real and reactive power are expressed in terms of real and imaginary parts of the network admittance and network voltages.

3.3 Proposed sensitivity analysis method

3.3.1 Change in power injections in Cartesian coordinates

To explain the concept behind the proposed sensitivity method, the simple system presented in Figure 3.1 is considered. V and I denote for load voltage and current, respectively. P+jQ denotes for load power. It is worth noting that the developed expressions in this section have an assumption of constant power model for load and DG units.

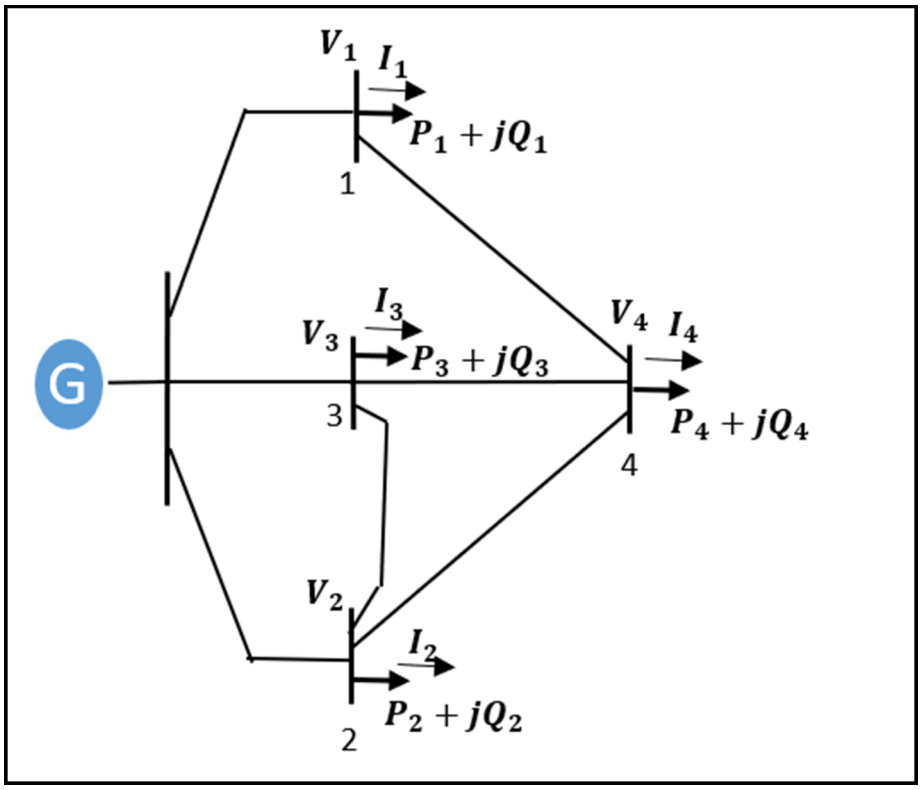

Figure 3.1 Simple power system

Any increment in the power injection (ΔP or ΔQ) at any node "x" will increase the voltage at node "i" by $\Delta V_i = \Delta V_{r,i} + j\Delta V_{im,i}$. The new voltage of node $i\epsilon\ M$ can be then expressed as $V_i + \Delta V_i = (V_{r,i} + \Delta V_{r,i}) + j(V_{im,i} + \Delta V_{im,i})$. Similarly, the load current will also be varied by $\Delta I_i = \Delta I_{r,i} + j\Delta I_{im,i}$, resulting in an expression for the new current as $I_i + \Delta I_i = (I_{r,i} + \Delta I_{r,i}) + j(I_{im,i} + \Delta I_{im,i})$. To find an expression for the voltage sensitivity to real power injection, let the load of node "i" at the 1st instant be $S_{\mathrm{i},1} = P_{\mathrm{i},1} + jQ_i$ and the load at the 2nd instant be $S_{\mathrm{i},2} = P_{\mathrm{i},2} + jQ_i$. According to (3.6), the real power at both instants can be written as:

$$P_{\mathrm{i},1} = V_{r,i}I_{r,i} + V_{im,i}I_{im,i}$$

$$P_{\mathrm{I},2} = (V_{r,i} + \Delta V_{r,i})(I_{r,i} + \Delta I_{r,i}) + (V_{im,i} + \Delta V_{im,i})(I_{im,i} + \Delta I_{im,i})$$

The change in the real power $\Delta P_i = P_{\mathrm{i},2} - P_{\mathrm{i},1}$ is written as:

$$\begin{aligned}\Delta P_i \;=\; & I_{r,i}\Delta V_{r,i} + V_{r,i}\Delta I_{r,i} + \Delta V_{r,i}\Delta I_{r,i} \\ & + I_{im,i}\Delta V_{im,i} + \; V_{im,i}\Delta I_{im,i} + \Delta V_{im,i}\Delta I_{im,i}\end{aligned} \tag{3.10}$$

It is worth mentioning that the smaller the value of ΔP_i (implying terms of ΔV_i &ΔI_i are also small), the closer the two operating points are the better the estimation of the sensitivity coefficients. The terms $\Delta V_{r,i}\Delta I_{r,i}$ and $\Delta V_{im,i}\Delta I_{im,i}$ of (3.10) represents very small values and therefore can be ignored. Accordingly, (3.10) can be written as:

$$\Delta P_i = I_{r,i}\Delta V_{r,i} + V_{r,i}\Delta I_{r,i} + I_{im,i}\Delta V_{im,i} + \; V_{im,i}\Delta I_{im,i} \tag{3.11}$$

To find an expression for the voltage sensitivity to reactive power injection, let the load at node "i" at the 1st instant be $S_{\mathrm{i},1} = \mathrm{P} + jQ_{\mathrm{i},1}$ and the load at the 2nd instant be $S_{\mathrm{i},2} = \mathrm{P} + jQ_{\mathrm{i},2}$. According to (3.7), the reactive power at both instants can be expressed as:

$$Q_{\mathrm{i},1} = V_{im,i}I_{r,i} - V_{r,i}\, I_{im,i}$$
$$Q_{\mathrm{i},2} = (V_{im,i} + \Delta V_{im,i})(I_{r,i} + \Delta I_{r,i}) - (V_{r,i} + \Delta V_{r,i})(I_{im,i} + \Delta I_{im,i})$$

The reactive power change $\Delta Q_i = Q_{\mathrm{i},2} - Q_{\mathrm{i},1}$ can be written as:

$$\begin{aligned}\Delta Q_i = V_{im,i}\Delta I_{r,i} + \; & \Delta V_{im,i}I_{r,i} + \Delta V_{im,i}\Delta I_{r,i} \\ & -V_{r,i}\Delta I_{im,i} - \; \Delta V_{r,i}I_{im,i} - \Delta V_{r,i}\Delta I_{im,i}\end{aligned} \tag{3.12}$$

By ignoring the terms $\Delta V_{im,i}\Delta I_{r,i}$ and $\Delta V_{r,i}\Delta I_{im,i}$, (3.12) becomes:

$$\Delta Q_i = -\, I_{im,i}\Delta V_{r,i} + V_{im,i}\Delta I_{r,i} + I_{r,i}\Delta V_{im,i} - V_{r,i}\Delta I_{im,i} \tag{3.13}$$

It is clear from (3.11) and (3.13) that the real and reactive power changes are expressed in terms of real and imaginary parts of the network voltages and currents.

3.3.2 Analytical derivation of power injections

In this section, mathematical expressions that link network voltages to node power injections are derived.

The expressions presented in (3.11) and (3.13) represent the change in active or reactive power injection in Cartesian coordinates. Dividing (3.11) by amount of real power injection at bus "x" (ΔP_x) yields:

$$\frac{\Delta P_i}{\Delta P_x} = I_{r,i}\frac{\Delta V_{r,i}}{\Delta P_x} + V_{r,i}\frac{\Delta I_{r,i}}{\Delta P_x} + I_{im,i}\frac{\Delta V_{im,i}}{\Delta P_x} + V_{im,i}\frac{\Delta I_{im,i}}{\Delta P_x} \tag{3.14}$$

By taking the limit of the expression in (3.14) as $\Delta P_x \rightarrow 0$, (3.14) becomes:

$$\frac{\partial P_i}{\partial P_x} = I_{i,r}\frac{\partial V_{i,r}}{\partial P_x} + V_{i,r}\frac{\partial I_{i,r}}{\partial P_x} + I_{i,im}\frac{\partial V_{i,im}}{\partial P_x} + V_{i,im}\frac{\partial I_{i,im}}{\partial P_x} \tag{3.15}$$

Similarly, dividing (3.13) by an amount of ΔQ_x and taking the limit of the expression as $\Delta Q_x \rightarrow 0$, we obtain:

$$\frac{\partial Q_i}{\partial Q_x} = -I_{i,im}\frac{\partial V_{i,r}}{\partial Q_x} + V_{i,im}\frac{\partial I_{i,r}}{\partial Q_x} + I_{i,r}\frac{\partial V_{i,im}}{\partial Q_x} - V_{i,r}\frac{\partial I_{i,im}}{\partial Q_x} \tag{3.16}$$

Where $\frac{\partial P_i}{\partial P_x}$ and $\frac{\partial Q_i}{\partial Q_x}$ represent the partial derivatives of the real and reactive power of node "i" with respect to active and reactive power injected into node x, respectively. $\frac{\partial V_{i,r}}{\partial P_x}$, $\frac{\partial V_{i,im}}{\partial P_x}$, $\frac{\partial I_{i,r}}{\partial P_x}$, $\frac{\partial I_{i,im}}{\partial P_x}$ and $\frac{\partial V_{i,r}}{\partial Q_x}$, $\frac{\partial V_{i,im}}{\partial Q_x}$, $\frac{\partial I_{i,r}}{\partial Q_x}$, $\frac{\partial I_{i,im}}{\partial Q_x}$ represent the partial derivatives of the voltage and current (real and imaginary parts) of bus "i" with respect to active and reactive power injected into

node “x”, respectively. The partial derivatives $\frac{\partial I_{i,r}}{\partial P_x}, \frac{\partial I_{i,im}}{\partial P_x}, \frac{\partial I_{i,r}}{\partial Q_x}$ and $\frac{\partial I_{i,im}}{\partial Q_x}$ can be obtained by taking the derivation of (3.3) and (3.4) with respect to active or reactive power injection as follows:

$$\frac{\partial I_{i,r}}{\partial P_x} = \sum_{\mathrm{j}\,\epsilon\, N} \left(G_{ij} \frac{\partial V_{j,r}}{\partial P_x} - B_{ij} \frac{\partial V_{j,im}}{\partial P_x} \right) \qquad i\epsilon\, M \tag{3.17a}$$

$$\frac{\partial I_{i,r}}{\partial Q_x} = \sum_{\mathrm{j}\,\epsilon\, N} \left(G_{ij} \frac{\partial V_{j,r}}{\partial Q_x} - B_{ij}\, \frac{\partial V_{j,im}}{\partial Q_x} \right) \qquad i\epsilon\, M \tag{3.17b}$$

$$\frac{\partial I_{i,im}}{\partial P_x} = \sum_{\mathrm{j}\,\epsilon\, N} \left(G_{ij}\, \frac{\partial V_{j,im}}{\partial P_x} + B_{ij} \frac{\partial V_{j,r}}{\partial P_x} \right) \qquad i\epsilon\, M \tag{3.17c}$$

$$\frac{\partial I_{i,im}}{\partial Q_x} = \sum_{\mathrm{j}\,\epsilon\, N} \left(G_{ij}\, \frac{\partial V_{j,im}}{\partial Q_x} + B_{ij} \frac{\partial V_{j,r}}{\partial Q_x} \right) \qquad i\epsilon\, M \tag{3.17d}$$

Where $\frac{\partial V_{j,r}}{\partial P_x}, \frac{\partial V_{j,r}}{\partial Q_x}, \frac{\partial V_{j,im}}{\partial P_x}$ and $\frac{\partial V_{j,im}}{\partial Q_x}$ are partial derivations referred to the node j. M represents number of PQ buses. By substituting (3.3), (3.4) and (3.17) into (3.15) and (3.16), we obtain:

$$\begin{aligned} \frac{\partial P_i}{\partial P_x} = & \sum_{j\,\epsilon\, M} \left(G_{ij} V_{i,r} \frac{\partial V_{j,r}}{\partial P_x} - B_{ij} V_{i,r}\, \frac{\partial V_{j,im}}{\partial P_x} \right) \\ & + \frac{\partial V_{i,r}}{\partial P_x} \sum_{j\,\epsilon\, N} \left(G_{ij} V_{j,r} - B_{ij}\, V_{j,im} \right) \\ & + \sum_{j\,\epsilon\, M} \left(G_{ij} V_{i,im} \frac{\partial V_{j,im}}{\partial P_x} + B_{ij} V_{i,im} \frac{\partial V_{j,r}}{\partial P_x} \right) \\ & + \frac{\partial V_{i,im}}{\partial P_x} \sum_{j\,\epsilon\, N} \left(G_{ij}\, V_{j,im} + B_{ij} V_{j,r} \right) \qquad i\epsilon\, M \end{aligned} \tag{3.18}$$

$$\frac{\partial Q_i}{\partial Q_x} = \sum_{j \in M} \left(G_{ij} V_{i,im} \frac{\partial V_{j,r}}{\partial Q_x} - B_{ij} V_{i,im} \frac{\partial V_{j,im}}{\partial Q_x} \right) + \frac{\partial V_{i,im}}{\partial Q_x} \sum_{j \in N} \left(G_{ij} V_{j,r} - B_{ij} V_{j,im} \right) - \sum_{j \in M} \left(G_{ij} V_{i,r} \frac{\partial V_{j,im}}{\partial Q_x} + B_{ij} V_{i,r} \frac{\partial V_{j,r}}{\partial Q_x} \right) - \frac{\partial V_{i,r}}{\partial Q_x} \sum_{j \in N} \left(G_{ij} V_{j,im} + B_{ij} V_{j,r} \right) \qquad i \in M \tag{3.19}$$

It is clear from (3.18) and (3.19) that right hand side is written in terms of the partial derivation of node voltages (real and imaginary parts) with respect to active or reactive power injected at node "x". For $i \in M$, (3.18) and (3.19) can be organized as:

$$\frac{\partial P_i}{\partial P_x} = \sum_{\substack{j \in M \\ i \neq j}} \left(G_{ij} V_{i,r} + B_{ij} V_{i,im} \right) \frac{\partial V_{j,r}}{\partial P_x} + \left(G_{ii} V_{i,r} + B_{ii} V_{i,im} + \sum_{j \in N} \left(G_{ij} V_{j,r} - B_{ij} V_{j,im} \right) \right) \frac{\partial V_{i,r}}{\partial P_x} + \sum_{\substack{j \in M \\ i \neq j}} \left(G_{ij} V_{i,im} - B_{ij} V_{i,r} \right) \frac{\partial V_{j,im}}{\partial P_x} + \left(G_{ii} V_{i,im} - B_{ii} V_{i,r} + \sum_{j \in N} \left(G_{ij} V_{j,im} + B_{ij} V_{j,r} \right) \right) \frac{\partial V_{i,im}}{\partial P_x} \tag{3.20}$$

$$\frac{\partial Q_i}{\partial Q_x} = \sum_{\substack{j \in M \\ i \neq j}} \left(G_{ij} V_{i,im} - B_{ij} V_{i,r}\right) \frac{\partial V_{j,r}}{\partial Q_x}$$
$$+ \left(G_{ii} V_{i,im} - B_{ii} V_{i,r} - \sum_{j \in N} \left(G_{ij} V_{j,im} + B_{ij} V_{j,r}\right) \right) \frac{\partial V_{i,r}}{\partial Q_x}$$
$$- \sum_{\substack{j \in M \\ i \neq j}} \left(G_{ij} V_{i,r} + B_{ij} V_{j,im}\right) \frac{\partial V_{j,im}}{\partial Q_x}$$
$$+ \left(-G_{ii} V_{i,r} - B_{ii} V_{i,im} + \sum_{j \in N} \left(G_{ij} V_{j,r} - B_{ij} V_{j,im}\right) \right) \frac{\partial V_{i,im}}{\partial Q_x} \qquad (3.21)$$

3.3.3 Build up the proposed model: ABCD matrix

To find the partial derivatives of node voltages (real and imaginary parts) with respect to active and reactive power injection at node "x", (3.20) and (3.21) are performed for each bus i ϵ M. In a matrix form, the system of equations can be organized as:

$$\underbrace{\begin{bmatrix} \overbrace{\begin{matrix} a_{11} & \cdots & a_{1i} & \cdots & a_{1M} \\ \vdots & & \vdots & & \vdots \\ a_{i1} & \cdots & a_{ii} & \cdots & a_{iM} \\ \vdots & & \vdots & & \vdots \\ a_{M1} & \cdots & a_{Mi} & \cdots & a_{MM} \end{matrix}}^{A} & \overbrace{\begin{matrix} b_{11} & \cdots & b_{1i} & \cdots & b_{1M} \\ \vdots & & \vdots & & \vdots \\ b_{i1} & \cdots & b_{ii} & \cdots & b_{iM} \\ \vdots & & \vdots & & \vdots \\ b_{M1} & \cdots & b_{Mi} & \cdots & b_{MM} \end{matrix}}^{B} \end{bmatrix}}_{R} \begin{bmatrix} \frac{\partial V_r}{\partial P_x} \\ \frac{\partial V_{im}}{\partial P_x} \end{bmatrix} = \begin{bmatrix} \frac{\partial P_1}{\partial P_x} \\ \vdots \\ \frac{\partial P_i}{\partial P_x} \\ \vdots \\ \frac{\partial P_M}{\partial P_x} \end{bmatrix} \qquad (3.22)$$

$$\underbrace{\begin{bmatrix} \overbrace{c_{11}..c_{1i}..c_{1M}}^{C} & \overbrace{d_{11}..d_{1i}..d_{1M}}^{D} \\ \vdots & \vdots \\ c_{i1}..c_{ii}..c_{iM} & d_{i1}..d_{ii}..d_{iM} \\ \vdots & \vdots \\ c_{M1}..c_{Mi}..c_{MM} & d_{M1}..d_{Mi}..d_{MM} \end{bmatrix}}_{T} \begin{bmatrix} \frac{\partial V_r}{\partial Q_x} \\ \frac{\partial V_{im}}{\partial Q_x} \end{bmatrix} = \begin{bmatrix} \frac{\partial Q_1}{\partial Q_x} \\ \vdots \\ \frac{\partial Q_i}{\partial Q_x} \\ \vdots \\ \frac{\partial Q_M}{\partial Q_x} \end{bmatrix} \quad (3.23)$$

Where $\frac{\partial V_r}{\partial P_x} = \left[\frac{\partial V_{1,r}}{\partial P_x} .. \frac{\partial V_{i,r}}{\partial P_x} .. \frac{\partial V_{M,r}}{\partial P_x}\right]^T$ and $\frac{\partial V_{im}}{\partial P_x} = \left[\frac{\partial V_{1,im}}{\partial P_x} .. \frac{\partial V_{i,im}}{\partial P_x} .. \frac{\partial V_{M,im}}{\partial P_x}\right]^T$ are sensitivity vectors of real and imaginary parts of PQ voltages with respect to active power injection at node "x", respectively. $\frac{\partial V_r}{\partial Q_x} = \left[\frac{\partial V_{1,r}}{\partial Q_x} .. \frac{\partial V_{i,r}}{\partial Q_x} .. \frac{\partial V_{M,r}}{\partial Q_x}\right]^T$ and $\frac{\partial V_{im}}{\partial Q_x} = \left[\frac{\partial V_{1,im}}{\partial Q_x} .. \frac{\partial V_{i,im}}{\partial Q_x} .. \frac{\partial V_{M,im}}{\partial Q_x}\right]^T$ are sensitivity vectors of real and imaginary parts of PQ voltages with respect to reactive power injection at node "x", respectively. "^{T}" denotes for transpose. From (3.22), we can see that the matrix R consists of two submatrices A and B. The elements of A represent the coefficients associated with the sensitivities $\frac{\partial V_r}{\partial P_x}$ while the elements of B represent the coefficients associated with the sensitivities $\frac{\partial V_{im}}{\partial P_x}$. Similarly, we can see from (3.23) that the matrix T consists of two submatrices C and D. The elements of C represent the coefficients associated with the sensitivities $\frac{\partial V_r}{\partial Q_x}$ while the elements of D represent the coefficients associated with the sensitivities $\frac{\partial V_{im}}{\partial Q_x}$. In a general form, (3.22) and (3.23) can be expressed as:

$$[A \quad B]\begin{bmatrix} \frac{\partial V_r}{\partial P_x} \\ \frac{\partial V_{im}}{\partial P_x} \end{bmatrix} = \left[\frac{\partial P}{\partial P_x}\right] \quad , [C \quad D]\begin{bmatrix} \frac{\partial V_r}{\partial Q_x} \\ \frac{\partial V_{im}}{\partial Q_x} \end{bmatrix} = \left[\frac{\partial Q}{\partial Q_x}\right] \quad (3.24)$$

Where $\frac{\partial P}{\partial P_x}$ and $\frac{\partial Q}{\partial Q_x}$ are sensitivity vectors of the active and reactive power of PQ nodes with respect to active and reactive power injection at node "x", respectively. The ijth element of the matrix can be found as (where both i and j ϵ M):

$$a_{ij} = \begin{cases} G_{ii}V_{i,r} + B_{ii}V_{i,im} + \sum_{j \in N} \left(G_{ij}V_{j,r} - B_{ij}\, V_{j,im}\right) & j = i \\ G_{ij}V_{i,r} + B_{ij}V_{i,im} & otherwise \end{cases} \quad (3.25a)$$

$$b_{ij} = \begin{cases} G_{ii}V_{i,im} - B_{ii}V_{i,r} + \sum_{j \in N} \left(G_{ij}\, V_{j,im} + B_{ij}V_{j,r}\right) & j = i \\ G_{ij}V_{i,im} - B_{ij}V_{i,r} & otherwise \end{cases} \quad (3.25b)$$

$$c_{ij} = \begin{cases} G_{ii}V_{i,im} - B_{ii}V_{i,r} - \sum_{j \in N} \left(G_{ij}\, V_{j,im} + B_{ij}V_{j,r}\right) & j = i \\ G_{ij}V_{i,im} - B_{ij}V_{i,r} & otherwise \end{cases} \quad (3.25c)$$

$$d_{ij} = \begin{cases} -G_{ii}V_{i,r} - B_{ii}V_{i,im} + \sum_{j \in N} \left(G_{ij}V_{j,r} - B_{ij}\, V_{j,im}\right) & j = i \\ -G_{ij}V_{i,r} - B_{ij}V_{i,im} & otherwise \end{cases} \quad (3.25d)$$

To obtain the voltages V_{re} and V_{im}, one may use the information gathered from SCADA and nodal measurements. Alternatively, the linear power flow method developed in Cartesian coordinates in (Martí et al., 2013) can be used as:

$$\begin{bmatrix} G & -B \\ B & G \end{bmatrix} \begin{bmatrix} V_{re} \\ V_{im} \end{bmatrix} = \begin{bmatrix} I_p \\ I_q \end{bmatrix}$$

Where $I_p$and I_q are vectors of the real and imaginary parts of load currents. V_{re} and V_{im} are vectors of network voltage parts. G and B are submatrices of a modified admittance matrix. These quantities and parameters are explained in detail in (Martí et al., 2013).

The power injection at a particular bus is independent of power injections of other buses. Therefore, the partial derivation $\frac{\partial P_i}{\partial P_x}$ and $\frac{\partial Q_i}{\partial Q_x}$ can be found as:

$$\frac{\partial P_i}{\partial P_x} = \frac{\partial Q_i}{\partial Q_x} = \begin{cases} 1 & i = x \\ 0 & otherwise \end{cases} \quad (3.26)$$

Similar system of equations presented in (3.24) can be used to find the partial derivatives with respect to other power injections (i.e. for power injections at node x ϵ N). Based on the expressions illustrated in (3.24-3.26), we can conclude the following points:

- A and B are developed to find the voltage sensitivities to active power injections while B and C are developed to find the voltage sensitivities to reactive power injections.
- The submatrices A, B, C and D are the same regardless of the node on which the active or reactive power is injected. The only change is the value of $\frac{\partial \mathrm{P_i}}{\partial \mathrm{P_x}}$ or $\frac{\partial \mathrm{Q_i}}{\partial \mathrm{Q_x}}$.
- It is clear that D=-A, and B=C for non-diagonal elements.
- The size of A, B, C , and D is M×M while the size of $\frac{\partial V_r}{\partial P_x}, \frac{\partial V_{im}}{\partial P_x} \frac{\partial V_r}{\partial Q_x}, \frac{\partial V_{im}}{\partial Q_x}, \frac{\partial P}{\partial P_x}$ and $\frac{\partial Q}{\partial Q_x}$ is M×1.

Once the partial derivations $\frac{\partial V_{i,r}}{\partial P_x}$, $\frac{\partial V_{i,im}}{\partial P_x}$ or $\frac{\partial V_{i,r}}{\partial Q_x}$, $\frac{\partial V_{i,im}}{\partial Q_x}$ are obtained, the voltage sensitivity coefficients can be easily computed. Since the voltage magnitude of bus "i" $|V_i|$ can be represented by $|V_i| = ({V_{i,r}}^2 + {V_{i,im}}^2)^{1/2}$, the voltage sensitivities of bus "i" to power injections at node "x" can be found as:

$$\frac{\partial |V_i|}{\partial P_x} = \frac{1}{|V_i|} \left(V_{i,r} \frac{\partial V_{i,r}}{\partial P_x} + V_{i,im} \frac{\partial V_{i,im}}{dP_x} \right) \quad (3.27a)$$

$$\frac{\partial |V_i|}{\partial Q_x} = \frac{1}{|V_i|} \left(V_{i,r} \frac{\partial V_{i,r}}{\partial Q_x} + V_{i,im} \frac{\partial V_{i,im}}{dQ_x} \right) \quad (3.27b)$$

3.3.4 Effect of PV buses

The PV buses can also be considered in the sensitivity analysis. When active or reactive power is injected at any node of the network, some system voltages may change. Consequently, reactive power injections will be required at PV buses (i.e. ΔQ_g) to keep constant voltages at those buses. Any increment in active or reactive power injection at bus "x" (i.e. Δu_x) will cause a change in the voltages of PV buses (i.e. ΔV_g). This can be represented as:

$$\frac{\partial |V_g|}{\partial u_x} \Delta u_x + \frac{\partial |V_g|}{\partial Q_g} \Delta Q_g = 0 \tag{3.28}$$

Where $\frac{\partial |V_g|}{\partial u_x}$ is the vector of PV bus sensitivities with respect to active or reactive power injection at bus "x". $\frac{\partial |V_g|}{\partial Q_g}$ is a matrix of PV bus sensitivities with respect to reactive power injection at these buses. ΔQ_g is the change vector of reactive power injections at PV buses. For any increment in active or reactive power injection at any bus, the change in the node voltage sensitivities (including impact of PV buses) can be expressed as:

$$\Delta |\mathrm{V}| = \frac{\partial |\mathrm{V}|}{\partial u_x} \Delta u_x + \frac{\partial |\mathrm{V}|}{\partial Q_g} \Delta Q_g \tag{3.29}$$

Where $|\mathrm{V}|$ is a vector of node voltage magnitudes. $\frac{\partial |\mathrm{V}|}{\partial u_x}$ is the vector of node voltage sensitivities with respect to active or reactive power injection at "x" node. $\frac{\partial |\mathrm{V}|}{\partial Q_g}$ is a matrix of the voltage sensitivities with respect to reactive power injection at PV buses. Dividing (3.29) by Δu_x and substituting $\frac{\Delta Q_g}{\Delta u_x}$ (equation (3.28)) into (3.29) we obtain:

$$\frac{\Delta |\mathrm{V}|}{\Delta u_x} = \frac{\partial |\mathrm{V}|}{\partial u_x} - \frac{\partial |\mathrm{V}|}{\partial Q_g} \left[\frac{\partial |V_g|}{\partial Q_g}\right]^{-1} \frac{\partial |V_g|}{\partial u_x} \tag{3.30}$$

From (3.30), it is clear that the $\frac{\Delta|V|}{\Delta u_x}$ depends on the voltage sensitivity calculation illustrated in (3.27). A flowchart of the proposed voltage sensitivity analysis is shown in Figure 3.2.

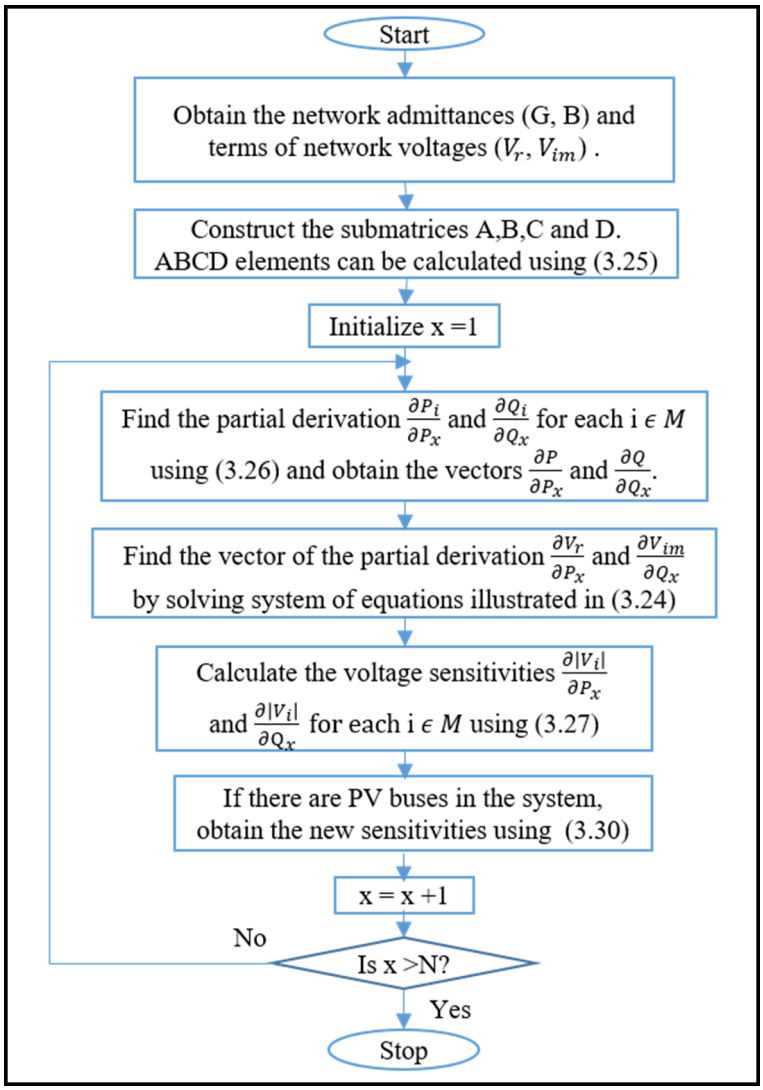

Figure 3.2 A flowchart of the proposed voltage sensitivity method

3.4 Simulation results

To validate the accuracy of the proposed sensitivity analysis method, 75-bus, 11 kV distribution system (Figure 3.3) is considered in this work. It is assumed that the network hosts 22 DG units (each with a rating of 3MVA). No output powers are generated by DG units unless

otherwise is mentioned. The system data and parameters can be found in (UKGDS, 2005). The study network and the proposed algorithm are implemented in MATLAB environment. To improve the readability of the figures, in this article, the first two digits of each bus number are omitted (i.e. 1175 will be 75).

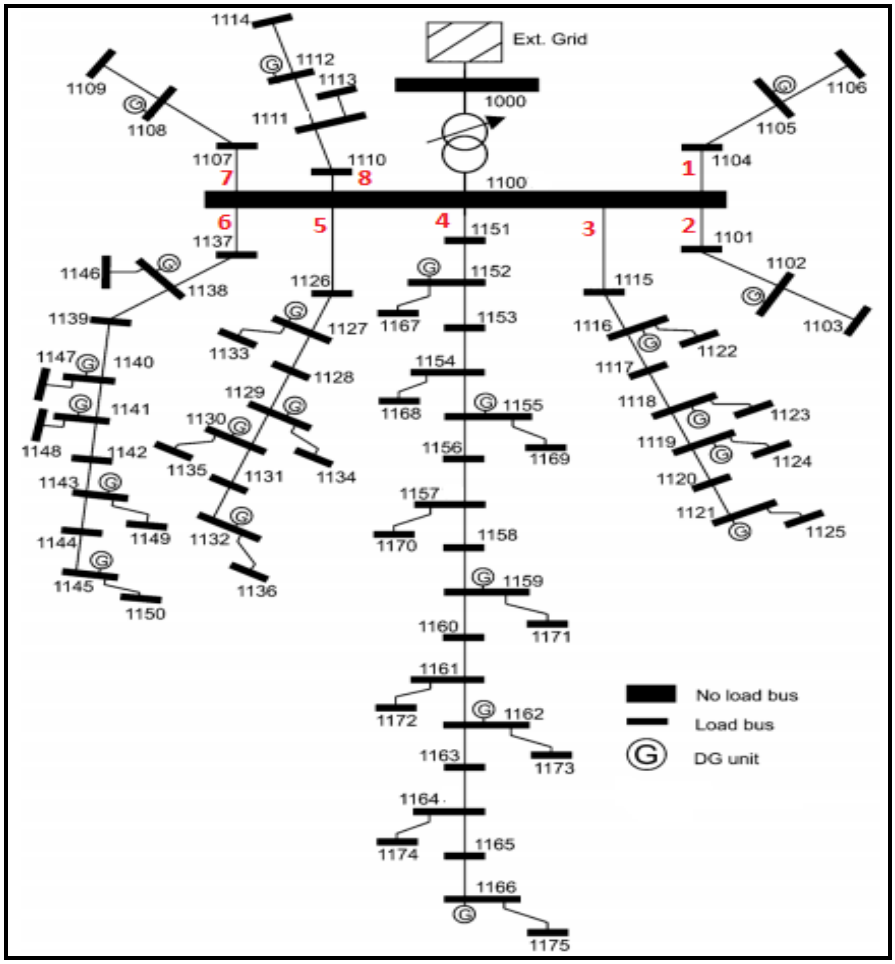

Figure 3.3 Topology of the test system
Taken from Alzaareer et al. (2020b)

3.4.1 Verification at base load condition

In this section, the voltage sensitivity coefficients ($d|V|/dP$ and $d|V|/dQ$) are computed at base load condition using ABCD method. The coefficients are demonstrated in the matrices shown in Figure 3.4. From both matrices, we can see that the sensitivity coefficients are

positive. This demonstrates the fact that injecting active or reactive power into power network will definitely increase the voltage magnitudes. The higher values of the self-sensitivity coefficients compared with the cross-sensitivity coefficients demonstrate also the accuracy of the proposed method. Indeed, power injection at a specific bus can increase its own voltage magnitude more than the voltage magnitudes of other buses. This is because system impedances mainly affect the power flow. Moreover, it is clear that the sensitivity coefficients of a specific node due to power injections into the same feeder is much higher than the coefficients due to power injections into other feeders.

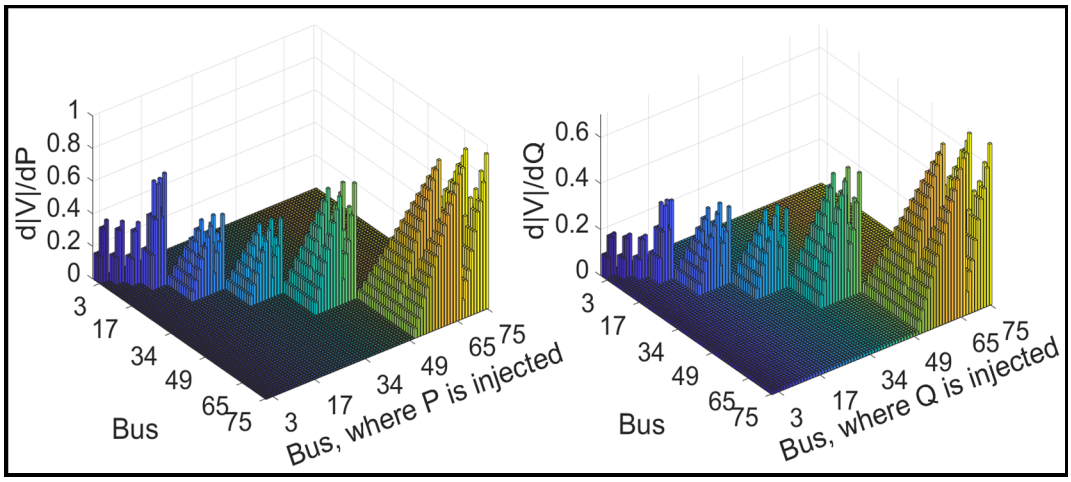

Figure 3.4 $d|V|/dP$ and $d|V|/dQ$ sensitivity coefficients at base load condition using ABCD method

Figure 3.5 shows sensitivity matrices obtained using the inverse of J (J^{-1}). By comparing the matrices obtained using ABCD method with the ones obtained using J^{-1}, we can notice that the matrices are very close to each other, rather they almost seem the same matrices.

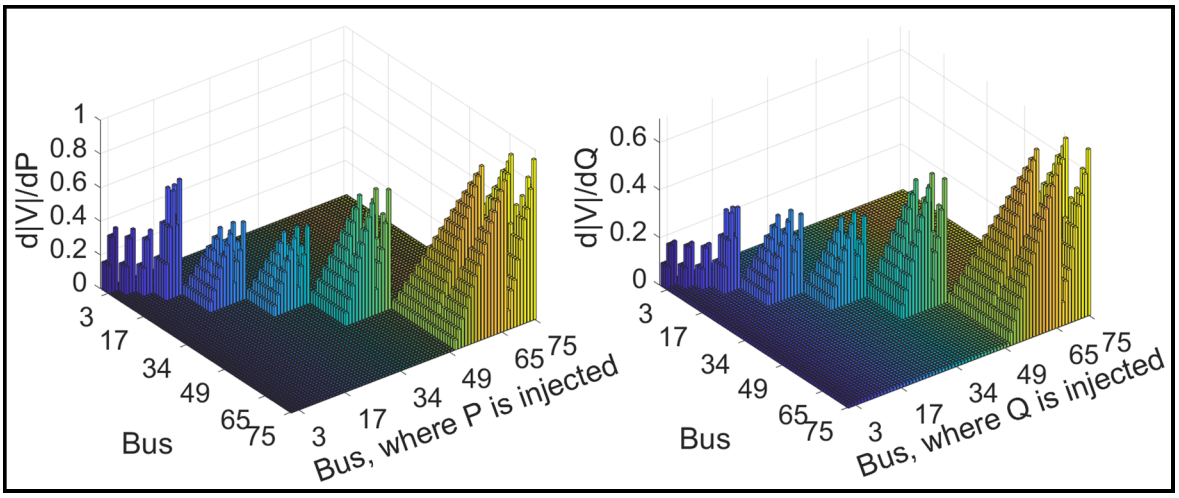

Figure 3.5 $d|V|/dP$ and $d|V|/dQ$ sensitivity coefficients at base load condition using inverse of J

Power flow calculations point out that V_{75} is the lowest voltage among network buses. The $d|V|/dP$ and $d|V|/dQ$ coefficients of bus 75 obtained via ABCD method are illustrated in Figure 3.6. Since the sensitivities to power injections into other feeders are very small, they aren't included in this figure.

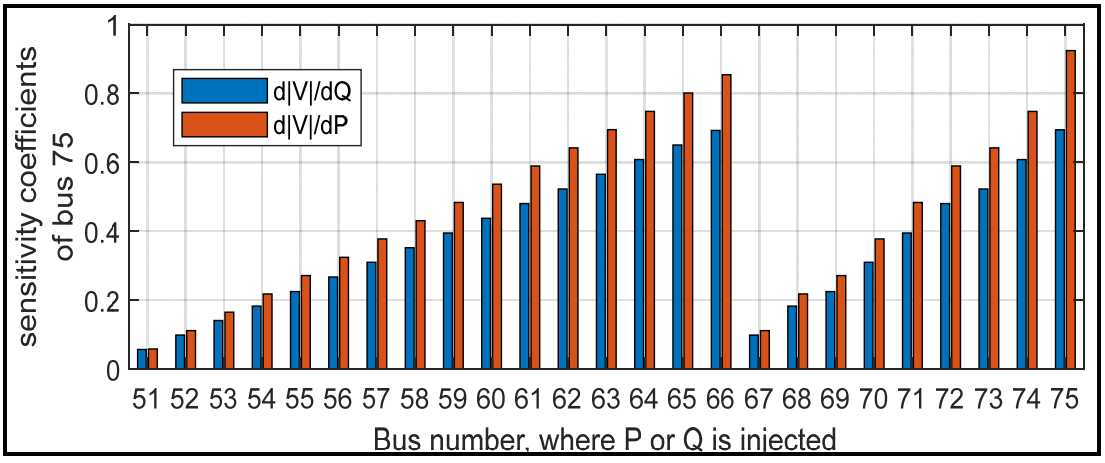

Figure 3.6 Voltage sensitivity coefficients of bus 75 with respect to active and reactive power injections at base load condition

From Figure 3.6, it is clear that the sensitivity coefficients of bus 75 due to power injections Q_{75} or P_{75} are higher than the sensitivity coefficients to power injections into other buses. Moreover, the sensitivity coefficients of bus 75 due to power injections Q_{66} or P_{66} are the

second largest among all the sensitivity coefficients. The expressions for the submatrices A, B, C, and D shown in (3.25) demonstrate this point, which show that their elements directly depend on the coupling admittances between system nodes. Since the bus 66 is the nearest node to bus 75, the sensitivity coefficients of bus 75 to power injections into node 66 is the largest cross-sensitivity. Verification of the self-sensitivity coefficients and the largest cross-sensitivity coefficients of bus 75 validates the proposed method for sensitivity analysis.

The verification of voltage self-sensitivity coefficients and the largest cross-sensitivity coefficients of node 75 (which has the lowest voltage) at base load condition is also investigated, in detail. This verification is investigated by assessing the performance of the sensitivity coefficients in voltage prediction. The predicted voltages are obtained by multiplying the sensitivity with the amount of the active or reactive power injection (or reduction). A comparison of the predicted voltages (obtained using the proposed method, inverse of J method, and perturb-and-observe (P&O) method presented in (Sansawatt et al., 2012)) with the actual voltages are then done. The actual voltages are obtained using power flow calculations. Power flow was performed after each step of power reduction or power injection, at a time.

To verify the self-sensitivity coefficients of bus 75 (obtained at base case condition), 1.0 p.u of its own active (or reactive) load power with step 0.1 p.u are deducted. To verify the largest cross-sensitivity coefficients of bus 75, 1.0 p.u of bus 66 active (or reactive) load power with step 0.1 p.u are deducted. Figure 3.7 shows a comparison between the predicted and the actual voltages of bus 75 due to active (or reactive) power reductions at bus 75 (or bus 66). It shows that the errors between the predicted voltages using ABCD method and the ones obtained using other methods are very small. It is also clear that as the load power reduction increases, the errors increase. Moreover, the errors due to the self-sensitivities are smaller than the ones due to the cross-sensitivities. Besides, the errors due to $d|V|/dQ$ sensitivities are smaller than the ones due to $d|V|/dP$ sensitivities. These characteristics coincide with the results obtained using the inverse of J.

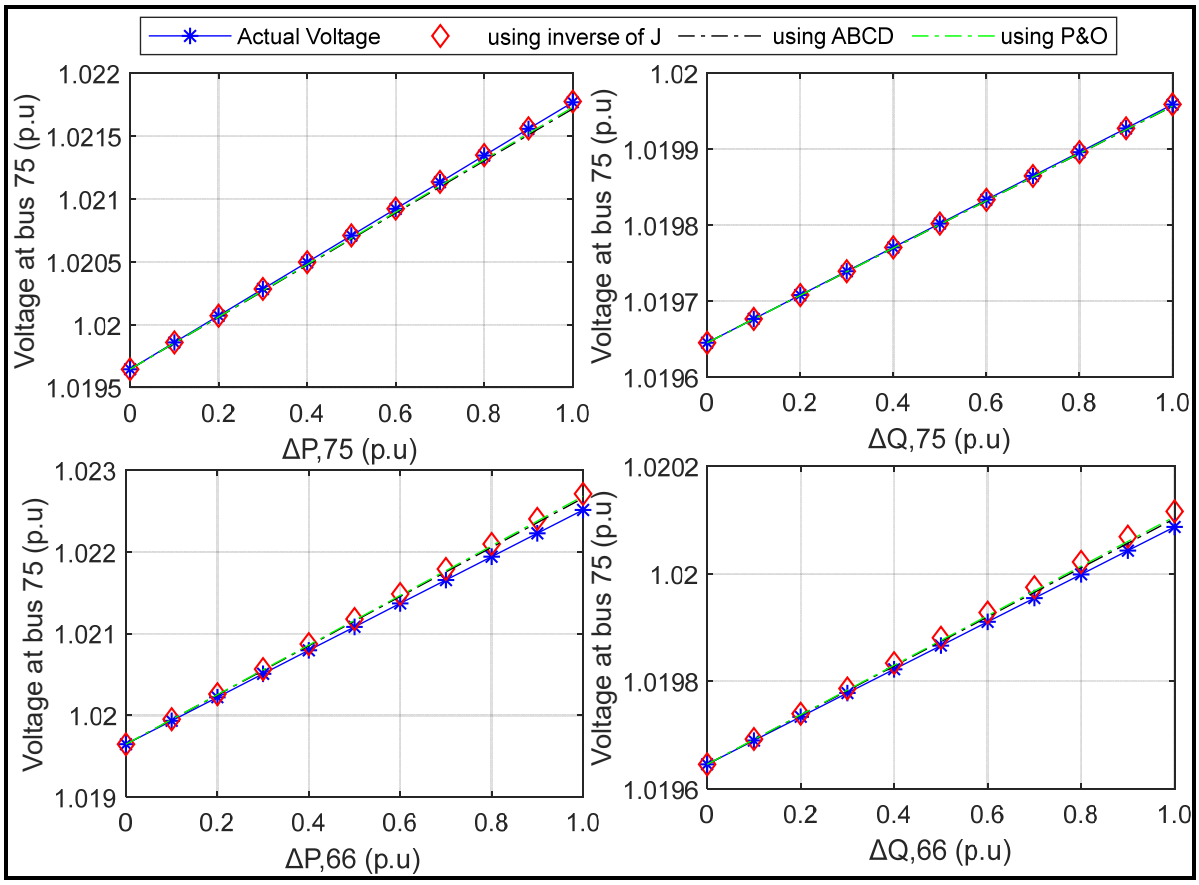

Figure 3.7 A comparison between the actual and the predicted voltages of bus 75 due to active and reactive power reductions at buses (75 and 66) for load base condition

The percent errors between the actual voltages and the predicted ones of node 75 are summarized in Table 3.1. The percent errors in Table 3.1 are very small (in the order of 10^{-02} to 10^{-07}). These percent errors are considered common in the sensitivity coefficients that are used for prediction and control in nonlinear power networks. This provides a rigorous justification for the accuracy of ABCD method.

Table 3.1 The errors (%) in the voltage V_{75} at load base condition

ΔQ Or ΔP (p.u)	**Self-sensitivity to:**				**Cross-sensitivity to:**			
	P_{75}		Q_{75}		P_{66}		Q_{66}	
	Using J^{-1} ($\times 10^{-4}$)	**Using ABCD ($\times 10^{-4}$)**	**Using J^{-1} ($\times 10^{-4}$)**	**Using ABCD ($\times 10^{-4}$)**	**Using J^{-1} ($\times 10^{-3}$)**	**Using ABCD ($\times 10^{-3}$)**	**Using J^{-1} ($\times 10^{-4}$)**	**Using ABCD ($\times 10^{-4}$)**
0	0	0	0	0	0	0	0	0
0.1	0.056	5.648	0.0017	0.237	1.837	1.340	2.806	1.468
0.2	0.224	11.18	0.0071	0.471	3.694	2.700	5.620	2.944
0.3	0.504	16.60	0.0160	0.701	5.571	4.081	8.440	4.426
0.4	0.896	21.90	0.0286	0.928	7.468	5.481	11.26	5.914
0.5	1.399	27.10	0.0447	1.151	9.385	6.902	14.09	7.410
0.6	2.014	32.17	0.0643	1.370	11.32	8.342	16.93	8.912
0.7	2.739	37.14	0.0876	1.586	13.27	9.803	19.78	10.42
0.8	3.575	41.99	0.1144	1.798	15.25	11.28	22.63	11.93
0.9	4.522	46.73	0.1448	2.007	17.24	12.78	25.49	13.45
1.0	5.579	51.36	0.1787	2.212	19.26	14.30	28.36	14.98

3.4.2 Verification at different loading conditions

To verify the voltage sensitivity coefficients at different operating conditions, the self-sensitivity and the largest cross sensitivity of bus 75 are also selected for this purpose. As section A of simulation results, 1.0 p.u of the active (or reactive) load powers with step 0.1 p.u are deducted. The only difference is that as the operating condition is changed, the sensitivity coefficients will be also updated. Accordingly, the predicted voltages are obtained by taking the summation of the individual multiplication (multiplication of the sensitivity with the amount of power change for each step). Table 3.2. shows the percent errors between the sensitivities obtained using ABCD method and the ones obtained via inverse of J method.

Table 3.2 The errors (%) in the updated sensitivities

ΔQ Or ΔP (p.u)	**Self-sensitivity to:**		**Cross-sensitivity to:**	
	$d\|V_{75}\|/dP_{75}$	$d\|V_{75}\|/dQ_{75}$	$d\|V_{75}\|/dP_{66}$	$d\|V_{75}\|/dQ_{66}$
0	0.00257	0.000544	0.001473	0.001983
0.1	0.00256	0.000538	0.001445	0.001979
0.2	0.00253	0.000532	0.001416	0.001976
0.3	0.00250	0.000526	0.001387	0.001973
0.4	0.00247	0.000520	0.001358	0.001969
0.5	0.00243	0.000514	0.001330	0.001966
0.6	0.00240	0.000508	0.001302	0.001962
0.7	0.00237	0.000502	0.001273	0.001959
0.8	0.00247	0.000496	0.001245	0.001955
0.9	0.002312	0.000490	0.001217	0.001952
1.0	0.002281	0.000484	0.001189	0.001949

A comparison between the actual and the predicted voltages of bus 75 due to active (or reactive) power reductions at bus 75 (or bus 66) is shown in Figure 3.8. The percent errors in the predicted voltage using the proposed method are summarized in Table 3.3. It can be concluded from these results that the errors in the sensitivities and the predicted voltages are also very small.

By comparing the predicted voltages using ABCD method shown in Table 3.1 with the ones shown in Table 3.3, we can notice that the errors are smaller in case of updating the sensitivities in each step (i.e. with the changes in system operating conditions). This demonstrates the necessary for updating the sensitivities in voltage control.

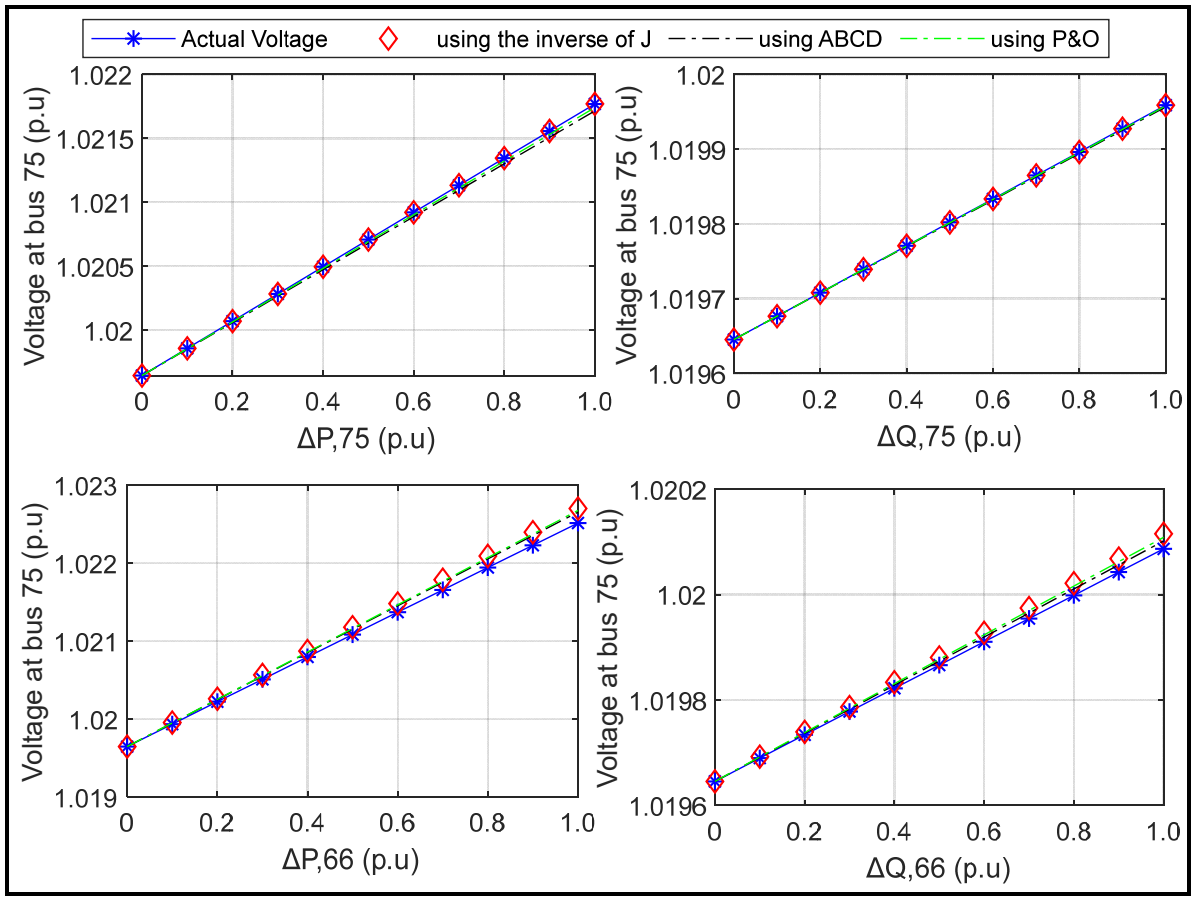

Figure 3.8. A comparison between the actual and the predicted voltages of bus 75 due to active and reactive power reductions at buses (75 and 66) for different loading conditions

3.4.3 Verification during DG power influences

To verify the voltage sensitivities during the influence of DG power, it is assumed that DG units can supply reactive power up to 3MVAR and make active power curtailments up to 3MW. This amount of power supply or curtailment represents a high value and can cause distinct variations in network voltage as well as the voltage sensitivities. Thus, the verification during DG power influences can provide a good demonstration on the accuracy of the proposed sensitivity method. Moreover, different voltages far away from the DG unit are considered for verification. 3.0 MW curtailment (or MVAR injection) by DG_{59} with step 0.3MW (or 0.3MVAR) are done. The sensitivity coefficients will be updated during each step. Accordingly, the predicted voltages are obtained by taking the summation of the individual

multiplication (multiplication of the sensitivity with the amount of power change for each step).

Table 3.3 The errors (%) in V_{75} due the updated sensitivities

ΔQ Or ΔP (p.u)	**Self-sensitivity due to:**		**Cross-sensitivity due to:**	
	$\boldsymbol{P_{75}}$	$\boldsymbol{Q_{75}}$	$\boldsymbol{P_{66}}$	$\boldsymbol{Q_{66}}$
0	0	0	0	0
0.1	5.648×10^{-5}	2.373×10^{-6}	1.340×10^{-4}	1.468×10^{-5}
0.2	1.122×10^{-4}	4.721×10^{-6}	2.686×10^{-4}	2.938×10^{-5}
0.3	1.672×10^{-4}	7.042×10^{-6}	4.039×10^{-4}	4.409×10^{-5}
0.4	2.216×10^{-4}	9.336×10^{-6}	5.398×10^{-4}	5.882×10^{-5}
0.5	2.752×10^{-4}	1.160×10^{-5}	6.763×10^{-4}	7.355×10^{-5}
0.6	3.281×10^{-4}	1.384×10^{-5}	8.134×10^{-4}	8.830×10^{-5}
0.7	3.803×10^{-4}	1.606×10^{-5}	9.511×10^{-4}	1.030×10^{-4}
0.8	4.317×10^{-4}	1.824×10^{-5}	1.089×10^{-3}	1.178×10^{-4}
0.9	4.825×10^{-4}	2.041×10^{-5}	1.228×10^{-3}	1.326×10^{-4}
1.0	5.325×10^{-4}	2.254×10^{-5}	1.367×10^{-3}	1.474×10^{-4}

A comparison between the actual and the predicted voltages due to reactive power injections (or active power curtailments by DG_{59}) can be found in Figure 3.9. The predicted voltages are done using ABCD method and the inverse of J method. The percent errors in the sensitivities and in the predicted voltages are summarized in Table 3.4 and Table 3.5, respectively. Although large power injections are considered in this case and considering different voltages far away from DG unit, it is clear that the errors are still very small. The errors in the sensitivities and in the predicted voltages are in order of 10^{-02} (or 10^{-01}) and 10^{-04} (or 10^{-03}), respectively. This also provides a rigorous justification for the accuracy of ABCD method. It is also clear that the percent errors in the sensitivities of nodes in the same feeder (the feeder owning the DG) are higher than the precent errors in the sensitivities of nodes of other feeders.

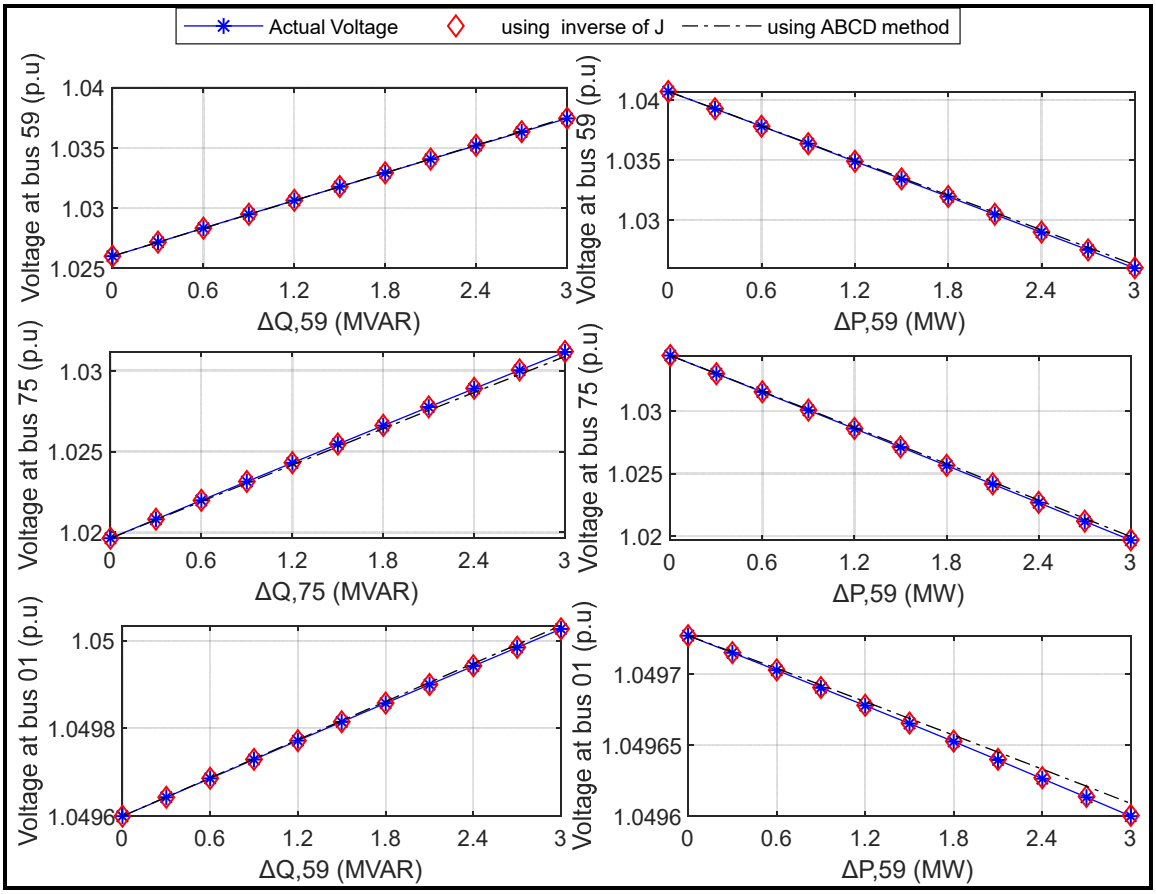

Figure 3.9 A comparison between the actual and the predicted voltages of some buses due to reactive power injection (active power curtailment) by DG_{59}

3.4.4 The performance assessment in online voltage control

To assess the performance of the proposed sensitivity method through transient simulation studies, multi-step optimization problem formulated in (Valverde et al., 2013) is used for voltage control in this section. This problem is formulated as:

$$min \sum_{k=0}^{n-1} \|\Delta Q(t+k)\|_F^2 + \|\varepsilon\|_G^2 \qquad 3.31$$

Subjected to:

$$-\varepsilon_1 A + V_i^{min} \le V_i(t+k) \le V_i^{max} + \varepsilon_2 A$$

$$V_i(t+k) = V_i(t+k-1) + \frac{\partial |V|}{\partial Q} \Delta Q_i(t+k)$$

$$\Delta Q^{min} \le \Delta Q(t+k) \le \Delta Q^{max}$$

$$Q^{min} \le Q(t+k) \le Q^{max}$$

Where ΔQ represents the vector of changes in reactive power injection by DG units. $\varepsilon = [\varepsilon_1, \varepsilon_2]^{\mathrm{T}}$ is the vector of slack variables used to relax the voltage constraints. n is number of prediction steps. '$^{\mathrm{T}}$' represents array transposition. 'A' denotes a unitary vector. F and G are a weight matrices used to penalize the reactive power injections and the slack variables, respectively. $V_i(t+k)$ is the predicted voltage magnitude of bus i. $V_i(t+k-1)$ is the previous voltage magnitude. $\frac{\partial |V|}{\partial Q}$ is the sensitivity matrix of bus voltage magnitudes with respect to reactive power injection by DG units. Q denotes a vector of the reactive power injected by DG units.

Table 3.4 The errors (%) in the sensitivities during DG influence

ΔQ (MVAR) Or ΔP (MW)	$\frac{d\lvert V_{59}\rvert}{dQ_{59}}$	$\frac{d\lvert V_{75}\rvert}{dQ_{59}}$	$\frac{d\lvert V_{01}\rvert}{dQ_{59}}$	$\frac{d\lvert V_{59}\rvert}{dP_{59}}$	$\frac{d\lvert V_{75}\rvert}{dP_{59}}$	$\frac{d\lvert V_{01}\rvert}{dP_{59}}$
0	0.319	1.220	0.014	0.325	0.525	0.017
0.3	0.205	1.172	0.016	0.435	0.596	0.019
0.6	0.092	1.124	0.018	0.547	0.667	0.022
0.9	0.019	1.076	0.020	0.660	0.740	0.024
1.2	0.130	1.030	0.022	0.774	0.815	0.026
1.5	0.240	0.984	0.025	0.889	0.890	0.028
1.8	0.350	0.939	0.027	1.006	0.966	0.031
2.1	0.458	0.895	0.029	1.124	1.044	0.033
2.4	0.565	0.852	0.031	1.244	1.123	0.035
2.7	0.671	0.809	0.033	1.365	1.203	0.038
3.0	0.776	0.767	0.035	1.487	1.285	0.040

Table 3.5 The errors (%) in different voltages during DG influence

ΔQ (MVAR) Or ΔP (MW)	**power injection Q_{59}**			**power injection P_{59}**		
	V_{59}	V_{75}	V_{01}	V_{59}	V_{75}	V_{01}
0	0	0	0	0	0	0
0.3	0.0007	0.0033	0.00004	0.0011	0.0017	0.00005
0.6	0.0010.	0.0065	0.00010	0.0027	0.0037	0.00011
0.9	0.0011	0.0096	0.00016	0.0037	0.0059	0.00018
1.2	0.0008	0.0125	0.00022	0.0067	0.0084	0.00026
1.5	0.0002	0.0153	0.00029	0.0092	0.0111	0.00034
1.8	0.0007	0.0179	0.00037	0.0121	0.0139	0.00043
2.1	0.0020	0.0204	0.00045	0.0153	0.0171	0.00053
2.4	0.0035	0.0228	0.00054	0.0189	0.0204	0.00063
2.7	0.0053	0.0250	0.00064	0.0204	0.0241	0.00074
3.0	0.0074	0.0271	0.00074	0.0271	0.0279	0.00085

It is clear from (3.34) that the voltages are evaluated inside the optimization problem using the sensitivities $\frac{\partial |V|}{\partial Q}$. These sensitivities are obtained using (3.23) and (3.27), and updated after each step. It is worth noting that the sensitivities can be updated due to changing the submatrices C and D.

In this scenario, all DG units are installed in the grid. No more than 0.3 MVAR of reactive power is allowed to be injected by each DG unit for each control action. The cost of using the slack values are higher than the cost of using the reactive power by 800 times. The acceptable limits for voltages are assumed to be [0.98, 1.04] p.u. This work randomly assumes that the control actions take place every 10 seconds. This period can be replaced by any another period (i.e. 1 second, 5 second, … etc.). It is worth noting that this period is selected to consider the calculation time, measurement collection time, the time required to transmit the new control set-points of DG units, and the dead time required to avoid making decisions based on

measurements taken during transients. The measurements in this work is the reactive power output by DG units. It is also assumed that the loads are operated at their maximum to create undervoltage problem. Thus, reactive power outputs by DG units are the controls for voltage regulations. The optimization software LINGO and MATLAB are both used to investigate the results.

Some of network voltages and reactive power outputs by DG units are shown in Figure 3.10 and Figure 3.11, respectively. It is clear that the controller, with the aid of the proposed sensitivity analysis, was able to gradually regulate the voltages. Figure 3.11 shows that some units (i.e. DG at bus 05) are operated at a lower amount of power. This is to prevent any violation of the upper voltage near bus 05.

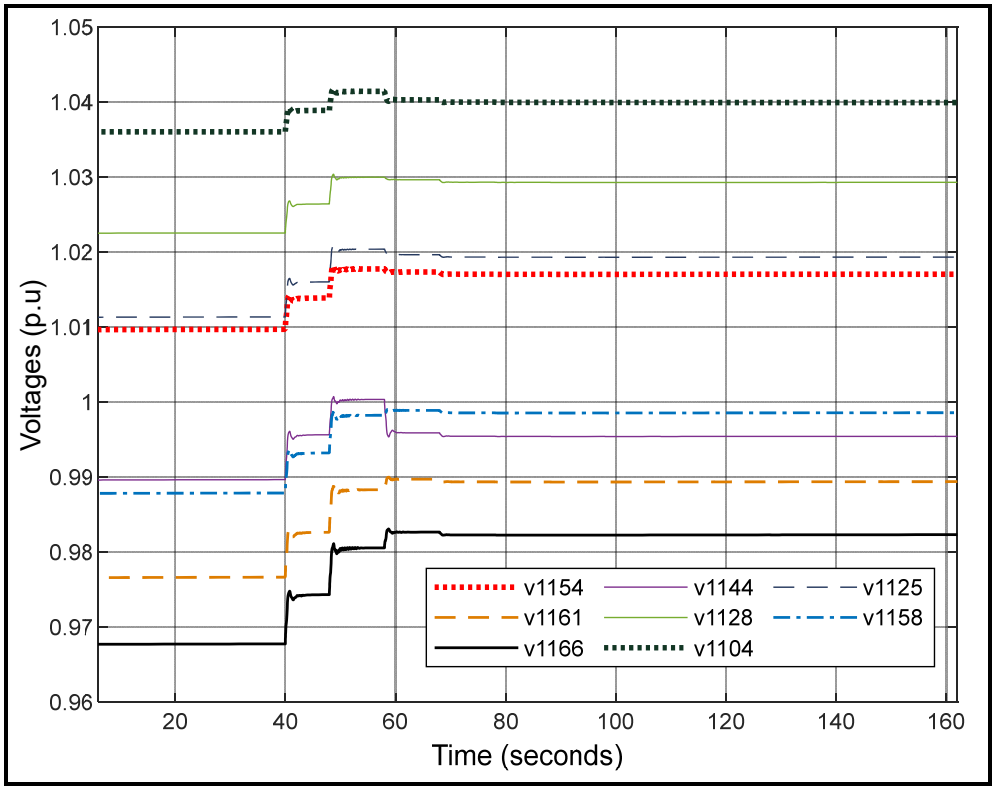

Figure 3.10 Some bus voltages during transient analysis

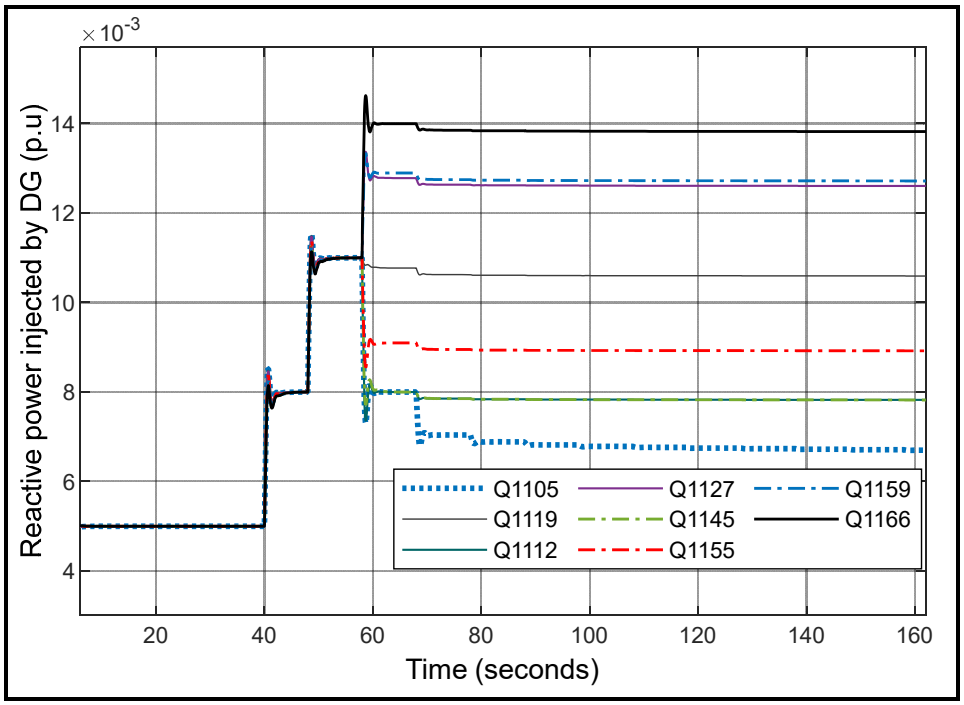

Figure 3.11 Some reactive power outputs by DG units

Figure 3.11 also shows that the DG installed at bus 66 has to participate in power injection more than other units. This is because V66 is the most problematic voltage. We can also see that the nearest DG units to the region of the violated voltages have to participate more than the other units.

The total compensated amount of reactive powers and the voltage profiles of two cases, namely, Vuncontrolled and Vcontrolled, are illustrated in Figure 3.12 and Figure 3.13, respectively. Based on the simulation results, it is concluded that the proposed sensitivity analysis is suitable for online applications and has a logical performance for managing reactive powers among DG units.

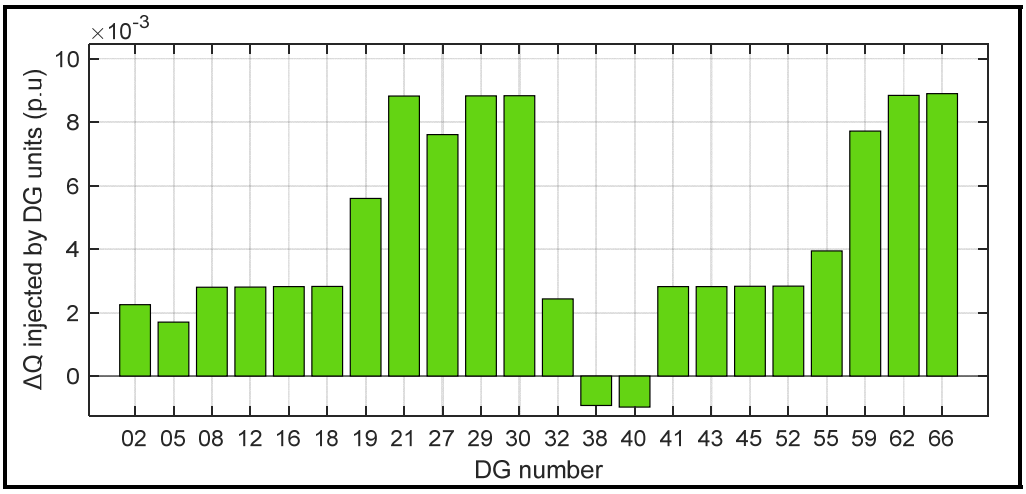

Figure 3.12 The total change in reactive power injections by DG units

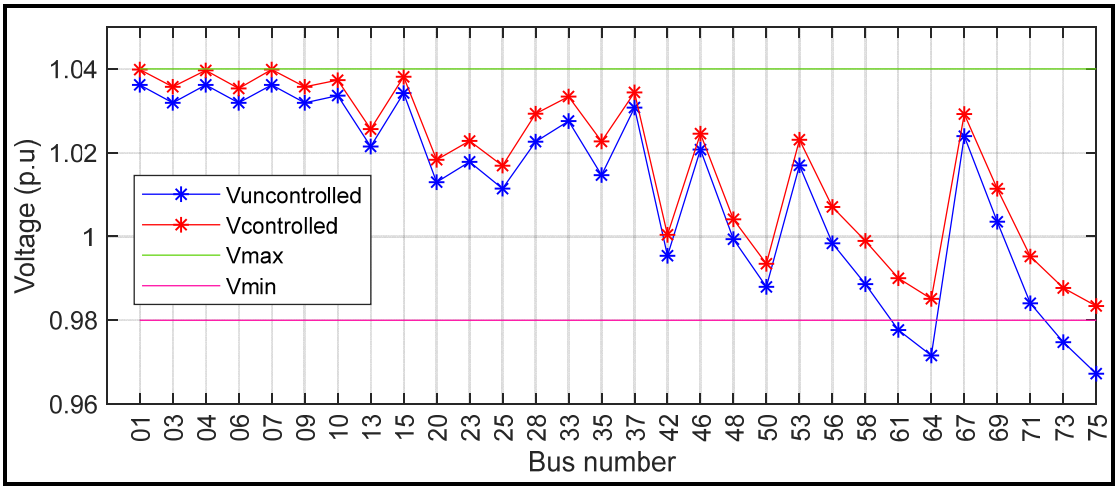

Figure 3.13 Voltage profile during the two cases: controlled and uncontrolled

3.4.5 Dynamic simulation studies

The actual performance of the proposed sensitivity analysis through dynamic simulation is assessed in this section. The system is operated at condition where there is no violation in the voltage. It is assumed that DG_{75} has the power profile (for 15s) shown in Figure 3.14. It is also assumed that the lower voltage limit is 0.98 p.u. Control action takes place when the voltage exceeds the lower limit. New settings are then held for 4s. The obtained voltage at bus 66

(where the DG is connected) and the set points of DG unit are presented in Figure 3.14. The results show that both sensitivity approaches provide almost the same amount of reactive power and, hence, almost the same voltage profile.

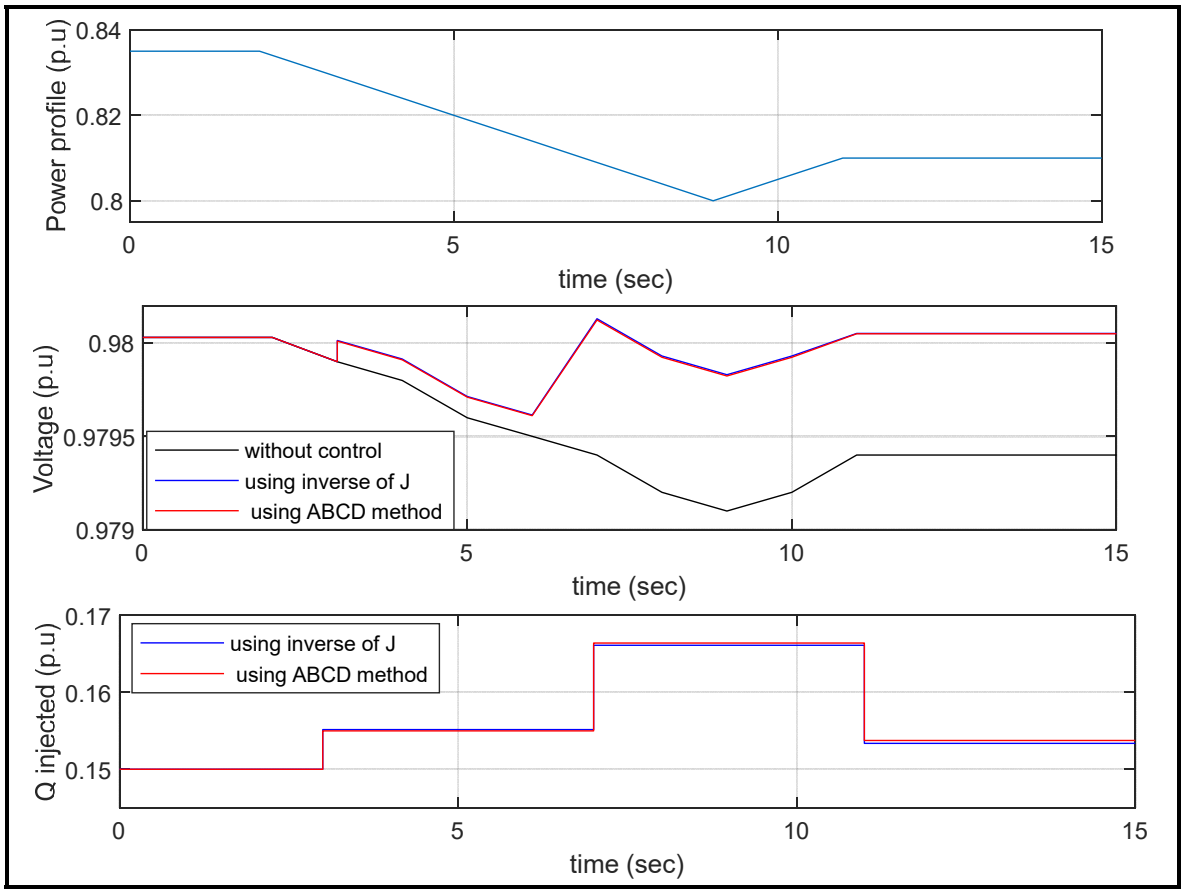

Figure 3.14 Dynamic simulation studies

3.4.6 Calculation speed

To show the calculation speed of the proposed approach, the scenario presented in section 3.4.1 is selected for this purpose. The results show that the execution time of the proposed method is 0.41s. In contrast, 0.64s is required to execute Jacobian-based sensitivity analysis method. It is clear that the proposed method was able to reduce the computation time by 38.91%. This reduction in the calculation time will be much higher in cases of practical networks or in the

context of optimization techniques. The results are obtained using an i7–8850 CPU@ 2.60 GHz laptop.

3.5 Conclusions

In this study, a new and fast sensitivity approach is developed to find the voltage sensitivity coefficients in smart grids. The proposed approach has been validated on a radial distribution network including several DG units under different scenarios. The numerical values of the sensitivity coefficients and the comparison with the results of other techniques validate the accuracy of the proposed method. The results show that the errors in the values of sensitivity coefficients or in voltage prediction are very small, which demonstrate that ABCD model has almost the same level of the accuracy of J^{-1} method. The results also showed that the proposed method can successfully account for any change in the operating conditions.

The proposed method is also validated using dynamic and transient analysis to show that the ABCD model is able to continuously update the sensitivities. This also demonstrates the potential application of the proposed sensitivity method in online applications. The results also showed that the proposed method is able to efficiently manage the voltages by accurate dispatching of control variables.

CHAPTER 4

DEVELOPMENT OF NEW IDENTIFICATION METHOD FOR GLOBAL GROUP OF CONTROLS FOR ONLINE COORDINATED VOLTAGE CONTROL IN ACTIVE DISTRIBUTION NETWORKS

Khaled Alzaareer[1], Maarouf Saad[1], Hasan Mehrjerdi[2], Dalal Asber[3] and Serge Lefebvre[3]

[1] Département of Electrical Engineering, École de Technologie Supérieure, 1100 Notre-Dame Ouest, Montréal, Québec, Canada H3C 1K3
[2] Department of Electrical Engineering, Qatar University, University Street, Doha, Qatar 2713
[3] Power Systems and Mathematics, Research Institute of Hydro-Quebec 1740 Boul Lionel-Boulet, Varennes, Québec, Canada J3X 1S1

Paper published in *IEEE Transactions on Smart Grid*, September 2020

Abstract

The incorporation of distributed generation (DG) units in distribution network voltage control may create operational conflicts with other conventional voltage control devices. Structural changes of networks can also increase the possibility to create control interactions. Control rules-based voltage control methods are not suitable for large scale networks where large number of control choices are available. Similarly, optimization-based voltage control methods are impractical to implement since many control variables have to be used to obtain the optimal solution. Therefore in this paper, a new technique for choosing a global group of the most effective control variables considering the ones with low cost is proposed for voltage regulation in distribution networks. This technique is based on the concept of electrical distances between the voltage control devices and network nodes to derive a correction index (CI). The index represents the level of effectiveness of each control variable with respect to all violated voltages. The index is implemented in two phase algorithms (top–down and bottom-up) to identify the global group of control variables. The proposed technique takes into consideration five aspects: the effectiveness, availability, and cost of the control variables as well as the

structural changes of networks and the coordination between control variables to simultaneously eliminate the violation in the voltages. The technique is fast and suitable to be implemented for online voltage control. The proposed method is successfully examined on the modified IEEE 123 distribution system under different scenarios.

Keywords: Voltage Control; Controls Selection; Controls Coordination; Electrical Distances; Active Distribution Systems.

4.1 Introduction

Voltage control is one of the operational challenges in active distribution networks. The integration of multiple DG units into distribution networks can cause over/under voltage problems as well as operational conflicts with other conventional voltage control devices, such as on load tap changers (OLTC), Voltage Regulators (VRs), and Capacitor Banks (CBs) (Ranamuka et al., 2016). These problems can grow as distribution networks meet structural changes (Ranamuka et al., 2015). Thus, it is required to operationally update the voltage control devices in active distribution networks.

One of the favorable ways of reducing the adverse impacts of the operational conflicts among DG units and conventional voltage control devices is control coordination. Generally speaking, the coordinated voltage control (CVC) techniques can update the control actions based on control rules or optimization techniques.

A novel method for CVC in active distribution systems is developed (Elkhatib et al., 2011). The method is based on installing remote terminal units at DG units to communicate with each other. A method for CVC in active distribution systems based on control rules algorithm is proposed (Kulmala et al., 2014). A Dynamic Master/Slave Scheme for voltage control in active distribution networks is presented (Moursi et al., 2014). A coordinated method based on power flow sensitivity factor for output control of multiple DG units are detailed (Jupe et al., 2010). An online combined local and remote voltage control in the presence of induction machine-

based DG unit is presented (Viawan et al., 2007). A CVC method for coordination of OLTC, VR, and DG unit is presented (Muttaqi et al., 2015). The method is based on the concept of control zone, line drop compensation, as well as the controllers' parameters. A real-time voltage control for distribution systems employing plug-in electric vehicles, DG, and OLTC is proposed (Azzouz et al., 2015). However, all the above-mentioned studies do not consider the coordination process in case of multiple conventional voltage control devices and multiple DG units. An online CVC strategy is developed in order to operationally avoid the impact of simultaneous responses of multiple voltage control devices and DG units (Ranamuka et al., 2013). However, it does not consider the impacts of non-simultaneous operations of DG units and the conventional devices. To minimize the impact of non-simultaneous operations, an online CVC by allowing voltage control devices to operate in accordance with a priority scheme is proposed (Ranamuka et al., 2015). However, control rules-based CVC methods are not suitable for large networks where a large number of control choices are available or when many various objectives are included in the control. In these cases, defining of control rules is a complex task.

Different techniques for Optimization-based CVC in active distribution networks have been presented in the literature. A method is developed for voltage regulation in active distribution systems by formulating a large-scale optimization problem and solving it using a genetic algorithm-based solver (Senjyu et al., 2008). A strategy for CVC in active distribution networks using a dynamic programming method is proposed (Kim et al., 2012). A comprehensive decentralized Volt/VAr control strategy for coordination of conventional control devices and synchronous machine-based DG units in distribution networks is proposed (Viawan et al., 2008). A multiple line drop compensation voltage control technique for under-load tap changer transformers is proposed (Choi et al., 2001), where the desired tap positions are obtained by solving an integer optimization problem. A strategy for short-term scheduling of DG units and conventional voltage control devices is proposed (Borghetti et al., 2010) for implementing optimal voltage control in active distribution networks. A mutation fuzzy adaptive particle swarm optimization method for CVC is proposed (Yang et al., 2015). A Trust Region Sequential Quadratic Programming technique for CVC in active distribution networks

is presented (Sheng et al., 2015). However, by using optimization-based methods, large number of control variables have to be activated to obtain the best solution, which is not suitable for practical systems. Moreover, those works do not fully consider the impacts of structural changes in voltage control.

The wide distribution of controls and the possibility of occurring many voltage violations among the network makes it is hard to provide coordination of the controls while activating only the required number of controls. Moreover, it is not easy to rank the most effective control variables during multi violated voltages while considering a set of aspects. Thus and in order to avoid the problems associated with the two kinds of CVC methods, this work proposes a new method to identify and coordinate a set of the cheaper and most effective control variables (only the required number) for CVC in active distribution networks. The proposed method is capable of ranking the control variables to multi violated voltages (not only one violated voltage) while considering a set of aspects, especially the cost. It is also capable to simultaneously (with no time delay) eliminate all the multi violations with only the most effective controls, low computational efforts and high speed. The proposed method does not aim to find the optimal voltage control, which requires operation of most, if not all, the control variables, but provides a group of the most effective control variables to simultaneously eliminate the violation in voltage, taking into accounts the cost of controls. Thus, the result of this method provides a feasible solution for practical implementation.

The proposed method employs a correction index based on the concept of electrical distances between the voltage control devices and network nodes to rank the controls. The index represents the level of effectiveness of each control variable with respect to the violated voltages. Then, the index is implemented in two phase algorithms (top–down and bottom-up) to identify the global group of controls that are the most efficient to simultaneously eliminate the violation in voltages.

The key contributions of this study are:

- Using optimization-based CVC methods, large number of controls have to be activated to obtain the best solution, which is not suitable for practical systems. Solution infeasibility is one of the main problems for optimization-based methods. In contrast, the proposed method can guide the network operators to select a global set of the most effective control variables (only the required number) to eliminate the violation in the voltages, which is feasible for practical implementation.
- Compared with control rules-based CVC methods, the proposed method is suitable for large networks where a large number of control choices exist or when many various objectives are included in the control. Defining of control rules is a complex task in those cases. Moreover, most of the rules-based methods are not capable to simultaneously eliminate the violations due to the time delay associated with conventional controls.
- The proposed method shows a high level of flexibility such that it can take into consideration the five aspects below to eliminate the violation in the voltages: the effectiveness, availability, and the cost of each control action as well as the structural changes of networks and the coordination among control actions.
- Since the proposed technique mainly depends on the concept of electric distances, it is able to effectively account for the impact of structural changes in the grid.

The remainder of the paper is organized as follows. Section II shows the calculation of the electrical distances between the control variables and network voltages. Section III formulates the correction index to determine the level of effectiveness of each control variable with respect to the violated voltages. Section IV describes how the most effective control variables are identified using the two-phase algorithm. Section V shows simulation results and Section VI shows the conclusions.

4.2 Calculation of the electrical distances

4.2.1 Sensitivities of network voltages to control variables

OLTC, VRs, CBs, and DG units are the main voltage control devices in modern distribution grids. Under a particular condition, the voltage magnitude at bus i of the network for small changes in control variables can be easily obtained.

For DG units, the sensitivities of network voltages to the power injected by DG units into the network can be found using the inverse Jacobian matrix, $\boldsymbol{J^{-1}}$ as:

$$\begin{bmatrix}\boldsymbol{\Delta\theta}\\ \boldsymbol{\Delta V}\end{bmatrix} = [\boldsymbol{J^{-1}}]\begin{bmatrix}\boldsymbol{\Delta P}\\ \boldsymbol{\Delta Q}\end{bmatrix}$$

$$\begin{bmatrix}\boldsymbol{\Delta\theta}\\ \boldsymbol{\Delta V}\end{bmatrix} = \begin{bmatrix}\boldsymbol{\frac{\partial\theta}{\partial P}} & \boldsymbol{\frac{\partial\theta}{\partial Q}}\\ \boldsymbol{\frac{\partial V}{\partial P}} & \boldsymbol{\frac{\partial V}{\partial Q}}\end{bmatrix}\begin{bmatrix}\boldsymbol{\Delta P}\\ \boldsymbol{\Delta Q}\end{bmatrix} \quad (4.1)$$

Where ΔP and ΔQ represent the vectors of nodal change in active and reactive power, respectively. ΔV and $\Delta\theta$ represent the vectors of nodal change in voltage magnitudes and angles, respectively. $\partial\theta/\partial P$ and $\partial\theta/\partial Q$ are the sensitivity vectors of nodal voltage angle to real and reactive power injection, respectively. $\partial V/\partial P$ and $\partial V/\partial Q$ are the sensitivity vectors of nodal voltage magnitude to real and reactive power injection, respectively.

Let us assume that a DG unit is connected at x^{th} node for the distribution network with n number of nodes. Thus, the change in voltage magnitudes at network nodes due to the output variation of DG unit at x^{th} node can be found as:

$$[\boldsymbol{\Delta V_1}, \dots \boldsymbol{\Delta V_i}, \dots, \boldsymbol{\Delta V_x}, \dots, \boldsymbol{\Delta V_n}]^{\boldsymbol{T}} = \left[\frac{\boldsymbol{\partial V_1}}{\boldsymbol{\partial P_x}}, \dots, \frac{\boldsymbol{\partial V_i}}{\boldsymbol{\partial P_x}}, \dots, \frac{\boldsymbol{\partial V_x}}{\boldsymbol{\partial P_x}}, \dots, \frac{\boldsymbol{\partial V_n}}{\boldsymbol{\partial P_x}}\right]^{\boldsymbol{T}} \boldsymbol{\Delta P_x} + \left[\frac{\boldsymbol{\partial V_1}}{\boldsymbol{\partial Q_x}}, \dots, \frac{\boldsymbol{\partial V_i}}{\boldsymbol{\partial Q_x}}, \dots, \frac{\boldsymbol{\partial V_x}}{\boldsymbol{\partial Q_x}}, \dots, \frac{\boldsymbol{\partial V_n}}{\boldsymbol{\partial Q_x}}\right]^{\boldsymbol{T}} \boldsymbol{\Delta Q_x} \tag{4.2}$$

Where 'i' denotes the ith node and 'n' represents number of network buses. Simplify, for the ith node:

$$\boldsymbol{\Delta V_i} = \frac{\boldsymbol{\partial V_i}}{\boldsymbol{\partial P_x}}\ \boldsymbol{\Delta P_x} + \frac{\boldsymbol{\partial V_i}}{\boldsymbol{\partial Q_x}}\ \boldsymbol{\Delta Q_x} \tag{4.3}$$

The term associated with active power injected by a DG unit, $(\boldsymbol{\partial V_i}/\ \boldsymbol{\partial P_x})\ \boldsymbol{\Delta P_x}$, depends on the type of DG unit and its operation. However, the term associated with reactive power injection, $(\boldsymbol{\partial V_i}/\ \boldsymbol{\partial Q_x})\ \boldsymbol{\Delta Q_x}$ can be used for voltage control. Thus, the value of $\boldsymbol{\partial V_i}/\boldsymbol{\partial Q_x}$ is used to obtain sensitivity of ith bus voltage with respect to the DG unit connected at xth node.

Remark: In some overvoltage cases (i.e. in cases where reactive power output by DG units does not have sufficient capacity for voltage correction), the output active power can also be used for voltage control. Thus, the term $(\boldsymbol{\partial V_i}/\ \boldsymbol{\partial P_x})$ is used to obtain sensitivity of ith bus voltage with respect to the active power output by DG unit connected at xth node.

To find the sensitivity of ith bus voltage with respect to conventional control variables, it is necessary to formulate the power flow equations of the network at fixed operating point (i.e. at the current operating point) as follows:

$$\boldsymbol{H(V, u) = 0} \tag{4.4}$$

Where H is the set of equations for reactive power injected at all PQ buses. V and u represent the vectors of bus voltages and control variables, respectively.

By taking the derivative of (4.4), we obtain:

$$\boldsymbol{H_V\, dV + H_u\, du = 0} \tag{4.5}$$

Where H_V and H_u are the partial derivatives of the injected reactive power with respect to the voltages and control variables, respectively. Based on (4.5), the sensitivities of network voltages with respect to a conventional control variable u_j can be found as:

$$\boldsymbol{\frac{\partial V}{\partial u_j} = -\,[H_V\,]^{-1}\;H_{u_j}} \tag{4.6}$$

The term $[H_V\,]^{-1}$ can be directly found using the inverse of Jacobian matrix. H_{u_j} is a known vector and represents how the injected reactive power changes with varying the control variable u_j (i.e. Δu_j). Thus, the change in network voltages due to the variation in the control variables can be found as:

$$\boldsymbol{[\Delta V] = \left[\frac{\partial V}{\partial u}\right][\Delta u]} \tag{4.7}$$

Let us assume that the voltage control device is connected at x^{th} node for the distribution system with n number of nodes. Thus, the change in the voltages due to the variation in the control variable located at x^{th} node can be found as:

$$\boldsymbol{[\Delta V_1, \dots, \Delta V_i, \dots, \Delta V_x, \dots, \Delta V_n\,]^T =} \left[\frac{\partial V_1}{\partial u_x}, \dots \frac{\partial V_i}{\partial u_x}, \dots \frac{\partial V_x}{\partial u_x}, \dots, \frac{\partial V_n}{\partial u_x}\right]^T \Delta u_x \tag{4.8}$$

Where 'i' denotes the i^{th} node and 'n' represents number of network buses. Simplify, for the i^{th} node:

$$\boldsymbol{\Delta V_i = \frac{\partial V_i}{\partial u_x}\ \Delta u_x} \tag{4.9}$$

Thus, the value of $\boldsymbol{\partial V_i / \partial u_x}$ is used to the obtain sensitivity of ith bus voltage with respect to the conventional controls (i.e. CBs, and VRs).

4.2.2 Determination of electrical distances

The calculation of the electrical distances between network buses depends on the relative variation in voltage magnitudes between two nodes due to a change in reactive power injection at one of the nodes. In other words, the coupling between any two buses can be found by the maximum attenuation of the voltage variation between the two buses as follows:

$$\boldsymbol{\Delta V_i = \alpha_{ij}\, \Delta V_j} \tag{4.10}$$

Where $\boldsymbol{\alpha_{ij}}$ represents the attenuation between the two nodes i and j. The respective attenuation between any control variable device located at xth and any node i in the network can be derived by dividing the elements of the voltage sensitivity vector stated in (4.2) or (4.8) by the $\boldsymbol{\partial V_x / \partial Q_x}$ or $\boldsymbol{\partial V_x / \partial u_x}$ as:

$$\boldsymbol{\alpha_{ix} = \frac{\partial V_i}{\partial Q_x} / \frac{\partial V_x}{\partial Q_x} \qquad for\ DG\ units} \tag{4.11a}$$

$$\boldsymbol{\alpha_{ix} = \frac{\partial V_i}{\partial u_x} / \frac{\partial V_x}{\partial u_x} \qquad for\ convenional\ controls} \tag{4.11b}$$

It is clear from (4.11) that any change in reactive power injection (i.e. ΔQ) at bus x could cause a change in the voltages at buses x and i by ΔV_x and ΔV_i, respectively. The change in the voltage at a corresponding node due to reactive power injection at its own bus is greater than power injection at other nodes. This means that α_{ix} has a numerical value between 0 and 1.

The electrical distance between any control variable located at x^{th} node and any node in the network D_{ix} can be derived by:

$$\boldsymbol{D_{ix} = -Log\ (\alpha_{ix}.\alpha_{xi})} \tag{4.12}$$

The normalized electrical distance $\boldsymbol{d_{ix}}$ can be given by:

$$\boldsymbol{d_{ix} = \frac{D_{ix}}{max(D_{1x}, D_{2x}, \dots, D_{nx})}} \tag{4.13}$$

In this section, the electrical distances between voltage control devices and network nodes (i.e. sensitivities of the network voltages to voltage controls) are calculated. The distances can be used to sort the promising control variables for any violated voltage, but there is no coordination between these control variables. The coordination is necessary since each control variable has an effect on more than one node voltage. In the next section, these electrical distances will be implemented to develop an index that sorts and chooses the most efficient controls to bring back the violated voltages within an acceptable range.

4.3 Formulation of the correction index

In order to obtain the global group of most effective control devices to simultaneously eliminate all violated voltages, this section introduces a new index (correction Index) to measure the effectiveness of each control variable to eliminate all the violations in network voltages. The index is based on the critical distances (i.e. sensitivities) between each control variable and network nodes.

In the previous section, we showed that d_{ix} illustrated in (4.13) represents the normalization of the electrical distance between the control variable device located at x^{th} node and any node in the network. The normalized electrical distance equation (4.13) considers the effectiveness of each control.

The availability of the control can also be taken into account by using a parameterization for the control variables such that $u_x = 0, 1$ or -1 represents the present value, the maximum value or the minimum value of the control variable. However, the previous formula does not include the control cost.

For each control variable u_x, let d_x be the vector of electrical distances between network nodes and the control variable u_x as:

$$\boldsymbol{d_x} = [\boldsymbol{d_{1x}}, \boldsymbol{d_{2x}}, \dots, \boldsymbol{d_{ix}}, \dots, \boldsymbol{d_{nx}}] \tag{4.14}$$

If C_x is considered as the unit cost of the x^{th} control variable, the vector d_x can be modified as follows:

$$\boldsymbol{d'_x} = \frac{\boldsymbol{d_x}}{\boldsymbol{C_x}} \tag{4.15}$$

Given a control u_x, the corrective index CI can be calculated by finding the summation of d'_{ix} with respect to all the violated voltages as follows:

$$\boldsymbol{CI_x} = \sum_{\boldsymbol{i=1}}^{\boldsymbol{N}} \boldsymbol{d'_{ix}} \tag{4.16}$$

Where N is the number of violated voltages and CI_x is the index for the control u_x. This index measures the ability of a control variable to bring all violated voltages within acceptable limits by taking into account its availability, effectiveness, and cost.

A flowchart of the CI calculation is shown in Figure 4.1

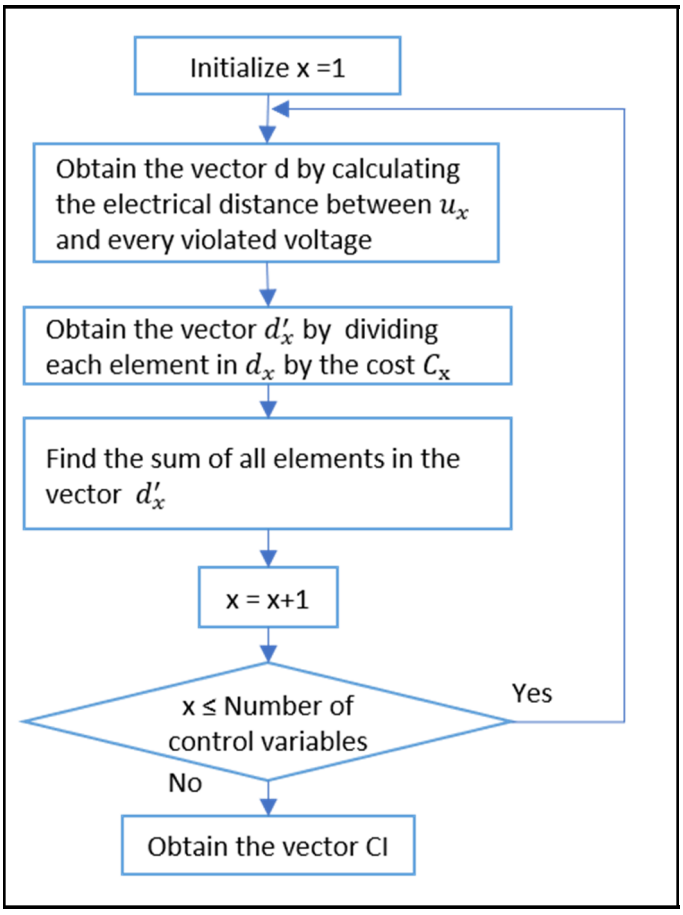

Figure 4.1 A flowchart of CI calculation

4.4 Identifying of the global control group

The development of methods to identify a group of control variables to simultaneously correct the voltages in active distribution networks is necessary. In this section, a two-phase algorithm (top-down and bottom-up) is proposed for this purpose. Top-down and bottom-up are both strategies of data treatment and knowledge organizing, utilized widely in a diversity of fields. The computation effort for the top-down and bottom-up phases is very low and therefore it is suitable for online voltage control.

The basic idea behind the top-down method is that the main task is divided into multiple smaller subtasks. These subtasks are further divided until the obtained subtasks can be simply

understood and make it easier to design or implement. Thus, it can be considered as a step-by-step process in which each subtask is separately analyzed for solving the large problem. In contrast, the bottom-up method works in an inverse manner for top-down method. The bottom-up method defines a set of rules for the individual performances and the interactions and then are combined into the entire problem by proceeding with the inference of the full performance. Figure 4.2 shows the process direction for the two approaches.

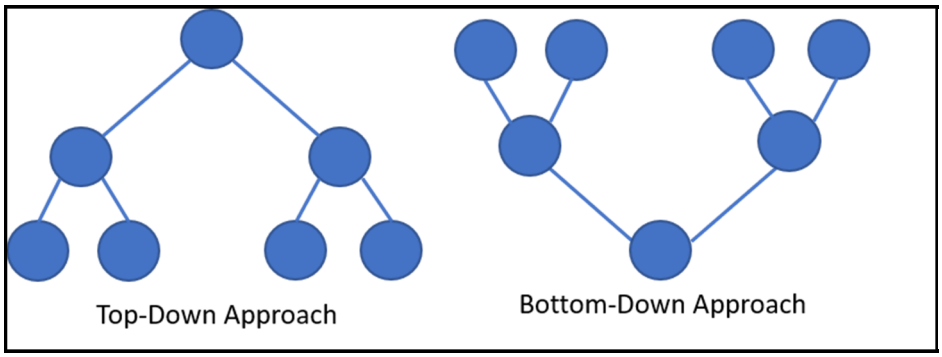

Figure 4.2 Top-Down approach vs. Bottom-Down approach

Since the subproblems in top-down method aren't connected in a manner so that they can communicate well, redundancies can be obtained. However, the bottom-up approach implements the concept of the information hiding and, thus, it can omit the redundancies. One of the main applications of the bottom-up approach is testing.

In this work, the two approaches have been suggested for identifying the global group of controls for voltage control in active distribution networks. The top-down approach uses aggregate control to obtain the global group, which is then allocated to individual control variables on the basis of their ranking in CI index. The bottom-up approach employs individual control variables to test the voltage estimation process.

In the first phase (top-down selection), the index vector CI is reordered in descending order, and the control variables (started from the highest rank to the lowest rank) are chosen until all of the violated voltages are eliminated. Thus, this phase tries to choose the control variables with lowest cost and highest effectiveness. By this attempt, the result set from this phase may

include excessive controls and consequently increase the overall cost. In the worst case, some voltages may violate the opposite voltage limit. To solve these problems, a second phase (bottom-up selection) is employed.

4.4.1 Top-down phase (phase I)

Let Γ be a vector of all violated voltages, i.e., $\Gamma = [V_1, V_2, \ldots, V_N]$ and φ be the set of the most effective control variables to eliminate the violations in network voltages. Phase I obtains the set φ by choosing the control variables with highest CI values. To estimate how much each variable affects the violated voltage, the vector Γ is increased by the value of the control variable sensitivity. This selection is performed sequentially until all violated voltages are within the normal voltage limits. Given N_c as the available number of control variable and x as an index for control variable, the main steps to obtain φ during the top-down phase can be explained in the flowchart shown in Figure 4.3.

4.4.2 Bottom-up phase (phase II)

As mentioned before, top-down strategy might contain more control actions than necessary. This may occur when controls with low CI, like repeated taps of VRs for example, are selected to complete the control process. This high cost control variable (low CI) may be redundant to other control variables in set φ.

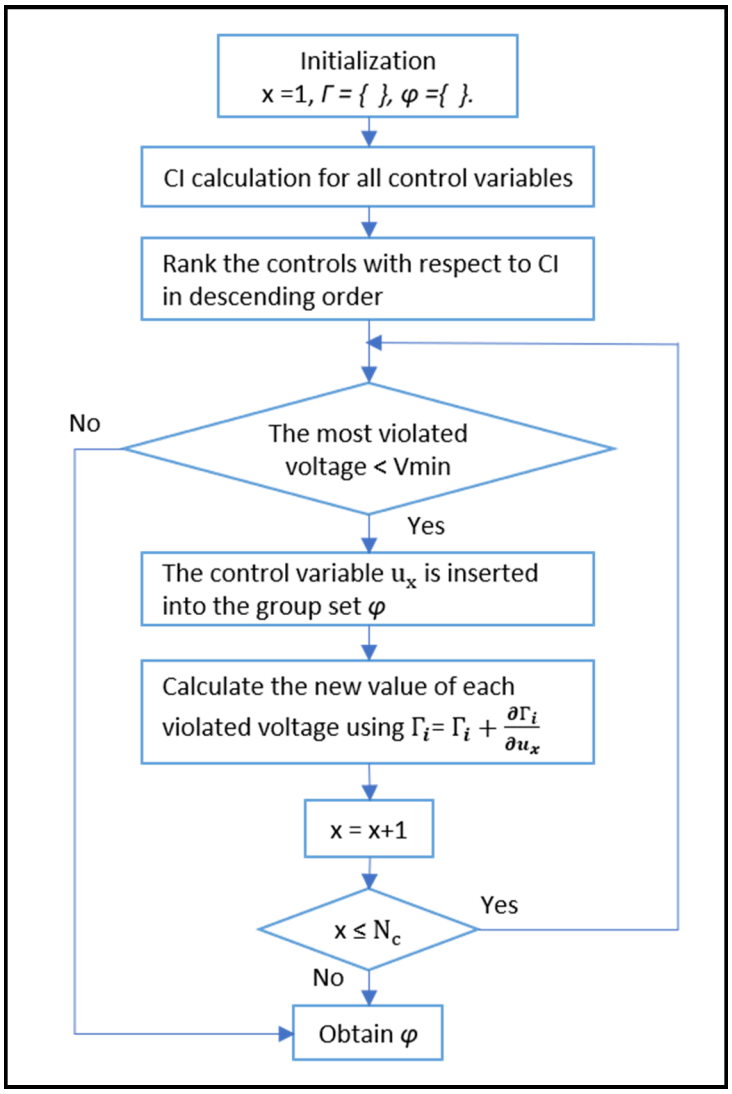

Figure 3.3 A flowchart of the Top-Down phase of the proposed method

To refine the obtained set of control variables φ, phase II evaluates all the control variables in φ, starting from the ones with the higher cost, and eliminates the unnecessary ones. Thus, this phase ranks the controls in φ in ascending order. To estimate how much eliminating each control variable affects the voltages obtained by phase 1 (let £ = { V_1 , V_2…} is the vector of the voltages obtained by phase 1), the value of its sensitivity is subtracted from £. The control variable is considered useless if its removing from φ does not reduce the voltages to a value smaller than Vmin. The set φ′ is the result set by this phase. To obtain a better refinement process, phase 2 can also be performed for each control step k of control variables in the

obtained set φ' starting from the higher step to the lower step. φ'' is the final result set of the most effective controls with low cost.

Given N'_c N''_c as the available numbers of control variables in the group φ and φ'respectively, and x as an index for control variable in the set φ, the main steps to refine φ during the phase II can be explained in the flowchart shown in Figure 3.4.

Remark: the previous steps for the two-phase algorithm takes into account only the undervoltage cases. However, the steps can be modified such that the proposed method considers overvoltage cases. This can be achieved by comparing the most violated voltage with the upper acceptable voltage limit Vmax in phase I. Since the availability takes a negative sign during overvoltage cases (i.e. the term $\partial V_i/\partial u_x$), the new value of violated voltages in the voltage evaluation process will definitely be reduced (instead of increased) by their sensitivities. Similarly, during phase II, the most violated voltage will be compared with Vmax.

4.4.3 Implementation of the proposed voltage control scheme

Figure 3.5 offers an overview of the proposed global voltage control method. It is proposed that the control scheme is implemented using a distribution management system (DMS) for online voltage control. DMS uses pseudo measurements of load and DG generation, and information on system structural changes as inputs. Pseudo measurements can be replaced by installing monitoring devices at the corresponding buses. To transfer the updated information about the status of set-points reference value for DG units and the status of conventional voltage control devices to the control center, DG units and conventional voltage control devices are also proposed to be integrated with a supervisory control and data acquisition (SCADA) system.

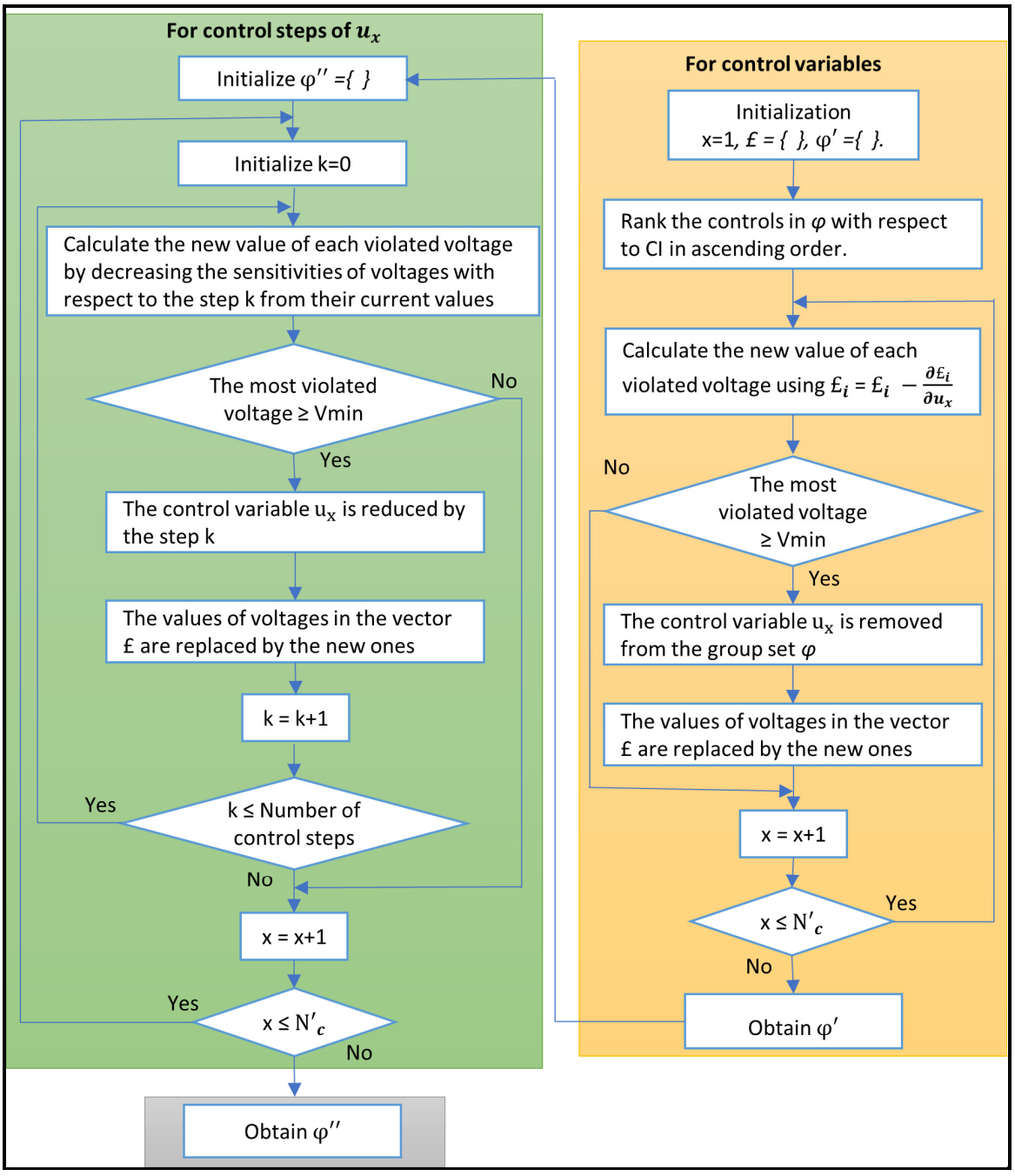

Figure 4.4 A flowchart of the bottom-up phase of the proposed method

Since system reconfiguration can be done online, the structural changes can easily be obtained. If there are no structural changes in the network, the previous values of electric distance are used in the analysis.

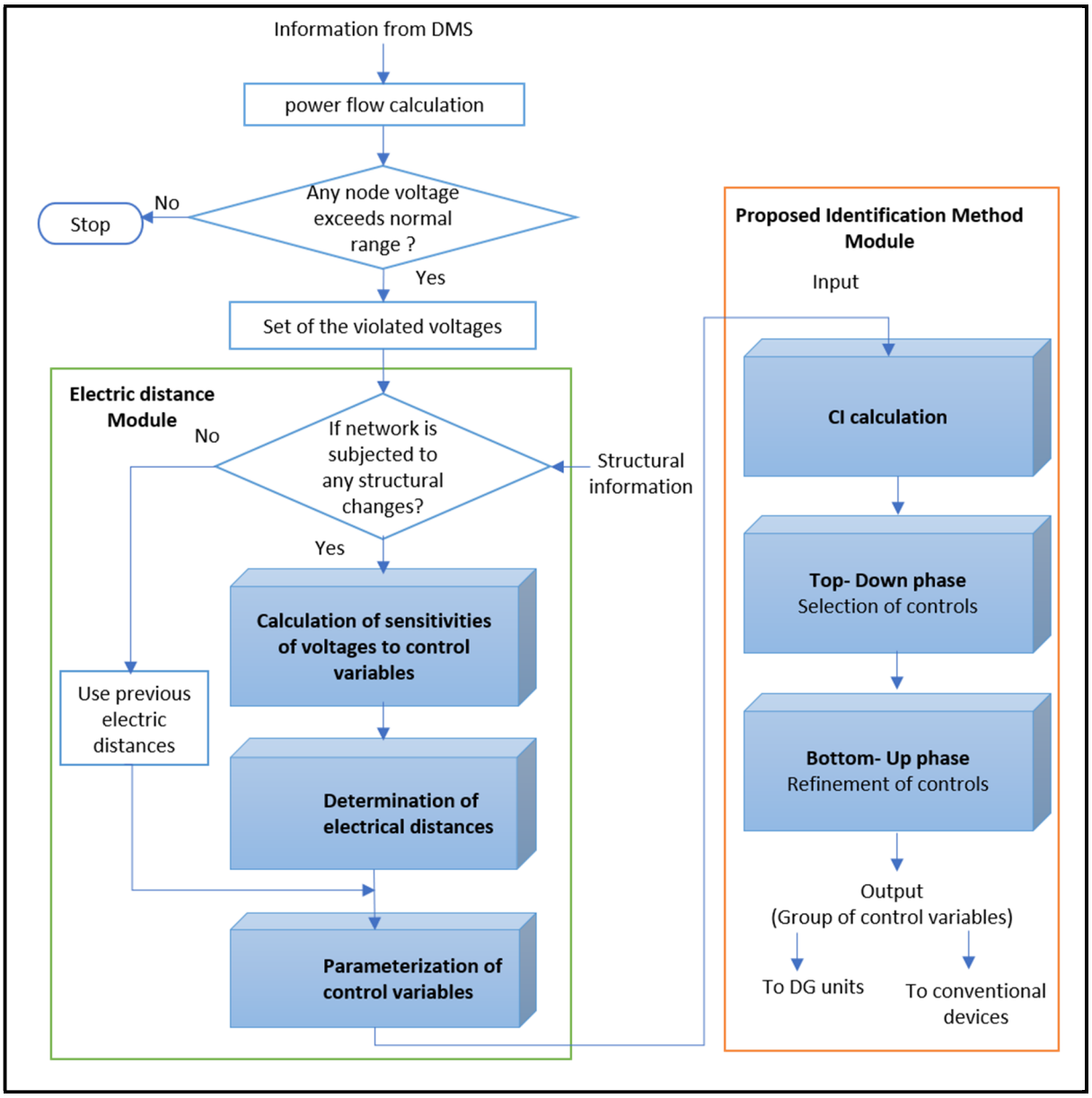

Figure 4.5 An overview of the proposed global voltage control

4.5 Test system and simulation results

To check the validity of the proposed identification technique in coordinated voltage control, the modified IEEE 123-bus distribution network has been used for simulation. The system and

the proposed voltage control approach were simulated in OpenDSS through MATLAB environment. Several scenarios are considered to evaluate the validity of the proposed algorithm in choosing the global group of controls.

The IEEE 123 distribution network was designed as a multi-phase unbalanced system (PES DTF, 2010). In this work, the network is modified to be a three-phase balanced grid as the study in (Zhao et al., 2017). Figure 4.6 represents the one-line diagram of the study system. The normal voltage limits of this system is [0.95, 1.03] p.u. In the modified IEEE 123-bus system, there are three VRs and four CBs. Ten DG units (each with a capability of 400KW and 250KVAR) are also installed at 10 buses.

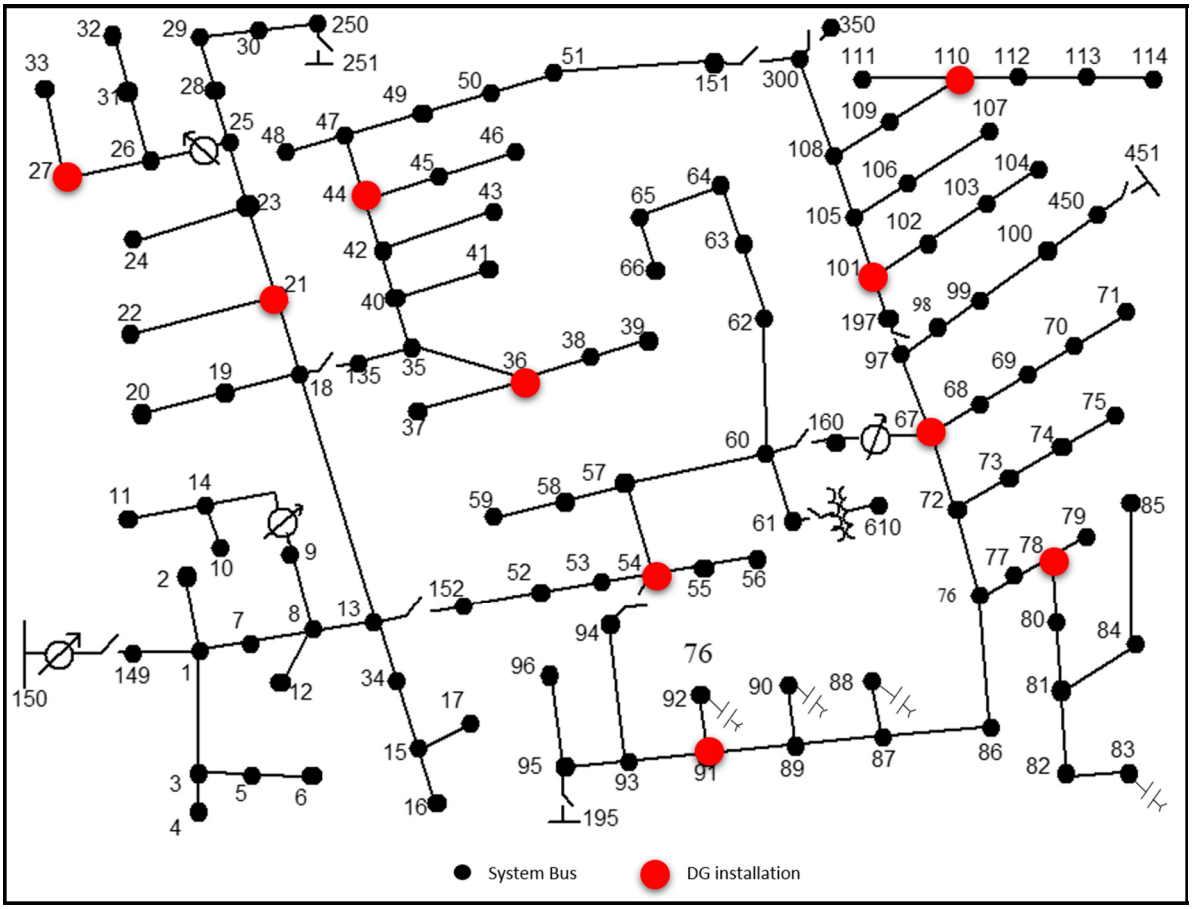

Figure 4.6 The modified IEEE 123-bus system

In this work, the output power by DG units, CBs and VRs were considered available for voltage control. Since time delay for OLTC operation is relatively long, it is not included in the voltage control method proposed in this paper. However, if needed, OLTC can also be included in the proposed method by considering its time delay in the availability aspect.

Actually, the cost values assigned to control variables are directly related to the cost of the device to provide ancillary services. Since the controller can distinguish between the cheap and expensive controls, this paper assumes that the cost of change of reactive power injected by DG units are smaller than the costs of other control variables. This is to obtain a higher voltage support by generating reactive power by DG units. Reduction in tap and switching operations is necessary for reducing their maintenance cost and increase in its lifetime and, thus, a much higher cost could be assigned to them rather than other controls. The cost can be determined by network operators based on the type of control variables. Other factors can also be considered such as the age and the required maintenance of the control variable. In this paper, the cost values are chosen by taking into account the type of control variable. The cost values reflect the relative cost of each control. This work also assumes that there are some differences in the cost for each type of control variables. This just to show ability of the proposed method to distinguish between the controls belonging to the same type.

The availability and cost of the different types of control variables are presented in Table 4.1. Shunt capacitor C_{90} and DG unit DG_{78} are operated at their maximum capacity, i.e., C_{90} =DG_{78} =1 (100%). Thus, these controls are not available for control.

Table 4.1a Availability and cost of voltage regulators

Location	**Availability**	**Cost ($)**
9-14	100%	1000
25-26	100%	1000
160-67	100%	1000

Table 4.1b Availability and cost of shunt capacitors

Bus No.	KVAR	Availability	Cost ($)
83	600	75%	120
88	50	50%	90
90	50	0	90
92	50	100%	90

Table 4.1c Availability and cost of KVAR of DG units

DG location	Capability (KVAR)	Availability	Cost ($)
21	250	10%	23
27	250	50%	25
36	250	50%	25
44	250	75%	25
54	250	50%	20
67	250	100%	25
78	250	0%	20
91	250	75%	23
101	250	100%	20
110	250	100%	23

4.5.1 Scenario one: undervoltage scenario

4.5.1.1 Case 1

In this case, one operating point is chosen as the representative scenario to examine the validity of the proposed technique in selection the control groups. The system operates at high demand and low power generation by DG units. This results in low voltages at some nodes. After computing the electrical distances between control variables and the violated nodes, the proposed method for selection of control variables was employed to obtain the set of the most effective control variables considering the ones with low cost to eliminate the violation in the voltages. The CI values are calculated and presented in Table 4.2 in decreasing order. The table shows that CI values of control variables C_{90} and DG_{78} equals to zero. This because the states of both control variables are at their maximum capacity and therefore there is no available control actions to activate.

Table 4.2 CI values of undervoltage scenario

Control No	CI	Control No	CI	Control No	CI
DG_{101}	0.0196	DG_{27}	0.0063	DG_{21}	0.00085
DG_{110}	0.0154	DG_{36}	0.0058	VR_{25}	0.00058
DG_{67}	0.0144	C_{83}	0.0043	VR_{9}	0.00028
DG_{91}	0.0124	C_{92}	0.0025	DG_{78}	0.0
DG_{54}	0.0100	VR_{160}	0.0022	C_{90}	0.0
DG_{44}	0.0096	C_{88}	0.0012		

From CI calculations, it is also clear that most DG units occupy higher ranks while VRs are at low ranks. This is the philosophy of the proposed technique to give the priority for DG units for voltage support. This was achieved by including the cost aspect in the analysis.

The high CI value in Table 4.2 represents the most effective control with low cost. Top down phase sequentially selects the control variables from Table 4.2 to obtain the lower voltage level (i.e. Vmin= 0.95 p.u) . Bottom-up phase enhances the solution of phase 1 by removing unnecessary control variables. The obtained set of control variables is shown in Table 4.3. It is clear that phase I chooses the first seven control variables of Table 4.3 with a total cost of 161 $. Phase II tried to refine the solution by eliminating the useless control actions, but no one is detected.

Table 4.3 Group of the controls obtained via the two phases of case 1

	Top-Down (Phase I)	**Bottom-Up (Phase II)**
Group of Controls	$DG_{101}, DG_{110}, DG_{67}, DG_{91}, DG_{54}, DG_{44}, DG_{27}$	$DG_{101}, DG_{110}, DG_{67}, DG_{91}, DG_{54}, DG_{44}, DG_{27}$
Cost	161 $	161 $

If the cost aspect was neglected from CI calculation, the global group of control variables would be $VR_{160}, VR_{25}, DG_{101}, DG_{110}, DG_{67}, C_{83}, DG_{91}$, and VR_9 with a total cost of 3211$. This difference in the cost illustrates the necessary for including the cost aspect in the analysis.

The obtained voltage profiles under three conditions: without control, control using the proposed method and control using an optimization problem (with an objective function to minimize the changes in the control variables) are shown in Figure 4.7. It is clear that the proposed method is successfully able to mitigate the violation in voltages.

In this case, the results obtained by phase II match the ones obtained by phase I. This means that there is no redundant in the control variables of the set φ. In other words, any elimination of controls obtained by phase I would cause a violation in the lower level of normal limits (i.e 0.95 p.u).

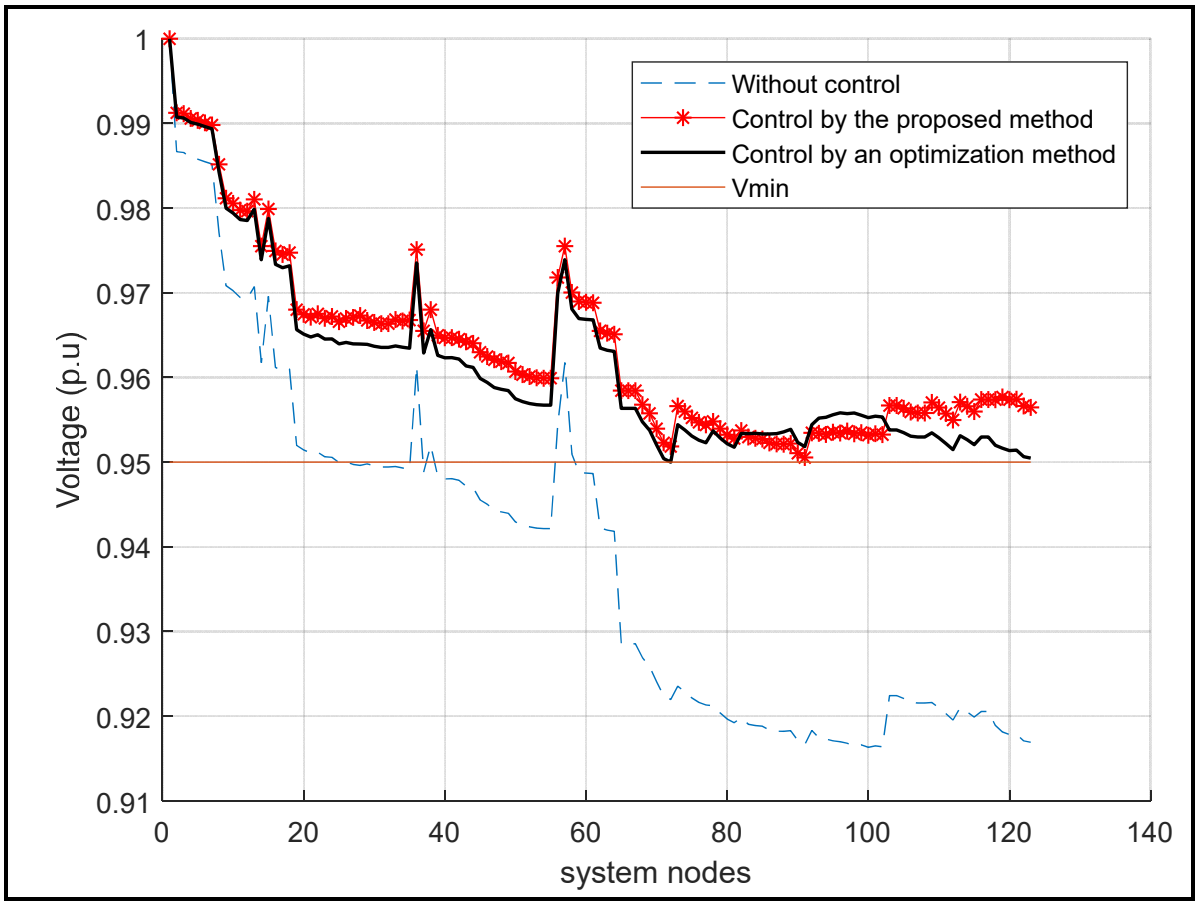

Figure 4.7 A comparison between the estimated voltage profile obtained by the proposed method and the profiles obtained under other conditions of case 1

It is worth mentioning that it was found from the results that most of control variables are used for voltage control through the optimization method. In contrast, only the required controls are used for voltage control during the proposed method. Moreover, it was noticed that the control variables obtained by the proposed method have to participate more than other controls during the optimization method. This validates the accuracy of CI index in selecting the most effective controls. It was also noticed that the control variable with the highest rank have to participate more than other selected controls, which proves the effectiveness of the index CI.

4.5.1.2 Case 2

To show the validity of bottom-up phase in the refinement process, the system is operated at a more severe condition than the previous one. The obtained set of control variables is shown in Table 4.4. It is clear that phase I chooses the first eleven control variables of Table 4.2 with a total cost of 1396 $. Phase II eliminates one control variable, reducing the cost 1306$. To achieve a better refinement, phase II is also performed for step actions of each control variable of the obtained set. The results showed that the bottom-up phase was able to eliminate 14 taps of the control variable VR_{160}, reducing the total cost to 431$ (assuming that the cost for each tap = 1000/16 $).

Table 4.4 Group of the controls obtained via the two phases of case 2

	Top-Down (Phase I)	**Bottom-Up (Phase II)**
Group of Controls	$DG_{101}, DG_{110}, DG_{67}, DG_{91}, DG_{54}, DG_{44}, DG_{27}, DG_{36}, C_{83}, C_{92}, VR_{160}$	$DG_{101}, DG_{110}, DG_{67}, DG_{91}, DG_{54}, DG_{44}, DG_{27}, DG_{36}, C_{83}, VR_{160}$(tap=2)
Cost	1396$	431 $

Table 4.5 compares some of the violated voltages with the new estimated values obtained by the two phases. It is clear that the voltages obtained by the phase I is higher than or equal to the ones obtained by the phase II. This due to the fact that the top-down phase overestimates the control requests to get the lower voltage level. From the results, it is also shown that the voltage at bus 102 is the most violated one. The top-down phase chose many control actions until the most violated voltage was larger than Vmin. This phase tried to mitigate the violation in voltages by selecting controls of low cost such as the reactive power output by DG units. However, the DG units have no enough ability to solve the problem. Controls with higher cost are then included in the group to solve the problem. The bottom-up phase refined the solution obtained by phase 1 by removing the useless actions while maintaining the most violated voltage greater than Vmin.

Table 4.5 Estimated violated voltages with the obtained group of case 2

Bus no	Without control	Top-Down	Bottom-Up
13	0.9543	0.977	0.977
35	0.9389	0.9589	0.9587
48	0.9914	0.9525	0.9522
91	0.9003	1.0352	0.9521
114	0.9008	1.0362	0.9543

The comparison between the estimated voltage profile obtained by the two phases and the profiles under other conditions are shown in Figure 4.8. It is clear that the proposed method is successfully able to mitigate the violation in voltages. We can also see that the voltages obtained by phase I is higher than or equal to the ones obtained by phase II.

The high difference in the voltages at the end of the curve occurs due to the action of control variable VR_{160}. The availability of VR_{160} is 100% which means that there are 16 taps to enact. During phase I, the control variable VR_{160} with its full availability is chosen for control. However during phase II, the bottom- up phase eliminates the useless control actions of VR_{160} (14 taps in this case). This demonstrates the necessary of the bottom-up phase in the selection process to eliminate the unnecessary actions and, hence, reduce the total cost.

4.5.1.3 Case 3

This case shows the performance of the proposed method when most of DG units are installed at the far end of the system. Moreover, this scenario deals with cases where multi DG units are installed at one node or one feeder. Thus, the DG units: DG_{21}, DG_{27}, DG_{36}, DG_{44}, and DG_{54} shown in Figure 4.5 are changed to be placed at the nodes 110, 104, 71, 75 and 85 respectively (but the numbers assigned with DG units remain unchanged despite of changing their locations).

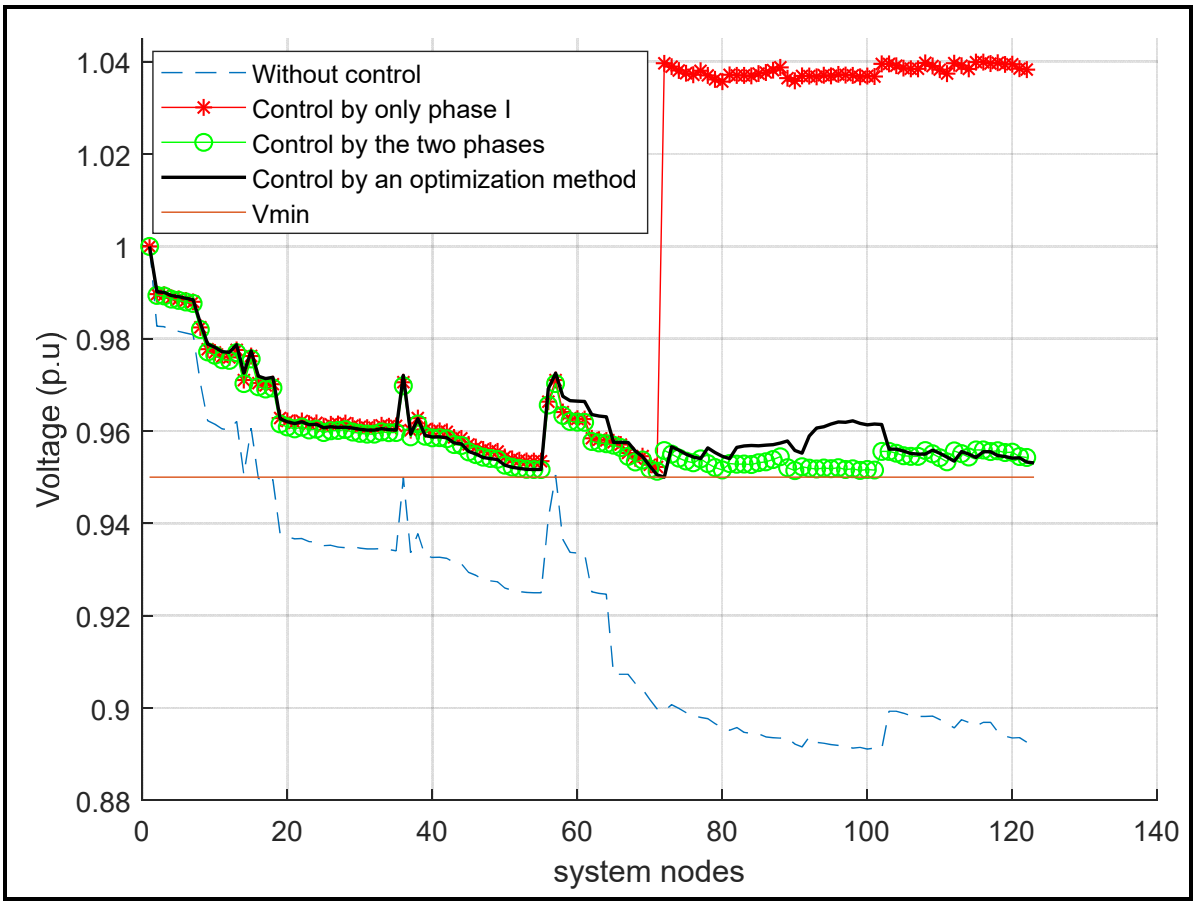

Figure 4.8 A comparison between the estimated voltage profile obtained by the two phases and the profiles obtained under other conditions of case 2

In this scenario, the system also operates at high demand and low power generation by DG units. The obtained set of control variables with the total cost are shown in Table 4.6.

Table 4.6 Group of the controls obtained via the two phases of case 3

	Top-Down (Phase I)	**Bottom-Up (Phase II)**
Group of Controls	$DG_{101}, DG_{110}, DG_{67}, DG_{44}, DG_{91}$	$DG_{101}, DG_{110}, DG_{67}, DG_{44}, DG_{91}$
Cost	116 $	116$

The comparison between the estimated voltage profile obtained by the proposed method and the profiles under other conditions are shown in Figure 4.9. From the results, it is clear that the proposed method was successfully able to eliminate the violations in the voltage by selecting and refining a global group of controls.

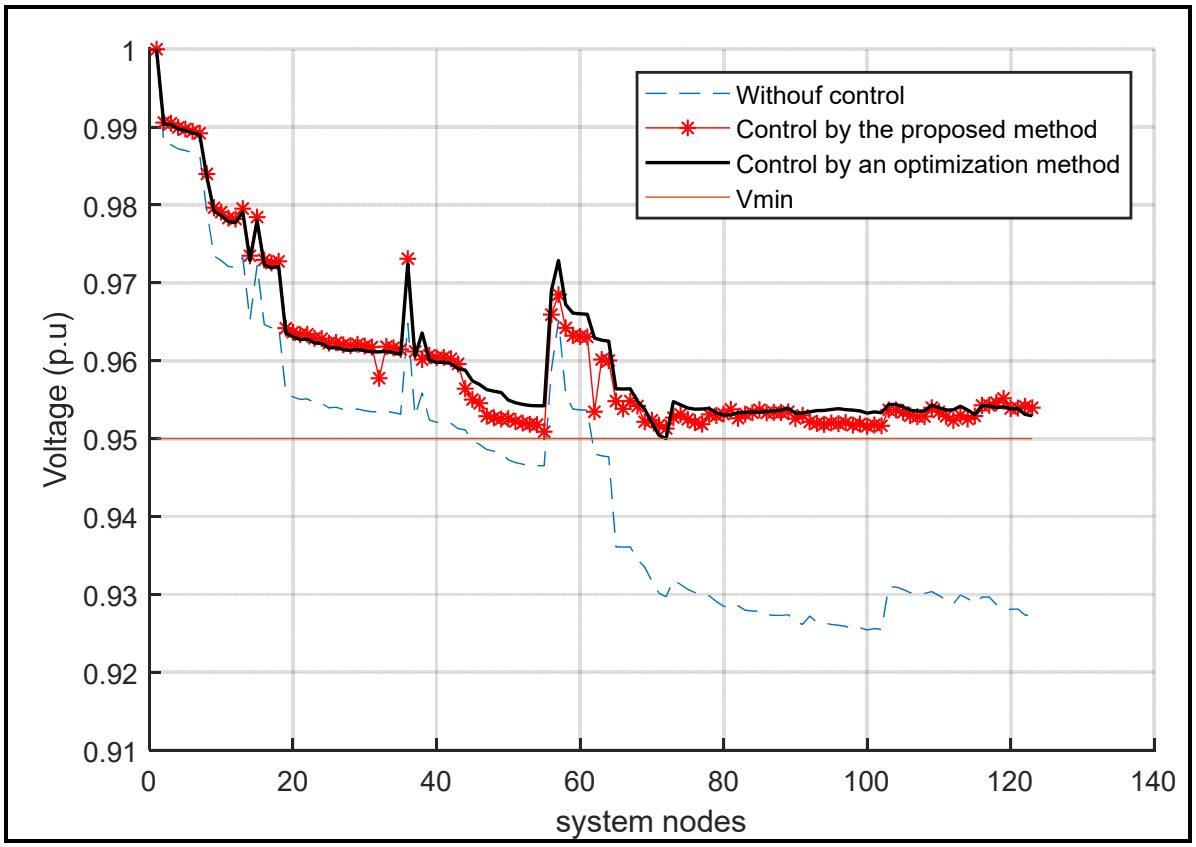

Figure 4.9 A comparison between the estimated voltage profile obtained by the proposed method and the profiles obtained under other conditions of case 3

Since most of the voltages are violated at the far end of the system, we can see that all the selected controls are available near their regions. This validates the accuracy of the proposed controller in the selection process. We can also see that the increase amount in the voltages at the region of 0-60 nodes is less than the amount shown in case 1. This is due to the fact that more controls are required to be activated in the region of 0-60 nodes of case 1.

From Table 4.6 we can also see that although two DG units are located at the same node (DG_{21} and DG_{110}), the controller selects DG_{110} while the unit DG_{21} is ignored. This is due to fact that the proposed method takes into account the availability of control variables in the analysis.

4.5.2 Scenario two: structural changes scenario

To check the validity of the proposed technique during structural changes, the first case of undervoltage scenario is repeated but with closing the switch (151-300) and opening the switch (97-197) of the test system. This will make a change in the values of electric distances between nodes. The result of CI values and the group of the most effective controls (during both phases) are presented in Table 4.7 and Table 4.8 respectively.

It can be seen from table 4.7 that the CI index has a different value and ranking from those presented in scenario 1. Consequently, we can find that there is a change in the result group of control. The bottom-up phase was able to eliminate four control variables (useless ones), saving a cost of 95$. Therefore, the proposed method is able to account for the effect of topology changes in the system. This because the proposed algorithm is based on the concept of the electrical distances.

Table 4.7 CI values of structural changes scenario

Control No	**CI**	**Control No**	**CI**	**Control No**	**CI**
DG_{101}	0.0148	DG_{27}	0.0063	DG_{21}	0.00085
DG_{67}	0.0144	DG_{36}	0.0058	VR_{25}	0.00058
DG_{91}	0.0124	C_{83}	0.0043	VR_{9}	0.00028
DG_{110}	0.0116	C_{92}	0.0025	DG_{78}	0.0
DG_{54}	0.0100	VR_{160}	0.0022	C_{90}	0.0
DG_{44}	0.0096	C_{88}	0.0012		

Table 4.8 Group of the controls obtained via the two phases of scenario 2

	Top-Down (Phase I)	**Bottom-Up (Phase II)**
Group of Controls	$DG_{101}, DG_{67}, DG_{91}, DG_{110}, DG_{54}, DG_{44}, DG_{27}, DG_{36}, C_{83}$	$DG_{101}, DG_{67}, DG_{91}, DG_{110}, C_{83}$
Cost	276 $	181 $

The comparison between the estimated voltage profile obtained by the two phases and the profiles under other conditions are shown in Figure 4.10. It is clear that the proposed method is successfully able to mitigate the violation in voltages by only the obtained five control variables.

4.5.3 Scenario three: overvoltage scenario

In this scenario, the system operates at low power demand and high-power generation by DG units. This results in overvoltage at some nodes. For overvoltage cases, active power curtailments can be included as control variables but with a high cost. KW Capability, availability, and cost of DG units are shown in Table 4.9. The KVAR data presented in Table 4.1c are also used for overvoltage control but with an assumption that the availability is in a negative direction (i.e. the KVAR availability is 100% for DG_{78} and 0% for DG_{110}).

The CI values for controls are calculated and ranked. The results showed that most of KVAR controls occupy higher ranks than active power curtailments due to taking into accounts the cost aspect. By performing the proposed method for identifying the global group of control, we found that the units DG_{78}, DG_{54}, DG_{21}, DG_{27}, DG_{36}, and $DG_{91}$are selected for KVAR control while the units DG_{110}, DG_{67} and DG_{78} are selected for active power curtailment in order to eliminate all the violated voltages.

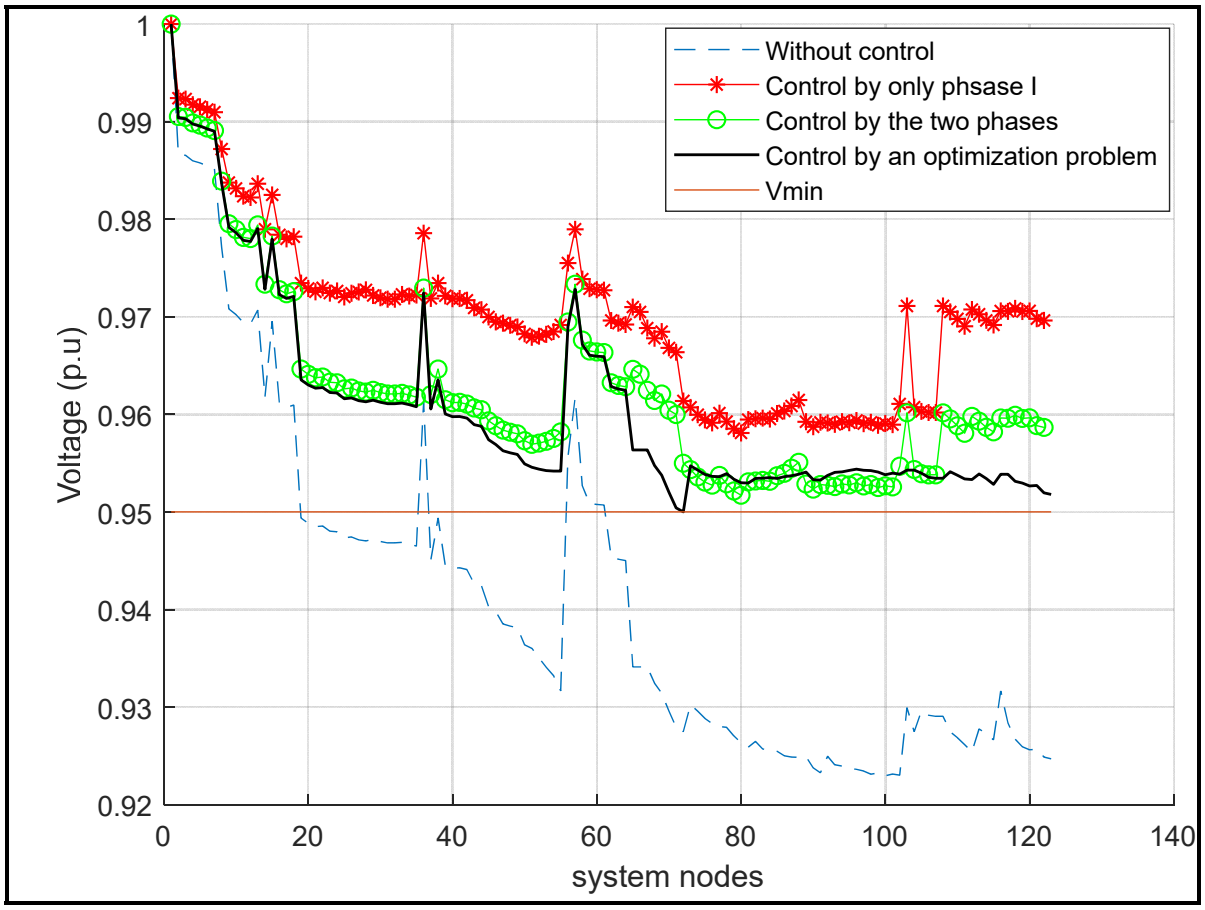

Figure 4.10 A comparison between the estimated voltage profile obtained by the two phases and the profiles obtained under other conditions for scenario 2

Since the availability for DG_{110}, DG_{101}, DG_{67} for overvoltage control is 0%, they aren't selected in the global group of controls. If the cost was not included in the analysis, we will find that most of DG units will be selected for active power curtailments instead of KVAR control. This is due to the fact that most of DG units have high levels of KW availability compared with KVAR capability.

Table 4.9 KW availability and cost of DG units

DG location	capability (KW)	Availability	Cost ($)
21	350	90%	300
27	350	70%	300
36	350	80%	300
44	350	90%	300
54	350	70%	300
67	350	90%	300
78	350	80%	300
91	350	70%	300
101	350	70%	300
110	350	90%	300

The comparison between the estimated voltage profile obtained by the proposed method and the profiles under other conditions are shown in Figure 4.11. It is clear that the proposed method is successfully able to mitigate the violation in the voltages.

4.5.4 Dynamic simulation studies

The applicability of the proposed technique for online voltage control can be examined through dynamic response. The operating condition presented for the case one of undervoltage scenario is repeated for this scenario. The only change is that all DG units are assumed to be solar PV systems. To get a dynamic response, the test system is operated under rapid solar variations. The solar changes start by declining from 100% at t = 0 sec to 0.09% at t=34ses. Then, the changes are stopped for 6 sec. After that, the solar changes start to increase to reach 100% at t = 72 sec. The same cycle is repeated until 120 sec is completed.

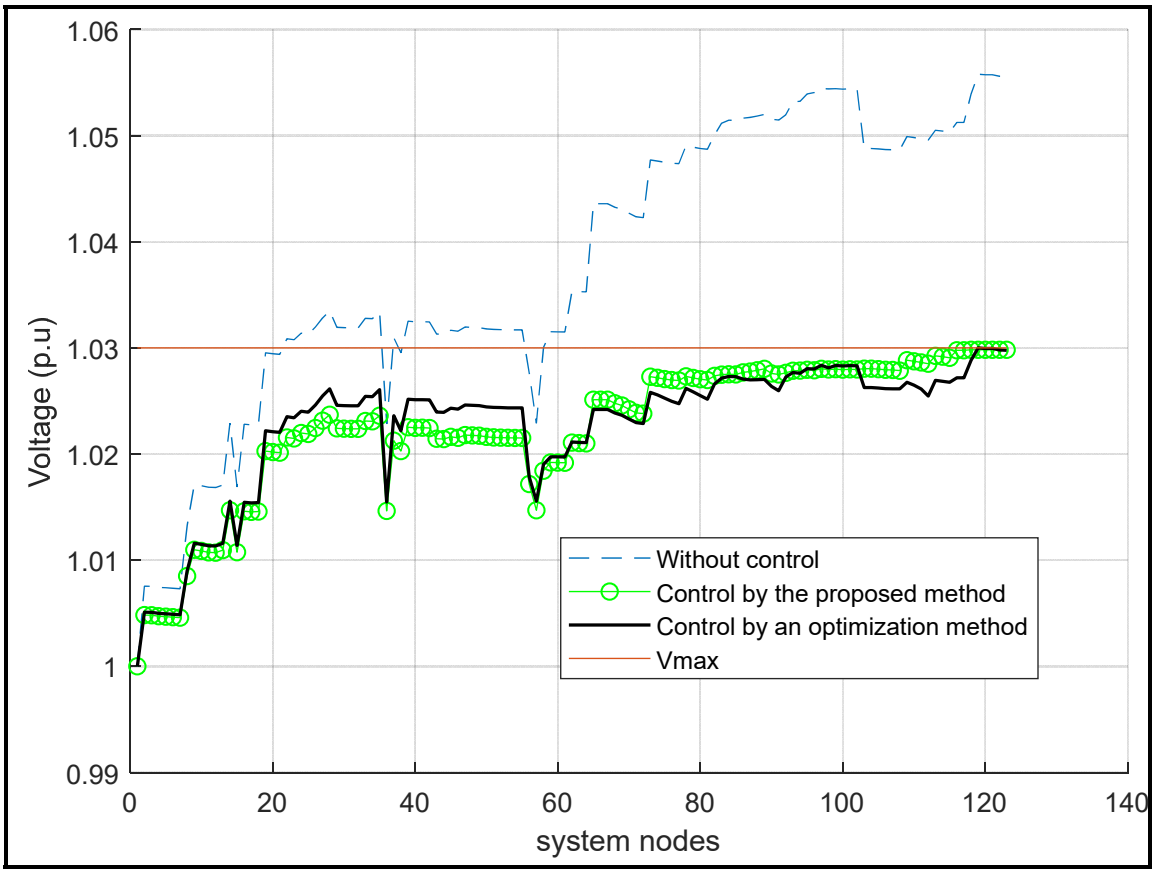

Figure 4.11 A comparison between the voltage profile obtained by the proposed method and the profiles obtained under other conditions for scenario 3

Remark: The obtained controls in the global set in the corresponding case are all DG units. Thus, in order to show the speed of the proposed method, it is assumed that the control actions will take place during seconds. However, control adjustments can be required every minute, 15 minutes, or every day. This is governed by (a) the time delay associated with conventional controls and (b) the available input data to the controller (i.e. load and DG generation).

The node having the most violated voltage, node 85, is chosen for dynamic studies. The comparison between the estimated voltages of node 85 obtained by the proposed method and the voltages with no control is presented in Figure 4. 12. It is clear that the proposed method for voltage control has a very fast response. This is due to the fact that the proposed method has a very simple calculation.

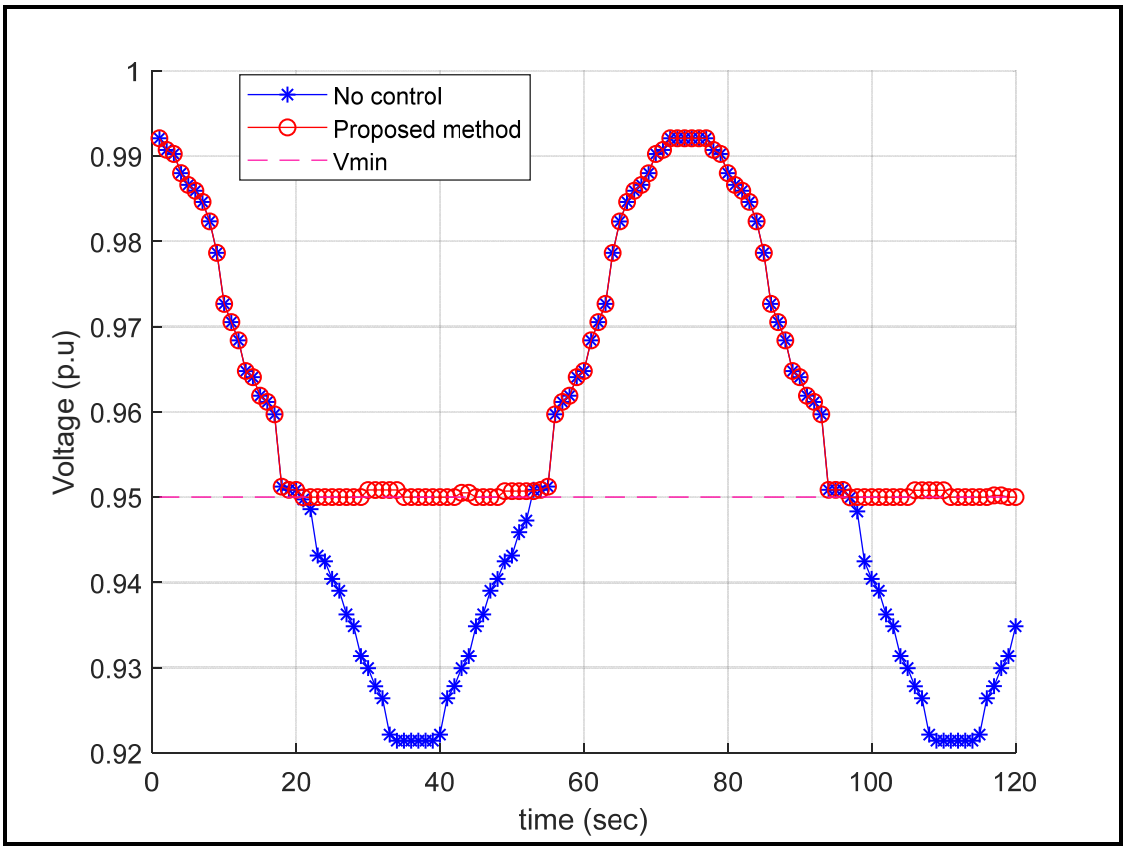

Figure 4. 12 The comparison between the estimated voltages of node 85 obtained by the proposed method and the voltages with no control

4.6 Conclusions

In this work, a new identification method to determine a global group of controls for online CVC for active distribution systems is developed. Only the most effective control variables with the low-cost ones are identified as a global group to simultaneously bring back all the violated voltages inside the normal voltage limits. The proposed technique takes into the consideration the effectiveness, availability, and cost of the control variables as well as the structural changes of networks and the coordination between control variables to simultaneously correct all violated voltages. This method depends on the concept of electrical distances between control variables and system buses. The top-down and bottom-up phases are used to achieve the selection process.

Tests were conducted on the Modified IEEE 123-bus network. The control variables were successfully grouped in terms of their effectiveness and cost to mitigate the violation in the voltages. Activation of the control variables of the obtained group demonstrates that all violated voltages are restored inside the normal limits with a low cost. Thus, the proposed method can guide the network operator to choose the minimum number of controls to eliminate the violations in voltages.

Since the proposed identification algorithm mainly depends on the concept of the electrical distances, the proposed method was effectively also able to account for the effect of topology changes in the grid. The proposed method was also checked in a dynamic simulation. Dynamic results demonstrate the efficacy of the proposed method in voltage control with fast response time.

Further work is required to take into account the OLTC in the proposed voltage considering its time delay and in a dynamic analysis. The transient performance of distribution network under the action of the proposed method and under different scenarios is also part of our vision.

CHAPTER 5

IMPEDANCE SENSITIVITY-BASED CORRECTIVE METHOD FOR ONLINE VOLTAGE CONTROL IN SMART DISTRIBUTION GRIDS

Khaled Alzaareer[1], Maarouf Saad[1], Dalal Asber[2], Serge Lefebvre[2] and Laurent Lenoir[2]

[1] Département of Electrical Engineering, École de Technologie Supérieure,
1100 Notre-Dame Ouest, Montréal, Québec, Canada H3C 1K3
[2] Power Systems and Mathematics, Research Institute of Hydro-Quebec
1740 Boul Lionel-Boulet, Varennes, Québec, Canada J3X 1S1

Paper published in *Electric Power Systems Research*, April 2020

Abstract

With the rapid increase in hosting large penetration levels of Distributed Generation (DG), voltage stability problem has raised a main concern for distribution networks. This study proposes a new centralized voltage control method following a security purpose for active distribution grids. The method is based on a sensitivity analysis to optimally dispatch the control variables. The sensitivity analysis uses a Thevenin- based load impedance margin (TLIM) derived from the nodal measurements to take into the consideration the changes in the system operation, especially those caused by the rapid-response devices of DGs. Sensitivity of load and equivalent impedances to control variables is investigated via the derivation of nodal voltage and current with respect to control variables. Accordingly, the contribution of each control variable in change TLIM and, hence, in voltage control can accurately be obtained. The changes of the impedances of pilot bus, which has the smallest value among all the TLIMs, are formulated in a multi-step optimization problem in terms of impedance sensitivities for the optimal dispatch of controls. The proposed sensitivities and their application in voltage control are successfully validated by a 11-kV distribution grid including 77 bus and hosting 22 DG units. Simulation results show the validity and the accuracy of the proposed sensitivity method in voltage control during different scenarios.

Keywords: Voltage Control; Sensitivity Analysis; Load Impedance Margin; Smart Grids; Distributed Generation; Distribution Networks.

5.1 Introduction

Integration of a high penetration level of DG units has brought significant operational problems upon the distribution networks (Atwa et al., 2010). Over and under voltages are one of the main problems caused by the intermittent generation of DGs. Since DG units have the ability to provide ancillary services, numerous research efforts have focused to utilize DG units in voltage control. A review of the voltage control models proposed for smart distribution networks is presented (Evangelopoulos et al., 2016). The optimization-based technique is one of these approaches to obtain the optimal output power of DG units.

A coordinated voltage control for active distribution networks is proposed (Richardot et al., 2006) to show the ability of DG units to regulate the system voltage. A coordinated voltage control for distribution networks is presented (Biserica et al., 2011) to maintain voltages at their set-point value. A centralized voltage control model based on sensitivity analysis is proposed (Zhou et al., 2007) to minimize the curtailment in active power production of DG units. A short-term scheduling of a distribution system is presented (Borghetti et al., 2010) to minimize the variation in the output of DG units and node voltages. An optimal voltage control is developed (Oshiro et al., 2011) to reduce the voltage deviation in distribution networks using DG units. An optimal voltage control to minimize the deviation in the voltage at pilot bus and the power production by DG units is proposed (Castro et al., 2016). A nonintrusive control strategy using voltage and reactive power for distribution systems based on PV and the nine-zone diagram is presented (Dou et al., 2019). A new mutation fuzzy adaptive particle swarm optimization algorithm is presented (Yang et al., 2015) to mitigate the overvoltage and minimize total loss in active distribution systems. A new Coordinated voltage control in distribution networks including several distributed energy resources is developed (Kulmala et al., 2014). A multiagent-based dispatching scheme for distributed generators for voltage

support on distribution feeders is presented (Baran et al., 2007). A coordinated voltage control of tap changers and DG units is presented (Jakus et al., 2015) to maximize daily DGs production and minimize the daily losses. A voltage control framework for day-ahead operation is presented (Degefa et al., 2015) with the objective to minimize the power losses and voltage violations in active distribution grids. The voltage control scheme developed (Li et al., 2018) aims to enable high solar penetrations in distribution systems while minimizing the voltage deviations and tap operations. An advanced voltage control scheme is proposed (Olival et al., 2017) for smart microgrids to maximize power generated by DG units. A control approach exploits the reactive power capability of DG units to minimize the power losses and mitigating overvoltages (Kryonidis et al., 2019). An optimal power flow is used for voltage control in medium voltage networks with the objective to minimize the curtailment of DG units and reduce the shedding of controllable loads (Meirinhos et al., 2017). The aforementioned methods formulate the problem as a single step optimization. To compensate the modeling inaccuracies, a Model Predictive Control (MPC) is proposed (Valverde et al., 2013) to correct the voltages in active distribution networks. Multi-step optimization is used in the literature to speed-up the computation and to avoid numerical problems (Alamo et al., 2015), (Guo et al., 2017). It can be also used for large scale systems.

Generally speaking, the target voltage or normal operating limits of optimization-based voltage control may follow a security or economical purpose. However, all models proposed in the literature are designed for economic purposes (i.e. minimize the control cost or network losses) or voltage deviation minimization. All researchers focus only on keeping voltage magnitudes of distribution network within normal limits. However, the acceptable voltage magnitude cannot ensure that the system is stable (Lof et al., 1992). According to (Kundur et al., 1994), for a highly reactive power compensated system, voltage instability could happen even if the voltage magnitude is close to the nominal value.

The continuity in integration high penetration levels of DGs in distribution grids could impose a new challenge on network stability. This is due to displacement of a significant portion of the synchronous generation and increase the electrical distances between nodes (Nazari et al.,

2014). Moreover, DG unavailability (or outage) and the continuously fast load increase can also significantly affect the voltage stability in distribution networks. Besides, some types of DG units (i.e. fixed speed wind turbines) always consume reactive power, which may cause voltage instability in distribution systems (Liu et al., 2014). Another essential issue is that when transmission networks meet accidents, the voltage stability in distribution systems may be affected during post disturbances periods. For all these reasons, it is necessary to pay more attention for voltage control following security purposes (i.e. voltage stability issues) in future distribution grids.

Several techniques have been proposed for voltage stability analysis in distribution networks: continuation power flow CPF (Dou et al., 2017), probabilistic evaluation (Liu et al., 2015) and modal analysis technique (Chou et al., 2014). However, all these approaches require extensive calculations that are not suitable for real-time applications. Several voltage stability indicators have been presented by reducing the distribution network into two-bus system (Gubina et al., 1997), (Jasmon et al., 1991), (Hamada et al., 2010). However, those indicators are derived only at one operating point and none of them can involve the dynamic nonlinear behavior of loads.

Since power systems are highly nonlinear, the equivalent network would be adequate for voltage stability assessment under different conditions. With the development of phasor measurement units (PMUs), the situational awareness of the network operators is increased by developing new approaches for voltage stability assessment. In the meanwhile, to include the dynamic nonlinear behavior of power systems, the developed equivalent nodal analysis (Wang et al., 2011) was extended to be used in distribution networks (Alzaareer & Saad, 2018) for voltage stability assessment. The same concept was also used to detect the voltage instability of fixed-speed induction generator in distribution networks (Liu et al., 2014). The equivalent nodal analysis is simple such that Thevenin circuit seen by a load bus can be easily obtained and, then, incorporated into voltage stability assessment. Moreover, the parameters of equivalent impedances can be updated in case of the changes in the system operation, especially those caused by the rapid-response devices of DGs.

The existing Thevenin based methods have a lack of guiding information regarding the decisions of control measures. Thus, performing sensitivity analysis on the parameters of the Thevenin circuits is necessary for voltage stability prediction and control. The information of how each control variable contributes in voltage control is an important issue for network operators.

In this regard, this paper proposes a voltage control model following a security purpose by applying the optimal changes of DG production. On the basis of that, a sensitivity analysis is proposed on the terms of TLIM, which is derived from equivalent nodal analysis, to investigate the optimal dispatch of control variables. The key contributions of this study are:

- Using the common optimization methods for voltage control in distribution networks, the normal operating limits of voltage follow an economical purpose. In contrast, this work uses a voltage stability index, namely TLIM, as a target for voltage control in distribution networks. In other words, not only the voltage profile is considered as a main goal in this study, but also the voltage stability is taken into account.
- The sensitivity analysis is presented for the first time in order to evaluate the sensitivity of the load and the equivalent impedances of a load bus to control variables. These sensitivities are derived via the derivation of nodal voltage and current with respect to control variables. The proposed sensitivities provide an analysis of not only how other buses affect the impedances of a specific load bus but also how the specific bus can affect the impedances of other load buses.
- Compared with the well-known sensitivity techniques that oriented to find the contribution of each control variable in change of voltage stability margin, the proposed sensitivity approach does not require a detailed system model and complex calculation to find the critical point via CPF or the singularity of Jacobian matrix. This feature makes the proposed sensitivity method suitable for real-time voltage control in distribution networks.
- Simulation results successfully verify the proposed impedance sensitivities and validate that they can accurately find the optimal dispatch of control variables and demonstrate their accuracy in voltage control.

The rest of the paper is as follows: Section 2.2 presents the Equivalent Nodal Analysis to formulate TLIM. Section 2.3 uses the sensitivity analysis to derive the change of TLIM due to control variable changes. The optimization-based Voltage Control Scheme is presented in section 2.4. Section 2.5 shows the results and discussion.

5.2 Thevenin based load impedance margin TLIM

TLIM is an index for estimating the voltage stability margin, derived from the equivalent nodal analysis and based on Thevenin's equivalent theory. In general, the nodal current equation of any power system can be written as [V]=[Z][I]. Where Y is the network bus admittance, I and V are bus current and voltage vectors, respectively. The network buses can be classified into generator buses G = {1,…, M}, load buses L = {M+1,…, N} and Tie buses T = {N+1, …, R}. By eliminating the tie buses and reorganizing the nodal equation, we can obtain:

$$\begin{bmatrix} V_G \\ V_L \end{bmatrix} = \begin{bmatrix} Z_{GG} & Z_{GL} \\ Z_{LG} & Z_{LL} \end{bmatrix} \begin{bmatrix} I_G \\ -I_L \end{bmatrix} \tag{5.1}$$

Where Z is the network impedance matrix. From (5.1), the load voltage can be expressed as:

$$V_L = Z_{LG}\, I_G \; - Z_{LL}\, I_L \tag{5.2}$$

The term $Z_{LG}\, I_G$ can be written as:

$$\begin{aligned} Z_{LG}\, I_G &= (\, Z_{i1} I_1 + \cdots + Z_{iM} I_M) \\ &= \sum_{j \,\epsilon\, G} Z_{ij} I_j \end{aligned} \tag{5.3}$$

and the term $Z_{LL}\, I_L$ can be written as:

$$Z_{LL}\, I_L = (Z_{i1} I_{M+1} + \cdots + Z_{ii} I_i + \cdots + Z_{iN} I_N) = \left(Z_{ii} + \sum_{\substack{j \,\epsilon\, L \\ i \neq j}} Z_{ij} \frac{I_j}{I_i} \right) I_i \qquad (5.4)$$

Thus, the voltage at load bus i ϵ L, can be obtained as:

$$V_i = \sum_{j \,\epsilon\, G} Z_{ij}\, I_j - \left(Z_{ii} + \sum_{\substack{j \,\epsilon\, L \\ i \neq j}} Z_{ij} \frac{I_j}{I_i} \right) I_i \qquad (5.5)$$

where I_i and I_j are the current injected at load buses i and j respectively; Z_{ii} and Z_{ij} are the self and coupling impedance of bus i respectively and can be directly obtained using the submatrix Z_{LL}.

Since (5.5) can be written in terms of the Thevenin parameters as $V_i = V_{eq,i} - Z_{eq,i} I_i$, we conclude that:

$$Z_{eq,i} = Z_{ii} + \sum_{\substack{j \,\epsilon\, L \\ i \neq j}} Z_{ij} \frac{I_j}{I_i} \qquad (5.6)$$

Where $V_{eq,i}$ and $Z_{eq,i}$ are the equivalent voltage and impedance referred to load bus i respectively. Based on the Thevenin equivalent theory, the maximum power transfer to a load bus occurs when the load impedance $|Z_L|$ matches the equivalent impedance of the rest of the system $|Z_{eq}|$. TLIM at any load bus i can then be obtained as:

$$TLIM_i = \frac{|Z_{L,i}| - |Z_{eq,i}|}{|Z_{L,i}|} \qquad i \,\epsilon\, L \qquad (5.7)$$

Where $Z_{L,i}$ is the load impedance of bus i and can be found as:

$$Z_{L,i} = \frac{V_i}{I_i} \tag{5.8}$$

Where V_i and I_i are the measured voltage and current at bus i respectively. Based on (5.6) - (5.8), it is clear that the load and the equivalent impedances are based on the nodal current and voltage measurements and the network impedance matrix. This means that this approach requires PMUs to be installed at the load buses to measure the nodal voltage and current. The nodal measurements and the data of Y matrix are sent through Supervisory Control and Data Acquisition (SCADA) system onward to control center. The calculations are then done in control center to obtain the optimal changes in control variables. Those changes are sent to update the reference set-points of controls.

Remark: For practical systems, appropriate PMU placement techniques can be performed first while ensuring the full observability of the network. PMUs can be installed at critical buses where the power is supplied to a couple of nodes or feeders. Thus, all the downstream nodes of each critical bus can be seen as one lumped load impedance. This issue is not part of the present paper and will be studied in our future works.

The value of the TLIM ranges from 0 to 1, and TLIM $= 0$ represents the instability point where $|Z_{eq}|=|Z_L|$ (as proposed in other Thevenin- based indices (Liu et al., 2014),(Li et al., 2017),(Matavalam et al., 2017)). For large power systems, the smallest value among all the TLIMs can be selected to represent the system margin (i.e. pilot node) as (Wang et al., 2011):

$$TLIM = min\ (TLIM_i) \qquad i \in L \tag{5.9}$$

To show the behavior of the proposed TLIM in determining the distance to voltage instability, let us consider the R–X diagram in Figure 5.1. If the load impedance $|Z_L|$ is moved from B to B′ or the radius of the equivalent impedance $|Z_{eq}|$ is increased from A to A′, the TLIM will

decrease. If $|Z_L|$ is located inside the circle with a radius $|Z_{eq}|$, the system is unstable. Therefore, it is necessary to keep $|Z_L|$ far away from the circle of Z_{eq} to maintain a safe stability and operation.

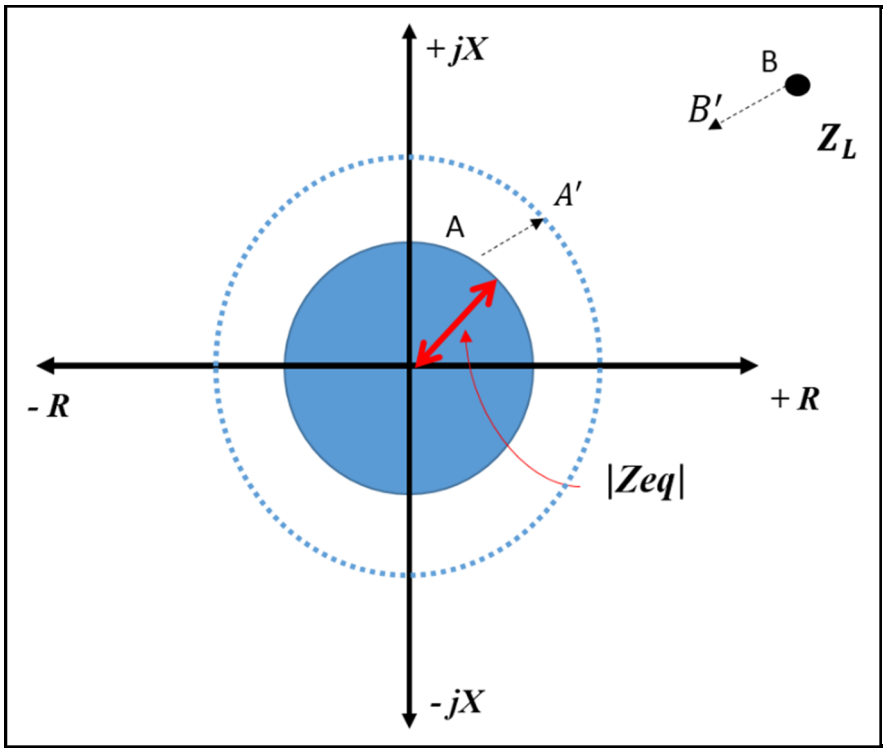

Figure 5.1 R–X diagram for TLIM

It is worth mentioning that $|Z_{eq}|$ is not a constant value and varies following the dynamic behavior of power systems. Since the derived TLIM is based on equivalent nodal analysis, it can easily capture any change in system operation and, hence, the increment or decrement in $|Z_{eq}|$ as illustrated in (5.6).

5.3 TLIM-based sensitivity analysis

According to section 5.2, any change in load power consumption (i.e. load current) or voltage of load bus i will result in an increase or decrease in the load impedance. Similarly, any change in the current or voltage of other load buses will result in an increment or decrement in the

equivalent impedance seen by the load bus i. To explain how control variables can vary the impedances referred to a load bus, let us consider the small distribution system shown in Figure 5.2.

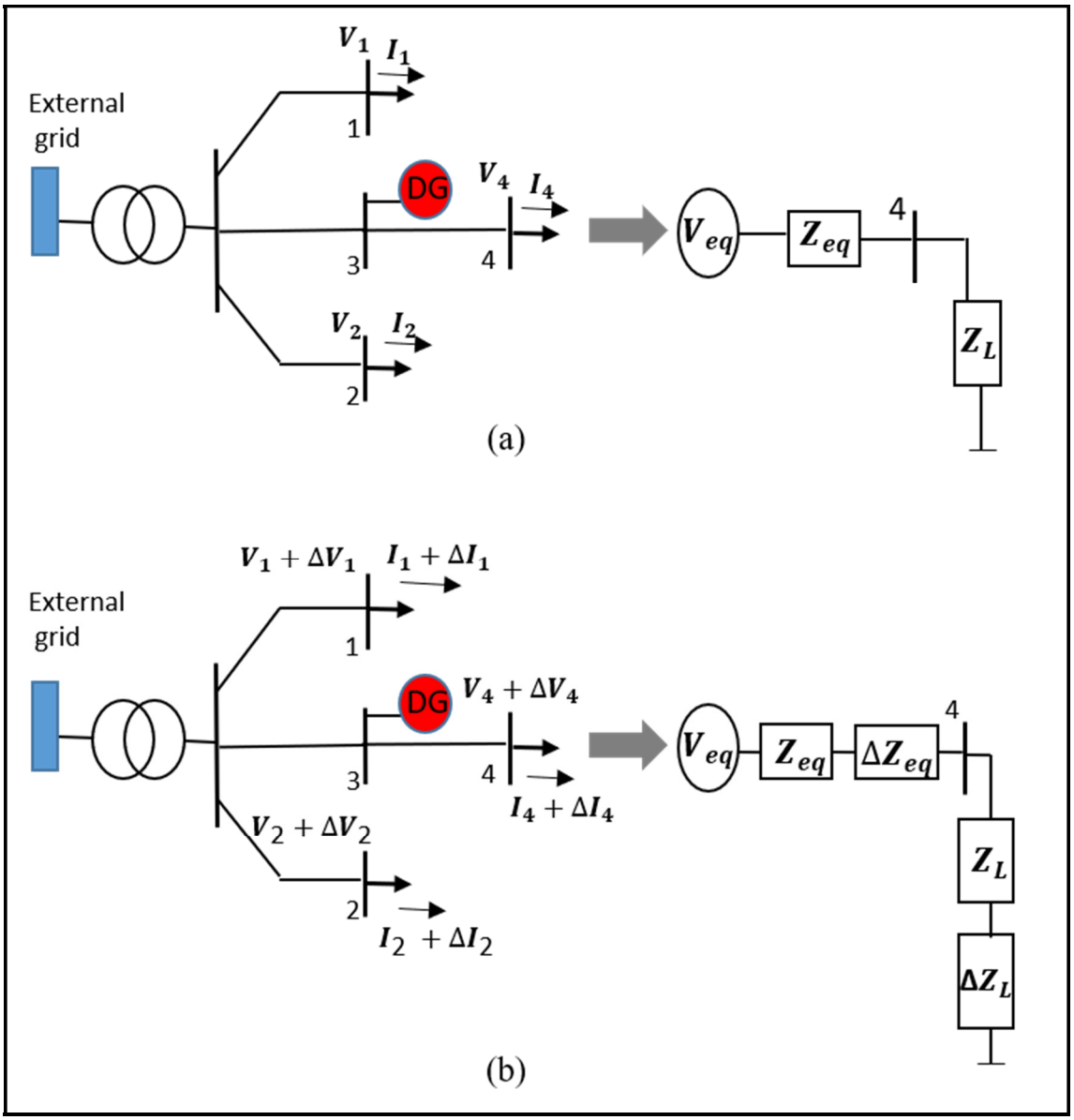

Figure 5.2 Simple distribution system with simplified circuit referred to bus 4
(a) before and (b) after injecting power by DG

The network consists of 3 load buses (1, 2 & 4) and one bus for DG installation (bus 3). It is assumed that DG unit operates with constant output power. As we explained in section II, to assess the voltage stability at bus 4, the network can be simplified to Thevenin equivalent circuit as shown in Figure 5.2a. Any increase or decrease in power injected by DG unit will cause the voltages and branch currents to change by ΔV_L, ΔI_L respectively. By referring to (5.6) & (5.8), we can conclude that the load and the equivalent impedances referred to a load bus 4 will vary by ΔZ_L, ΔZ_{eq} respectively, as shown in Figure 5.2b. Accordingly, the voltage stability of any load bus can be estimated as expressed in (5.7).

However, no further information is available to guide the decisions of control measures. To provide such information, sensitivity analyses on the load and the equivalent impedances is performed in this study to examine the impact of control variables (i.e. nodal power injection) on these impedances. Accordingly, the contribution of each control variable in change TLIM can be easily obtained. This helps network operators to take a global measure to improve the nodes voltages as well as the voltage stability.

5.3.1 Sensitivity of load bus voltages to control variables

Sensitivity of a load bus voltage to any change in control variable u_x can be calculated as:

$$\frac{dV_i}{du_x} = e^{j\theta_i}\left(\frac{d|V_i|}{du_x} + j|V_i|\frac{d\theta_i}{du_x}\right) \tag{5.10}$$

Where $|V_i|$ and θ_i are the node i voltage magnitude and angle respectively. Assuming that the control variables are only the power injected by DG, $d|V_i|/du_x$ and $d\theta_i/du_x$ can be obtained from the inverse of Jacobian matrix J as:

$$\begin{bmatrix}\Delta|V| \\ \Delta\theta\end{bmatrix} = [J]^{-1}\begin{bmatrix}\Delta P \\ \Delta Q\end{bmatrix} = \begin{bmatrix}\frac{\partial|V|}{\partial P} & \frac{\partial|V|}{\partial Q} \\ \frac{\partial\theta}{\partial P} & \frac{\partial\theta}{\partial Q}\end{bmatrix}\begin{bmatrix}\Delta P \\ \Delta Q\end{bmatrix} \tag{5.11}$$

Where $\partial|V|/\partial P$ and $\partial|V|/\partial Q$ are the sensitivity vectors of nodal voltage magnitude to real and reactive power injection, respectively. $\partial\theta/\partial P$ and $\partial\theta/\partial Q$ are the sensitivity vectors of nodal voltage angle to real and reactive power injection, respectively.

5.3.2 Sensitivity of load currents to control variables

The load current at any bus i can be calculated as:

$$I_i = \frac{S_i^*}{V_i^*} \tag{5.12}$$

Where S_i is complex power of bus i. Thus, the sensitivity of any load current to control variable can be obtained by:

$$\frac{dI_i}{du_x} = \frac{d\left\{\frac{S_i^*}{V_i^*}\right\}}{du_x} = \frac{V_i^* \frac{dS_i^*}{du_x} - S_i^* \frac{dV_i^*}{du_x}}{V_i^{*2}} \tag{5.13}$$

At constant load impedance, the term S_i^* can be written as:

$$S_i^* = \frac{|V_i|^2}{Z_{L,i}} \tag{5.14}$$

Thus, the sensitivity S_i^* to control variable can be calculated as:

$$\frac{dS_i^*}{du_x} = \frac{2\,V_i}{Z_{L,i}} \frac{dV_i}{du_x} \tag{5.15}$$

By substituting (5.14) & (5.15) into (5.13), we obtain:

$$\frac{dI_i}{du_x} = \frac{I_i}{V_i^*}\left(2\frac{dV_i}{du_x} - \frac{dV_i^*}{du_x}\right) \tag{5.16}$$

5.3.3 Sensitivity of load impedances to control variables

The sensitivity of load impedance $Z_{L,i}$ to control variable u_x can be found by taking the derivation of (5.8) with respect to u_x:

$$\frac{dZ_{L,i}}{du_x} = \frac{d\left\{\frac{V_i}{I_i}\right\}}{du_x} = \frac{I_i\frac{dV_i}{du_x} - V_i\frac{dI_i}{du_x}}{{I_i}^2} \tag{5.17}$$

By substituting (5.16) into (5.17), we obtain:

$$\frac{dZ_{L,i}}{du_x} = \frac{\left(1 - \frac{2V_i}{V_i^*}\right)\frac{dV_i}{du_x} + \frac{V_i}{V_i^*}\frac{dV_i^*}{du_x}}{I_i} \tag{5.18}$$

5.3.4 Sensitivity of equivalent impedances to control variables

The sensitivity of the equivalent impedance referred to a load bus i to control variable u_x can be calculated by taking the derivation of (5.6) with respect to u_x as:

$$\frac{dZ_{eq,i}}{du_x} = \sum_{\substack{j \in L \\ i \neq j}} Z_{ij}\frac{d\left(\frac{I_j}{I_i}\right)}{du_x} = \sum_{\substack{j \in L \\ i \neq j}} Z_{ij}\ \frac{I_i\ \frac{dI_j}{du_x} - I_j\frac{dI_i}{du_x}}{{I_i}^2} \tag{5.19}$$

By substituting (5.16) for the buses i & j into (5.19), we obtain:

$$\frac{dZ_{eq,i}}{du_x} = \sum_{\substack{j=1 \\ i \neq j}} \frac{Z_{ij} I_j}{I_i} \left(\frac{2}{V_j^*} \frac{dV_j}{du_x} - \frac{2}{V_i^*} \frac{dV_i}{du_x} - \frac{1}{V_j^*} \frac{dV_j^*}{du_x} + \frac{1}{V_i^*} \frac{dV_i^*}{du_x} \right) \tag{5.20}$$

5.3.5 Calculation the change of TLIM

By obtaining the sensitivities $dZ_{L,i}/du_x$ and $dZ_{eq,i}/du_x$, we can obtain that:

$$\Delta Z_{L,i} = \sum_{x=1}^{M} \frac{dZ_{L,i}}{du_x} \Delta u_x \tag{5.21}$$

$$\Delta Z_{eq,i} = \sum_{x=1}^{M} \frac{dZ_{eq,i}}{du_x} \Delta u_x \tag{5.22}$$

Whrere $\Delta Z_{L,i}$ & $\Delta Z_{eq,i}$ are the change in the load and equivalent impedances referred to load bus i respectively. Δu_x represents the change in the control variable x. M represents the number of control variables. The new TLIM that results due to the changing in control variables can be found as:

$$TLIM_{i,new} = \frac{\left|Z_{L,i} + \Delta Z_{L,i}\right| - \left|Z_{eq,i} + \Delta Z_{eq,i}\right|}{\left|Z_{L,i} + \Delta Z_{L,i}\right|} \tag{5.23}$$

From (5.21)-(5.23), it is clear that the change in any control variable (i.e. the power injected) at a particular load bus will not only affect the voltage stability (TLIM) of its own bus, but also

the stability of other buses. According to (5.18) & (5.20), the proposed sensitivities can be used to investigate the coupling effect of the load buses in TLIM and to assess the impact of change of the power injected by any DG to the load and the equivalent impedances and, hence, voltage stability.

5.4 Voltage control scheme

The voltage control approach proposed in this study is based on a multi-step optimization to smoothly correct the voltages. The approach is inspired from MPC to predict the behavior of the system over interval of n discrete steps (Valverde et al., 2013). Since the pilot bus can determine the overall performance of the network, the main objective in this study is to minimize the deviation in the margin (TLIM) of the pilot bus. Accordingly, a standard Quadratic Programming problem can be formulated as:

$$min \sum_{k=0}^{n-1} \left\| Ref - TLIM_p(t+k) \right\|^2 \tag{5.24}$$

Ref is the target value for the index TLIM and equals 1. t represents the time instant and n represents the length of the prediction or control horizon. $\mathrm{TLIM_p(t+k)}$ is the predicted voltage stability margin of pilot bus given the measurements at time instant t. By substituting (5.23) into (5.24), (5.24) becomes:

$$min \sum_{k=0}^{n-1} \left\| \frac{|Z_{eq,p} + \Delta Z_{eq,p}(t+k)|}{|Z_{L,p} + \Delta Z_{L,p}(t+k)|} \right\|^2 \tag{5.25}$$

Where $\mathrm{\Delta Z_{L,p}(t+k)}$ and $\mathrm{\Delta Z_{eq,p}(t+k)}$ represent the change of the load and the equivalent impedances referred to pilot bus at time $\mathrm{t+k}$ respectively. The subletter p denotes for pilot bus. By substituting (5.21) & (5.22) into (5.25), we obtain:

$$min \sum_{k=0}^{n-1} \left\| \frac{\left| Z_{eq,p} + \sum_{x=1}^{M} \frac{dZ_{eq,p}}{du_x} \Delta u_x(t+k) \right|}{\left| Z_{L,p} + \sum_{x=1}^{M} \frac{dZ_{L,p}}{du_x} \Delta u_x(t+k) \right|} \right\|^2 \tag{5.26}$$

Where $\Delta u_x(t+k)$ is the change of control variable x at time $t+k$. For practical purposes, another objective function can be included to minimize the changes of the control variables. As a result, the following optimization problem can be used:

$$Min \quad w \sum_{k=0}^{n-1} \left\| \frac{\left| Z_{eq,p} + \frac{dZ_{eq,p}}{du} \Delta u(t+k) \right|}{\left| Z_{L,p} + \frac{dZ_{L,p}}{du} \Delta u(t+k) \right|} \right\|_G^2 + (1-w) \sum_{k=0}^{n-1} \| \Delta u(t+k) \|_G^2 + \| \varepsilon \|_H^2 \tag{5.27}$$

Subject to:

$$-\varepsilon_1 A + V_i^{min} \le V_i(t+k) \le V_i^{max} + \varepsilon_2 A$$

$$V_i(t+k) = V_i(t+k-1) + \frac{\partial |V|}{\partial u} \Delta u_i(t+k)$$

$$\Delta Q_x{}^{min} \le \Delta Q_x(t+k) \le \Delta Q_x{}^{max}$$

$$\Delta P_x{}^{min} \le \Delta P_x(t+k) \le \Delta P_x{}^{max}$$

$$P_x{}^{min} \le P_x(t+k) \le P_x{}^{max}$$

$$Q_x{}^{min} \le Q_x(t+k) \le Q_x{}^{max}$$

Where $0 \le w \le 1$ is to penalize each objective function. $\frac{dZ_{L,p}}{du} = [\frac{dZ_{L,p}}{dP}, \frac{dZ_{L,p}}{dQ}]$ and $\frac{dZ_{eq,p}}{du} = [\frac{dZ_{eq,p}}{dP}, \frac{dZ_{eq,p}}{dQ}]$ are the sensitivity vectors of the load and equivalent impedances of pilot bus to control variables respectively. $\frac{dZ_{L,p}}{dP}, \frac{dZ_{eq,p}}{dP}$ and $\frac{dZ_{L,p}}{dQ}, \frac{dZ_{eq,p}}{dQ}$ represent the sensitivity vectors

of the load and equivalent impedances of pilot bus to real and reactive power injected by DGs respectively. $\Delta u = [\Delta P, \Delta Q]^T$ represents the vector of changes of control variables. 'T' represents array transposition. ΔP & ΔQ represents the vector of changes of real and reactive power injected by DGs respectively. $\varepsilon = [\varepsilon_1, \varepsilon_2]^T$ is the vector of slack variables used and relax the voltage constraints. 'A' denotes a unitary vector. G is a weight matrix used to penalize the "expensive" generation control variables. The weight matrix H is used to penalize the slack variables. $V_i(t+k)$ is the predicted voltage magnitude of bus i given the measurements at time instant t. $V_i(t+k-1)$ is the measured voltage magnitude of bus i at time instant t. $\frac{\partial |V|}{\partial u} = [\frac{d|V|}{dP}, \frac{d|V|}{dQ}]$ is the sensitivity matrix of bus voltage magnitudes with respect to the control variables. P_x& Q_x are the real and reactive power injected by DG 'x' respectively. ΔP_x & ΔQ_x are the change in real and reactive power injected by DG 'x' respectively. $\Delta P_x{}^{min}$, $\Delta P_x{}^{max}$, $\Delta Q_x{}^{min}$and $\Delta Q_x{}^{max}$ represent the limits for the change in real and reactive power injected by DG 'x'. DG limits are included in the optimization problem (i.e. the third and fourth constraints) to protect the equipments (i.e. machines or inverters) against fast ramping and to create a cautious environment for distributing the control actions. However, those limits can be provided for use in the constraint set according to data provided by equipment's manufactures.

Remark: Several algorithms can be used to solve the optimization problem. They are very known methods for researchers. However, since the objective of this work is not to show how optimization problems can be solved, any optimization modeling tool can be used to obtain the optimal changes in control variables.

It is worth mentioning that the proposed method is more flexible such that it can incorporate conventional voltage control devices in the optimization problem to avoid any interaction between control variables. This requires the following changes in the optimization problem:

- Modify the vector of changes of control variables (Δu) in (5.27) to contain those other devices (i.e. $\Delta u = [\Delta P, \Delta Q, \Delta VCD_1, \Delta VCD_2, \dots \Delta VCD_i]^T$) where ΔVCD_i represent the

change in the ith other voltage control device (i.e. the voltage set-point of voltage regulators).

- Add new constraints to the optimization problem such as the limits of voltage control devices and capacitor banks integer positions.
- As expressed in equations (5.18) and (5.20), the sensitivities $\frac{dZ_{eq,p}}{du}$ and $\frac{dZ_{L,p}}{du}$ depend on the sensitivity $\frac{dV}{du_x}$. As shown in section 5.1, if the control variables are only the power injected by DG, the term $\frac{dV}{du_x}$ can be directly obtained from the inverse of Jacobian matrix J. However, for other control variables, the term $\frac{dV}{du_x}$ can be found by linearizing the power flow equations $F(V, u_x) = 0$ as (assuming that the load parameter is constant at current operating point):

$$\frac{dF}{dV}\Delta V + \frac{dF}{du_x}\Delta u_x = 0$$

Where $\frac{dF}{dV}$ equals to Jacobian matrix at the base case and $\frac{dF}{du_x}$ is known. Thus, $\frac{\Delta V_i}{\Delta u_x}$ (or $\frac{dV}{\mathrm{du_x}}$) can be easily found.

The proposed method is also flexible such that it can incorporate remotely controlled switches in the optimization problem. This also requires to modify the vector of changes of control variables (Δu) in equation (5.27) to contains remotely controlled switches and to add new constraints to the optimization problem such as the connection status of remotely controlled switches. If the control variable is a remotely controlled switch, the term $\frac{dV}{du_x}$ can be approximated by computing the variations of the bus voltages due to remotely controlled switch action. This information can be easily extracted from the solution of two power flow runs with a remotely controlled switch action.

The proposed algorithm can be implemented in the control center of distribution network as follows:

1. The data of network admittance matrix Y and the nodal measurements are collected from SCADA system and PMUs.
2. If the network is subjected to structural changes, update the admittance matrix Y. Otherwise, use the previous matrix.
3. If the network is subjected to DG unavailability, recalculate the submatrix Z_{LL}. Otherwise, use the previous Z_{LL}.
4. Calculate the load and the equivalent impedances and TLIM for the interested load buses using (5.6), (5.7) & (5.8), and determine the pilot bus.
5. Calculate the voltage and current sensitivities of pilot bus to control variables using (5.10) & (5.16).
6. Calculate the sensitivities of the load and equivalent impedances of pilot bus to control variables using (5.18) & (5.20).
7. Construct and solve the optimization problem in (5.27) and apply the control actions.

If all voltages are within the normal range, process is finished. Otherwise, go to step 4.

5.5 Simulation results

To verify the applicability and robustness of the proposed method, 77-bus, 11 kV distribution grid shown in Figure 5.3 is used as a test system. The network consists of 22DG units and 53 load bus. The system base is 100 MVA. The line parameters and load data are available in (UKGDS, 2005). The system and the proposed approach have been simulated in MATLAB under different operating conditions. LINGO software was interfaced with MATLAB to solve the real time optimization problem.

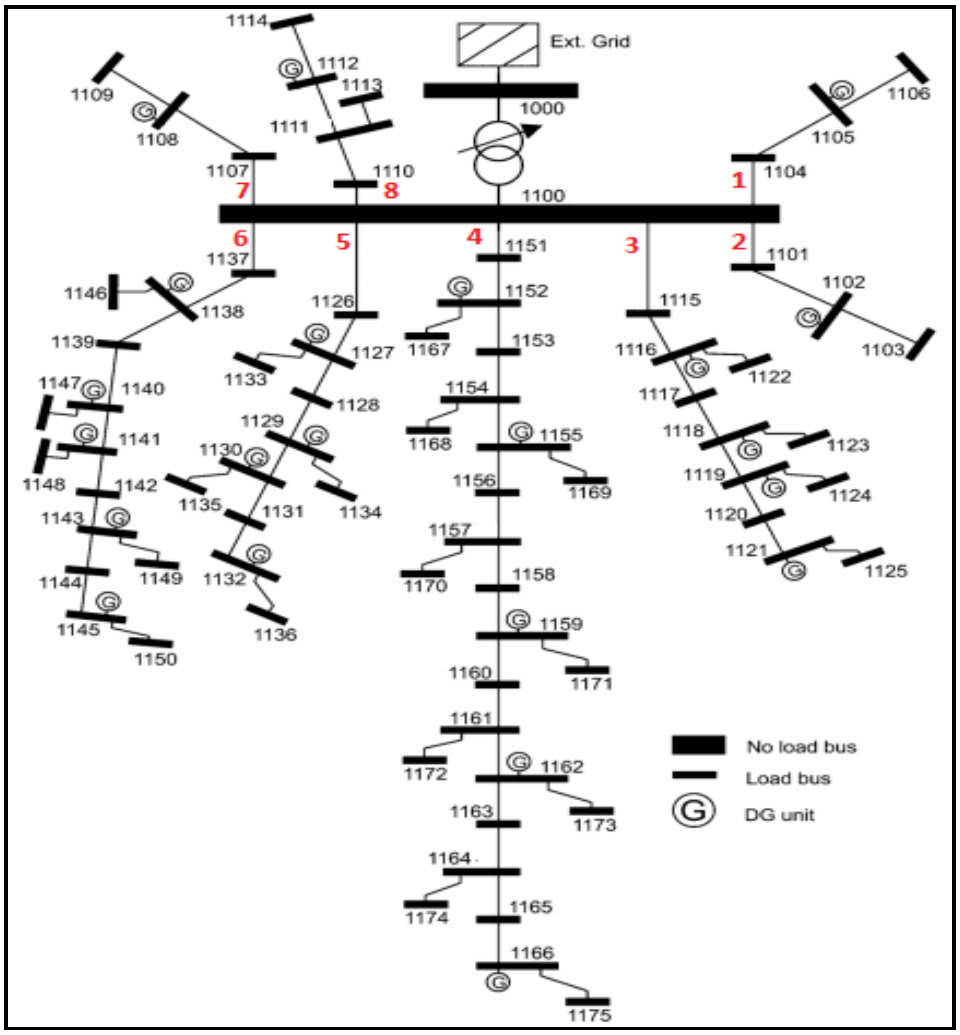

Figure 5.3 Topology of the test system
Taken from Valverde et al. (2013)

5.5.1 Verification of the impedance—based sensitivities

In this scenario, the system is operated under base load condition with no DG integrated to the system. The sensitivities $|dZ_L/dP|, |dZ_L/dQ|$ and $|dZ_{eq}/dP|, |dZ_{eq}/dQ|$ of the load buses are demonstrated in Figures. 5.4 and 5.5 respectively. It is clear from Figure 5.4 that all the sensitivities are positive, which indicates that increase in nodal active or reactive power injection will increase the load impedances. In contrast, the positive values of sensitivities in Figure 5.5 indicate that increase in nodal active or reactive power injection will decrease the equivalent impedances. The resulted matrices also show that the diagonal elements are

dominant which means that the change of power injection at a specific bus has a higher impact on its own Z_L and Z_{eq} than the change power at other buses. This due to fact that the power flow across the network reduces impact of power injection at a specific bus on other buses while the change at its own bus cast such impact without any losses across the network. It is also noticed that the sensitivity of the load and equivalent impedances of a particular bus to power injection at other buses in the same feeder are higher than the sensitivity due to power injection at the buses of other feeders. For example, the sensitivity of Z_L and Z_{eq} of bus 1175 to power injection at any bus in feeder 4 are higher than the sensitivity due to power injection in other feeders. The modest sensitivity in the region near the bus 1103 and bus 1175 can be demonstrated by noticing that the nodes near the bus 1103 are located at nodes far away from the bus 1175 and on other feeders.

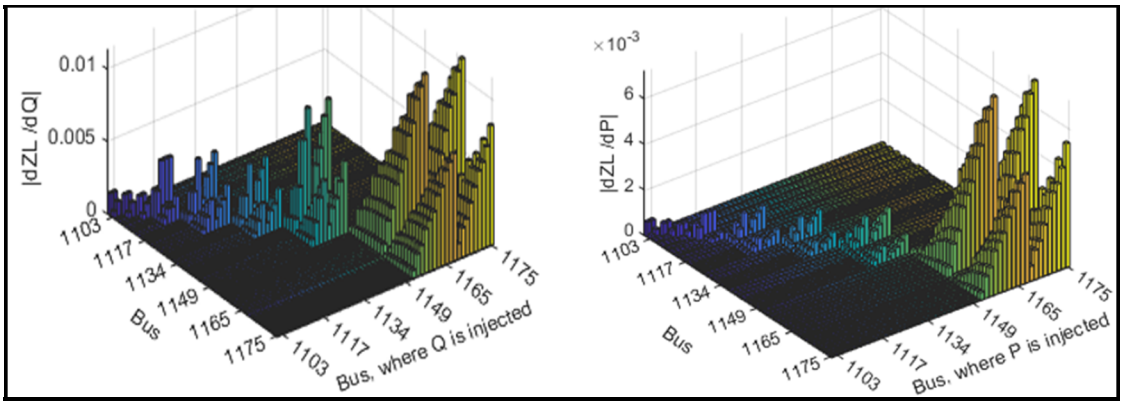

Figure 5.4 $|Z_L/dP|$ and $|Z_L/dQ|$ sensitivitymatrices for base condition

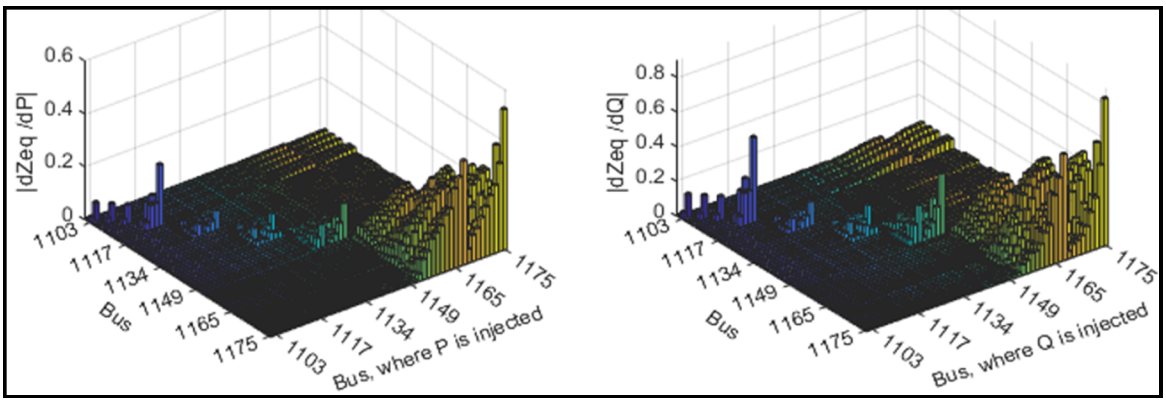

Figure 5.5 $|Z_{eq}/dP|$ and $|Z_{eq}/dQ|$ sensitivity matrices for base condition

It is worth mentioning that the sensitivities of Z_{eq} of the buses located at the end of feeders 4 and 6 are significantly greater than those of the buses located at the beginning of the feeders or at the other feeders as shown in Figure 5.5. This is due to fact that injecting power at the buses of the end of the feeders 4 or 6 has a higher impact on other buses than injecting the power at the beginning of the feeder or the other feeders. The high difference between the sensitivities can be explained from (5.20) which shows that the equivalent impedance sensitivity depends on the sum of the coupling effects between buses.

From (5.18) and (5.20), we can find that the proposed sensitivities are closely related to the sensitivity terms of $[\,J]^{-1}$. The numerical values of the sensitivities illustrate the strong relation to the values of $[\,J]^{-1}$. For example, the bus 1175 self-sensitivity term of $[\,J]^{-1}$ is higher than its cross-sensitivity terms. Moreover, the bus 1175 largest cross-sensitivity term is obtained with bus 1165 which is the nearest location to bus 1175. This justifies the higher sensitivities of the impedances of bus 1175 to power injection at its own location and the nearest buses over other locations.

From the results, it is noticed that changing the impedances is not a local problem in which Z_L and Z_{eq} of a load bus are changed due to a disturbance (i.e. change in power injection) in its own bus or other buses network. Verification of the sensitivities of Z_L and Z_{eq} of bus 1175 to active and reactive power injection at its own bus and bus 1165 demonstrates the validity of the proposed sensitivities.

5.5.2 Impedance sensitivity-based voltage control

Application of the equivalent nodal analysis (similar to TLIM) in voltage stability assessment has been studied in (Li et al., 2018), (Nazari et al., 2014). Thus, this work focusses only on examination of the applicability and accuracy of the proposed sensitivities $|dZ_L/du|$ and $|dZ_{eq}/du|$ in voltage control. Application of the proposed method for a weak system and during contingency cases will be studied in the next future work.

In this test, it is assumed that the rating for DG units are 3.5-MVA with 2.6 MW of maximum capacity. For each step of corrective actions, DG units are allowed to change their active and reactive power not more than 0.3 MW and 0.3 MVAr respectively. The cost of using the active power and slack values are higher than the cost of using the reactive power by 10 and 800 times respectively. The normal voltage limits are considered to be within [0.98, 1.04] p.u. The controller uses only the reactive power for voltage control while the active power is only used when any voltage reaches the emergency upper limit (= 1.06 p.u in this study). It is also assumed that the controller updates the set points of control variables every 10 seconds and collects the measurements 8 seconds after updating the set points.

5.5.2.1 Under voltages scenario

In this case, the network operates at maximum power demand so that some buses suffer from low voltage. Since all voltages are below the emergency upper limit, the reactive power outputs of DG units are only used for voltage correction. Figure 5.6a shows the voltages regulation starting at t= 40 s and changing every 10s by adjusting the set point of DG units. The measured voltages, currents and the sensitivities are also updated every 10s to achieve the correct voltage control. The curves in Figure 5.6b correspond to the most representative voltages of both DG and load buses.

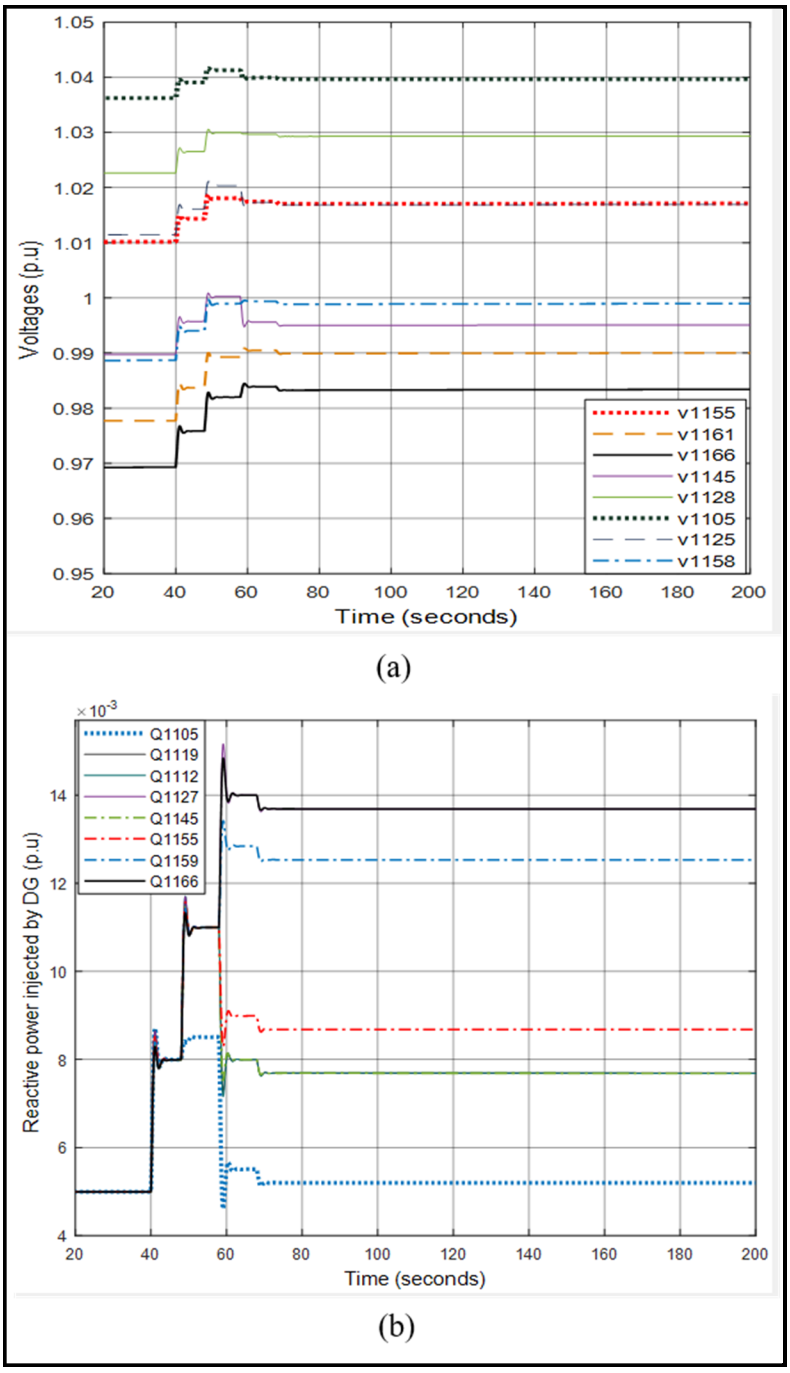

Figure 5.6 (a) Bus voltages & (b) Reactive power output of the DGs for scenario 1

It is clear that the controller can improve the voltages gradually until the latter are brought back inside the normal limits. Once the voltages are restored inside the normal limits, the controller does not request further increase in reactive power. This condition is met at 70s. It is also

shown from Figure 5.6b that although most of the DG units provide reactive power, DG located at bus 1105 was requested to still operate at the lower amount of reactive power. This is because the voltages near bus 1105 (i.e. v1105) would violate the upper limit of 1.04 p.u. It is also noticed that DG located at 1166 provide the higher amount of reactive power because v1166 is the most problematic voltage.

When all under voltages are corrected, the total compensated amount of reactive power is given in Figure 5.7. It is clear that not all the DG units are used for voltage support. Some units still operate at lower amount of reactive power while others absorb reactive power.

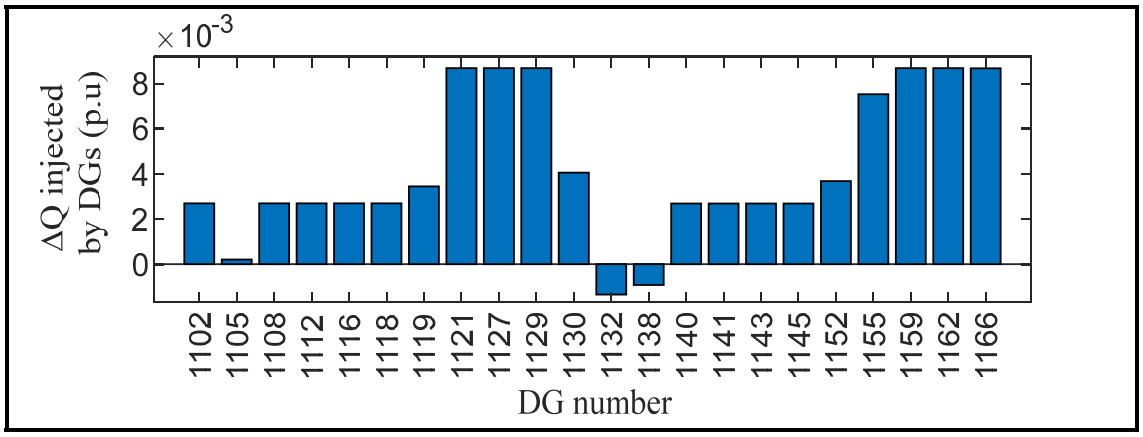

Figure 5.7 The total compensated reactive power outputs by DGs for scenario 1

The node voltage profiles of two cases, namely, Vuncontrolled and Vcontrolled, are shown in Figure 5.8. It is shown that the proposed approach can correct the voltages by generating 9.57MVar reactive power in total.

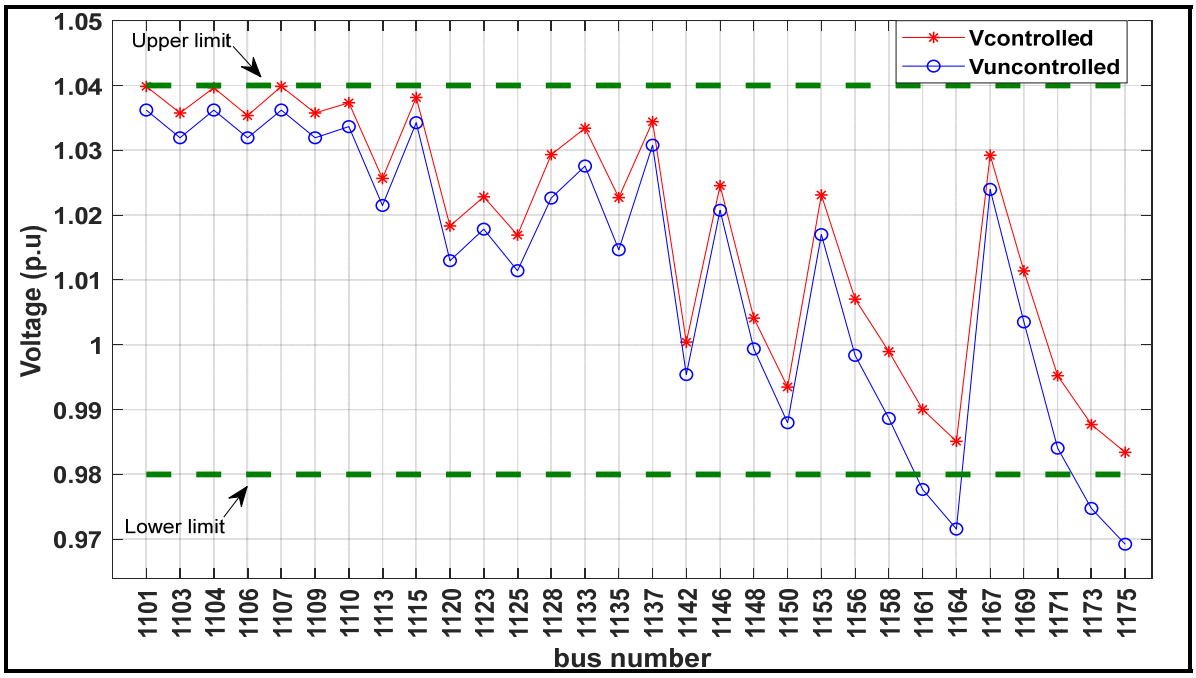

Figure 5.8 Voltage profile of the network for scenario 1

To show the accuracy of the proposed sensitivities $|dZ_L/dQ|$ and $|dZ_{eq}/dQ|$, the contribution of each DG in the change of the impedances of the pilot bus, bus 1110, among some control actions is presented in Figure 5.9. It can be seen that the dominant change occurred by DG located near the pilot bus, DG at 1112. Contribution of other DGs in the change of the impedances of the pilot bus is almost equal. This is because the pilot bus has a weak coupling effect with other DGs located at other feeders. Although the system is successfully stable in this scenario, the proposed voltage control was able to improve the value of TLIM by 0.018%.

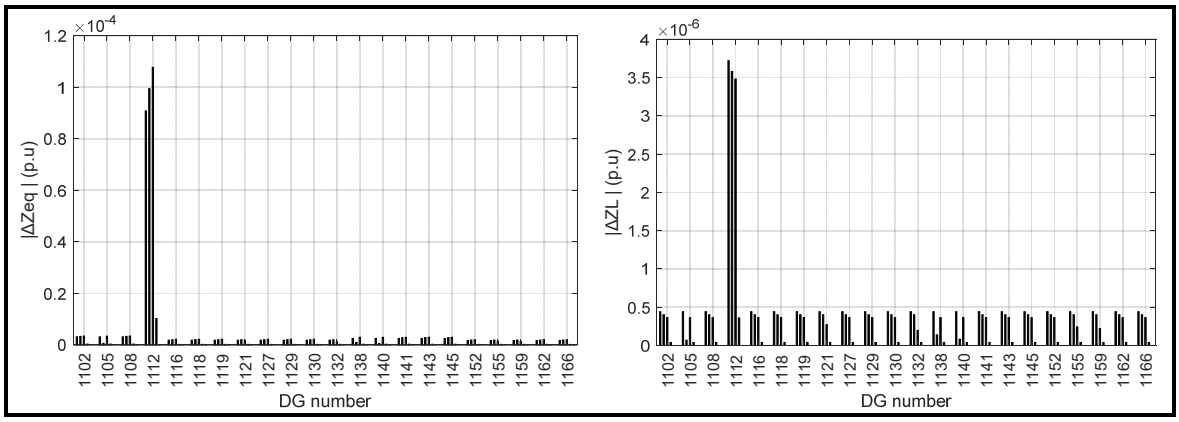

Figure 5.9 The change of the load and equivalent impedance of pilot bus caused by each DG among some control actions for scenario 1

5.5.2.2 DG unavailability

In this scenario, the system was operated so that all voltages are within normal voltages. It was assumed that the network met an outage of two DG units, located at the buses 1166 and 1162, at t= 0 s. This created low voltage conditions at some buses of feeder 4. Figure 5.10 shows the voltages regulation and the changes in the reactive power starting at t=40 s. It is clear that the rest of DG units can improve the voltages in case of the outage of some DG units.

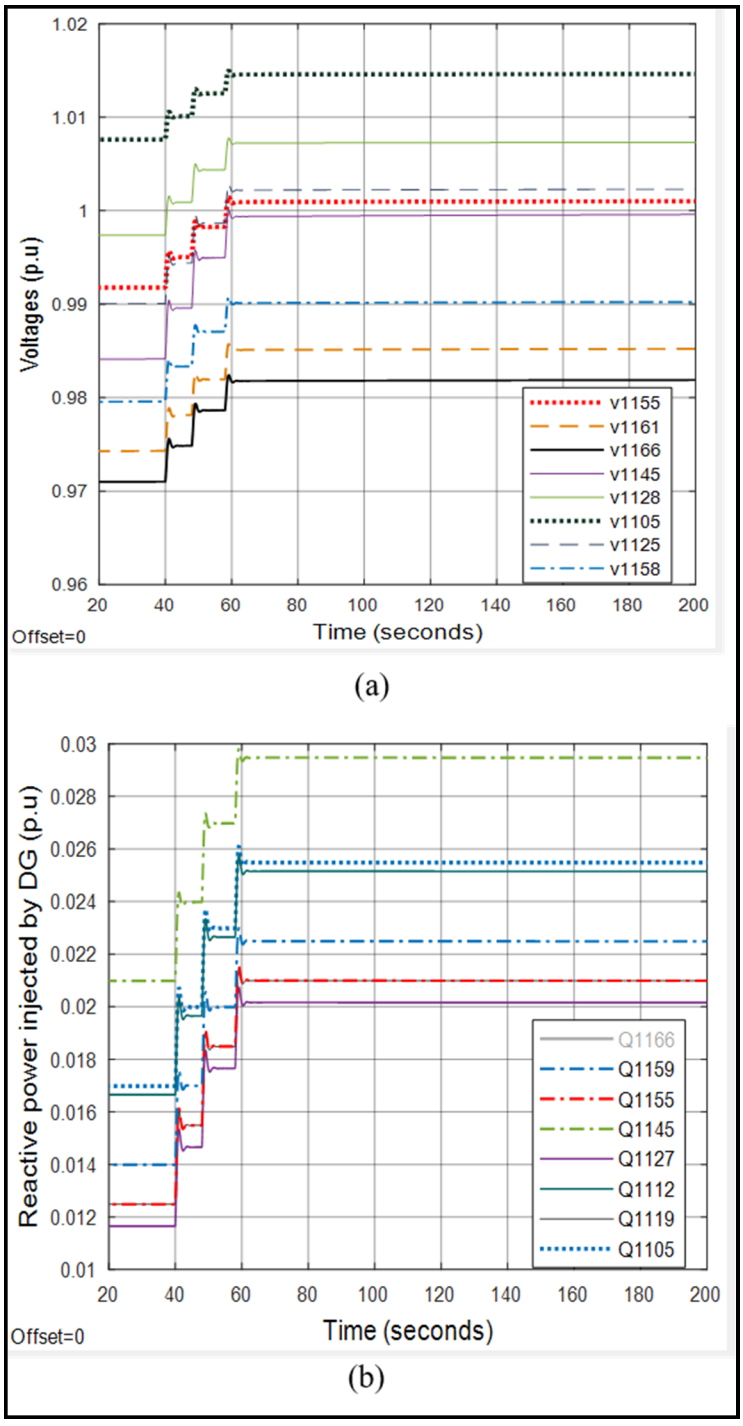

Figure 5.10 (a) Bus voltages &(b) Reactive power output of the DGs for scenario 2

To show the accuracy of the proposed sensitivities$|dZ_L/dQ|$ and $|dZ_{eq}/dQ|$, the contribution of each DG in the change of the impedances of pilot bus, bus 1175, among some control actions is presented in Figure 5.11.

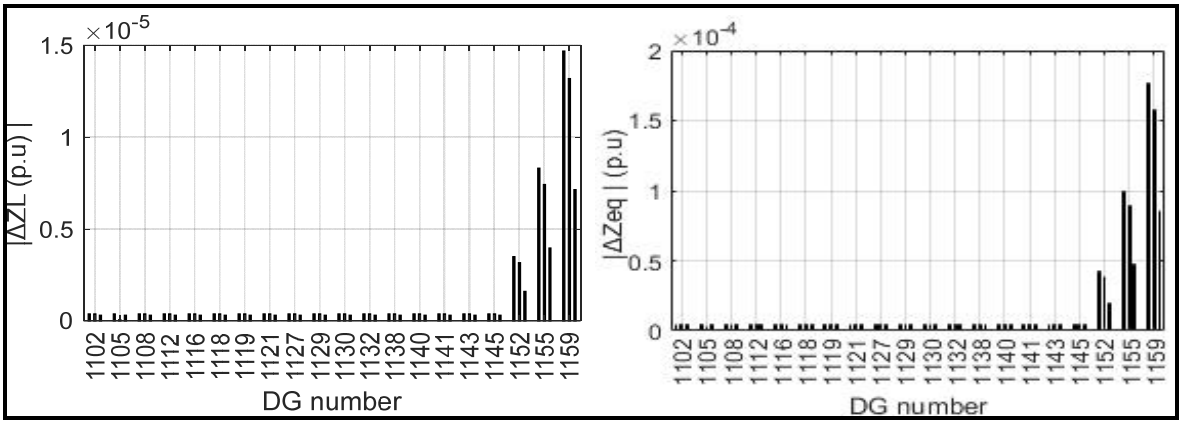

Figure 5.11 The change of the load and Equivalent impedance of pilot bus caused by each DG among some control steps for scenario 2

It can be seen that the dominant change occurred by the DGs located near pilot bus, bus 1175, and at the same feeder (located at buses 1159, 1155 & 1152). The results also show the weak coupling effect of the pilot bus with other DGs located on other feeders. In this scenario, the proposed voltage control was able to improve the value of TLIM by 0.19%.

5.5.2.3 Overvoltage scenario

To show the validity of the proposed voltage control during overvoltage conditions, the system was operated at low power consumptions and high power generated by DG units. Figure 5.12a shows the voltages regulation starting at t= 20 s by adjusting the set point of DG units. Since there are some voltages exceeded the emergency upper limit, the controller used the reactive and active power outputs of DG units for voltage correction. Figure 5.12b shows the reduction in reactive power outputs while Figure 5.13 shows the reduction in active power outputs of some DG units.

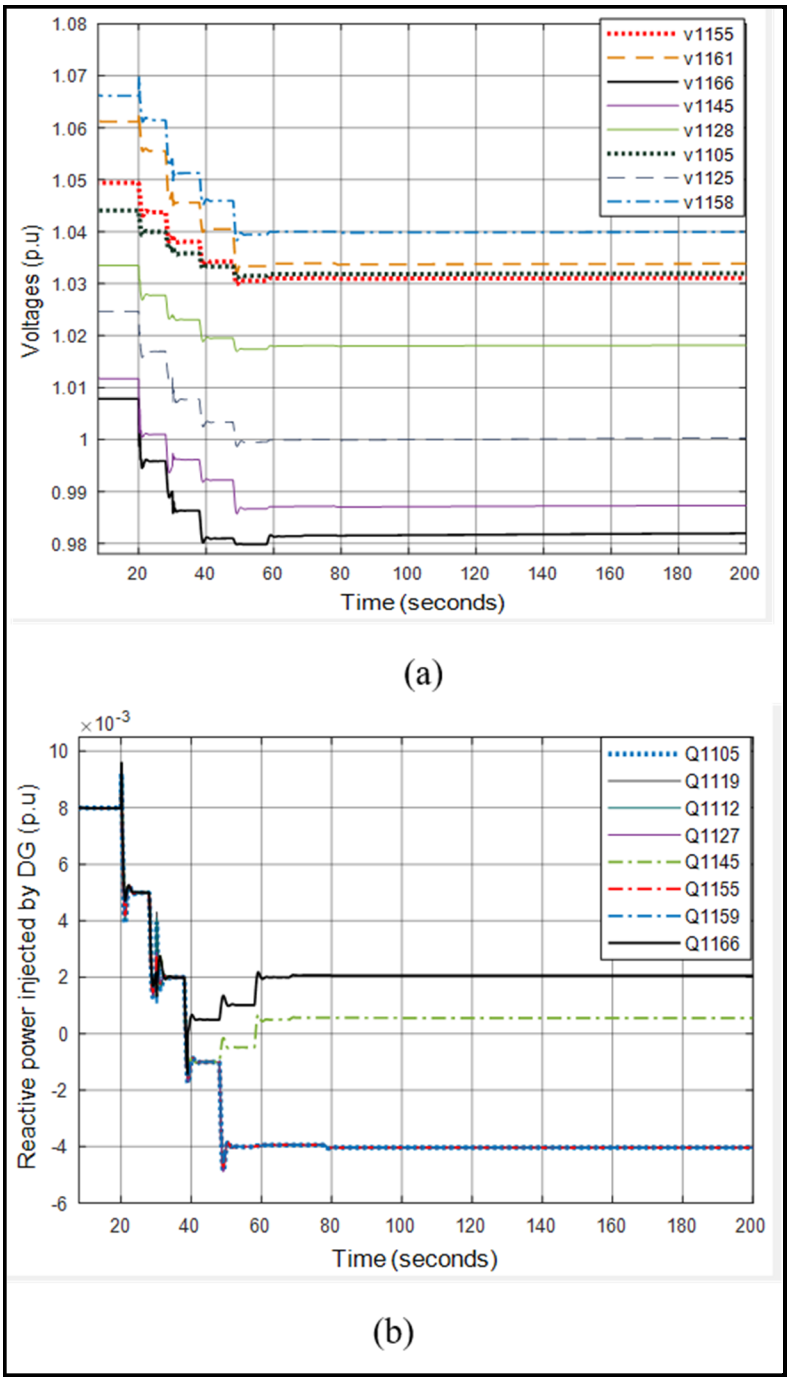

Figure 5.12 (a) Bus voltage & (b) Reactive and
of some DGs for scenario 3

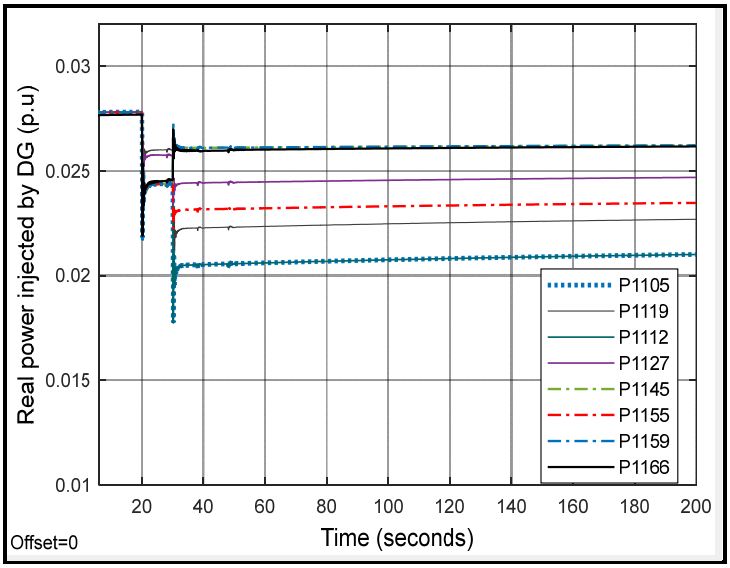

Figure 5.13 Active power output of some DGs for scenario 3

It is clear that as all the voltages are restored to non-emergency region, the controller only uses the reactive power outputs for voltage correction. This met at t = 40 s. It is also shown that although most of the DG units absorbed reactive power, DG units located at the buses 1166 and 1145 were requested to still generate reactive power. This is because the voltages v1166 and v1145 would violate the lower limit of 0.98 p.u.

To show the accuracy of the proposed sensitivities $|dZ_L/dP|$ and $|dZ_{eq}/dP|$, the contribution of the change in active power outputs by each DG in the change of the impedances of pilot bus, bus 1110, is presented in Figure 5.14. It can be seen that the dominant change occurred by DG located near pilot bus, DG at 1112, among the two control actions.

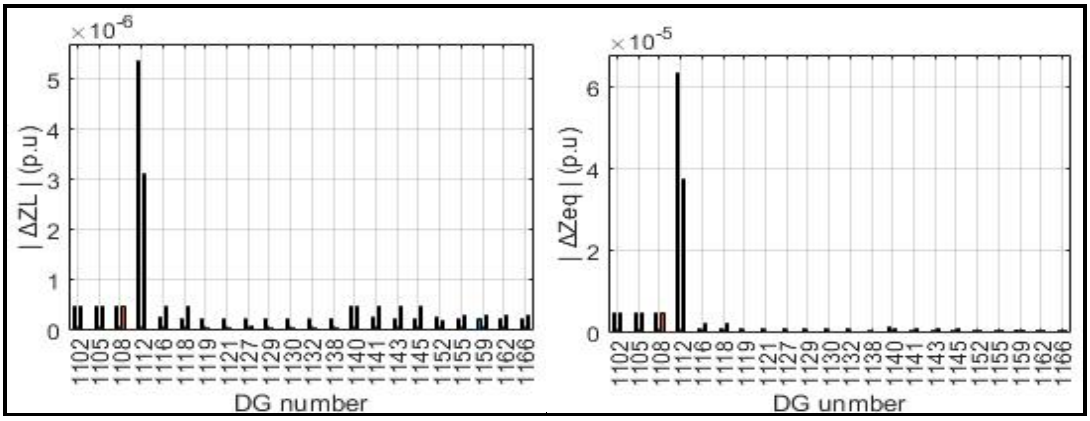

Figure 5.14 The change of the load and equivalent impedance of pilot bus caused by the change in the real power output by each DG for Scenario 3

5.5.2.4 Under voltage scenario (Emergency scenario)

To show the validity of the proposed voltage control during an extreme low voltage, it is assumed that the network is operated at high power consumptions and low power generated by DG units. Figure 5.15a shows the voltages regulation starting at t= 20 s by adjusting the set point of DG units. Figure 5.15b shows the gradual increase in reactive power outputs of some DG units. It is clear that as all the voltages are successfully brought back inside the normal limits by optimally dispatch the reactive power output by DG units. It can be seen from Fig.15.b that there is an overshoot in the control. This is due to the effect of slack values which used to relax some voltages.

To show the accuracy of the proposed sensitivities $|dZ_L/dQ|$ and $|dZ_{eq}/dQ|$, the contribution of the change in active power outputs by each DG in the change of the impedances of pilot bus, bus 1175, is presented in Figure 5.16. It can be seen that the dominant change occurred by DG located near pilot bus, DG located among feeder 4. In this scenario, the proposed voltage control was able to improve the value of TLIM by 1.92%.

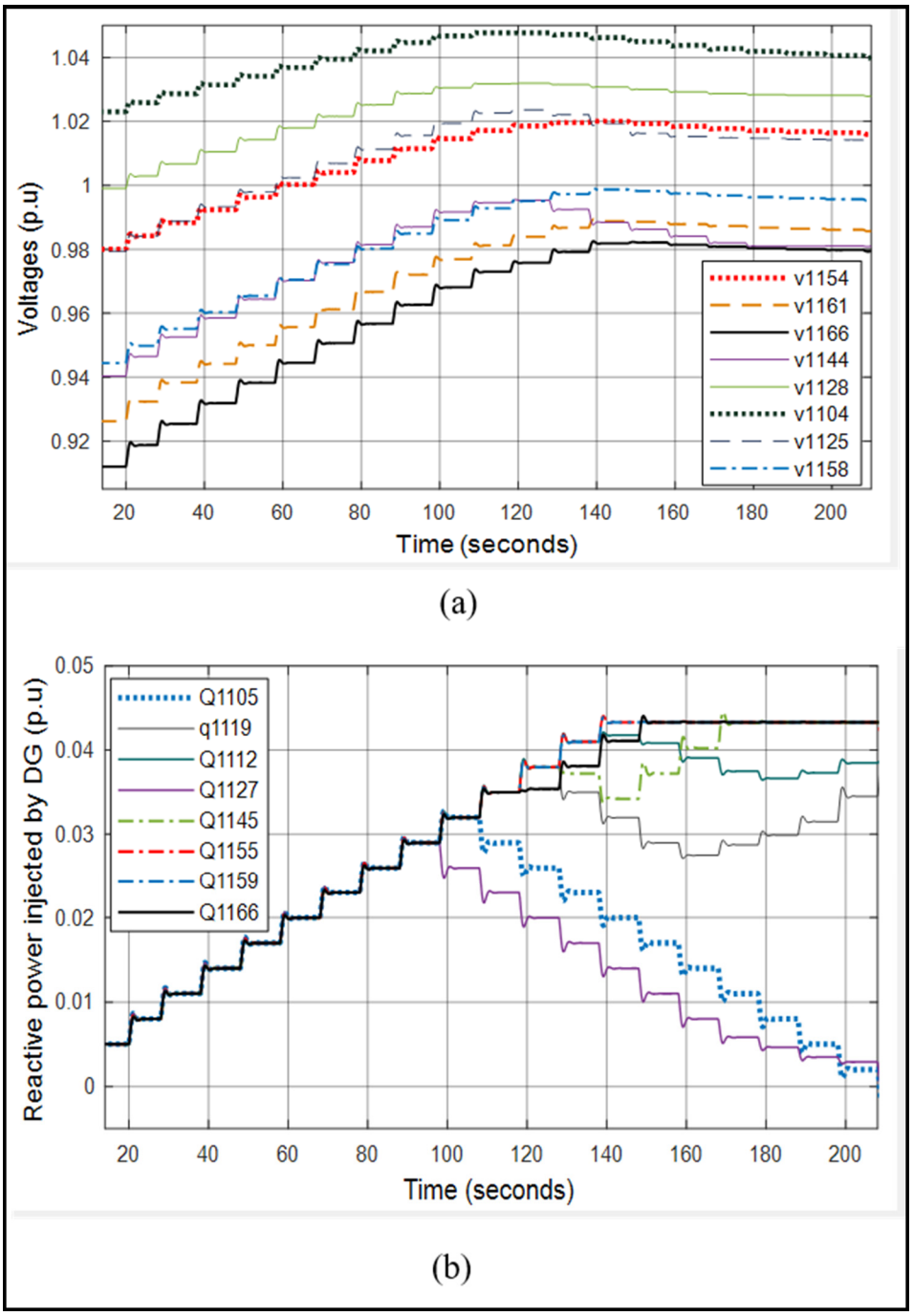

Figure 5.15 (a) Bus voltage & (b) Reactive power output of the DGs for scenario 4

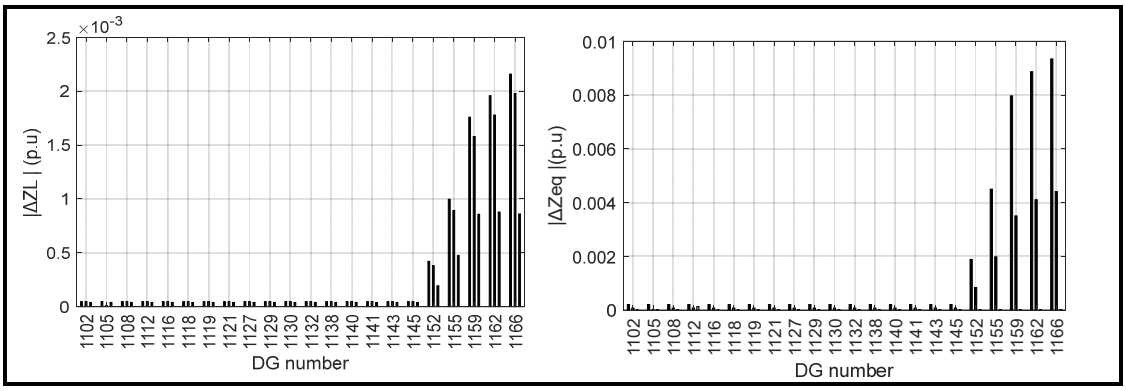

Figure 5.16 The change of the load and equivalent impedance of pilot bus caused by each DG among some control steps for scenario 4

5.6 Conclusions

This paper presents a new centralized voltage control method following a security purpose to optimally dispatch the control variables of active distribution grids. The method is based on the sensitivity of load and equivalent impedances to control variables. The method helps the distribution network operators to make a global voltage correction considering voltage stability issues inside distribution networks. Simulation results show that the sensitivities of the load and equivalent impedances can accurately be used to quantitatively analyze the impact of change of power injections to the impedances. The results also show the accuracy and the validity of the proposed method in voltage control during different scenarios: normal and emergency operating conditions. It is also clear that the proposed method is applicable for real-time voltage control in the distribution network. This can be noticed from the frequent updated of the set points of control variables (every 10 s in this work).

Our future work is to develop appropriate PMU placement techniques to obtain the equivalent impedances with a full observability of the distribution systems. Moreover, application of the proposed method for a weak system and during contingency cases will be studied.

CHAPTER 6

MIQCP-BASED MULTI-MODES ONLINE POWER EXCHANGE CONTROL AT T/D INTERFACE

Khaled Alzaareer[1], Maarouf Saad[1], Hasan Mehrjerdi[2], Dalal Asber[3] and Serge Lefebvre[3]

[1] Département of Electrical Engineering, École de Technologie Supérieure, 1100 Notre-Dame Ouest, Montréal, Québec, Canada H3C 1K3
[2] Department of Electrical Engineering, Qatar University, University Street, Doha, Qatar 2713
[3] Power Systems and Mathematics, Research Institute of Hydro-Quebec 1740 Boul Lionel-Boulet, Varennes, Québec, Canada J3X 1S1

Paper submitted to *IEEE Transactions on Smart Grid*, August 2020

Abstract

Control of power exchange between transmission and distribution systems is one of the new requirements of modern power networks. The high production from Distributed Generated units (DGs) of Distribution Networks (DNs) and during light loading can increase the connection point voltage and, in turn, cause problems for Transmission Networks (TNs). In contrast, active DNs are strongly requested to support TNs (i.e. providing ancillary services) during its unexpected system failures. Thus, this work proposes an online centralized method to meet the requirements issued by international Demand Connection Codes (DCC) at Transmission/Distribution (T/D) interface or fulfill demand response (DR) requirements from TN as well as DN voltages. A linear power flow taking into accounts the voltage dependence of loads is utilized to formulate the problem as a mixed-integer quadratically constrained optimization problem (MIQCP), which can be solved efficiently to its global optimum solution. To increase the responsibility degree of DNs in fulfilling DCC (or TN) requirements, controllable loads are involved in the control strategy. The proposed method was tested on a 11kV, 75-bus distribution network including several DGs.

Keywords: Voltage Control; TN Support; Distribution Networks; Power Exchange; Distributed Generation; T/D Interface.

6.1 Introduction

The adoption of DGs has been raised in the recent years. With high penetration levels of DGs, the expansion in creating additional conventional generating units or transmission lines may be eliminated or reduced. This depends on the capability of DGs in locally providing ancillary services and separated active and reactive power control. The IEEE Std 1547.4 (Photovoltaics et al., 2009) considers utilization of DGs in islanded operation to supply the power to the islanded network and expand their capabilities for the overall TN support. In other words, DNs are requested to provide ancillary services by exporting reactive power to the TN. However, injecting power into TN may add new challenges to TN operator in the regard of voltage control (Lin, 2016). Currently, DN operators are not responsible for power exchange control at T/D interface. TN operator is responsible for managing this problem. However future requirements will be posed for DN operators to manage the power exchange. One of these requirements is issued by the 'Network Code on Demand Connection' of the European Network of Transmission System Operators for Electricity (ENTSO-E) (European Commission, 2016). According to this code, the reactive power transfer should be inside a range depending on the import or export capability. The TN may ask the DN not to deliver reactive power at times of low demands or it may ask the DN for reactive power injection during unexpected system failure. On other side, DNs may require the TN to provide reactive power during the system management. Therefore, such a code is beneficial for both networks to keep the system secure and reliable.

By incorporating DGs and conventional control devices, DNs will have higher degree of responsibility for system support (D'Adamo et al., 2009). However, there are open questions about how to steer the power exchange at T/D interface from DN side. It is requested that DNs have the ability to maintain their own voltages while managing the power exchange at T/D interface. Although some works deal with the role of DNs in TN support, employing DNs for online power exchange control and considering practical issues has not yet been fully studied.

A coordinative sub-transmission voltage control for reactive power management between TN and DNs is proposed (Ke et al., 2018). However, all the decisions are done by high voltage side. The enhanced utilization of voltage control variables by maximizing the DGs reactive power output is proposed (Keane et al., 2010). A method for minimizing the reactive power transfer by the TN to the DNs is presented (Ochoa et al., 2011). Reactive power management at T/D interconnection is proposed (Ali et al., 2015). An optimal reactive power control for transmission connected distribution network with wind farms is proposed (Stock et al., 2016). A model predictive control for reactive power control in transmission connected DNs is proposed (Stock et al., 2016). However, these works present passive control methods and do not aim to solve the problem online. Most of them are oriented to solve the problem over multi periods of time. Moreover, most of them depend on non-linear power flow equations to perform optimal power flow technique for problem solving. The problem is formulated as mixed-integer nonlinear optimization problem (MINLP). This kind of problems is associated with complexity and computationally expensive features. Although there are many techniques to solve MINLP problems, the optimal solution may not be obtained within the constraints of online applications. They may provide suboptimal solution, and no guarantee to obtain the optimality.

Other methods based on real-time measurements are used for TN support. A centralized control method is used to regulate the reactive power output by DGs to support TN is used (Morin et al., 2016), (Valverde & Cutsem, 2013b). However, the high required number of monitoring devices is one of the main challenges in these methods.

In addition to the challenges associated with the aforementioned methods, they are oriented to handle only one mode of operation. They are limited to control the reactive power exchange while active power exchange is left unchanged. They also utilize only the utility-owned devices for problem control ignoring the customer response.

Although DR programs have been widely used for network support through peak shaving and load shifting, utilizing DR for voltage regulation has not yet been fully studied. A DR program is developed for voltage control in active DNs (Zakariazadeh, et al., 2014). This study considers only the emergency scenarios. The electric appliances are used for voltage control through demand curtailment (Christakou, et al., 2014), (Petinrin &, Shaaban., 2014). However, only load was used as a DR resource. Besides, these works did not consider the power exchange control at T/D interface.

The main challenges associated with power exchange at T/D interface can be summarized as:

- Although several DGs, along with the conventional voltage regulation devices, are available for control in DNs, their impacts may not be enough to meet the requirements at T/D interface or DR requirements From TN. Their operation is usually limited by their locations. Thus, involving loads in power exchange control can increase the flexibility level of DNs for TN support.
- Due to the continuous changes in system operation condition (i.e. the changes of system demand and generation or unexpected disturbances) of power system, multi-periods based control methods are not enough for power exchange control. Instead of that, an online control method is required.
- Formulation the problem as combinatorial nonlinear optimization problems (i.e. optimal power flow) requires complex calculations. Besides, they do not guarantee that the optimal solution will be reached.
- The voltage dependent characteristics of loads have a significant impact on power consumptions and thus in voltage control, especially with the integration of DGs in DNs which may change the unidirectional characteristics of the power flow. Taking into account these load characteristics increases the accuracy of the problem control.
- It is impractical to use large number of monitoring devices for power exchange control. TN voltage support from DNs side requires cost-effective control methods.
- Despite the physical coupling between TN and DNs, very limited information exchange and coordination exist between the operators. Power exchange control based on an interactive mechanism between TN and DNs makes the problem complex and consumes

more time. Thus, the decoupling between the TN control and DNs control is the best choice for online power exchange control.

- Flexible multi-mode control method is strongly required for future power system operation. For instance, keeping the reactive power exchange at T/D interface within a range cannot fulfill the DR requirements from TN.

In this regard, this paper proposes an online control method to regulate the active and reactive power exchange between TN and DNs as well as DNs voltages. The analysis is done at the distribution level without any interaction with TN. A linear power-flow method considering the load voltage dependence characteristics is used for problem formulation. The control problem is formulated as MIQCP problem, which can be solved efficiently to its global optimum solution. To increase the responsibility degree of DNs for problem control, controllable loads, along with DGs and shunt capacitors, are involved in the control. The proposed control method provides the option for DNs to operate in different modes: isolated mode, active and passive modes (i.e. fulfilling the requirements issued by DCC at T/D interface) or DR mode (i.e. fulfilling the DR requirements from TN).

The key contributions of this work are:

- Development of a flexible online control framework for DN to steer the power exchange at T/D interface. Compared to other control methods, the problem is formulated as MIQCP to be solved efficiently to its global optimum solution. Besides, the framework can work under different modes: isolated mode, passive mode, active mode and DR mode. This allows TN voltage (or voltage stability) problem to be handled by utilizing control variables in DNs without creating operational issues in DNs.
- Control not only the reactive power exchange at T/D interface but also the active power exchange.
- Coordination among the customer-owned devices and utility-owned devices for voltage and T/D power exchange control.

The rest of the paper is organized as follows. Section II presents the control operation modes of DNs. Section III presents the linear power flow approach used for problem formulation. Power exchange formulas and MIQCP problem formulation are presented in section IV. Simulation results are shown in section V while Section VI includes the conclusions.

6.2 Control Modes of DNs

With the continuous integration of DGs in power networks, DN operators will be able to operate in different modes. The operation modes can be classified as:

6.2.1 Isolated Mode

Some of DNs may choose to be operated as isolated networks. In this mode no real and reactive power exchange at T/D interface.

6.2.2 Passive Mode

DN operators also have the choice to operate in passive participation mode in voltage support. In this mode, DNs are required to limit the reactive power exchange Q_{ex} inside the cost-free region as shown in Figure 6.1. In some countries and in case of exceeding the cost-free range, DNs are billed for the cost of the excess reactive energy (Kurzidem, 2011). Passive DNs do not take on any responsibilities or obligations with regard to active voltage support in TN. Reactive energy is only billed once certain limits are violated. The limits are symmetrical on both sides of the reactive power base line. Based on Figure 6.1, the limits of cost-free range can be divided into two parts:

- For large absolute values of active power exchange P_{ex}, the limits of the cost-free region are set by the power factor limit pf_{lim}. For example, in Switzerland, $pf_{lim} \geq 0.9$ of either the maximum imported or exported active power. The limits of the reactive power exchange Q_{lim}^{pf} depend on the predefined pf_{lim} and the active power exchange as:

$$pf_{lim} = \frac{Q_{lim}^{pf}}{P_{ex}}$$

- For small values of P_{ex}, the limits are defined as $\pm Q_{lim}$ on both sides of the reactive power base line. The limits of the reactive power exchange Q_{lim} are defined based on the specifications of substation power transformer.

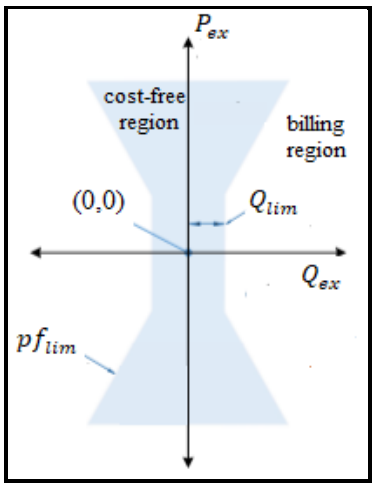

Figure 5.1 Passive Mode of DN operation

It is worth mentioning that $Q_{ex} < 0$ (or $P_{ex} < 0$) means that DN exports reactive (or active) power to the TN while $Q_{ex} > 0$ (or $P_{ex} > 0$) means that DN imports reactive (or active) power from the TN.

6.2.3 Active Mode

DN operators also have the choice to operate in active participation mode in voltage support. In this mode, DNs are obliged to use their available reactive power to support the TN voltage V_T when it is necessary, without compromising the active power (Kurzidem, 2011). If the setpoint voltage V_T^S is reached, the reactive power exchange is considered "compliant". This

mode is applied for reactive power exchange in any direction (i.e. importation or exportation). Figure 6.2 presents the compliance principle. If the DN exports (or imports) reactive power when V_T is lower (or higher) than V_T^S, it is considered to be compliant.

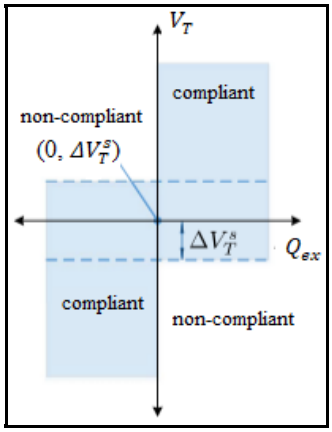

Figure 6.2 Active Mode of DN operation

6.2.4 DR Mode

DNs may also be requested to control both active and reactive power exchange at T/D interface to meet DR requirements from TN. Figure 6.3 shows the operation region of DR mode.

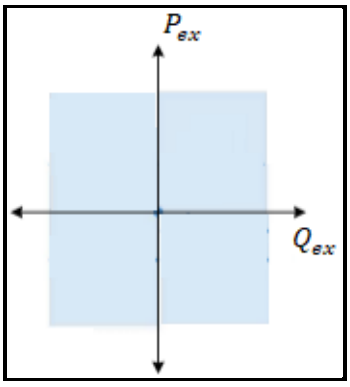

Figure 6.3 DR Mode of DN operation

6.3 Linear power flow

The power flow approach presented in (Martí et al., 2013) represents a set of linear equations that include the voltage dependent characteristics of the loads. Two components (constant impedance and constant current) are used to model the loads. The load model is described as:

$$\frac{P}{P_O} = C_1\left(\frac{V}{V_O}\right)^2 + C_2\left(\frac{V}{V_O}\right) \tag{6.1a}$$

$$\frac{Q}{Q_O} = C_1'\left(\frac{V}{V_O}\right)^2 + C_2'\left(\frac{V}{V_O}\right) \tag{6.1b}$$

where P and Q represent the active and reactive power consumption, respectively. V is the load voltage. The zero subscript denotes the nominal values. The coefficients C_1, C_1', C_2 and C_2' are governed by the conditions $C_1 + C_2 = 1$ and $C_1' + C_2' = 1$. According to (Martí et al., 2013), this load model is used to derive a linear power flow equation. Each load can be represented by a current source in parallel with an admittance. The values for the equivalent admittance (G_L and B_L) and equivalent current source ($I_{L,p}$ and $I_{L,q}$) for each load are described as:

$$G_L = \frac{C_1 P_O}{{V_O}^2}, \quad B_L = -\frac{C_1' Q_O}{{V_O}^2} \tag{6.2a}$$

$$I_{L,p} = \frac{C_2 P_O}{V_O}, I_{L,q} = -\frac{C_2' Q_O}{V_O} \tag{6.2b}$$

Accordingly, the power flow equations can be described as (Martí et al., 2013):

$$\begin{bmatrix} G & -B \\ B & G \end{bmatrix}\begin{bmatrix} V^{re} \\ V^{im} \end{bmatrix} = \begin{bmatrix} I_p^L \\ I_q^L \end{bmatrix} \tag{6.3}$$

For N number of network buses, G and B are submatrices (each of N×N dimension) of the real and the imaginary parts of the new admittance matrix, respectively. V^{re} and V^{im} are vectors (each of N×1 dimension) of the real and the imaginary parts of the node voltages, respectively.

I_p^L and I_q^L are vectors (each of N×1 dimension) of the parts of the load currents. Based on (5.3), the power flow equations at bus i can be expressed as:

$$\sum_{j=1}^{N} \left(G_{i,j}V_j^{re} - B_{i,j}V_j^{im}\right) = I_{p,i}^L \tag{6.4}$$

$$\sum_{j=1}^{N} \left(G_{i,j}V_j^{im} + B_{i,j}V_j^{re}\right) = I_{q,i}^L \tag{6.5}$$

Where i and j denote for system buses. To include the effect of DGs, (6.4) and (6.5) can be replaced by:

$$\sum_{j=1}^{N} \left(G_{i,j}V_j^{re} - B_{i,j}V_j^{im}\right) = I_{p,i} \tag{6.6}$$

$$\sum_{j=1}^{N} \left(G_{i,j}V_j^{im} + B_{i,j}V_j^{re}\right) = I_{q,i} \tag{6.7}$$

Where

$$I_{p,i} = I_{p,i}^{Load} - I_{p,i}^{DG}$$
$$I_{q,i} = I_{q,i}^{Load} - I_{q,i}^{DG}$$

The terms $I_{p,i}^{DG}$ and $I_{q,i}^{DG}$ are parts of the current injection by the DG located at bus i. The negative sign for the two parts indicates for power injection into the grid (i.e. negative load).

6.4 Problem formulation

6.4.1 Power exchange and power factor at T/D interface

According to (6.6) and (6.7), the active and reactive power exchange between TN and DN can easily be obtained. If it is assumed that V_{sub} is the voltage magnitude at the substation bus and I_{sub} is the current drawn from the substation, the power at T/D interface S_{sub} can be calculated as:

$$\begin{aligned} S_{sub} &= V_{sub} I_{sub}^{*} \\ &= V_{sub}(I_{p,sub} - \mathrm{j} I_{q,sub}) \end{aligned} \tag{6.8}$$

Where * denotes the complex conjugate. Thus, the active and reactive power imported by DN can be calculated as (Ahmadi et al., 2014):

$$\begin{aligned} P_{ex} &= V_{sub} I_{p,sub} \\ &= V_{sub} \sum_{j=1}^{N} \left(G_{sub,j} V_j^{re} - B_{sub,j} V_j^{im} \right) \end{aligned} \tag{6.9}$$

$$\begin{aligned} Q_{ex} &= -V_{sub} I_{q,sub} \\ &= -V_{sub} \sum_{j=1}^{N} \left(G_{sub,j} V_j^{im} + B_{sub,j} V_j^{re} \right) \end{aligned} \tag{6.10}$$

Where the subscript *sub* denotes the substation bus. For the active and reactive power exported to TN, the I_{sub} should be switched to "negative", and thus (6.9) and (6.10) will be multiplied by a negative sign. Depending on the requirements of system operation, the exchange power P_{ex}, Q_{ex}, or both can be controlled.

The power factor PF at T/D interface can also be calculated as:

$$PF = \frac{P_{ex}}{(P_{ex}^2 + Q_{ex}^2)^{1/2}} = \frac{I_{p,sub}}{\left(I_{p,sub}^2 + I_{q,sub}^2\right)^{1/2}} \quad (6.11)$$

6.4.2 MIQCP power formulation

This work aims to control the power exchange at T/D interface by formulating the problem as MIQCP optimization problem. The objective function is to minimize the cost of control variables and the deviation of the substation voltage V_{sub} as:

$$Min\ obj = \sigma\, w_1(C^{ca} + C^{DG} + C^{cl}) + w_2 \Delta V_{sub} \quad (6.12)$$

where C^{ca}, C^{DG} and C^{cl} represent the change cost of the capacitors, output power of DGs and the controllable loads, respectively. $\Delta\mathrm{V}_{sub}$ represents the deviation at the substation voltage. w_1 and w_2 are weight coefficients ($w_1, w_2 \epsilon\ [0,1]$) used to penalize the terms of the objective function. The weight coefficients are subjected to the condition $w_1 + w_2 = 1$. Since the cost objective function is usually very high compared to the voltage deviation objective function, a correction coefficient σ is used to normalize the objective terms. It is worth mentioning that a) the outputs of DGs can only be curtailed, not increased; b) the controllable loads can be turned on/off to provide only active power response; c) the active power compensation (active power output by DGs and controllable loads) will not be used unless the reactive power compensation (reactive power output by DGs and capacitor banks) fails to fulfill the network requirements.

The optimization problem formulated in this study is also based on a multi-step optimization to smoothly correct the voltages over interval of n discrete steps. Thus, each term in (6.12) as well as ε can be expressed as:

$$C^{ca} = \sum_{=0}^{n-1} \sum_{i=1}^{N_{ca}} C_i^{Ca} \left(e(i)\Delta C_i(t+k)\right)^2 \tag{6.13a}$$

$$C^{DG} = \sum_{k=0}^{n-1} \sum_{i=1}^{N_{DG}} \left[C_{Q,i}^{DG} \left(\Delta Q_i^{DG}(t+k)\right)^2 + C_{P,i}^{DG} \left(\Delta P_i^{DG}(t+k)\right)^2 \right] \tag{6.13b}$$

$$C^{cl} = \sum_{k=0}^{n-1} \sum_{i=1}^{cl} C_{P,i}^{cl} \left(\Delta P_i^{cl}(t+k)\right)^2 \tag{6.13c}$$

$$\Delta \mathrm{V}_{sub} = \sum_{k=0}^{n-1} \left(Ref - \mathrm{V}_{sub}(t+k)\right)^2 \tag{6.13d}$$

Where C_i^{Ca}, $C_{Q,i}^{DG}$ $C_{P,i}^{DG}$ and $C_{P,i}^{cl}$ are the cost of the change in the capacitor steps of load i, the reactive and active power output by DG i, and the change in the controllable load i, respectively. ΔC_i, ΔQ_i^{DG}, ΔP_i^{DG}, and ΔP_i^{cl} represent the change in the capacitor steps of load i, the reactive and active power output by DG i, and the controllable load i, respectively. N_{ca}, N_{DG}, and N_{cl} are the number of the capacitors, DGs, and the controllable loads used for the control. Ref represents the reference substation voltage. $e(i)$ represents the status of "on" or "off" of the capacitor at bus i. t+k denotes the predicted quantity given the data at time t instant.

To relax the constraints of the quantities at T/D interface as well as DN voltages, the objective function illustrated in (6.12) should include slack variables ε. Thus, the term (6.13e) is also added to (6.12).

$$\Delta \mathrm{V}_{sub} = \sum_{k=0}^{n-1} \left(Ref - \mathrm{V}_{sub}(t+k)\right)^2 \tag{6.13e}$$

$\varepsilon_{1,i}$ and $\varepsilon_{2,i}$ are slack variables used to relax the voltage constraint at bus i. $C_i^{\varepsilon 1}$and $C_i^{\varepsilon 2}$are the cost of using the slack variable $\varepsilon_{1,i}$ and $\varepsilon_{2,i}$, respectively. $\varepsilon_{3,i}$ and $\varepsilon_{4,i}$ are slack variables used to relax the constraint at T/D interface. $C_i^{\varepsilon 3}$and $C_i^{\varepsilon 4}$ are the cost of using the slack variables $\varepsilon_{3,i}$ and $\varepsilon_{4,i}$, respectively. N_{ex} is the number of the controlled quantities at T/D interface.

Regarding the cost, the change of reactive power outputs by DGs is considered cheap controls while the active power output by DGs is considered an expensive control. Due to the payment imposed for the users, it is assumed that the cost of controllable loads is also more expensive than the cost of active power output by DGs. To avoid the frequent switching of the capacitors, their cost is considered more expensive than reactive power output by DGs.

Remark 1: Price functions can be derived for cost models. However, this issue is not the target of this work and will be considered in our future works.

The objective function presented in (12-13) is subjected to:

a. Distribution network constraints:

- Node voltages

The nodal voltage limits can be expressed as:

$$-\varepsilon_{1,i} + V_i^{min} \le V_i(t+k) \le V_i^{max} + \varepsilon_{2,i} \tag{6.14}$$

$$\begin{aligned} V_i(t+k) = V_i(t+k-1) &+ \sum_j^{N_{ca}} \frac{\partial V_i}{\partial C_j} e(j) \Delta C_j(t+k) \\ &+ \sum_j^{N_{DG}} \frac{\partial V_i}{\partial Q_j} \Delta Q_j^{DG}(t+k) + \sum_j^{N_{DG}} \frac{\partial V_i}{\partial P_j} \Delta P_j^{DG}(t+k) \\ &+ \sum_j^{N_{cl}} \frac{\partial V_i}{\partial P_j} \Delta P_j^{cl}(t+k) \end{aligned} \tag{6.15}$$

Where $V_i(t+k)$ is the predicted voltage magnitude of bus i while $V_i(t+k-1)$ is the previous voltage magnitude of bus i. $\frac{\partial V_i}{\partial C_j}$, $\frac{\partial V_i}{\partial Q_j}$, and $\frac{\partial V_i}{\partial P_j}$ are the voltage sensitivity of bus i to the change in the capacitor j, reactive and active power injected at bus j, respectively . V_i^{min} and V_i^{max} represent the bus voltage limits.

- Discrete control variables
  Since the capacitors are operated as discrete control variables, the status of "on" or "off" of the capacitor at bus i can be constrained as:

$$e(i) = 0 \; or \; 1 \tag{6.16}$$

- The changes in the control variables:
  The limits of the change in the control variables of each step are:

$$\Delta C_{i,min} \leq \Delta C_i(t+k) \leq \Delta C_{i,max} \tag{6.17a}$$

$$\Delta Q_{i,min}^{DG} \leq \Delta Q_i^{DG}(t+k) \leq \Delta Q_{i,max}^{DG} \tag{6.17b}$$

$$\Delta P_{i,min}^{DG} \leq \Delta P_i^{DG}(t+k) \leq \Delta P_{i,max}^{DG} \tag{6.17c}$$

$$\Delta P_{i,min}^{cl} \leq \Delta P_i^{cl}(t+k) \leq \Delta P_{i,max}^{cl} \tag{6.17d}$$

The capacity of each control variable is constrained as:

$$C_{i,min} \leq C_i(t+k) \leq C_{i,max} \tag{6.18a}$$

$$Q_{i,min}^{DG} \leq Q_i^{DG}(t+k) \leq Q_{i,max}^{DG} \tag{6.18b}$$

$$P_{i,mi}^{DG} \leq P_i^{DG}(t+k) \leq P_{i,max}^{DG} \tag{6.18c}$$

$$P_{i,min}^{cl} \leq P_i^{cl}(t+k) \leq P_{i,max}^{cl} \tag{6.18d}$$

Where C_i, P_i^{DG}, Q_i^{DG}, P_i^{cl} are the status of the capacitor i, the active and reactive power injected by the DG i, and the demand of the controllable load i, respectively. The subscript "min" and "max" denote the change limits.

The limits $P_{i,max}^{cl}$ and $P_{i,min}^{cl}$ can be determined based on the demand curtailment contract or percentage of curtailed demand λ as:

$$P_{i,max}^{cl} = \lambda P_i \,, \quad P_{i,min}^{cl} = -\lambda P_i \tag{6.19}$$

- Branch currents:
  The branch capacity limits can be constrained as:

$$I_{ij}{}^2(t+k) \leq I_{ij,max}^2 \tag{6.20}$$

The magnitude of the current flowing through branch *ij* is calculated as:

$$\begin{aligned} I_{ij} &= |Y|\left|\left(V_i - V_j\right)\right| \\ &= \left|G_{ij} + jB_{ij}\right|\left|\left(V_i{}^{re} - V_j{}^{re}\right) + j\left(V_i{}^{im} - V_j{}^{im}\right)\right| \\ &= \left(G_{ij}{}^2 + B_{ij}{}^2\right)^{1/2}\left((V_i{}^{re} - V_j{}^{re})^2 + (V_i{}^{im} - V_j{}^{im})^2\right)^{1/2} \end{aligned}$$

$$\begin{aligned} I_{ij}{}^2(t+k) = \; & \left(G_{ij}{}^2 + B_{ij}{}^2\right)\left(\left(V_i{}^{re}(t+k) - V_j{}^{re}(t+k)\right)^2\right. \\ & \left. + \left(V_i{}^{im}(t+k) - V_j{}^{im}(t+k)\right)^2\right) \end{aligned} \tag{6.21}$$

- T/D interface constraints

  The T/D interface constraints can be determined based on the operation mode as follows**:**

- For isolated mode:

  The active and reactive power exchange at T/D interface should be:

$$P_{ex} = Q_{ex} = 0$$

Thus, the T/D constraints are:

$$-\varepsilon_{3,1} \leq V_{sub}(t+k)\sum_{j=1}^{N}\big(G_{sub,j}V_j^{re}(t+k) - B_{sub,j}V_j^{im}(t+k)\big) \leq \varepsilon_{4,1} \quad (6.22)$$

$$-\varepsilon_{3,2} \leq -V_{sub}(t+k)\sum_{j=1}^{N}\big(G_{sub,j}V_j^{im}(t+k) + B_{sub,j}V_j^{im}(t+k)\big) \leq \varepsilon_{4,2} \quad (6.23)$$

Where $\varepsilon_{3,1}$, $\varepsilon_{3,2}$, $\varepsilon_{4,1}$, and $\varepsilon_{4,2}$ denote the ith slack variable for the constraints at T/D interface (i.e. $\varepsilon_{3,i}$ and $\varepsilon_{4,i}$ of equation (13.e)).

- For passive mode:

  The power factor at T/D exchange should maintain within a specific range. Thus, the T/D constraint can be expressed as:

$$PF_{min} \leq |PF(t+k)| \leq PF_{max}$$

Or

$$PF_{min}^2 \leq PF^2(t+k) \leq PF_{max}^2 \quad (6.24)$$

Where $PF(+k)$ is the predicted power factor at the interface point while PF^{min} and PF^{max} represent the power factor limits. By substituting (6.11) into (6.24), the constraint can be formulated as:

$$(1 - PF_{min}^2)I_{p,sub}^2(t+k) - PF_{min}^2 I_{q,sub}^2(t+k) \geq -\varepsilon_3 \tag{6.25}$$

$$(1 - PF_{max}^2)I_{p,sub}^2(t+k) - PF_{max}^2 I_{q,sub}^2(t+k) \leq +\varepsilon_4 \tag{6.26}$$

The general formulas for $I_{p,sub}^2$ and $I_{q,sub}^2$ are illustrated in (6.27) and (6.28).

$$\begin{aligned} I_{p,sub}^2 &= \left(\sum_{j=1}^{N} \left(G_{sub,j} V_j^{re} - B_{sub,j} V_j^{im} \right) \right)^2 \\ &= \sum_{j=1}^{N} \left(G_{sub,j} V_j^{re} - B_{sub,j} V_j^{im} \right)^2 \\ &+ \sum_{x \neq j}^{N} \left[\left(G_{sub,j} V_j^{re} - B_{sub,j} V_j^{im} \right) \left(G_{sub,x} V_x^{re} - B_{sub,x} V_x^{im} \right) \right] \end{aligned} \tag{6.27}$$

$$\begin{aligned} I_{q,sub}^2 &= \left(\sum_{j=1}^{N} \left(G_{sub,j} V_j^{im} + B_{sub,j} V_j^{re} \right) \right)^2 \\ &= \sum_{j=1}^{N} \left(G_{sub,j} V_j^{im} + B_{sub,j} V_j^{re} \right)^2 \\ &+ \sum_{x \neq j}^{N} \left[\left(G_{sub,j} V_j^{im} + B_{sub,j} V_j^{re} \right) \left(G_{sub,x} V_x^{im} + B_{sub,x} V_x^{re} \right) \right] \end{aligned} \tag{6.28}$$

- For Active Mode

  The voltage at T/N point should maintain within a specific range as:

$$-\varepsilon_3 + V_{sub}^{min} \le V_{sub}(t+k) \le V_{sub}^{max} + \varepsilon_4 \tag{6.29}$$

- For DR mode

  The active and reactive power exchange at T/D interface should be:

$$P_{ex} = DR_P, Q_{ex} = DR_Q$$

Where DR_P and DR_Q are the active and reactive power requested by TN. If TN requests the DN to import power, then the constraints should be:

$$\begin{aligned} -\varepsilon_{3,1} + DR_P &\le V_{sub}(t+k)\sum_{j=1}^{N}\left(G_{sub,j}V_j^{re}(t+k) - B_{sub,j}V_j^{im}(t+k)\right) \\ DR_P + \varepsilon_{4,1} &\ge V_{sub}(t+k)\sum_{j=1}^{N}\left(G_{sub,j}V_j^{re}(t+k) - B_{sub,j}V_j^{im}(t+k)\right) \end{aligned} \tag{6.30}$$

$$\begin{aligned} -\varepsilon_{3,2} + DR_Q &\le V_{sub}(t+k)\sum_{j=1}^{N}\left(G_{sub,j}V_j^{im}(t+k) + B_{sub,j}V_j^{re}(t+k)\right) \\ DR_Q + \varepsilon_{4,2} &\ge V_{sub}(t+k)\sum_{j=1}^{N}\left(G_{sub,j}V_j^{im}(t+k) + B_{sub,j}V_j^{re}(t+k)\right) \end{aligned} \tag{6.31}$$

For power exportation, the power expressions illustrated in (6.30) and (6.31) are multiplied by a negative sign.

It is worth mentioning that the proposed algorithm can be embedded in a distribution management system (DMS) for online power exchange control, without needing for

measurement devices. Pseudo measurements of demand and DGs production, and network structure data can be considered as inputs for DMS. The control variables can also be equipped with SCADA system to transmit the real-time information about the status of control devices.

6.5 Test System and Simulation Results

To verify the validity of the proposed method, 77-bus, 11 kV distribution grid shown in Figure 6.4 is used as a test system. The network consists of 22DG units (each with 3.3 MVA of rating) and 53 load bus. The distribution network is connected to an external grid, modeled as a Thevenin equivalent. For system data, refer to (UKGDS, 2005). Three capacitors (each with 0.5 MVAR of rating) are also installed at three buses (bus 1125, 1134 and 1157). MATLAB interfaced with LINGO software was used to solve the optimization problem defined in the previous section and to investigate the optimal solution.

In this work, it is assumed that the normal limits of DN voltages are [0.97, 1.04] p.u and the percentage of curtailed demand λ is 15%. For each control step, the limits of the change in the active (or reactive) power output by each DG are ± 0.3 MW (or MVAR) while the limits of the change in the controllable load are ± 0.2 of λ. It is also assumed that each capacitor has five steps of 0.1 MVAR. The limits of the change in the capacitor for each control step is only one step. The cost of using the capacitors, the active power output by DGs, the controllable loads, and slack values are higher than the cost of using the reactive power by 50, 100, 200 and 1000 times, respectively. The coefficients w_1 and w_2 are both set at 0.5. The prediction horizon n is also set to be 3. In this study, the set-points of the controls are updated every 10 seconds while the data are collected 8 seconds after updating the set-points. The remaining time (6 secs) is proposed for calculating and transmitting the new set-points.

Due to the space limit, two scenarios are analyzed in this section: active mode scenario and DR mode scenario.

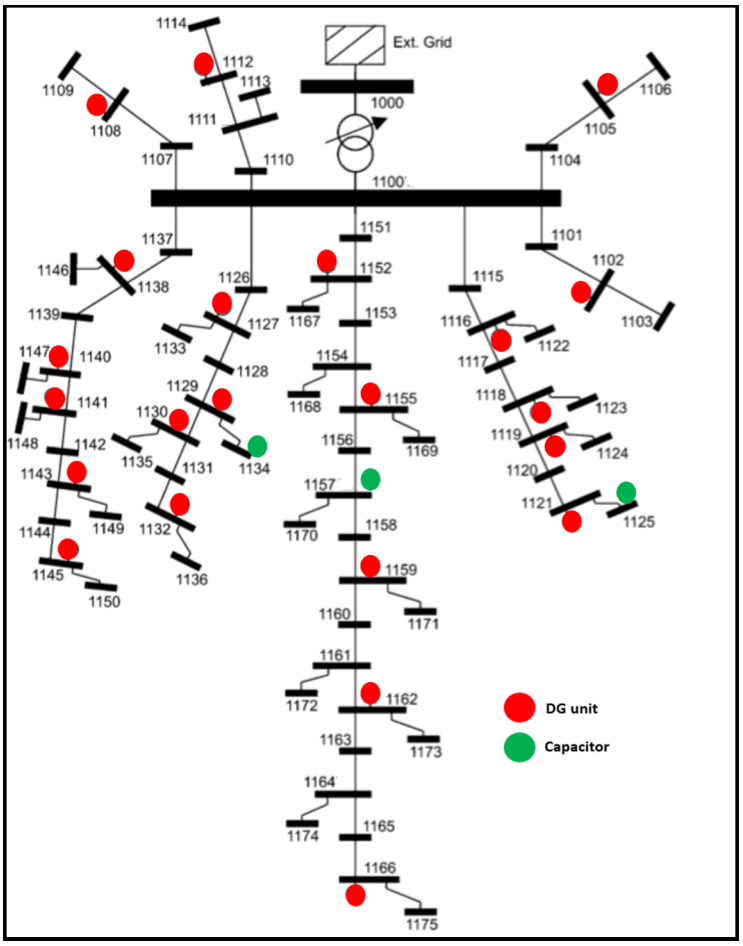

Figure 6.4 Topology of the test system

6.5.1 Active mode scenario

To demonstrate the performance of the proposed method during active mode, it is assumed that the high voltage side requests the DN to keep the voltage at node 1000 within the range [1.0 1.01] pu. Figure 6.5 shows the regulation of the high-voltage side (i.e. v1000). It is clear that the proposed method is able to correct the voltage v1000 by dispatching the DG reactive power outputs without need for other control variables. The dispatch of some DGs is presented in Figure 6.6. The DG reactive power injections increase over the different periods until DCC requirement is reached while maintain DN voltages within acceptable limits (see Figure 6.7). Figure 6.6 also shows that the DG located at bus 1105 provides the largest amount of power injections among DGs. This is because bus 1105 is the nearest bus to the external grid. In

contrast, the DG located at bus1166 (the furthest DG) provides the smallest amount of power. Since the voltage v1144 violates the upper voltage limit at t=68 sec, DG located at bus 1145 (the nearest DG to bus 1144) reduces its power injection at t=78 sec.

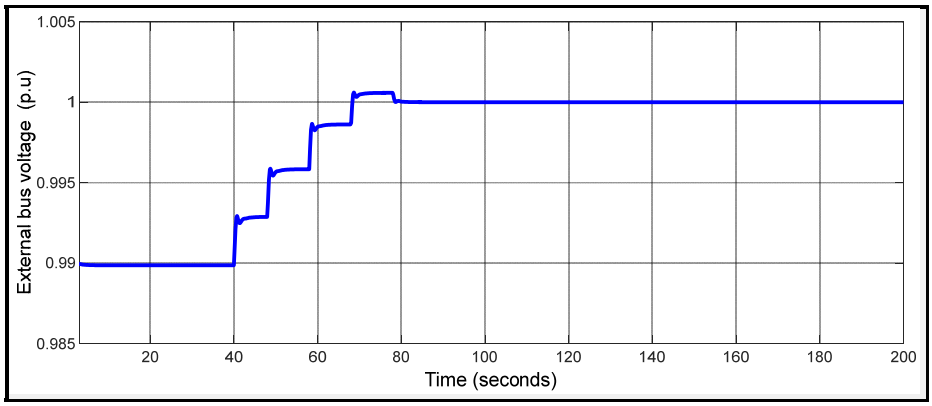

Figure 6.5 The voltage at node 1000

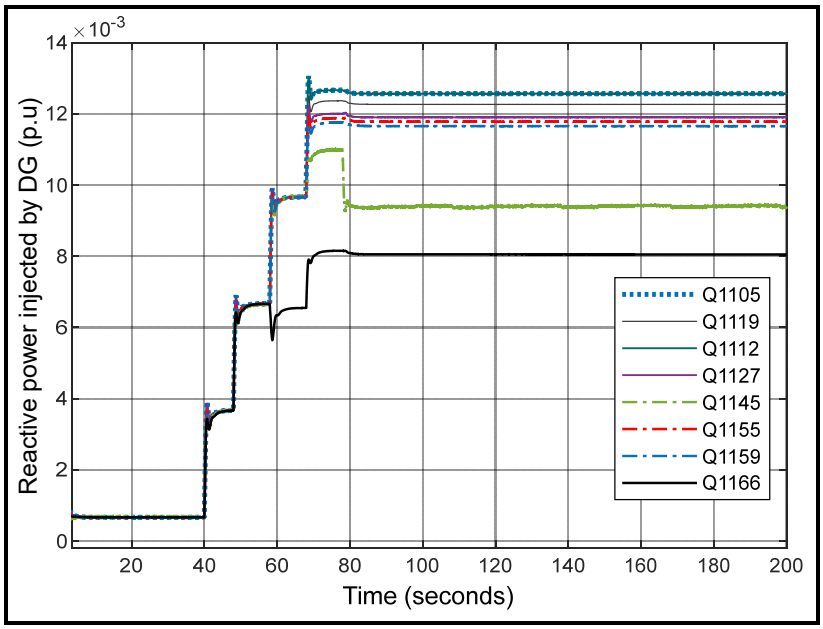

Figure 6.6 Some of DG reactive power outputs of scenario 1

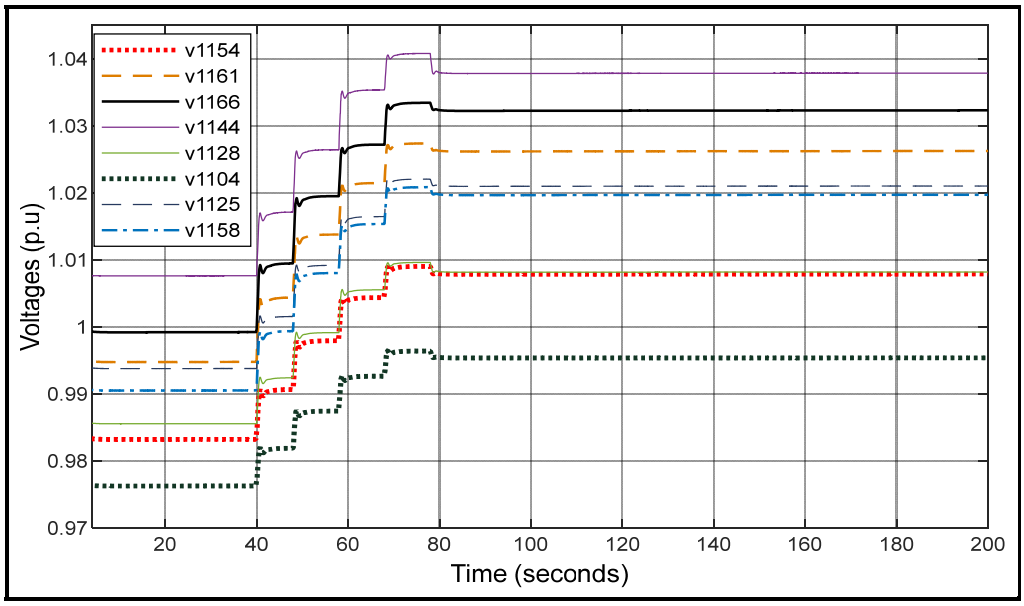

Figure 6.7 The voltage at the corresponding nodes of scenario 1

The dispatch results for all DGs and the network voltage profile are shown in Fig.8 and Figure 6.9, respectively.

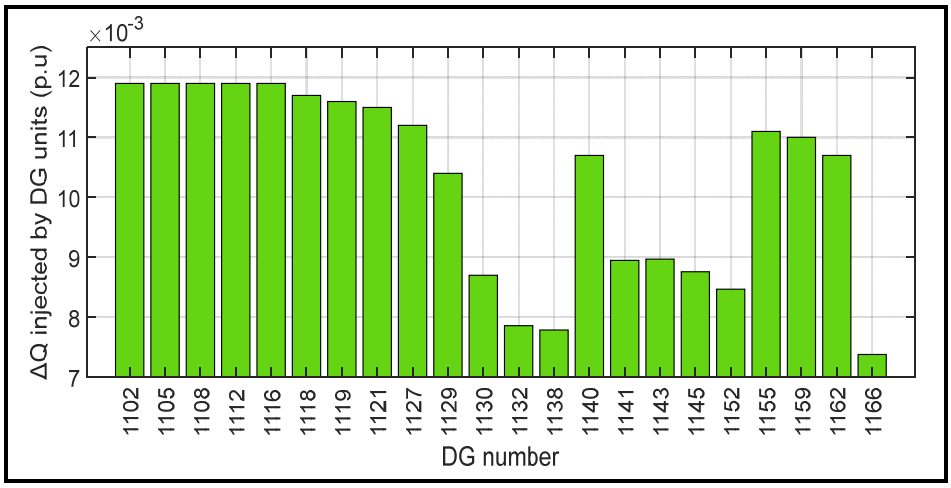

Figure 6.8 Dispatch results of DGs of scenario 1

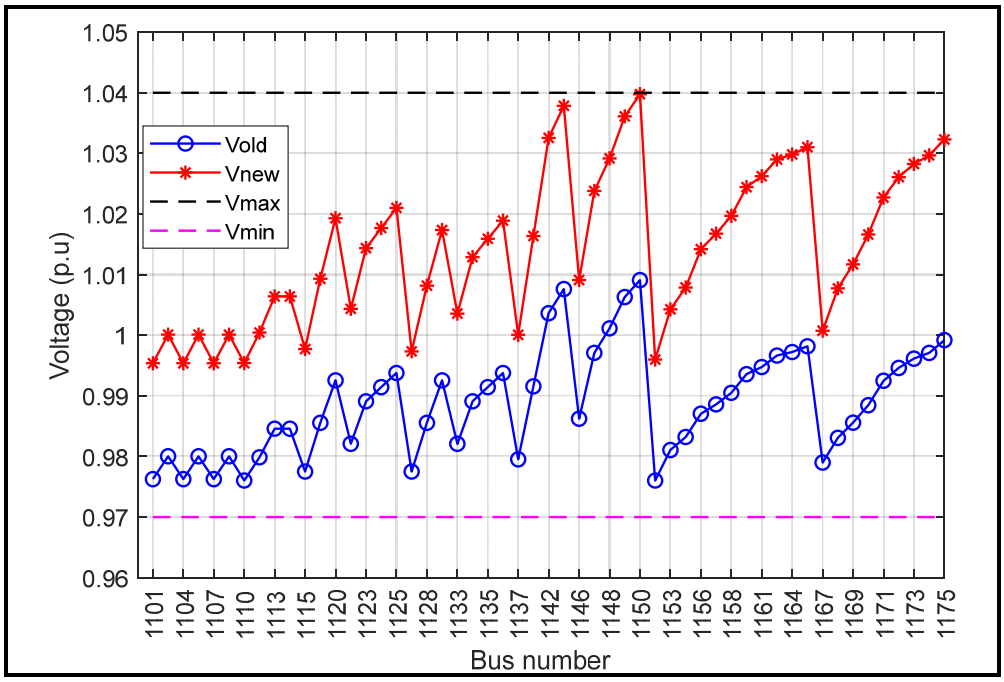

Figure 6.9 The network voltage profile of scenario 1

6.5.2 DR mode scenario

In this scenario, it is assumed that TN requests $DR_P = 0.26$ p.u and DR_Q= 0.25 p.u to be exported by the DN. Initially, the DN imports 0.05 p.u of reactive power and exports 0.2 pu of active power. Fig.10 and Fig.11 show the reactive and active power exchange at T/D interface, respectively. It is clear that the proposed method can meet the DCC requirements by dispatching the different types of control variables. The dispatch of some DGs is presented in Fig.12. The voltages at some corresponding node of DN are presented in Fig.13. Again, the DG located at bus 1105 provides the largest amount of power injections among all DGs. The DG located at 1145 also reduces its power injection at t=78 sec to prevent the voltage violation at bus 1144. The dispatch results for the control variables (DG reactive output power, capacitor banks, and the controllable loads) and the network voltage profile are shown in Fig.14 and Fig.15, respectively. The dispatch results show that some DGs absorbs reactive power and some capacitors are switched on. To meet DR requirements, some controllable loads are turned off. Since DGs cannot increase their power injections, they are not used for the power exchange control.

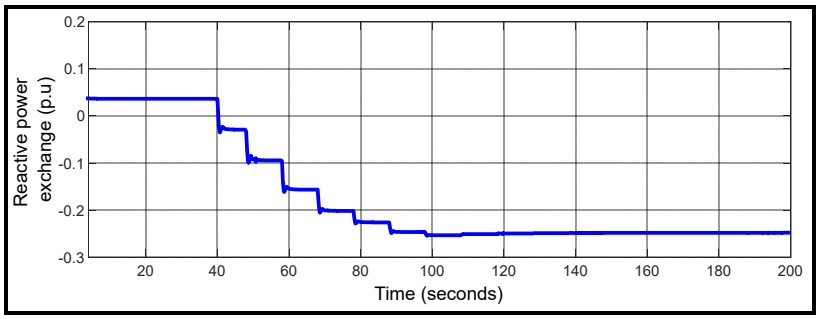

Figure 6.10 The reactive power exchange at T/D interface

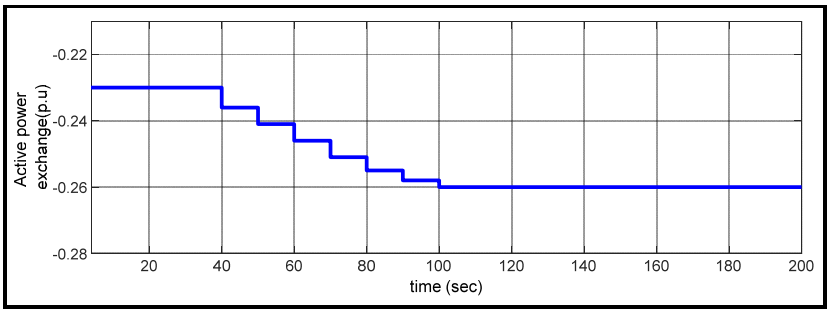

Figure 6.11 The active power exchange at T/D interface

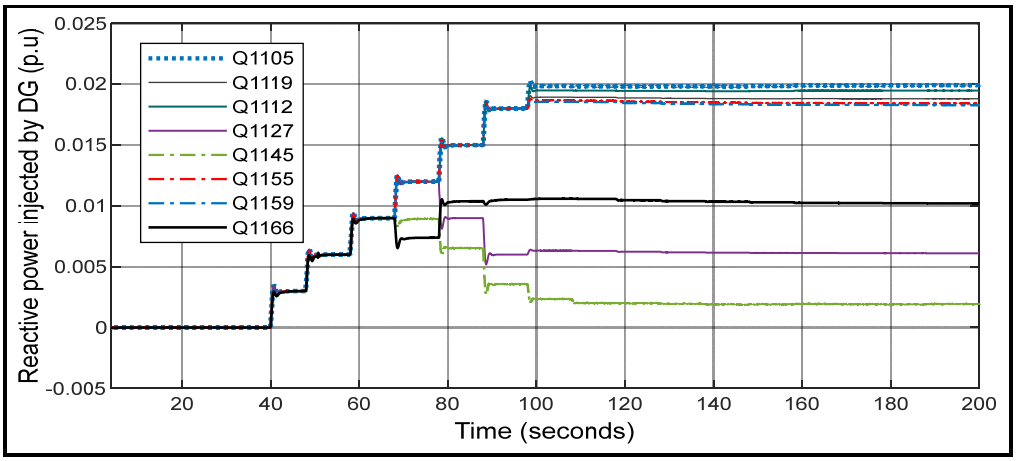

Figure 6.12 Some of DG reactive power outputs of scenario 2

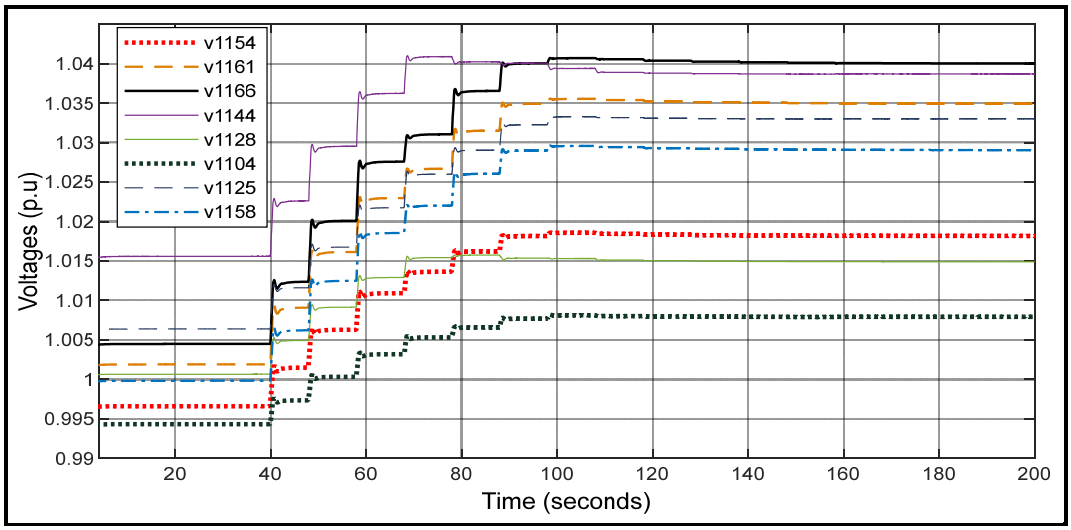

Figure 6.13 The voltage at the corresponding nodes of scenario 2

The dispatch results for the control variables (DG reactive output power, capacitor banks, and the controllable loads) and the network voltage profile are shown in Figure 6.14 and Figure 6.15, respectively. The dispatch results show that some DGs absorbs reactive power and some capacitors are switched on. To meet DR requirements, some controllable loads are turned off. Since DGs cannot increase their power injections, they are not used for the power exchange control.

Remark 2: In this work, the control actions take place every 10 secs. However, any time period (every minute, every hour, etc.) can be used for power exchange control.

Remark 3: It is worth noting that not all loads are controllable. However, this work assumes that all loads in the system are controllable to check the validity of the method. Moreover, a constraint can be added to the optimization problem to limit the number of controllable load status changes and make the problem more practical.

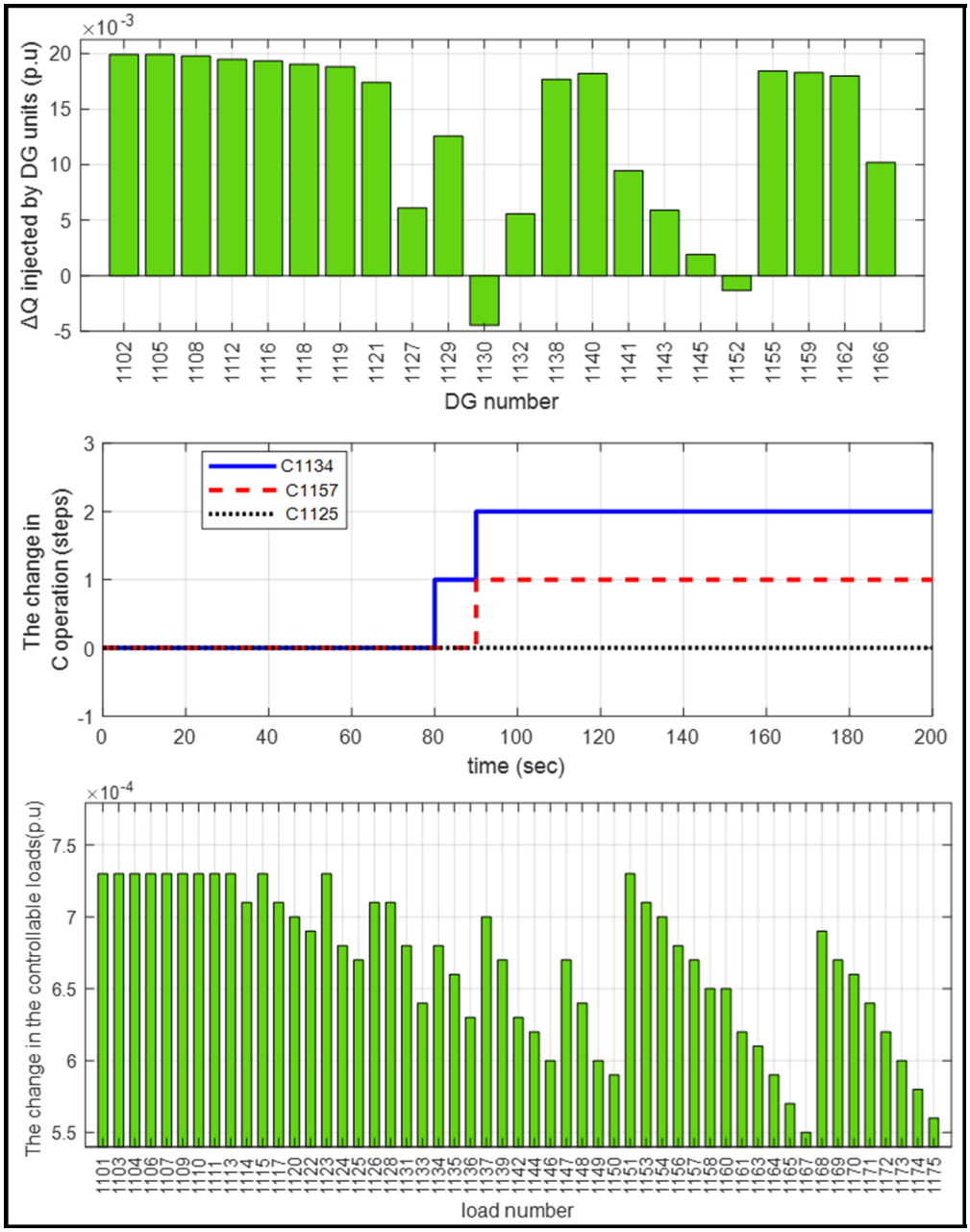

Figure 6.14 Dispatch results of the control variables of scenario 2

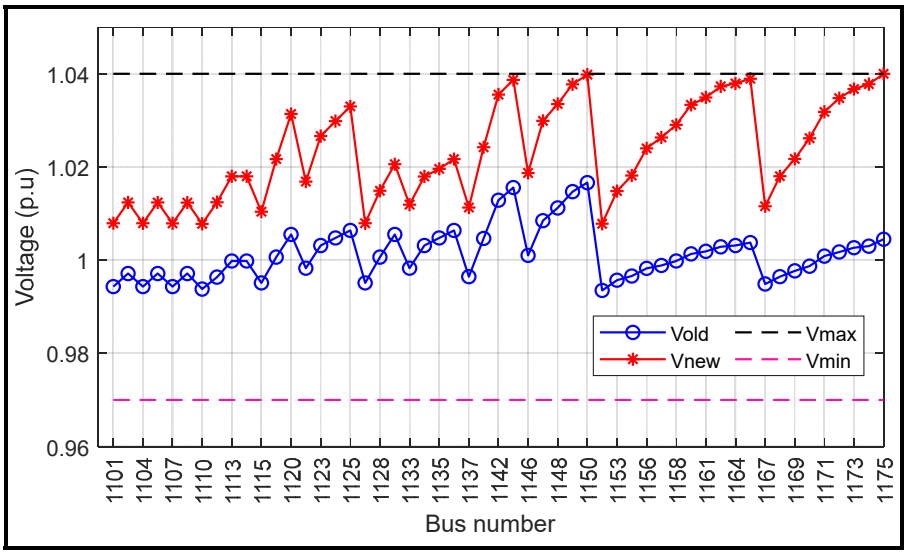

Figure 6.15 The network voltage profile of scenario 2

6.6 Conclusions

In this work, an online control framework for regulating the active and reactive power at T/D interface as well as DN voltages has been proposed. Tests are conducted on 77-bus, 11 kV distribution grid including different DG units. The results show that the proposed method can steer DN to operate under different operation modes. The network was able to fulfill the requirements of DCC or DR requirements from TN while maintaining DN voltages within normal limits. The simulations also show that the responsibility degree of DNs in providing ancillary services has been increased by incorporating the controllable loads into the control. The applicability of the proposed MIQCP problem in online control applications was demonstrated through the transient analyses.

CONCLUSION

This thesis focused on developing novel fast techniques for online CVC and T/D power exchange control for smart DNs. The techniques consider static voltage stability issues and HV side support. Simulation tests were conducted and validated on different standard distribution networks including different DG units. The main results of this project can be summarized as follows:

- A new fast method (ABCD model) has been proposed for voltage sensitivity analysis in smart DNs using direct analytical derivation. By comparing the matrices obtained using ABCD method with the ones obtained using J^{-1}, we noticed that the matrices are very close to each other, rather they almost seem the same matrices. Verification of the self-sensitivity coefficients and the largest cross-sensitivity coefficients (at base load condition and during different loading conditions) of the critical bus also demonstrated the accuracy of the proposed method for sensitivity analysis. The results also showed that the errors in the values of sensitivity coefficients or in voltage prediction are very small, which demonstrate a high level of accuracy. Besides, the proposed method can successfully account for any change in the operating conditions. The results show that the proposed method has the potential to be implemented in online applications.

- A new fast identification method for selecting a global group of controls for CVC in smart DNs was proposed. The results showed that the control variables were successfully grouped in terms of their effectiveness and cost to mitigate the violation in the voltages. The method was able to distinguish between the expensive and the cheap control variables. Activation of the control variables of the obtained group demonstrates that all violated voltages are restored inside the normal limits with low cost. The proposed method was successfully able to select the minimum number of controls to eliminate the violations in voltages. Since the proposed identification algorithm mainly depends on the concept of the electrical distances, the proposed method was effectively able to account for the effect of topology changes in the grid. The proposed method was also validated through dynamic

simulation to demonstrate the efficacy of the proposed method in voltage control with fast response time.

- A new online CVR method for smart DNs considering the static voltage stability was proposed via the sensitivity of the load and the equivalent impedances to control variables (i.e. parts of TLIM). Simulation results showed that the sensitivities of the load and equivalent impedances can accurately be used to quantitatively analyze the impact of change of power injections to the impedances. The contribution of each DG unit in change the impedances was carried out. By this method, the static voltage stability can be improved in real-time. The results also showed the accuracy and the validity of the proposed method in voltage control during different scenarios: normal and emergency operating conditions. It was also clear that the proposed method is applicable for real-time voltage control in DNs. This can be noticed from the frequent updated of the set points of control variables (every 10 s in this work).

- An online control framework for steering the active and reactive power at T/D interface as well as DN voltages was proposed. The results showed that the proposed method can steer DN to operate under different operation modes. The network was able to fulfill the requirements of DCC or DR requirements from TN while maintaining DN voltages within normal limits. The simulations also showed that the responsibility degree of DNs in providing ancillary services has been increased by incorporating the controllable loads into the control. The applicability of the proposed MIQCP problem in online control applications was demonstrated through the transient analyses.

Finally, we conclude that the developed approaches have ensured a good performance for CVC and T/D power exchange. The execution time of the proposed techniques is further reduced and therefore they can meet smart grid requirements.

RECOMMENDATION

Some limitations and problems can be highlighted in this thesis and can be considered as future works as follows:

- The methods proposed in this work for voltage control and T/D power exchange ignore substation OLTC action. It is not involved in the system control. It is known that OLTC needs more time (i.e. prolonged time delay), compared with other controls, to change its taps. The OLTC behavior can be taken into account in the proposed control techniques. However, the prolonged time delay associated with OLTC have to be considered through the control.

- This thesis developed the control methods assuming that DNs are balanced systems. However for systems with lower voltage rating, it is necessary to extend the proposed method to include the unbalanced issues. Since the proposed methods are generally based on the nodal current equation, it can simply consider the unbalanced characteristics by replacing each nodal voltage and current by three-phase voltage and current. The same procedure used in this thesis can be then followed to obtain the unbalance effect.

- This thesis research used a fast-centralized method for voltage stability assessment in distribution networks. The method is accurate and can capture the dynamic non-linear changes of power systems. However, there are some limitation regarding cost and the communication failure associated with such method. The scheme concept is based on wide area measurements collected throughout the network. Therefore, there are open choices to develop decentralized online methods for real-time voltage stability analysis. The decentralized based schemes do not rely on the wide area communication system and thus they are more reliable and have fast response after the disturbances.

- The proposed methods in this thesis represent the loads as constant impedances. This ignores the voltage dependent characteristics of loads. However, the loads can be generally modeled as constant power model, constant impedance model, constant current model,

exponential model, or polynomial model. Each model has specific characteristics that can affect the results obtained using of the proposed methods. Moreover, DG units can be modeled based on their operation modes: constant voltage, constant current, and constant power. These modes can also affect the obtained results. Thus, such voltage dependent characteristics can also be included in the analysis. To achieve the voltage dependent characteristics, one may express the active and reactive load powers as a function of voltage magnitude, nominal voltage magnitudes and modeling coefficients (ZIP). The proposed model can approximate the load voltage dependency using an impedance and current source, representing the quadratic voltage dependency and the linear voltage dependency, respectively. The polynomial coefficients can be obtained for a very good fit to the measured data. A curve-fitting procedure can be used to minimize the differences between the fitted values and the measured data for a specific number of voltage points within a specific range of network voltages.

- The cost of control variables is assumed to be constant in this work. However, price functions can be derived for cost models of control variables to prioritize the different resources. The price for shunt capacitors can be considered as constant because they are switched on or off with constant amounts of reactive power injection. Besides, they are manufactured with standardized capable switching times. In contrast, the price of controllable loads and DG units have to vary as the required response and power injection or curtailment amount. Many other factors can be considered for modeling the price function as condition changes and the manufacture characteristics. For photovoltaic-based DG, the cost of power curtailment will be greater when the curtailment amount is higher and when the curtailment occurs at lower power outputs. Moreover, the price of DG curtailment has to be different at each bus since each bus has different conditions for the power output. For controllable loads, the cost of the response is normally decreased as the required response amount increases. More users with higher response capacity will be recruited and thus the response cost will be lower.

- The proposed control methods are validated using academic test networks. However, it is required to show application of the proposed control methods for weak large-scale systems

and during contingency cases. Buses from large systems tend to behave differently from those belonging to smaller systems. In addition, larger systems are not as well conditioned as smaller systems. Some large and very large systems can be picked from the Matpower package for this purpose.

- This thesis uses the concept of Thevenin impedance match for voltage stability analysis. However, some researchers argue that this concept is not accurate for stability analysis (i.e. determining the voltage stability margin). In other words, the voltage instability or collapse may occur when the Thevenin equivalent impedance equals the load impedance. In this regard, a new formula for voltage stability margin can be developed such that all condition changes of the system are detected. An example for the new formula is to include the Thevenin equivalent voltage in margin formulation.

- This thesis provides a technique for power control at T/D interface and HV side support. The work considers a part of the interaction between TN and DNs. However, keeping the voltage at T/D interconnection point or controlling the reactive power at T/D interface does not assure the voltage stability of TNs. It is generally known that abnormal accidents in the area of high voltage network are not reported to distribution network operators. In other words, in cases in which the transmission network meets maintenance or outage of lines or generators, the distribution network operators cannot be able to know the voltage stability condition. Thus, the research is open about developing decentralized monitoring methods to reflect the operating state of HV network to distribution network, with limited operational data submitted by the HV network. One suggestion is to find a model for Thevenin equivalent parameter identification of TN, which considers the dynamic nonlinear system nature. This helps the distribution operators to avoid the operational interaction between TN and DNs by taking corrective or preventive actions without needing for DR signals from TN.

- Network partition methods can be involved for the voltage and T/D power exchange control. The partition method can be performed while ensuring that the intra-subarea voltage violation is solved by each subarea. The electrical distances and regional voltage

improvement capabilities can be used to achieve this purpose. This means that the control methods can be performed for each zone of the system, instead for the whole network. This can increase the reliability of the voltage and T/D power exchange control in distribution system while coordinating the voltage control devices throughout the network. The distributed control structures can also depend on intelligent agents for decision-making and computational sharing

LIST OF PUBLICATIONS

Alzaareer, K., & Saad, M. (2018). Real-time voltage stability monitoring in smart distribution grids. In *2018 International Conference on Renewable Energy and Power Engineering (REPE)* (pp. 13-17). IEEE.

Alzaareer, K., Saad, M., Mehrjerdi, H., Asber, D., & Lefebvre, S. (2020). Development of New Identification Method For Global Group of Controls For Online Coordinated Voltage Control In Active Distribution Networks. *IEEE Transactions on Smart Grid*, vol. 11, no. 5, pp. 3921-393.

Alzaareer, K., Saad, M., Asber, D., Lefebvre, S., & Lenoir, L. (2020). Impedance sensitivity-based corrective method for online voltage control in smart distribution grids. *Electric Power Systems Research, 181, 106188.*

Alzaareer, K., Saad, M., Mehrjerdi, H., El-Bayeh, C. Z., Asber, D., & Lefebvre, S. (2020). A new sensitivity approach for preventive control selection in real-time voltage stability assessment. *International Journal of Electrical Power & Energy Systems*, 122, 106212

Alzaareer, K., Saad, M., Mehrjerdi, H., Asber, D., & Lefebvre, S. A Fast Sensitivity Analysis Method For Voltage Control Applications With Distributed Generation. 2020 *IEEE Power Engineering Society General Meeting*.

Alzaareer, K., Saad, M., Mehrjerdi, H., El-Bayeh, C. Z., Asber, D., & Lefebvre, S. (2020) Voltage and Congestion Control in Active Distribution Networks Using Fast Sensitivity Analysis. *In 2020 5th International Conference on Renewable Energies for Developing Countries (REDEC)* (pp. 1-5). IEEE.

Alzaareer, K., Saad, M., Mehrjerdi, H., Asber, D., & Lefebvre, S. Realtime Control of Distributed Generation for Voltage Stability Improvement and HV Side Support. *International Conference on Technology and Policy in Electrical Power & Energy (ICT-PEP 2020).*

Alzaareer, K., Saad, M., Mehrjerdi, H., Asber, D., & Lefebvre, S. Development of an Index for Preventive Control Ranking and Selection for Voltage Stability Analysis. *First IEEE International Conference on Smart Technologies for Power, Energy and Control* (STPEC 2020).

Alzaareer, K., Saad, M., Mehrjerdi, H., Asber, D., & Lefebvre, S. Top-Down/Bottom-Up Method for Identifying a Set of Voltage Stability Preventive Controls. *International Conference on Technology and Policy in Electrical Power & Energy* (ICT-PEP 2020).

Alzaareer, K., Saad, M., Mehrjerdi, H., Asber, D., & Lefebvre, S. New Voltage Sensitivity Analysis for Smart Distribution Grids Using Analytical Derivation: ABCD Model. *International Journal of Electrical Power & Energy Systems*, (Submitted, Sep 2020).

Alzaareer, K., Saad, M., Mehrjerdi, H., Asber, D., & Lefebvre, S. MIQCP-Based Multi-Modes Online Power Exchange Control at T/D Interface. *IEEE Transactions on Smart Grid*. (Submitted, Aug 2020).

BIBLIOGRAPHY

ABB Pvt. Ltd. (Dec. 23, 2012). Network Manger SCADA/DMS Distribution Network Management. [Online]. Available: http://www.abb.com

Ahmadi, H., Martí, J. R., & Dommel, H. W. (2014). A framework for volt-VAR optimization in distribution systems. *IEEE Transactions on Smart Grid*, *6*(3), 1473-1483.

Ajjarapu, V., & Christy, C. (1992). The continuation power flow: a tool for steady state voltage stability analysis. *IEEE transactions on Power Systems*, *7*(1), 416-423.

Alamo, A. C. M., & Alberto, L. F. C. (2015, June). A multi-step optimization approach for power flow with transient stability constraints. In *2015 IEEE Eindhoven PowerTech* (pp. 1-6). IEEE.

Ali, S., & Mutale, J. (2015, September). Reactive power management at transmission/distribution interface. In *2015 50th International Universities Power Engineering Conference (UPEC)* (pp. 1-6). IEEE.

Alzaareer, K., & Saad, M. (2018, November). Real-time voltage stability monitoring in smart distribution grids. In *2018 International Conference on Renewable Energy and Power Engineering (REPE)* (pp. 13-17). IEEE.

Alzaareer, K., Saad, M., Mehrjerdi, H., Asber, D., & Lefebvre, S. (2020a). Development of New Identification Method For Global Group of Controls For Online Coordinated Voltage Control In Active Distribution Networks. *IEEE Transactions on Smart Grid.*

Alzaareer, K., Saad, M., Asber, D., Lefebvre, S., & Lenoir, L. (2020b). Impedance sensitivity-based corrective method for online voltage control in smart distribution grids. *Electric Power Systems Research, 181, 106188.*

Alzaareer, K., Saad, M., Mehrjerdi, H., El-Bayeh, C. Z., Asber, D., & Lefebvre, S. (2020c). Voltage and Congestion Control in Active Distribution Networks Using Fast Sensitivity Analysis. *In 2020 5th International Conference on Renewable Energies for Developing Countries (REDEC)* (pp. 1-5). IEEE.

Aolaritei, L., Bolognani, S., & Dörfler, F. (2018). Hierarchical and distributed monitoring of voltage stability in distribution networks. *IEEE Transactions on Power Systems*, 33(6), 6705-6714.

Aristidou, P., Valverde, G., & Van Cutsem, T. (2015). Contribution of distribution network control to voltage stability: A case study. *IEEE Transactions on Smart Grid*, 8(1), 106-116.

Atwa, Y. M., & El-Saadany, E. F. (2010). Optimal allocation of ESS in distribution systems with a high penetration of wind energy. *IEEE Transactions on Power Systems*, *25*(4), 1815-1822.

Azzouz, M. A., Shaaban, M. F., & El-Saadany, E. F. (2015). Real-time optimal voltage regulation for distribution networks incorporating high penetration of PEVs. *IEEE Transactions on Power Systems*, *30*(6), 3234-3245.

Bahmanyar, A. R., & Karami, A. (2014). Power system voltage stability monitoring using artificial neural networks with a reduced set of inputs. *International Journal of Electrical Power & Energy Systems*, 58, 246-256.

Bandler, J., & El-Kady, M. (1980). A unified approach to power system sensitivity analysis and planning, Part I: Family of adjoint systems. *In Proc. IEEE Int. Symp. Circuits Syst* (pp. 681-687).

Bandler, J. W., & El-Kady, M. A. (1982). A new method for computerized solution of power flow equations. *IEEE Transactions on Power Apparatus and Systems*, (1), 1-10.

Baran, M. E., & El-Markabi, I. M. (2007). A multiagent-based dispatching scheme for distributed generators for voltage support on distribution feeders. *IEEE Transactions on power systems*, *22*(1), 52-59.

Biserica, M., Berseneff, B., Besanger, Y., & Kiény, C. (2011, June). Upgraded coordinated voltage control for distribution systems. In *2011 IEEE Trondheim PowerTech* (pp. 1-6). IEEE.

Bolognani, S., & Zampieri, S. (2015). On the existence and linear approximation of the power flow solution in power distribution networks. *IEEE Transactions on Power Systems*, *31*(1), 163-172.

Borghetti, A., Bosetti, M., Grillo, S., Massucco, S., Nucci, C. A., Paolone, M., & Silvestro, F. (2010). Short-term scheduling and control of active distribution systems with high penetration of renewable resources. *IEEE Systems Journal*, *4*(3), 313-322.

Castro, J. R., Saad, M., Lefebvre, S., Asber, D., & Lenoir, L. (2016). Optimal voltage control in distribution network in the presence of DGs. *International Journal of Electrical Power & Energy Systems*, *78*, 239-247.

Chakravorty, M., & Das, D. (2001). Voltage stability analysis of radial distribution networks. *International Journal of Electrical Power & Energy Systems*, 23(2), 129-135.

Choi, J. H., & Kim, J. C. (2001). Advanced voltage regulation method of power distribution systems interconnected with dispersed storage and generation systems. *IEEE Transactions on Power Delivery*, *16*(2), 329-334.

Chou, H. M., & Butler-Purry, K. L. (2014, September). Investigation of voltage stability in three-phase unbalanced distribution systems with DG using modal analysis technique. In *2014 North American Power Symposium (NAPS)* (pp. 1-6). IEEE.

Christakou, K., Tomozei, D. C., Le Boudec, J. Y., & Paolone, M. (2013). GECN: Primary voltage control for active distribution networks via real-time demand-response. *IEEE Transactions on Smart Grid*, 5(2), 622-631.

Conti, S., Raiti, S., & Vagliasindi, G. (2010, July). Voltage sensitivity analysis in radial MV distribution networks using constant current models. In *2010 IEEE International Symposium on Industrial Electronics* (pp. 2548-2554). IEEE.

Corsi, S., & Taranto, G. N. (2008). A real-time voltage instability identification algorithm based on local phasor measurements. *IEEE transactions on power systems*, 23(3), 1271-1279.

D'Adamo, C., Jupe, S., & Abbey, C. (2009, June). Global survey on planning and operation of active distribution networks-Update of CIGRE C6. 11 working group activities. In *CIRED 2009-20th International Conference and Exhibition on Electricity Distribution-Part 1* (pp. 1-4). IET.

Degefa, M. Z., Lehtonen, M., Millar, R. J., Alahäivälä, A., & Saarijärvi, E. (2015). Optimal voltage control strategies for day-ahead active distribution network operation. *Electric Power Systems Research*, *127*, 41-52.

Dobson, I. (1992). Observations on the geometry of saddle node bifurcation and voltage collapse in electrical power systems. *IEEE Transactions on Circuits and Systems I: Fundamental Theory and Applications,* 39(3), 240-243.

Dou, X., Zhang, S., Chang, L., Wu, Z., Gu, W., Hu, M., & Yuan, X. (2017). An improved CPF for static stability analysis of distribution systems with high DG penetration. *International Journal of Electrical Power & Energy Systems*, *86*, 177-188.

Dou, X., Duan, X., Hu, Q., Shen, L., & Wu, Z. (2019). A nonintrusive control strategy using voltage and reactive power for distribution systems based on PV and the nine-zone diagram. *International Journal of Electrical Power & Energy Systems*, *105*, 89-97.

Elkhatib, M. E., El-Shatshat, R., & Salama, M. M. (2011). Novel coordinated voltage control for smart distribution networks with DG. *IEEE transactions on smart grid*, *2*(4), 598-605.

El Moursi, M. S., Zeineldin, H. H., Kirtley, J. L., & Alobeidli, K. (2014). A dynamic master/slave reactive power-management scheme for smart grids with distributed generation. *IEEE Transactions on Power Delivery*, *29*(3), 1157-1167.

European Commission, "Establishing a network code on demand connection," *Official Journal of the European Union*, vol. 59, pp. 1–45, August 2016.

Evangelopoulos, V. A., Georgilakis, P. S., & Hatziargyriou, N. D. (2016). Optimal operation of smart distribution networks: A review of models, methods and future research. *Electric Power Systems Research*, *140*, 95-106.

Ferreira, L. A. F. (1990). Tellegen's theorem and power systems-new load flow equations, new solution methods. *IEEE transactions on circuits and systems*, *37*(4), 519-526.

Gama, P. H. R. P., Flores, E. M., Alvarez, G. P., Mak, J., Guaraldo, N. J., Guardia, E. C., ... & Sanzoni, S. (2009, July). Incorporating distributed generation in the energy contracting strategy in a regulated environment. In *2009 CIGRE/IEEE PES Joint Symposium Integration of Wide-Scale Renewable Resources Into the Power Delivery System* (pp. 1-6). IEEE.

Gao, B., Morison, G. K., & Kundur, P. (1992). Voltage stability evaluation using modal analysis. *IEEE transactions on power systems*, 7(4), 1529-1542.

Garces, A. (2015). A linear three-phase load flow for power distribution systems. *IEEE Transactions on Power Systems*, *31*(1), 827-828.

Gharebaghi, S., Safdarian, A., & Lehtonen, M. (2019). A linear model for AC power flow analysis in distribution networks. *IEEE Systems Journal*, *13*(4), 4303-4312.

Glavic, M., Hajian, M., Rosehart, W., & Van Cutsem, T. (2011). Receding-horizon multi-step optimization to correct nonviable or unstable transmission voltages. *IEEE Transactions on Power Systems*, 26(3), 1641-1650.

Gönen, T. (1986). Electric Power Distribution System*, McGraw-Hill Book Company*.

Gubina, F., & Strmcnik, B. (1997). A simple approach to voltage stability assessment in radial networks. *IEEE Transactions on Power Systems*, *12*(3), 1121-1128.

Guo, J., Tonguz, O., & Hug, G. (2017, June). Impact of power system partitioning on the efficiency of distributed multi-step optimization. In *2017 IEEE Manchester PowerTech* (pp. 1-6). IEEE.

Gurram, R., & Subramanyam, B. (1999). Sensitivity analysis of radial distribution network–adjoint network method. *International Journal of Electrical Power & Energy Systems*, *21*(5), 323-326.

Hamada, M. M., Wahab, M. A., & Hemdan, N. G. (2010). Simple and efficient method for steady-state voltage stability assessment of radial distribution systems. *Electric Power Systems Research*, *80*(2), 152-160.

IEEE PES, Distribution Test Feeders, Sep. 2010. [Online]. Available: http://www.ewh.ieee.org/soc/pes/dsacom/testfeeders/index.html.

Iwamoto, S., & Tamura, Y. (1981). A load flow calculation method for ill-conditioned power systems. *IEEE transactions on power apparatus and systems*, (4), 1736-1743.

Jasmon, G. B., & Lee, L. H. C. C. (1991). Distribution network reduction for voltage stability analysis and loadflow calculations. *International Journal of Electrical Power & Energy Systems*, *13*(1), 9-13.

Jupe, S. C., Taylor, P. C., & Michiorri, A. (2010). Coordinated output control of multiple distributed generation schemes. *IET Renewable Power Generation*, *4*(3), 283-297.

Kamel, M., Karrar, A. A., & Eltom, A. H. (2017). Development and application of a new voltage stability index for on-line monitoring and shedding. *IEEE Transactions on Power Systems*, *33*(2), 1231-1241.

Ke, X., Samaan, N., Holzer, J., Huang, R., Vyakaranam, B., Vallem, M., ... & Nguyen, Q. (2018). Coordinative real-time sub-transmission volt–var control for reactive power regulation between transmission and distribution systems. *IET Generation, Transmission & Distribution*, *13*(11), 2006-2014.

Keane, A., Ochoa, L. F., Vittal, E., Dent, C. J., & Harrison, G. P. (2010). Enhanced utilization of voltage control resources with distributed generation. *IEEE Transactions on Power Systems*, *26*(1), 252-260.

Kersting, W. H. (2012). Distribution system modeling and analysis. CRC press.

Kurzidem. M, "Voltage support concept for the Swiss transmission system from 2011," 2011.

Kim, Y. J., Ahn, S. J., Hwang, P. I., Pyo, G. C., & Moon, S. I. (2012). Coordinated control of a DG and voltage control devices using a dynamic programming algorithm. *IEEE Transactions on Power Systems*, *28*(1), 42-51.

Kryonidis, G. C., Demoulias, C. S., & Papagiannis, G. K. (2019). A new voltage control scheme for active medium-voltage (MV) networks. *Electric Power Systems Research*, *169*, 53-64.

Kulmala, A., Repo, S., & Järventausta, P. (2014). Coordinated voltage control in distribution networks including several distributed energy resources. *IEEE Transactions on Smart Grid*, *5*(4), 2010-2020.

Kundur, P., Balu, N. J., & Lauby, M. G. (1994). *Power system stability and control* (Vol. 7). New York: McGraw-hill.

Kundur, P., Paserba, J., Ajjarapu, V., Andersson, G., Bose, A., Canizares, C., ... & Van Cutsem, T. (2004). Definition and classification of power system stability IEEE/CIGRE joint task force on stability terms and definitions. *IEEE transactions on Power Systems,* 19(3), 1387-1401.

Jakus, D., Vasilj, J., & Sarajcev, P. (2015, June). Voltage control in MV distribution networks through coordinated control of tap changers and renewable energy sources. In *2015 IEEE Eindhoven PowerTech* (pp. 1-6). IEEE.

Khatod, D. K., Pant, V., & Sharma, J. (2006). A novel approach for sensitivity calculations in the radial distribution system. *IEEE transactions on Power Delivery*, *21*(4), 2048-2057.
Kulmala, A., Repo, S., & Järventausta, P. (2014). Coordinated voltage control in distribution networks including several distributed energy resources. *IEEE Transactions on Smart Grid*, *5*(4), 2010-2020.

Li, C., Disfani, V. R., Pecenak, Z. K., Mohajeryami, S., & Kleissl, J. (2018). Optimal OLTC voltage control scheme to enable high solar penetrations. *Electric Power Systems Research*, *160*, 318-326.

Li, S., Tan, Y., Li, C., Cao, Y., & Jiang, L. (2017). A fast sensitivity-based preventive control selection method for online voltage stability assessment. *IEEE Transactions on Power Systems*, *33*(4), 4189-4196.

Lin, C., Wu, W., Zhang, B., Wang, B., Zheng, W., & Li, Z. (2016). Decentralized reactive power optimization method for transmission and distribution networks accommodating large-scale DG integration. *IEEE Transactions on Sustainable Energy*, *8*(1), 363-373.

Liu, J. H., & Chu, C. C. (2014). Long-term voltage instability detections of multiple fixed-speed induction generators in distribution networks using synchrophasors. *IEEE Transactions on Smart Grid*, *6*(4), 2069-2079.

Liu, K. Y., Sheng, W., Hu, L., Liu, Y., Meng, X., & Jia, D. (2015). Simplified probabilistic voltage stability evaluation considering variable renewable distributed generation in distribution systems. *IET Generation, Transmission & Distribution*, *9*(12), 1464-1473.

Liu, K., Wang, C., Wang, W., Chen, Y., & Wu, H. (2019). Linear power flow calculation of distribution networks with distributed generation. *IEEE Access*, *7*, 44686-44695.

Lof, P. A., Andersson, G., & Hill, D. J. (1993). Voltage stability indices for stressed power systems. *IEEE transactions on power systems*, 8(1), 326-335.

Lof, P. A., Smed, T., Andersson, G., & Hill, D. J. (1992). Fast calculation of a voltage stability index. *IEEE Transactions on Power Systems*, *7*(1), 54-64.

Lopes, J. P., Hatziargyriou, N., Mutale, J., Djapic, P., & Jenkins, N. (2007). Integrating distributed generation into electric power systems: A review of drivers, challenges and opportunities. *Electric power systems research*, 77(9), 1189-1203.

Maciejowski, J. M. (2002). *Predictive control: with constraints*. Pearson education.

Martí, J. R., Ahmadi, H., & Bashualdo, L. (2013). Linear power-flow formulation based on a voltage-dependent load model. *IEEE Transactions on Power Delivery*, *28*(3), 1682-1690.

Matavalam, A. R. R., & Ajjarapu, V. (2017). Sensitivity based thevenin index with systematic inclusion of reactive power limits. *IEEE Transactions on Power Systems*, *33*(1), 932-942.

Meirinhos, J. L., Rua, D. E., Carvalho, L. M., & Madureira, A. G. (2017). Multi-temporal optimal power flow for voltage control in MV networks using distributed energy resources. *Electric Power Systems Research*, *146*, 25-32.

Milosevic, B., & Begovic, M. (2003). Voltage-stability protection and control using a wide-area network of phasor measurements. *IEEE Transactions on Power Systems*, 18(1), 121-127.

Morin, J., Colas, F., Grenard, S., Dieulot, J. Y., & Guillaud, X. (2016, October). Coordinated predictive control in active distribution networks with HV/MV reactive power constraint. In *2016 IEEE PES Innovative Smart Grid Technologies Conference Europe (ISGT-Europe)* (pp. 1-6). IEEE.

Muttaqi, K. M., Le, A. D., Negnevitsky, M., & Ledwich, G. (2015). A coordinated voltage control approach for coordination of OLTC, voltage regulator, and DG to regulate voltage in a distribution feeder. *IEEE Transactions on Industry Applications*, *51*(2), 1239-1248.

Nazari, M. H., & Ilic, M. (2014). Dynamic modelling and control of distribution energy systems: comparison with transmission power systems. *IET Generation, Transmission & Distribution*, *8*(1), 26-34.

NR Electric Corporation. (Dec. 23, 2012). Distribution Management System. [Online]. Available: http://www.nrelect.com

Ochoa, L. F., Dent, C. J., & Harrison, G. P. (2009). Distribution network capacity assessment: Variable DG and active networks. *IEEE Transactions on Power Systems*, *25*(1), 87-95.

Ochoa, L. F., Keane, A., & Harrison, G. P. (2011). Minimizing the reactive support for distributed generation: Enhanced passive operation and smart distribution networks. *IEEE Transactions on Power Systems*, *26*(4), 2134-2142.

Olival, P. C., Madureira, A. G., & Matos, M. (2017). Advanced voltage control for smart microgrids using distributed energy resources. *Electric power systems research*, *146*, 132-140.

Oshiro, M., Tanaka, K., Senjyu, T., Toma, S., Yona, A., Saber, A. Y., ... & Kim, C. H. (2011). Optimal voltage control in distribution systems using PV generators. *International Journal of Electrical Power & Energy Systems*, *33*(3), 485-492.

Peschon, J., Piercy, D. S., Tinney, W. F., & Tveit, O. J. (1968). Sensitivity in power systems. *IEEE Transactions on Power Apparatus and Systems*, (8), 1687-1696.

Petinrin, J. O., & Shaaban, M. (2014, December). Voltage control in a smart distribution network using demand response. *In 2014 IEEE International Conference on Power and Energy (PECon) (pp. 319-324)*. IEEE.

Photovoltaics, D. G., & Storage, E. (2009). IEEE Application Guide for IEEE Std 1547™, *IEEE Standard for Interconnecting Distributed Resources with Electric Power Systems*.

Ranamuka, D., Agalgaonkar, A. P., & Muttaqi, K. M. (2016). Examining the interactions between DG units and voltage regulating devices for effective voltage control in distribution systems. *IEEE Transactions on Industry Applications*, *53*(2), 1485-1496.

Ranamuka, D., Agalgaonkar, A. P., & Muttaqi, K. M. (2015). Online coordinated voltage control in distribution systems subjected to structural changes and DG availability. *IEEE Transactions on Smart Grid*, *7*(2), 580-591.

Ranamuka, D., Agalgaonkar, A. P., & Muttaqi, K. M. (2013). Online voltage control in distribution systems with multiple voltage regulating devices. *IEEE Transactions on Sustainable Energy*, *5*(2), 617-628.

Richardot, O., Viciu, A., Besanger, Y., Hadjsaid, N., & Kiény, C. (2006, May). Coordinated voltage control in distribution networks using distributed generation. In *Transmission and Distribution Conference and Exhibition, 2005/2006 IEEE PES* (Vol. 1, pp. 1196-1201).

Sansawatt, T., Ochoa, L. F., & Harrison, G. P. (2012). Smart decentralized control of DG for voltage and thermal constraint management. *IEEE transactions on power systems*, *27*(3), 1637-1645.

Savier, J. S., & Das, D. (2007). Impact of network reconfiguration on loss allocation of radial distribution systems. *IEEE Transactions on Power Delivery*, *22*(4), 2473-2480.

Senjyu, T., Miyazato, Y., Yona, A., Urasaki, N., & Funabashi, T. (2008). Optimal distribution voltage control and coordination with distributed generation. *IEEE Transactions on power delivery*, *23*(2), 1236-1242.

Sheng, H., & Chiang, H. D. (2013). CDFLOW: A practical tool for tracing stationary behaviors of general distribution networks. *IEEE Transactions on Power Systems*, 29(3), 1365-1371.

Sheng, W., Liu, K. Y., Cheng, S., Meng, X., & Dai, W. (2015). A trust region SQP method for coordinated voltage control in smart distribution grid. *IEEE Transactions on Smart Grid*, *7*(1), 381-391.

Shivarudraswamy, R., & Gaonkar, D. N. (2012). Coordinated voltage regulation of distribution network with distributed generators and multiple voltage-control devices. *Electric Power Components and Systems,* 40(9), 1072-1088.

Short, T. A. (2014). Electric power distribution handbook. CRC press.

Smon, I., Verbic, G., & Gubina, F. (2006). Local voltage-stability index using Tellegen's theorem. *IEEE Transactions on Power Systems*, 21(3), 1267-1275.

Stock, D. S., Venzke, A., Hennig, T., & Hofmann, L. (2016, October). Model predictive control for reactive power management in transmission connected distribution grids. In *2016 IEEE PES Asia-Pacific Power and Energy Engineering Conference (APPEEC)* (pp. 419-423). IEEE.

Stock, D. S., Venzke, A., Löwer, L., Rohrig, K., & Hofmann, L. (2016). Optimal reactive power management for transmission connected distribution grid with wind farms. In *2016 IEEE Innovative Smart Grid Technologies-Asia (ISGT-Asia)* (pp. 1076-1082). IEEE.

Trias, A. (2012, July). The holomorphic embedding load flow method. *In 2012 IEEE Power and Energy Society General Meeting* (pp. 1-8). IEEE.

Uluski, B (2011). Distribution management systems. presented *at the CRN Summit*, Cleveland, OH, USA.

United Kingdom Generic Distribution Network (UKGDS). [Online]. Available: http://sedg.ac.uk

Vallem, M. R., Vyakaranam, B., Holzer, J. T., Elizondo, M. A., & Samaan, N. A. (2017, September). Power system decomposition for practical implementation of bulk-grid voltage control methods. In *2017 19th International Conference on Intelligent System Application to Power Systems (ISAP)* (pp. 1-6). IEEE.

Valverde, G., & Van Cutsem, T. (2013). Model predictive control of voltages in active distribution networks. *IEEE Transactions on Smart Grid*, *4*(4), 2152-2161.

Valverde, G., & Van Cutsem, T. (2013b). Control of dispersed generation to regulate distribution and support transmission voltages. In *2013 IEEE Grenoble Conference* (pp. 1-6). IEEE.

Viawan, F. A., & Karlsson, D. (2007). Combined local and remote voltage and reactive power control in the presence of induction machine distributed generation. *IEEE Transactions on Power Systems*, *22*(4), 2003-2012.

Viawan, F. A., & Karlsson, D. (2008). Voltage and reactive power control in systems with synchronous machine-based distributed generation. *IEEE transactions on power delivery*, *23*(2), 1079-1087.

Vu, K., Begovic, M. M., Novosel, D., & Saha, M. M. (1999). Use of local measurements to estimate voltage-stability margin. *IEEE Transactions on Power Systems*, 14(3), 1029-1035.

Walling, R. A., Saint, R., Dugan, R. C., Burke, J., & Kojovic, L. A. (2008). Summary of distributed resources impact on power delivery systems. *IEEE Transactions on power delivery*, *23*(3), 1636-1644.

Wang, Z., Cui, B., & Wang, J. (2016). A necessary condition for power flow insolvability in power distribution systems with distributed generators. *IEEE Transactions on Power Systems*, 32(2), 1440-1450.

Wang, Y., Pordanjani, I. R., Li, W., Xu, W., Chen, T., Vaahedi, E., & Gurney, J. (2011). Voltage stability monitoring based on the concept of coupled single-port circuit. *IEEE Transactions on Power Systems*, *26*(4), 2154-2163.

Wang, B., & Lan, K. (2011, March). Analysis of the distributed generation system and the influence on power loss. *In 2011 Asia-Pacific Power and Energy Engineering Conference* (pp. 1-4). IEEE.

Weckx, S., D'Hulst, R., & Driesen, J. (2014). Voltage sensitivity analysis of a laboratory distribution grid with incomplete data. *IEEE Transactions on Smart Grid*, *6*(3), 1271-1280.

Yang, H. T., & Liao, J. T. (2015). MF-APSO-based multiobjective optimization for PV system reactive power regulation. *IEEE Transactions on Sustainable Energy*, *6*(4), 1346-1355.

Yu, J., Li, W., Ajjarapu, V., Yan, W., & Zhao, X. (2014). Identification and location of long-term voltage instability based on branch equivalent. *IET Generation, Transmission & Distribution*, 8(1), 46-54.

Zad, B. B., Hasanvand, H., Lobry, J., & Vallée, F. (2015). Optimal reactive power control of DGs for voltage regulation of MV distribution systems using sensitivity analysis method and PSO algorithm. *International Journal of Electrical Power & Energy Systems*, *68*, 52-60.

Zakariazadeh, A., Homaee, O., Jadid, S., & Siano, P. (2014). A new approach for real time voltage control using demand response in an automated distribution system. *Applied Energy,* 117, 157-166.

Zhang, Y., Liu, M., Zhang, W., Sun, W., Hu, X., & Kong, G. (2018). Power System Voltage Correction Scheme Based on Adaptive Horizon Model Predictive Control. *Applied Sciences*, 8(4), 641.

Zhao, B., Xu, Z., Xu, C., Wang, C., & Lin, F. (2017). Network partition-based zonal voltage control for distribution networks with distributed PV systems. *IEEE Transactions on Smart Grid*, *9*(5), 4087-4098.

Zhou, Q., & Bialek, J. W. (2007). Generation curtailment to manage voltage constraints in distribution networks. *IET Generation, Transmission & Distribution*, 1(3), 492-498.

Zhou, Q., & Bialek, J. (2008, July). Simplified calculation of voltage and loss sensitivity factors in distribution networks. In *Proc. 16th Power Syst. Comput. Conf.(PSCC2008)*.

Zou, K., Agalgaonkar, A. P., Muttaqi, K. M., & Perera, S. (2011). Distribution system planning with incorporating DG reactive capability and system uncertainties. *IEEE Transactions on Sustainable Energy*, 3(1), 112-123.